Metrology-Based Process Modelling Framework for Digital and Physical Measurement Environments Integration

Zhang, Xi

Award date:
2013

Awarding institution:
University of Bath

Metrology-Based Process Modelling Framework for Digital and Physical Measurement Environments Integration

Xi Zhang

A thesis submitted for the degree of Doctor of Philosophy

University of Bath

Department of Mechanical Engineering

October 2013

Abstract

Process modelling is the activity of constructing and analyzing models, which are applicable and useful to solve predefined problems. It allows engineering process to be analyzed, and consequently leads to quality and efficiency improvement. As metrology becomes increasingly important in modern manufacturing, process modelling based on measurement techniques and operations becomes necessary and valuable. Measurement uncertainty, which is obtained from measurement operation, is regarded as a key factor in metrology-based process modelling. By analyzing measurement uncertainty, metrology-based process models can tangibly improve manufacturing quality and efficiency, improve the actualize communication between design and manufacturing, and, ultimately, achieve product lifecycle integration between design, manufacturing and verification functions.

Digital measurement models can simulate measurement process, and predict task-specific measurement uncertainty in the digital environment, before carrying out capital-consuming physical measurements. However, the integration between digital and physical measurement environments is not fully approved. Measurement uncertainty predicted by the digital measurement model may show little practical significance with that obtained from physical measurements. The quality of digital measurement result highly relies on input quantities loaded into the digital measurement model. And it is hardly possible to verify digital measurement results for all of the measurement scenarios because of the high variability and complexity of inspected features and measurement tasks.

This research has reviewed the fundamental technologies relating to measurement process modelling and measurement uncertainty evaluation in a digital environment, especially for coordinate measurement machines (CMMs). An initial verification work has been carried out by ‘measuring’ small features on a large-volume component in a realistic shop floor environment. This verification work has realized the limitations of the digital measurement model, and the challenge of integrating digital and physical measurement environments.

Based on the initial verification work, a Measurement Planning and Implementation Framework has been proposed, aiming to analyse and improve the relationship between digital and physical measurement environments. The Framework is deployed with the statistics methods to analyse measurement uncertainty obtained from the digital and the physical measurement environments, and quantitatively predict influence levels of measurement uncertainty contributors. The verification work of the Framework has been carried out in a finely-control laboratory environment with environmental control. The robustness of the Framework has been evaluated, indicating the potential of deploying statistical methods for measurement uncertainty analysis, which extends the utilization of measurement uncertainty for decision-making processes.

The contributions to knowledge of the research include:

(1) Verification of the performance of a digital CMM model under meaningful measurement scenarios;
(2) Development of a metrology-based process modeling framework to integrate digital and physical measurement environments through quantitative measurement uncertainty analysis.

Acknowledgement

Thank you to my supervisor, Prof. Paul Maropoulos, for the wide opportunities over the past few years. Thanks too to all of the 'The Laboratory for Integrated Metrology Applications (LIMA)' at Bath for making my PhD research such a valuable learning process.

I have greatly appreciated for being supported by Mr. Nick Orchard and Mr. Per Saunders, from *Rolls-Royce Plc*, for making the research rich with practical data and giving me vital experience in shop floor environment. Thanks to Prof. Alistair Forbes and Dr. Alan Wilson, from the *National Physical Laboratory (NPL)*, UK, for the intensive laboratory work which has leaded the scientific analysis and argumentation of the thesis. And thanks to Dr. Jon Balwin, from *MetroSage*, USA, and Mr. John Horst, from the *National Institute of Standards and Technology (NIST)*, USA, for explaining the latest developments of quality system integration. And thanks to Prof. Tang Xiaoqing and Dr. Du Fuzhou, from Beihang University, China, for helping me to structure the thesis. Thank you all for the enjoyable and beneficial workshops throughout my PhD research.

At last, I would like to thank my parents for all their love, patience and support.

Contents

List of Notations

ASME	American Society of Mechanical Engineers
CAD	Computer-Aided Design
CAM	Computer-Aided Manufacturing
CAPP	Computer-Aided Process Planning
CATIP	Computer-Aided Tactile Inspection Planning
CMM	Coordinate Measurement Machine
DOE	Design of Experiments
ECMM	Expert Coordinate Measurement Machine
GD&T	Geometric Dimensioning and Tolerancing
GPS	Geometrical Product Specifications
GUM	Guide to the Expression of Uncertainty in Measurement
IGES	Initial Graphics Exchange Specification
IPO	Input-Process-Output
ISO	International Standard Organization
JCGM	Joint Committee for Guides in Metrology
LSC	Least Squares Circle
MCC	Minimum Circumscribing Circle
MIC	Maximum Inscribed Circle
MZC	Minimum Zone Circle
NMIJ	National Metrology Institute of Japan
NML	National Measurement Laboratory
NPL	National Physical Laboratory
NURBS	Non-uniform rational B-spline
PTB	Physicalish-Technishe Bundesanstalt
PUNDIT	Predicts Uncertainty in Dimensional Inspection Techniques
QIF	Quality Information Framework
S/N Ratio	Signal-to-Noise Ratio
TDU	Tokyo Denki University
UES	Uncertainty Estimation Software
UML	Unified Modelling Language
UT	The University of Tokyo

VCMM	Virtual Coordinate Measurement Machine
VIM	International Vocabulary of Metrology

List of Figures

List of Tables

Chapter 1 Introduction

Dimensional Metrology is the science of calibrating and using physical measurement equipment to quantify the physical size of or distance from any given object [1]. In today's global competitive market, high product quality becomes increasingly important, and the accuracy assertion of the products becomes indispensable [2]. Consequently, dimensional metrology emerges as a critical step in manufacturing, driving product development and quality control at steady and strong pace [3]. Improved measurement capability will open the door to significant productivity benefits as improvements deliver.

Considerable progress has been made in dimensional measurement. In respect to hardware, laser-based measurement instruments have been developed, allowing measurement can be operated in contact, non-contact or hybrid manner. New measurement technologies and techniques are continuously adopted by high-value manufacturing line. In respect to software, measurement simulation packages are created by using various simulation techniques. The measurement simulation package can simulate the measurement process, and predict the measurement result. It allows measurement operations executed in the digital environment, and therefore, save financial and labour cost of executing physical measurements.

However, dimensional metrology still faces intense challenges to fulfil requirements from high-value manufacturing. The practices of dimensional metrology are lack of simplicity and standardization. Effective integration between digital and physical measurement environments is not implemented. And measurement process modelling has not been fully established.

In order to overcome these problems, a process model for measurement is imperative. This process model should promote the integration between digital and physical measurement environments, and release the potential of integrating measurement to Product Lifecycle Management (PLM) system. In this thesis, attempts have been towards this direction. A Measurement Planning and Implementation Framework has been implemented to integrate digital and physical measurement environments, and a

metrology-based process modelling has been developed, in particular for coordinate measurement machine (CMM).

In this chapter, the background of this research is presented in Section 1.1. Then the overall aims of the research are described in Section 1.2. Finally, Section 1.3 gives an organizational outline of the thesis.

1.1 Background

1.1.1 Metrology and measurement in high-value manufacturing

Global competition in high-value manufacturing requires high product quality and product complexity. To realize a proper function of a complex part, a product designer needs to assign sufficiently narrow tolerances to product features, while the manufacturer needs to produce the part to fulfil design requirements [4]. To achieve this goal, dimensional metrology becomes increasingly important.

Many world-leading high-value manufacturers have established the facilities and resources for effective measurements. Metrology has been generally realized as a part of manufacturers' strategy to achieve standardised methods for producing and sharing data around a global production network. The collection and analysis of measurement data is expected to be integrated into a production system - speeding up the decision making process and allowing changes to be made in real time wherever possible [5]. The need to continually assess the validity of measurement data is emerging. Measurement results are expected to be utilized in a more sensible manner [6].

New measurement technologies and techniques have been developed. As shown in Figure 1, the measurement instruments range from 3-axis coordinate measurement machine (CMM) to 6 degree-of-freedom articulated arms, and from contact point-to-point measurement to non-contact grid scanning [7]. These new measurement technologies and techniques are challenging and dislodging traditional approaches to established measurement practices, as manufacturing is becoming increasingly data driven [6].

Figure 1 Dimensional measurement instruments

1.1.2 Measurement process modelling

In manufacturing, process modelling deals with determination of appropriate operations and sequences to produce a tangible part from an engineering design [8]. With the booming development of computational techniques, the majority of process modelling activities have been accomplished with the aid of digital environments [9]. Extensive research efforts have been made in process modelling, and have demonstrated that process modelling is an effective and efficient technique for design and manufacturing integration [10].

Measurement process modelling uses computational techniques to design, analyse and optimize measurement processes. As metrology gets increasingly important in high-value manufacturing, measurement process modelling becomes a key in

production efficiency improvement and cost reduction [6]. Proper measurement process modelling can lead to a dramatic improvement in quality control and provide smooth integration of product lifecycle management (PLM) [11].

Measurement process modelling could be generally categorized into three levels:

- Direct measurement process modelling;
- Measurement uncertainty estimation;
- Robust measurement process modelling.

The details of these three levels are described in the following paragraphs.

- *Direct measurement process modelling*

Direct measurement process modelling can be seen as an interface between physical measurement operations and digital environment. As shown in Figure 2, features of measurement instruments and measurement operations are established in direct measurement process modelling. It visualizes physical measurement operations in digital environment, collects measurement results and outputs these data to assist product inspection and production quality control. Direct measurement process modelling allows the realization of a physical measurement process in a digital environment.

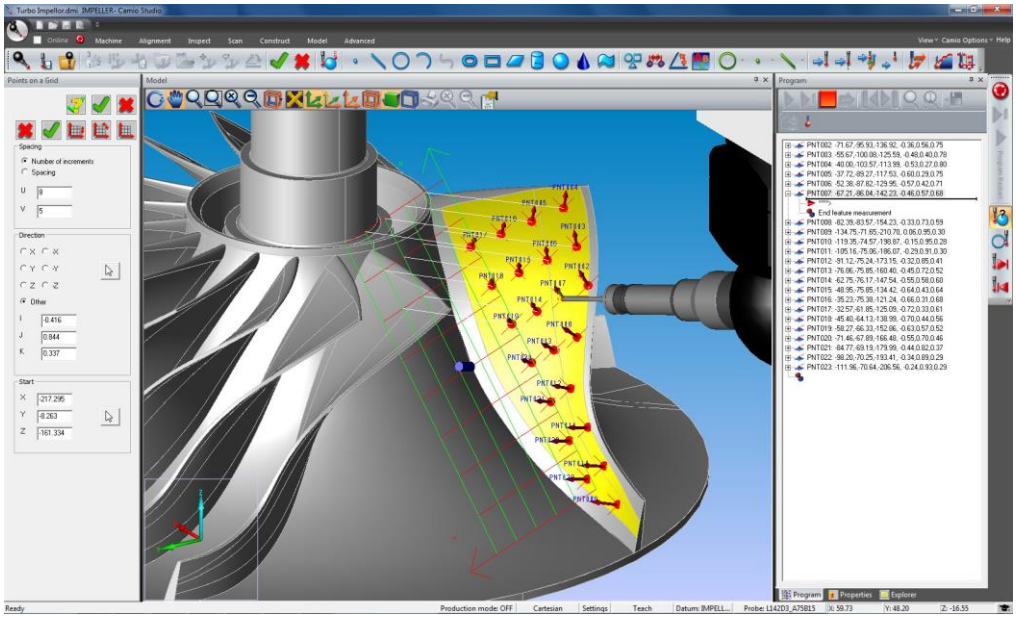

Figure 2 Online measurement simulation software

- *Measurement uncertainty estimation*

Measurement uncertainty estimation considers measurement uncertainty[*] as a key index of measurement process modelling. It allows end-users to configure measurement scenarios in a measurement model, and employs sophisticated quantitative analysis techniques to calculate task-specific measurement uncertainty [12], the measurement uncertainty of a specific feature for the configured measurement scenarios [13].

Process modelling for measurement uncertainty estimation allows knowing measurement results priory to physical measurement results, and therefore saves labour, time and resource cost from physical measurement operations [14]. Various endeavours have been made to verify the performance of uncertainty estimation models [15,16]. However, the verification work remains to be a challenge [17]. There is an enormous diversity and complexity of measurement tasks. Controlling uncertainty influence quantities in physical measurement is very expensive and difficult. It is virtually impossible to replicate all of measurement tasks in physical measurement environment.

- *Robust measurement process modelling*

Robust measurement process modelling considers measurement as an essential operation of product lifecycle, and therefore, aims to promote coherent integration of measurement operation into product lifecycle.

Robust measurement process modelling is still at an early stage. One of the major achievements is the introduction of the Qualify Information Framework (QIF) [18]. The QIF is an advanced measurement information-exchange platform, aiming to provide seamless data transition between design, machining, measurement and quality control. The genuine goal of the QIF is to enforce the total integration of PLM with the aim of metrology operations [11]. Although the structures and the schemas of the QIF are still under development, the QIF have shown promising prospect in terms of

[*] The details relating to measurement uncertainty can be referenced in Section 1.1.3.

manufacturing system integration. The proper adoption of the QIF will lead to the standardization of measurement systems, and therefore greatly promote measurement to integrate within manufacturing product lifecycle.

1.1.3 Measurement uncertainty and uncertainty analysis

Measurement uncertainty is the doubt that exists about the result of any measurement. Since no measurement is entirely accurate, a statement of measurement uncertainty is necessary to indicate the quality of measurement [19]. The fundamental concepts relating to measurement uncertainty have been provided in the International Vocabulary of Basic and General Terms in Metrology (VIM) [20] and the Guide to the Expression of Uncertainty in Measurement (GUM) [21].

Given the high diversity and complexity of measurement operations, task-specific measurement uncertainty has been introduced. Task specific uncertainty is the measurement uncertainty associated with the measurement of a specific feature using a specific measurement plan [13]. Task-specific measurement finely segments complex measurement processes into manageable operations. The introduction of task-specific measurement uncertainty allows the classification and standardization of measurement processes, and consequently, enhances measurement process automation and measurement system integration. In recent research, task-specific measurement uncertainty has emerged as a key concept in coordinate measurement [22].

Various researches on measurement uncertainty analysis have been carried out, e.g. conformance assessment [23], cost reduction [24] and risk management [25]. Enormous advances in computational science have made it feasible to deploy sophisticated quantitative analysis techniques to measurement uncertainty analysis. Measurement uncertainty analysis has gained increasing interests from academics and industry. Refining methods of measurement uncertainty analysis are expected to speed up the decision-making process in complex product manufacturing, and to improve product verification capability and capacity in global supply chain [6].

1.2 Overall aims

The overall aims of this research are to develop generic methodologies for measurement process modelling, and to integrate physical metrology systems within the digital environment, allowing smooth integration between digital and physical measurement environments.

The detailed aims and objectives will be discussed in Chapter 3.

1.3 Organization of the thesis

The thesis is organized in 8 chapters as follows:

In Chapter 1, the background related to this research is introduced and overall aims of the research are given.

In Chapter 2, a review of the related research is discussed. Three topics that are relevant to this research – coordinate measurement, computer-aided measurement planning and modelling and evaluation of task-specific measurement uncertainty using simulation, are reviewed.

In Chapter 3, the aims, objectives and the methodology of this research are given.

In Chapter 4, a pilot study on the digital measurement model is performed by carrying out physical measurement on a realistic component in shop floor environment. From the pilot study, the problems relating digital measurement verification are realized.

In Chapter 5, a Measurement Planning and Implementation Framework is proposed aiming to integrate digital and physical measurement uncertainty by statistically analysing task-specific measurement uncertainty.

In Chapter 6, the implementations of the Measurement Planning and Implementation Framework are presented, and the corresponding verification work are planned and carried out. The feasibility of the Framework is approved in a scientific manner.

Finally, Chapter 7 gives the conclusions and contributions to the knowledge of this research. The suggestions for future work are also outlines.

Chapter 2 Literature Review

2.1 Fundamentals of coordinate measurement

2.1.1 Fundamentals of measurement uncertainty

The highest-level guidelines for all forms of metrology activities are constructed in the International Vocabulary of Basic and General Terms in Metrology (VIM) [20] and the Evaluation of Measurement Data - Guide to the Expression of Uncertainty in Measurement (GUM) [21]. They provide the fundamentals of measurement and measurement uncertainty. They aim to solve popular metrology issues, such as traceability, accuracy, precision, uncertainty and error, etc. Since being drafted in 1997, the GUM and the VIM have been widely adopted by industrial applications and in academia.

1) The International Vocabulary of Basic and General Terms in Metrology (VIM)

The VIM [20] provides the "basic and general concepts and associated terms" in metrology. In the introduction, it is clarified that even the finest measuring process cannot confirm the measuring result as a single true value. The objective of a modern measuring process is to determine a set of information that contains an interval of the measuring results and the deviation from this interval, named as "measurement uncertainty". The vocabularies in metrology are rigorously defined or precisely described with detailed additional explanation. The VIM has defined critical considerations on practicing a measurement activity as below [20]:

- Measurement Result: set of quantity values being attributed to a measurand together with any other available relevant information;
- Uncertainty: non-negative parameter characterizing the dispersion of the quantity values being attributed to a measurand, based on the information used;
- Error: measured quantity value minus a reference quantity value;
- Accuracy: closeness of agreement between a measured quantity value and a true quantity value of a measurand;

- Precision: closeness of agreement between indications or measured quantity values obtained by replicate measurements on the same or similar objects under specified conditions;
- Metrological traceability: property of a measurement result whereby the result can be related to a reference through a documented unbroken chain of calibrations, each contributing to the measurement uncertainty.

In the annex part of the VIM, a series of concept diagrams have been given to further clarify the inter-relationships among the vocabularies and concepts.

2) The Evaluation of Measurement Data - Guide to the Expression of Uncertainty in Measurement (GUM)

The GUM [21] provides general mathematical rules for computing the measurement uncertainty. The GUM further developed the objective of measurement, that is "to establish a probability that this essentially unique value lies within an interval of measured quantity values, based on the information available from measurement" [20].

Besides the main text of the GUM [21], under the banner of "Evaluation of Measurement Data", there are seven titles of the documents to further support or explain the concepts in the GUM as listed in Table 1.

Table 1 Documents related to the GUM

Number	Title	Status
JCGM 100:2008	Evaluation of measurement data – Guide to the expression of uncertainty in measurement [21]	Approved
JCGM 104:2009	Evaluation of measurement data – An introduction to the "Guide to the expression of uncertainty in measurement" and related documents [26].	Approved
JCGM 101:2008	Evaluation of measurement data – Supplement 1 to the "Guide to the expression of uncertainty in measurement" – Propagation of distributions using a Monte Carlo method [27].	Approved
N/A	Evaluation of measurement data – The role of measurement uncertainty in conformity assessment.	Being prepared
N/A	Evaluation of measurement data – Concepts and basic principles.	Being prepared
N/A	Evaluation of measurement data – Supplement 2 to the "Guide to the expression of uncertainty in measurement" – Models with any number of output quantities.	Being prepared
N/A	Evaluation of measurement data – Supplement 3 to the "Guide to the expression of uncertainty in measurement" – Modelling.	Early stage of preparation
N/A	Evaluation of measurement data – Applications of the least-squares method.	Early stage of preparation

In JCGM100:2008, the main text of the GUM, it is re-enforced that the measurement result is only complete if it provides an estimate of the quantity concerned (the measurand interval) and a quantitative measure of the reliability of the estimate (known as the uncertainty). In order to relate the input quantities (or uncertainty sources) to generate a single measuring result, the GUM innovatively introduces a *GUM uncertainty framew*ork [27]. It is a mathematical model where the uncertainty and its components can be exactly computed by conceptualizing the standard uncertainty, the combined standard uncertainty and the expand uncertainty, and by utilizing the algorithms in the statistics and probability theorem, such as the probability density function (PDF) and coverage factor (as outlined in Figure 3).

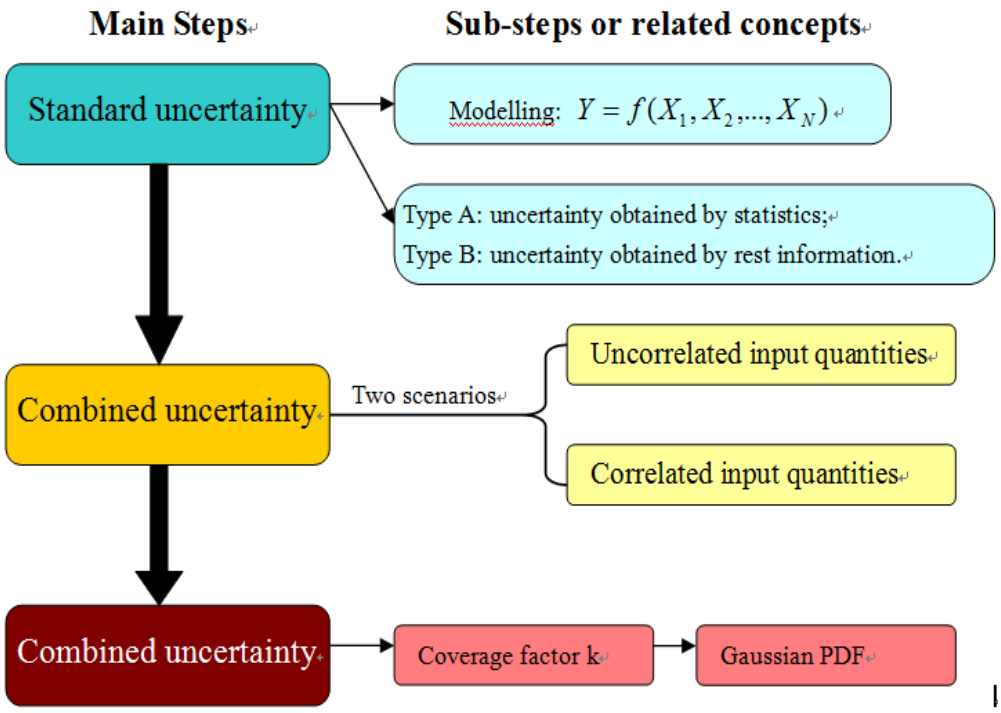

Figure 3 Outline of the uncertainty calculation in GUM

JCGM 104:2009, "An introduction to the GUM and related documents" [26], provides the general introduction the GUM to indicate the relationship between this fundamental Guide and its practical utilization in various measurement research fields. In particular, it points out the need to formalize the quality of a measured value through an appropriate measurement uncertainty statement.

JCGM 101:2006, "Supplement 1 to the GUM—Propagation of distributions using a Monte Carlo method" [27], is considered practically significant in cutting-edge metrology research (e.g. [28,29,30]). It describes a general numerical implementation of the propagation of distributions by using Monte Carlo method. The conditions for using the GUM need to be verified under different cases [31]. The Supplement 1 proves that, unlike the original GUM approach, the asymmetric distribution can treated by using the Monte Carlo Method and an estimate of the measuring interval and the associated standard uncertainty can be different from the approximate results (Figure 4). It provides an uncertainty calculation method based on the models as specified in the distributions themselves instead of the approximation to the model.

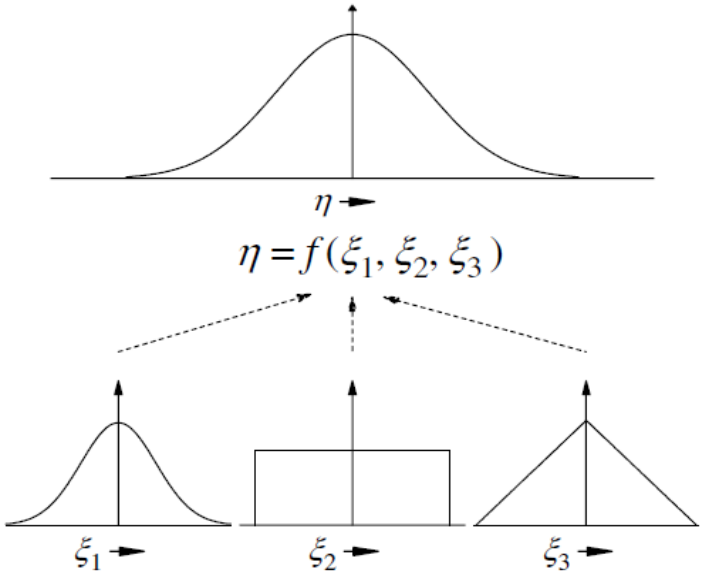

Figure 4 The basic concept of Monte Carlo Method: The knowledge given to possible values of each input quantity is expressed by a PDF and the knowledge of their interrelationship with the values of the output quantity (measurand) by the model function.

The rest of the GUM-related documents are not officially published yet. However, by intensive literature review and closely following the current research in metrology, concluding remarks can be conducted as below:

- They extend the GUM in various ways, aiming to maintain a balance between being updated with the current scientific advances and being stable as the essential reference documents [32];
- In "*Evaluation of measurement data – Concepts and basic principle"*, the Bayesian probability theorem is proposed to provide a self-consistent method permitting rigorous treatment of non-linear measurement models in measurement data evaluation [32];
- In *"Evaluation of measurement data – The role of measurement uncertainty in conformity assessment"*, the problem of calculating the conformance probability and the probabilities of the two types of error, given the distribution, the specification limits and the limits of the acceptance zone is addressed [33];
- In *"Evaluation of measurement data – Applications of the least-squares method*", the guidance on the application of the least-squares method is provided to data evaluation problems in metrology [34].

The topics in GUM supplements are abstracted from the latest research, of which topics reflect the key trends in the metrology researches. But the current researches on these topics are still unable to give a unified conclusion. There are challenges remaining in metrology research, hence requiring to be further explored.

2.1.2 GD&T standards - ASME Y14.5M

Geometric Dimensioning and Tolerancing (GD&T) is a global engineering language used in design, production and quality control. It is a system of symbols and conventions used to specify the allowable limit of departure from the intended geometry of a manufactured component. Primarily, it is aimed at ensuring interchangeability. [35]. Today GD&T and the CMM are inseparably linked. It is generally agreed that without the breaking-through invention of the CMM, efficient inspection in accordance with its principles would be very much more difficult, time-consuming and expensive.

The standard specifying GD&T on drawings is mainly ASME Y14.5M [36]. It classifies the dimensional variations (size) and the geometric variations (form, orientation, profile, position, run-out) in separate groups (Figure 5). This is because the types of variation that need to be controlled depend on functional and assembly requirements [37]. Datums can be spheres, cylinders, planes, lines or points, depending on the type of feature concerned.

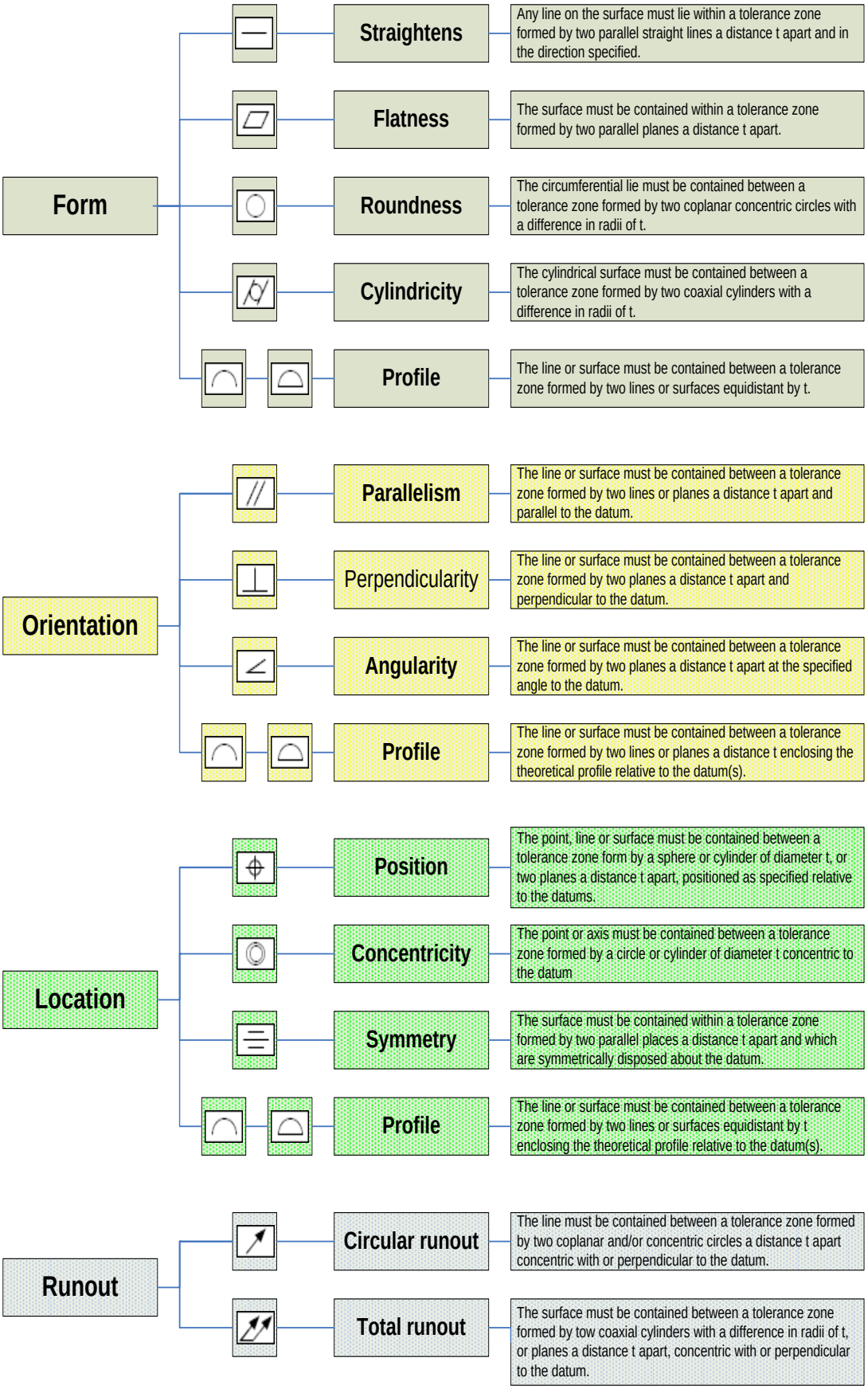

Figure 5 Tolerance classification in GD&T standards (concluded from ASME Y14.5 Standard [36])

As stated in ASME Y14.5M, the original purpose of GD&T is to describe the engineering intent of parts and assemblies [36]. Therefore, early research focussed on practicing GD&T in tolerance analysis in order to sustain the part assembly and functionality. As computer-added design (CAD) and computer-aided manufacturing (CAM) were overwhelmingly adopted, considerable research efforts have been made on extracting GD&T representations from CAD/CAM models and transforming the tolerance analysis in a statistical way to govern manufacturing processes precisely [38,39,40,41]. Shen et al. [42] proposed a semantic GD&T representation model, named the "constraint-tolerance-feature-graph" that is claimed to satisfy all tolerance analysis needs. Kong et al. [43] formulated an approach for the analysis of non-stationary tolerance variation during a multi-station assembly process with GD&T considerations.

Automated inspection is another area in which GD&T has been widely employed. By properly executing GD&T methods, automated inspection systems can reliably and effectively improve industrial manufacturing responsiveness, reduce the time-to-market life cycle, and increase product competition [44]. Hunter et al [44] established an approach to modelling and automating the part inspection process design through the integration of part GD&T in a knowledge-based system (KBS). Mohib et al [45] proposed a feature-based hybrid inspection planning, of which the first step is to interpret the CAD models to gather the relevant design information and GD&T specifications.

Since the development of non-contact scanning instruments, automated inspection systems for 3-D scanning measurements have been increasingly focused. GD&T analysis techniques are deployed in the 3-D scanning process. Prieto et al. [46,47] implemented an approach to inspect free-form surface dimensional and geometric tolerances using a set of 3D point clouds registered with a part CAD model and verifying the specified tolerances. Son et al. [48] studied an automated inspection planning system for free-form shape parts by laser scanning, which focused on scanning orientation and path determination by recognizing GD&T representations. Gao et al. [49] defined a Nominal Inspection Frame (NIF) for a nominal CAD model, in which every GD&T specification may be defined and specified, particularly for non-contact measurements.

To summarize, GD&T brings significant benefits to inspection activities. GD&T representation ensures that the component parts can be assembled into final with the intended functionality [36]. However, GD&T is sometimes mistakenly implemented due to the misunderstanding on design process [50]. Moreover, it is common to encounter the problems, e.g. lack of clarifying definitions in the feature locations, the orientation controls, and the variation specifications [51]. Zhang et al [52] points out that defining the GD&T requirements depends not only on capturing the functional requirements, but also on the cost and quality issues, and this becomes an even more challengeable element of the mechanical parts design. Maropoulos and Ceglarek [17] conclude that the GD&T is not adjusted for measurability analysis, and is not considered comprehensively for the planning of the measurement processes.

2.1.3 ISO GPS framework for CMM measurement

The original purpose of the ISO Geometrical Product Specification (GPS) framework is the integration of design and manufacturing. A product representative language is expected to be delivered in the ISO GPS framework to enable the communication between design engineers and manufacturing engineers.

The British Standard BS8888 provides an overview of the ISO GPS framework [53]. It explains the concept of ISO GPS framework as [53]:

- The GPS standards include several types of standards, dealing with the fundamental rules of specification, global principles and definitions and geometrical characteristics respectively;
- The GPS standards provide several kinds of geometrical characteristics, such as size, distance, angle, edge, form, orientation, location, roughness and waviness;
- The GPS standards define the workpiece characteristics as results of manufacturing processes and specific machine elements;
- The GPS standard can be applied at various steps of the product lifecycle, including design, manufacturing, metrology and quality assurance.

However, the standards under the ISO GPS framework have been developed by various ISO Technical Committees. There are still some standards missing or incomplete [54].

Given the nature of this research, ISO 14660, ISO 17450, ISO 10360 and ISO 15530 are reviewed. The bibliographic details of the standards are listed in Table 2. The contents of the standards are discussed individually in the following sub-sections.

Table 2 Mapping of ISO GPS Standards related to CMM measurement

Standard No.	Title	Sub-Part No.	Sub-Part title	Year
BS EN ISO 17450	General concepts	BS EN ISO 17450-1:2011	Model for geometrical specification and verification	2011
		DD ISO/TS 17450-2:2002	Basic tenets, specifications ,operators and uncertainties	2002
BS EN ISO 10360	Acceptance and reverification tests CMM.	BS EN ISO 10360-1:2001	Vocabulary	2001
		BS EN ISO 10360-2:2002	CMMs used for measuring size	2002
		BS EN ISO 10360-3:2001	CMMs with the axis of the rotary table as the fourth axis	2001
		BS EN ISO 10360-4:2001	CMMs used in scanning measuring mode	2001
		BS EN ISO 10360-5:2001	CMMs using single and multiple stylus contacting probing systems	2001
		BS EN ISO 10360-6:2001	Estimation of errors in computing Gaussian associated features	2001
DD CEN ISO/TS 15530	Technique for determining the uncertainty of measurement for CMM	DD CEN ISO/TS 15530-3:2007	Use of calibrated workpieces or standards	2007
		DD ISO/TS 15530-4:2008	Evaluating task-specific uncertainty using Simulation	2008

1) *ISO 17450 – General Concepts*

ISO 17450 [55,56] is designated to provide concepts for the ISO GPS framework. It aims to codify the geometric information of workpiece specifications in an unambiguous fashion to integrate design, manufacturing and inspection.

A model for geometrical specification and verification is provided in ISO 17450 – 1 [55]. The fundamental concept is that a range of deviations of workpiece geometrical specifications to be given to the workpiece's function should be considered at the product design stage. This design stage is named as 'geometrical specification', where

the geometrical information of the workpiece is specified and defined with tolerance values. The verification procedure must start from the defined tolerances.

ISO 17450 [55, 56] develops a set of the terms and definitions to enable how well a specification can express the workpiece function. To obtain ideal or non-ideal features, ISO 17450 – 1 [55] concludes a series of specific operations as listed in Table 3.

Table 3 Feature operations in ISO 17450 (concluded from [55]).

Operation	Description	Example
Partition	A particular subset of the real surface is identified for each surface to be verified.	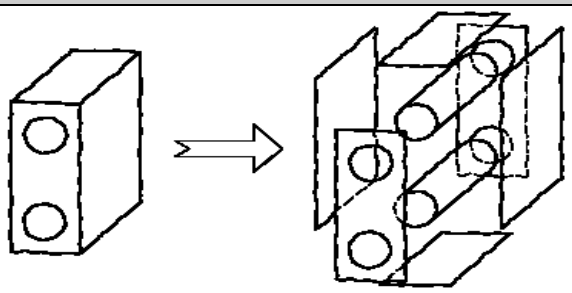
Extraction	A subset of the real feature is approximated using a physical extraction process generating to a finite set of point this feature operation	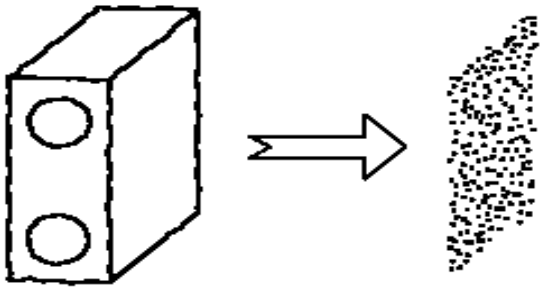
Filtration	The physical extraction process to reduce the information of the set of points to describe only the frequencies of merit for the verification of the particular surface-tolerance combination.	
Association	The filtered point set is used to estimate the closest fitting substitute geometry.	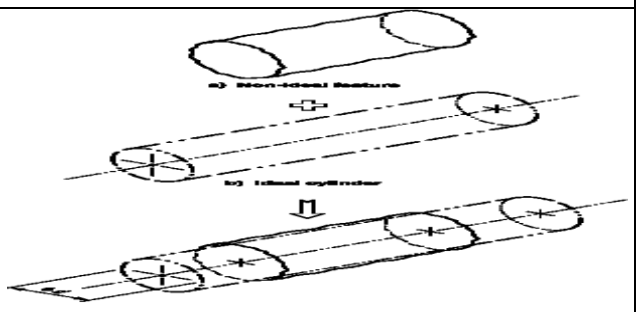
Collection	All the applicable surfaces are considered at the same time, when two or more surfaces are influenced by one tolerance.	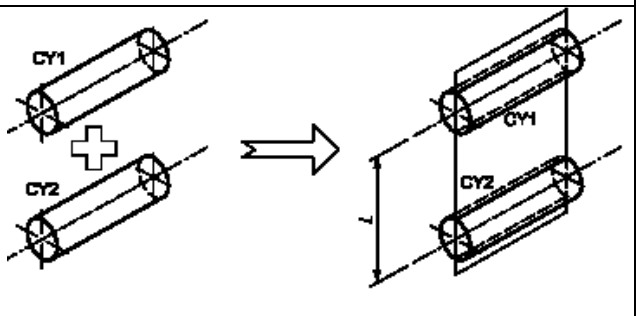

Construction	The ideal features are built from other features by respecting constraints.	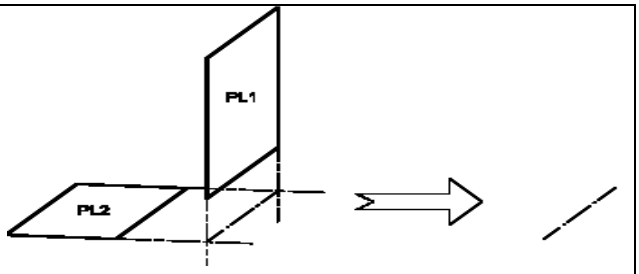
Reconstruction	A continuous feature (close or not) is created from an non-continuous feature (e.g. extracted feature)	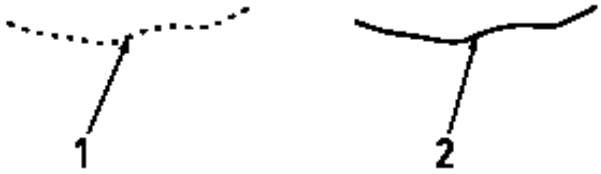

ISO 17450 has developed a novel operation-based system. It enables the designers to precisely express tolerances and requirements that have been determined based on part measurements and prototyping work [57]. If applying ISO 17450 properly, the extra effort in the product design stage to understand the functional requirements potentially saves considerable efforts in the manufacturing and support phases of the product lifecycle [58, 59]. However, ISO 17450 does not specify how to decide the closeness value between specification and verification, e.g., what data density and filter settings would be adequate for certain measurement tasks [60]. Moreover, the robustness of ISO 17450 methods are very likely to be challenged in modern manufacturing practices, where there are a large variety of workpiece features, machining techniques and measurement tasks.

2) ISO 10360 - Acceptance and Re-verification Tests for Coordinate Measuring Machines

ISO 10360, "Acceptance and Re-verification Tests for Coordinate Measuring Machines", describes the procedures to verify the CMMs. It properly downscales the procedures for judging CMM performance, and helps to make commercial decisions on specifying and purchasing CMMs.

In ISO 10360-2, "CMMs used for measuring size" [61], contains the basic background description and focus on size tests. It is stated that it is preferable to operate a CMM according to the manufacturers operating manual when carrying out

tests. Testing should also be done in conditions similar to those of the intended use. The errors in CMM measurement are divided into two sets:

- Volumetric Probing Error;
- Volumetric Length Measuring Error.

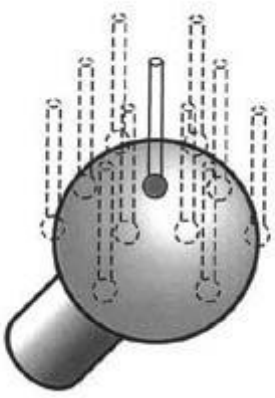

Figure 6 Determine Volumetric Probing Error

Volumetric Probe error is caused when the CMM probe approaches the work piece from different directions. As shown in Figure 6, to determine Volumetric Probe error, 25 point measurements are required to be made on the surface of a sphere, and then the measurement results are computed to get the deviation of points from the Gaussian associated sphere.

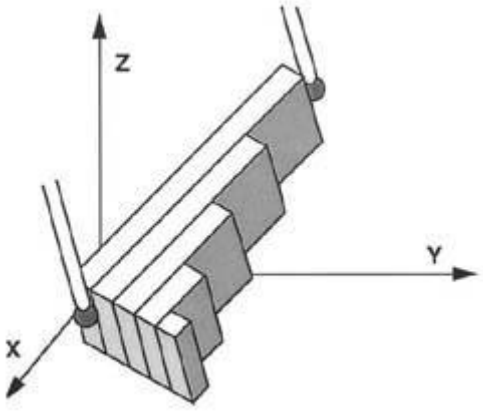

Figure 7 Determine Volumetric Length Measuring Error

Volumetric Length Measuring Error is the primary measure of the accuracy of a CMM. As shown in Figure 7, to determine Volumetric Length Measuring Error, five

different calibrated lengths are placed in seven different locations and/or positions and measured three times in each position for a total of 105 measurements.

ISO 10360-5, "CMMs Using Single and Multiple Stylus Contacting Probing Systems", covers the performance tests for contacting probing systems [62]. Volumetric Probing Error in ISO 10360-2 is taken out, and is integrated as 'single stylus probing system test' in ISO 10360 – 5. Noticeably, probing system performance is highly influenced by CMM performance. Probing system performance cannot be isolated and tested as "stand-alone specification". The tests procedures specified in ISO 10360-5 are sensitive to many errors produced by the complex "CMM" system. Therefore, in Annex B of ISO 10360-5, it is suggested to test probing system performance prior to testing CMM performance.

ISO 10360 is developed for 'standard' Cartesian CMMs. But as non-Cartesian CMM and optical systems gain more importance in applications, researchers have started to re-assess the effectiveness of testing procedures in ISO 10360. Reference objects such as step gauges can only be used for tactile photogrammetric systems which are working similar to CMMs [63]. ISO 10360 does not consider triangulation systems. Many optical systems are equipped by highly portable measuring sensors (e.g. camera stations) and perform variable measuring accuracy under different scales and system setups [64]. Extensive testing (as listed in ISO 10360) at the customer side brings up some problems or obscurities in the requirement specifications [65]. But as ISO 10360 has been updated recently, a few researchers claimed that ISO 10360 allows transferring test procedures to new measurement equipments based on an agreement between supplier and CMM user [66].

3) *ISO 15530 - Technique for Determining the Uncertainty of Measurement for CMM*

ISO 15530 deals with the general issues during CMM measurements tasks[*]. Major parts of ISO 15530 are incomplete. One of the most referenced parts is ISO 15530 – 4, Evaluating Task-Specific Measurement Uncertainty Using Simulation [67].

ISO 15530 – 4 aims to define the criteria for using computer simulation methods to determine task-specific measurement uncertainties. Computer simulation methods are expected to enable users to make quick judgements on the consistency of the measuring process or to carry quick conformance assessments on the work piece as required by ISO 14253 - 1.

ISO 15530 – 4 is the result of a long-term research focused on developing of Virtual CMM, a simulation techniques applied to CMM measurement [13]. It proposes three key concepts:

- Uncertainty Evaluation Software (UES);
- UES model and
- UES validation [67].

The UES is software used to provide uncertainty evaluation by simulating the overall CMM measuring process on a work piece. UES model is based on numerical procedures to handle input quantities (e.g. CMM types, environmental conditions) and to generate the measurement uncertainty. ISO 15530 – 4 provides two approaches for UES validation: physical experimental validation on calibrated artefacts and Computer-aided Verification and Evaluation (CVE).

At the time of writing the thesis, ISO 15530 - 4 is still in the first phase of the draft status, which means it does not have the full status of an international standard. But some researchers and software developers have already practiced ISO 15530 – 4 to guide their CMM measurement simulation activities. Summerhays et al.[14] developed a CMM measurement uncertainty prediction package, PUNDIT, given to ISO 15530 requirements. Baldwin et al [15] presented several application examples to demonstrate that simulation methods exhibit notable strength and versatility in predicting CMM measurement uncertainty. Phillips et al. [22] compared two commercially available UES, Virtual CMM and PUNDIT, and hence identified their

[*] This is the difference between ISO 15530 and ISO 10360. ISO 10360 is for judging CMM performance to serve the decision-making on CMM selection.

advantages and disadvantages. However, the credibility of UES results remains controversial. The study indicates the simulation results tend to be generally lower than physical measurements [22]. Further refinements in UES and ISO 15530 – 4 are necessary. Since ISO 15530 – 4 is designated for task-specific measurement uncertainty, which "is the measurement uncertainty associated with the measurement of a specific feature using a specific measurement plan [67]", a universal UES, which can comprehensively cover CMM measurement tasks, remains to be challenge to UES developers and CMM measurement simulation researchers.

2.1.4 Summary

The fundamentals of measurement uncertainty have been introduced in the VIM and the GUM, which aim to provide trustworthy guidance on metrology. The topics discussed in the GUM supplements represent the latest focal points in measurement uncertainty, e.g. conformity assessment, Monte-Carlo simulation method and post-measurement data analysis. They have provided a platform to guide research on using simulation techniques to predict measurement uncertainty, but these topics are still under development. Therefore, simulation techniques based on the VIM/GUM-approach need to be further explored and developed.

GD&T representation, ASME Y14.5M, ensures that component parts can be assembled into final products and function as per the design intent. But it is challenging to implement GD&T in a dual-communication manner, where both the designer's and manufacturer's requirements are unambiguously represented. Crucially to measurement and assembly, the GD&T is not adjusted for the measurability analysis, and is not considered comprehensively for the measurement processes. Therefore, simulation software based on GD&T concepts may not be able to interpret the design intent and the manufacturing processes correctly or comprehensively.

The ISO GPS framework aims to provide a product representative language to enable the tacit understanding between design and manufacturing. ISO 17450 [55, 56] presents an approach to decoding the geometric information of workpiece specifications in a fairly straightforward way, which has released the potential of using simulation software to predict the manufacturing, inspection and measurement

results. ISO 15530 [67] has specifically explored how to evaluate task-specific measurement uncertainty by using simulation software. The developments of the ISO GPS framework have shed light on deploying simulation techniques for evaluating CMM measurement uncertainty. However, as there may be a lack of consistency between ISO GPS standards, the simulation algorithm developed under ISO GPS standards should be used with considerable attention. Similarly, any simulation results need to be verified and validated.

Conclusively speaking, the fundamentals for measurement uncertainty have been developed and evolved. As theoretical attempts to defining measurement processes and measurement uncertainty emerged, predicting measurement uncertainty in a digital environment has become possible and popular. However, some inconsistencies between the measurement standards inhibit the development of uncertainty evaluation software (UES). The validation and verification of UES performance has become a necessary and vital task for the UES developer and user.

2.2 CMM Measurement Planning and Modelling

CMM measurement planning is an essential part of the design and manufacturing integration process [17]. It determines which features of a part to measure, what resources are needed, and how to arrange the measurement procedures. It aims to suggest the measurement strategy which achieves the desired measuring requirements as well as consuming minimum measurement cost and time. Parts acceptance or rejection is decided in the course of executing the measurement planning [68]. Therefore, CMM measurement planning has a significant effect on the product quality and production time influencing cost and production profits.

Modern manufacturing is increasingly challenged by tight tolerances for producing high quality and highly complex products. This leads to two major topics in CMM measurement planning and modelling – automated measurement planning and online measurement planning. Automated measurement planning provides accurate CMM measurement models by using computer-aided support tools, assisting to make decisions faster and better [68]. On-line measurement planning uses CMMs during the machining process to achieve real-time production quality control rather than

acceptance or rejection of parts at the end. Many researchers in measurement planning cover both of two topics, such as using computer-aided measurement planning for online measurement. Given to the nature of the research, we focus on the review of automated measurement planning [68].

Modern measurement process planning becomes a vital link to integrate design and manufacturing [68]. Generally, recent research in this area is developed to accomplish following the tasks:

- Recognizing CAD models and features;
- Optimizing inspection sequence;
- Determining detailed measuring strategy (e.g. probe selection, number and locations of measuring points, scanning speed);
- Generating measuring paths;
- Simulation and verification [69].

In terms of CMM measurement planning and modelling, the measuring stages are generally defines as:

- Inspection feature selection;
- Inspection sequencing optimization;
- Probing strategy determination;
- Collision-free probe path generation;
- CMM control command generation:
- Post-measurement data processing, e.g. statistical cost analysis [70].

The recent measuring planning systems either covered all of the six stages, or focused on accomplishing part of the stages.

2.2.1 Inspection feature selection

Feature selection and grouping is linked with feature recognition techniques in reverse engineering where the CAD-models of parts are not available. Since the CAD-models are usually available in CMM measurement planning, feature recognition is narrowed to feature selection and grouping. Inspection features are the dimensions and tolerances that have significant impact upon the parts' functionalities [71]. The purpose of feature selection and grouping is to determine which features are necessarily to be measured, and to group them in preparation in the following steps of

measurement planning, e.g. inspection sequencing. On a traditional shop floor, the selection and recognition of inspection features rely on the experiences of skilled inspection engineers [68]. Early research either required manual input to specify the inspection features, or automatically selected the inspection features only after carefully monitoring the machining process. In contrast, recent research developed feature selection techniques to the degree of full-automation. Inspection features can be directly recognised/extracted from the CAD model. Most of the advances in feature selection and grouping research happened not only in CMM measurement planning, but also in on-line inspection planning using CMM or other measuring instruments. Although the review was focused on CMM-based measuring planning, the research reviewed CMM measurement planning to a more advanced level.

For CMM-based inspection planning, Zhang et. al [72] proposed a feature-based inspection process planning system for CMM. To directly extract inspection features from CAD models, the system sequentially undergoes five functional modules, including tolerance feature analysis, accessibility analysis, clustering analysis, path generation and inspection process simulation. Liamiem and ElMaraghy [73] proposed a Computer-Aided Tactile Inspection Planning (CATIP) approach. Inspection features are selected based from CAD model together with tolerance requirements, and becomes the inputs of the system to optimize the inspection sequence. Hwang et al [74] proposed a CMM inspection planning system, selecting inspection features based on the tolerance specifications given by engineers.

Feature selection and grouping techniques for online measurement has made significant advances. Wong et al. [75] proposed a feature recognition approach for non-CMM inspection. This research classified the inspection features into seven categories : (1) distance between two parallel faces which can be a length (e.g. width, gap, slot, fin, height, protrusion, depth, recess or thickness, (2) diameter of a complete cylinder/hole, (3) diameter or radius of a partial cylinder/hole or a cylindrical face, (4) distance between a cylinder/hole and a parallel face, (5) distance between a pair of cylinders/holes, (6) Coordinate measurement (or profile) measurement of a curved surface (free-form or otherwise) with respect to a bounded reference plane, (7) combination of the above. Based on the feature classification, a wide range of

measuring instruments could be selected. Lee et at. [76] proposed a two-stage inspection process for the parts having many primitive features. The two stages are:
(1) Global inspection planning;
(2) Local inspection planning.
In Stage 1, the inspection features are selected by analysing features' relations and then grouped according to the extracted characteristics. In Stage 2, the features are decomposed into their constituent geometric elements (e.g. plane, circle) for the detailed measurement planning. Chung [77] developed an on-machining measurement planning for free-form surfaces. The free-form features trimmed by NURBS are translated by an IGES translator. The measurement codes are generated by means of coordinate transformation and the uniform sampling software is linked with the IGES. Cho and Seo [78] integrated the inspection process with the machining process by analysing the machined surface errors. The geometrical form of the machined surface is simulated in the system. Then the machining errors can be predicted by comparing the simulated machined surface with the designed surface.

To conclude, latest research in feature selection and grouping has developed to the automatic level by utilizing advanced digital engineering techniques. For CMM-based measurement planning, inspection features are recognized and classified mainly on the tolerance requirements. On-line inspection planning embraced diverse techniques (e.g. feature grouping) and has made more advances. When a part is measured on the same machining centre, the form of machining feature becomes more critical than the tolerance value. Therefore online measuring planning used different techniques to process the feature information and group them in another way.

2.2.2 Inspection sequence optimization

Optimizing the inspection sequences is closely linked with feature selection and grouping in measurement process planning. Some recent research treated inspection sequence optimization as part of feature selection and grouping, since features are grouped under the consideration of optimizing the inspection sequence. The sequencing of inspection features for CMM is mostly based on probe accessibility and on minimizing probe orientations.

The CATIP system [73] (reviewed in previous section) optimized the inspection sequence based on the probing accessibility and minimizing probe orientation. Zhang et al. [72] proposed a similar system structure, and executed the system with more detailed considerations. The feature-based CMM inspection planning system contains five function modules shown in Figure 8. The accessibility analysis module evaluates all the possible probe orientations for a surface feature and represents these probe orientations with an accessibility cone. The clustering analysis module arranges both the inspection probes into probe cells and the surface features into feature families so that the time for probe exchange can be minimised. Vafaeesefat and ElMaraghy [79] proposed a system to automatically define the probe accessibility. The system used the Stereo Lithography (STL) or Virtual Reality Model Language (VRML) to convert tolerance information into Probe Orientation Module (POM). Lu et al. [80] employed artificial neural network techniques to obtain the optimum inspection sequence. Hwang et al. [74] adopted Chvatal's greedy heuristic to minimize the number of part setups and probe orientations. And Hopfield neutral network was used to automatically generate optimal measuring sequence constrained by the feature natures, heuristic rules.

Figure 8 Flowchart of the proposed feature-based inspection process planning system [72]

From the above review, it can be concluded that probe accessibility and probing orientation are major considerations for CMM-based measuring sequencing. Inspection time and efficiency is also taken into account by some systems. Noticeably, most of sequencing systems employed knowledge-based techniques, such as clustering analysis, fuzzy logic or neutral networks [74]. These techniques have become suitable solutions for difficult and complex CMM measuring planning tasks.

2.2.3 Detailed probing strategy

Detailed sampling strategy mainly refers to topics relating to the CMM probe, e.g. determining the measuring point density and distribution. The most common type of CMM probe performs point-to-point contacting movements. Researchers focused on minimizing the number of measuring points and measuring time as well as maintaining measurement quality. The scanning probe collects sampling points by continuous movement along the part surface, and hence shortens the inspection time. As scanning probe technology matured, metrology researchers began to consider including scanning probes in measurement planning and process.

Most research on point-to-point CMM measurement planning employed a feature-based approach to determine proper measuring points. The density and distribution of measuring points are decided for each measuring feature by considering its tolerance value, geometric characteristics, and desired confidence level. Huang et al. [81] proposed a knowledge-based inspection planning system for CMMs. Part geometry, tolerance information and metrology expert knowledge were considered together to determine the numbers and positions of measuring points. They also applied their system to non-contact measuring systems. Cho et al [82] proposed a fuzzy system for determining the optimum number of measuring points for the online measurement system (Figure 9). The surface area, degree of tolerance and machine accuracy were used as inputs into a ‘fuzzy system’. The Hammersley’s algorithm is used to relocate the contacting measuring points on the target surfaces. Meanwhile, the non-contact measuring points are generated by relocating the measuring points.

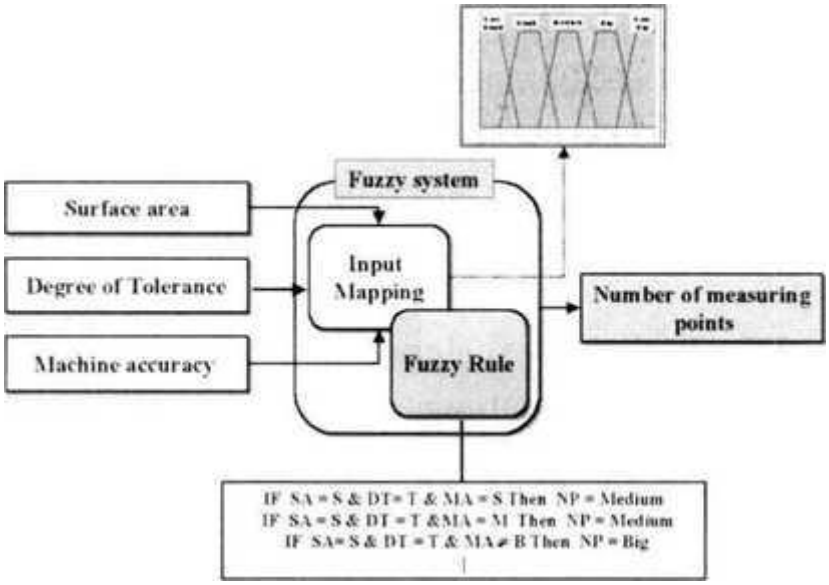

Figure 9. Fuzzy system structure to determine the number of measuring points [82].

The effect of selecting a particular sampling strategy has been recognized as a major component of measurement uncertainty [83]. This effect is caused by the systematic and random errors built-in the measurement systems [83]. Therefore, the CMM measurement errors were usually categorised into two sets, systematic error and random error, and the sampling strategy is optimized to reduce the two sets of errors using statistical methods. Dowling et al. [84] addressed statistical issues in feature-based measurement planning using CMM. The orthogonal least squares and minimum-zone methods were used to evaluate the measuring deviation for a specific feature. Jiang and Chiu [85] developed a statistical method for the determination of the number of measurement points for 2D rotational part features. But Elkott et al. [86] argued that research working on free-form feature measurement usually required large sample sizes to inspect free-form features, and did not adequately explore how to optimize the location of the measuring points. On the other hand, Zhao et al. [68] claimed that these shortcomings can be solved by a hybrid measurement system, which can automatically select a sampling algorithm that best fits the inspection surface.

Abundant attempts have also been made to find a suitable sampling strategy for form error evaluation. Form errors are the feature form deviations of a part resulting by the combined effect of all the error sources in a real manufacturing environment. Giovanni et al. [87] described form errors as ‘manufacturing signatures’, and tackled

the problem of determining sampling strategy starting from the characteristics of a surface which is attributable to the manufacturing methods. Cui et al. [88] concluded the mathematical representatives of form errors for various tolerance characteristics (Table 4). There are four form error evaluation methods frequently used, which are, least squares circle (LSC), minimum zone circle (MZC), maximum inscribed circle (MIC), and minimum circumscribing circle (MCC). Chan et al. [92] studied the influence of a number of points with equidistant sampling on the least square parameters of a circle. Liu et al. [89] have studied the effect of CMM measurement error on form tolerance using least squares and minimum zone methods. It is reported that the Taylor sensitivity coefficients were obtained by regression, but the procedure is not clearly described. Odayappan et al. [90] have studied the effect of sampling strategies for circles. They have given recommendations for the minimum number of points that have to be sampled for establishing the MZC, LSC, MCC and MIC. Cui et al. [88] assessed the measurement results by using different form error evaluation methods against CMM sampling. Some of the form error evaluation methods were proposed particularly for circular features [91,92]. But now research was also extended to free-form features [93,94].

Table 4 Mathematical representatives of form errors for tolerance characteristics [88]

Items	Data sets	Datum feature functions	Illustrations	Form errors
Flatness	$\{P_i\}=\{x_i,y_i,z_i\}$ $i=1,2,\cdots,n$	$z=ax+by+c$	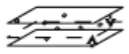	$\delta=\min\left(\max_{1\le i\le n}\{d_i\}-\min_{1\le i\le n}\{d_i\}\right)$ where, $d_i=\frac{z_i-ax_i-by_i-c}{\sqrt{a^2+b^2+1}}$
Planar straightness	$\{P_i\}=\{x_i,y_i\}$ $z_i=const$ $i=1,2,\cdots,n$	$y=ax+b$	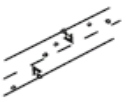	$\delta=\min\left(\max_{1\le i\le n}\{d_i\}-\min_{1\le i\le n}\{d_i\}\right)$ where, $d_i=\frac{y_i-ax_i-b}{\sqrt{a^2+1}}$
Spatial straightness	$\{P_i\}=\{x_i,y_i,z_i\}$ $i=1,2,\cdots,n$	$\frac{x-a}{l}=\frac{y-b}{m}=\frac{z}{1}$		$\delta=\min 2\max_{1\le i\le n}\{d_i\}$ where, $d_i=\frac{\left\|\begin{matrix} i & j & k \\ x_i-a & y_i-b & z_i \\ l & m & 1 \end{matrix}\right\|}{\sqrt{l^2+m^2+1}}$
Circularity	$\{P_i\}=\{x_i,y_i\}$ $z_i=const$ $i=1,2,\cdots,n$	$(x-a)^2+(y-b)^2=r^2$		$\delta=\min\left(\max_{1\le i\le n}\{d_i\}-\min_{1\le i\le n}\{d_i\}\right)$ where, $d_i=\sqrt{(x_i-a)^2+(y_i-b)^2}$
sphericity	$\{P_i\}=\{x_i,y_i,z_i\}$ $i=1,2,\cdots,n$	$(x-a)^2+(y-b)^2+(z-b)^2=r^2$		$\delta=\min\left(\max_{1\le i\le n}\{d_i\}-\min_{1\le i\le n}\{d_i\}\right)$ where, $d_i=\sqrt{(x_i-a)^2+(y_i-b)^2+(z_i-b)^2}$
Cylindricity	$\{P_i\}=\{x_i,y_i,z_i\}$ $i=1,2,\cdots,n$	$\frac{x-a}{l}=\frac{y-b}{m}=\frac{z}{1}$		$\delta=\min\left(\max_{1\le i\le n}\{d_i\}-\min_{1\le i\le n}\{d_i\}\right)$ where, $d_i=\frac{\left\|\begin{matrix} i & j & k \\ x_i-a & y_i-b & z_i \\ l & m & 1 \end{matrix}\right\|}{\sqrt{l^2+m^2+1}}$

Besides point-to-point measurement, the CMM scanning probe is attracting attention from academia as its technology matures. Complete characterization of scanning probe performances under various working conditions is in demand but still remains unexplored. Moreover, the emergence of a scanning probe adds extra options for CMM probe selection. Selecting the right type of CMM probe poses another challenge for CMM measurement planning.

2.2.4 Probing path generation

The research in probing path generation focused on automatically generating collision-free probing path when carrying out CMM measurement tasks.
Lu et al. [95] proposed an algorithm which uses a modified 3D octree ray tracing technique to search for the colliding obstacles in an octree database on a selected path. It also uses the global information about the obstacle vertices to reduce the zigzag nature of the path generated by the octree based methods. Albuquerque et al. [96] developed a collision-avoidance CMM inspection planning approach by defining the relationships between features and configuring the tolerance types. This research

considered mainly circular and prismatic features. Ainsworth et al. [97] developed a probe path generation system for free-form features. NURBS definition method was adopted to mathematically represent the shape of a free-form surface. The probing path was then generated through three stages: initial path generation, modification and verification. They defined the probing movement as either uni-directional or bi-directional. The implemented path planning software initially generates a measurement path for each selected entity, based on the CAD model. The system also allows users to modify the probing path parameters interactively. The final probing path is processed into machine executable programming code. They used a turbine blade which has an aerofoil shape to demonstrate their path generation system. Lin and Murugappan [98] proposed an approach for automatically generating a CMM probing path. It is assumed that the CMM probe is a point object. This assumption simplifies the detection of collision into a single point and the part and fixtures are not considered in this research.

To conclude the above review section, CMM probing path planning focuses on automatically generating an optimum collision-free path. Graphic representation methods are usually employed to recognise the feature shape, and hence to generate the probing points and trigger the probing movements. Usually there is a verification module, where the probing movements could be simulated in the digital environment; therefore the automatically generated probing path could be verified.

2.2.5 Post-measurement data processing

After the CMM completes its physical measurements, the measurement results collected from the parts are processed. This procedure is usually regarded as 'post-measurement data processing'. It addresses data analysis techniques which can improve the quality of the CMM measurement results. There are several broad types of post-measurement processing objectives, such as to enhance the accuracy, to filter the measurement 'noise' and to reduce the volume of measurement data collection. Generally, the techniques for post-measurement processing are deployed in two domains, design and production as shown in Figure 10. In the design domain, post-measurement data are processed to serve reverse engineering. In the production domain, post-measurement data are processed for quality control or cost analysis.

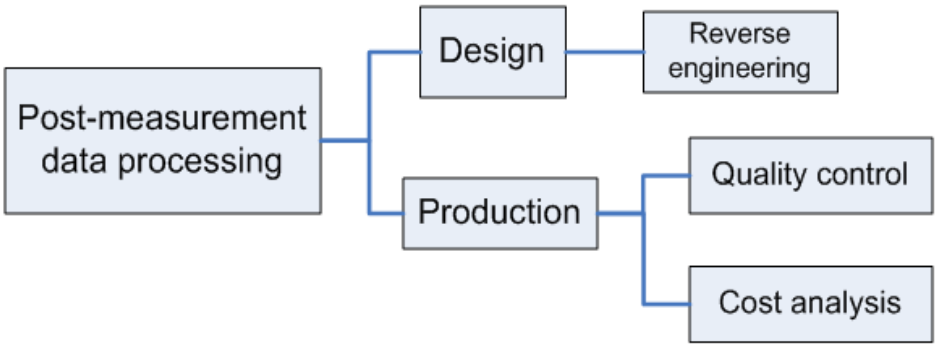

Figure 10 Areas where post-measurement data processing are served

The techniques for post-measurement data processing have been widely adopted in reverse engineering. The measurement results collected from the physical part are statistically analysed to approximately realize the designer's intents of a part, and hence to reversely create its CAD model in the digital world. Modern reverse engineering research efforts focus on restructuring complex features [99,100], deploying advanced measurement tools [101] and responding numerical control machining [102]. These allow the creation of a CAD model to be reused, modified and optimized [103].

The quality of manufactured products usually needs to be verified. Therefore, the measurement data sets are carefully processed in production for quality control purposes. Rajamohan et al. [104] assessed the effect of CMM probe size and measurement strategies on free-form features in terms of form deviation. Tosello et al. [105] analysed two CMM measurement systems to verify the manufacturing capabilities within the sub-mm level tolerance requirement for micro-product production. Fleischer et al. [106] employed advanced quality control charts, using exponentially weighted moving average (EWMA), to weight each measurement result against its error and statistically monitored the manufacturing quality.

CMM measurement data are also processed for the purpose of cost analysis. Kunzmann et al. [107] demonstrated that the manufacturing process capability index (C_p and C_{pk}) drifts due to the measurement uncertainty introduced from the inspection process. They argued that investing in proper measurement instruments can generate extra value to the entire manufacturing system. Forbes [23] deployed a Bayesian

decision-making approach to examine the measurement uncertainty impacts from the economical perspective, and optimized the decision-making on rejecting or accepting a part. The mathematical approach originated from the aero-engine shaft inspection, where the shaft tolerances on radius and form error were inspected using a CMM. Pendrill [108] developed a measurement uncertainty optimization model to balance the testing costs and the cost associated with the consumer's risk. Baldwin et al. [25] proposed a CMM cost analysis approach by incorporating Taguchi Loss Function. Despite of the above endeavours, research regarding the measurement cost and benefit analysing is insufficient. It would be helpful if the measurement benefits could be quantified, and could be demonstrated through focused research projects.

To conclude, post-measurement data processing is extensively adopted in reverse engineering and quality control. The data collected by CMM measurements is usually statistically processed in order to re-construct the parts' CAD model or finely control the production process. Recent research started to explore economical benefits by statistically analysing the post-measurement data. But few of the approaches have been progressed to focused research outcomes.

2.2.6 Summary

CMM measurement planning and modelling has been researched for decades. Recent CMM measurement planning has achieved significant improvements with the development of computer-aided design (CAD) and manufacturing (CAM) technologies. As shown in Figure 11, the research is assigned to solve the problems in: (1) inspection feature selection, (2) inspection sequencing optimization, (3) probing strategy determination, (4) probing path generation (5) CMM servo control, and (6) post-measurement data processing.

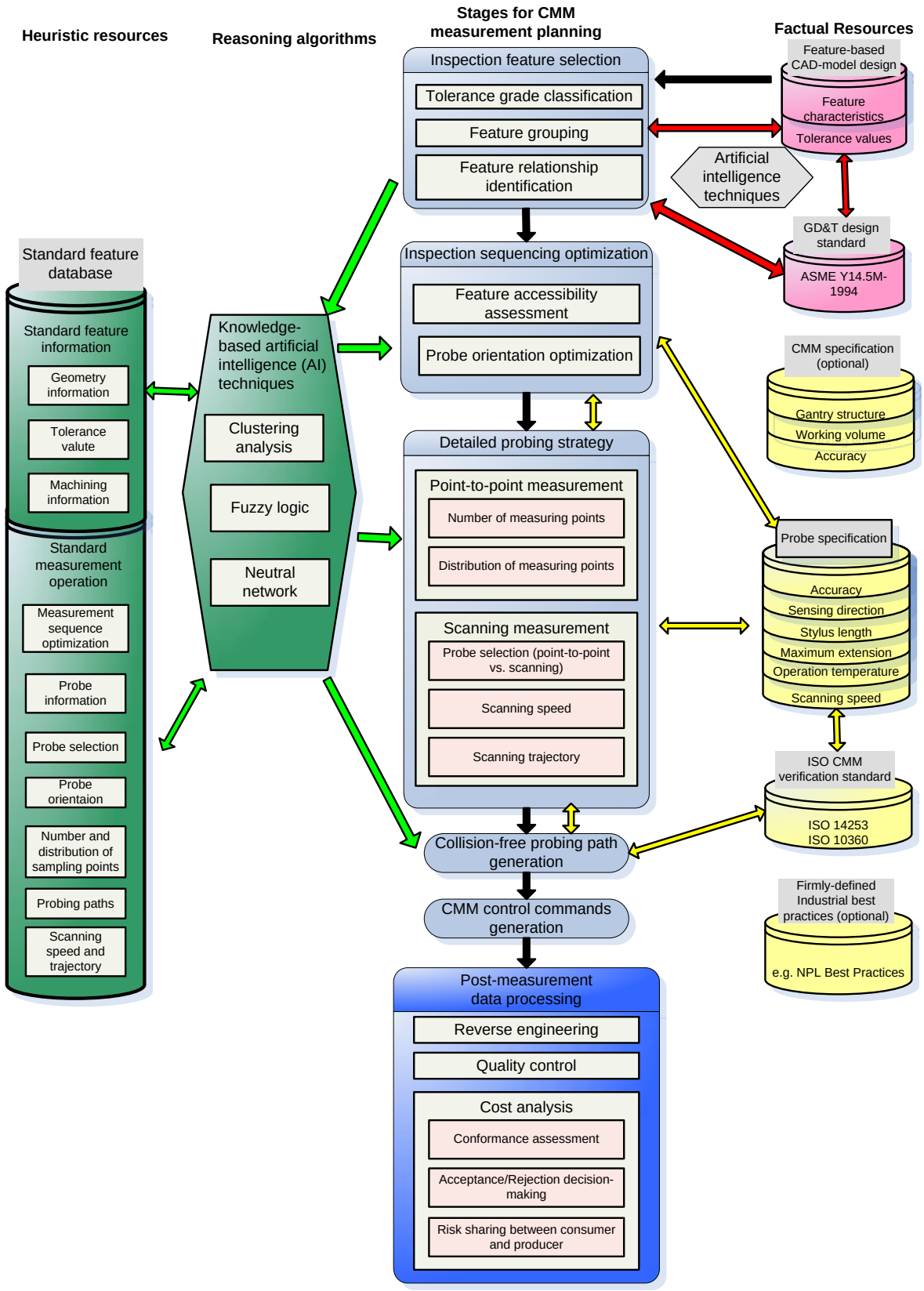

Figure 11 Conclusion of CMM measurement planning and modelling

Feature-based measurement planning has become the focus of recent research. Standard Feature Database*, which documents standardized measurement operations for each specific feature, have been proposed by various researchers. Due to the high complexity of CMM measurement planning, knowledge-based artificial intelligent techniques (e.g. clustering analysis, fuzzy logic) are frequently used to generate proper measurement strategies from a Standard Feature Database. Although Standard Feature Database poses certain challenges in real production practices, the concept itself remains an optimistic solution which is able to deliver real efficiency improvements for future CMM measurement planning.

Post-measurement data processing† has been developed. Measurement data sets are statistically processed to serve the requirements from reverse engineering, quality control and cost analysis. This introduces new research topics, e.g. conformance assessment, decision-making under uncertainty and risk sharing. Further explorations are still required in the post-measurement data processing area.

* As shown on the left-hand side of Figure 11.
† As highlighted in dark-blue in Figure 11.

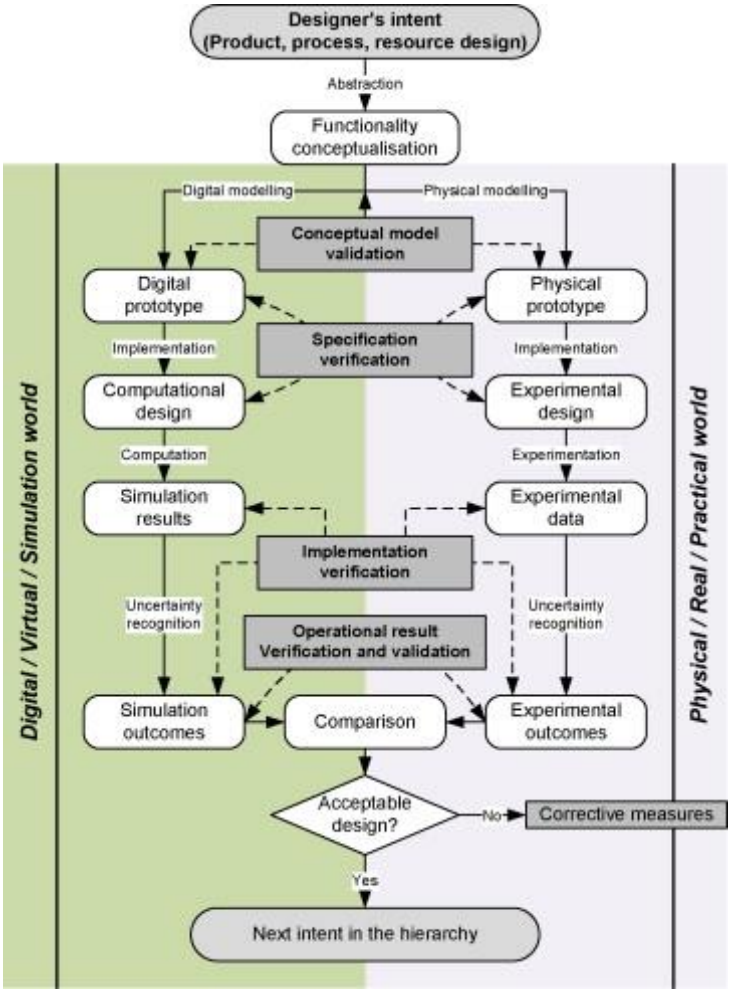

Figure 12. Measurement in digital and physical world [1]

To conclude, as CMM technologies and techniques are getting highly advanced, CMM measurement planning evolves as a necessary link to integrate design and manufacturing. As shown in Figure 12, measurement becomes integral to manufacturing processes, linking digital and physical worlds and interacting within the phases of design and manufacturing integration process. But its development in terms of measurement modelling and planning is embryonic when compared to processes and additional research is needed in CMM measurement modelling and planning.

2.3 Evaluation of task-specific measurement uncertainty using simulation

2.3.1 Requirements of uncertainty evaluating software (UES) as specified in ISO standard

The requirements for developing uncertainty evaluating software (UES) have been informatively specified in ISO 15530-4 [67], “Evaluating Task-Specific Measurement Uncertainty Using Simulation”.

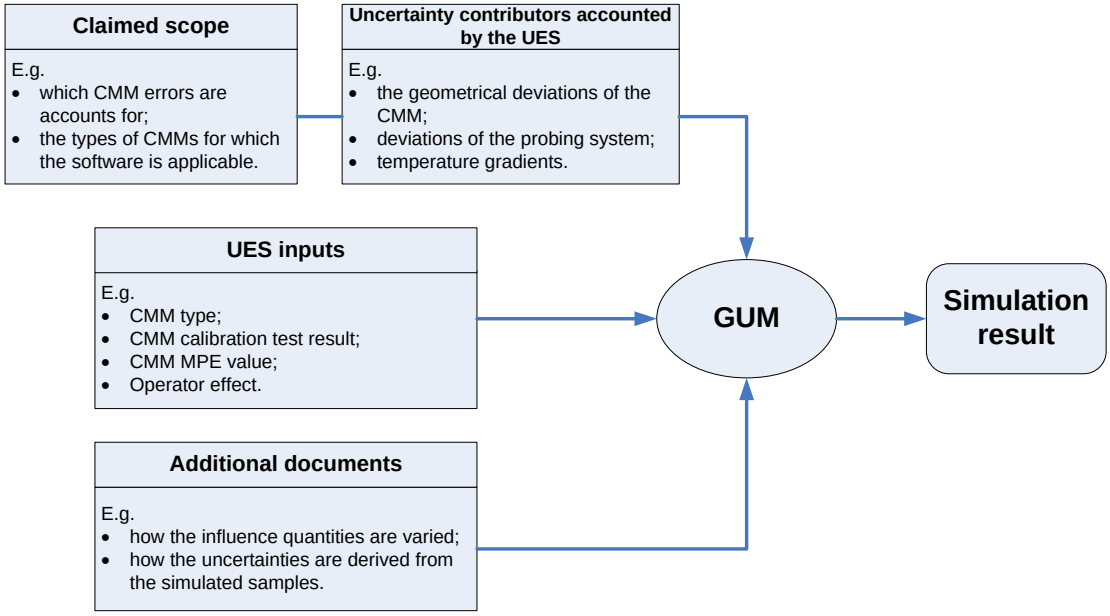

Figure 13. The UES requirements specified in ISO 15530-4 (concluded from [67]).

As shown in Figure 13, ISO 15530 – 4 claims that UES developers need to provide ‘a claimed scope’ of the UES (including specifying uncertainty contributors taken into account), the input quantities of the UES and additional documents involved to support the UES development. Meanwhile, ISO 15530 – 4 points that all of the statements provided by the UES developers need comply with GUM principles, and the UES results need to be consistent with the ‘claimed scope’ initially provided by the UES developer.

ISO 15530 – 4 provides a detailed checklist of the measurement uncertainty contributors for CMM measurement. The UES developers are suggested to reference

the checklist to identify the key influence factors in defining the ‘claimed scope’ of UES.

ISO 15530 – 4 points out that there can be two types of UES:

- Online UES – where the simulation is integrated into a specific CMM machine;
- Offline UES – where the simulation is implemented as an independent system on an external computer.

ISO 15530 – 4 describes the flowchart of the UES algorithm, which starts from a specific measurement task, and then mathematically calculates the measurement uncertainty taking into account the uncertainty contributors to the CMM measuring process. The mathematical method to determine the task-specific measurement uncertainty is also stated in the standard.

ISO 15530 – 4 has proposed the concept of Uncertainty Simulation Software (UES), and informatively specifies the requirements for the UES development. The special concerns in ISO 15530 -4 underline a key trend in computer-aided inspection - using the simulation method to determine task-specific measurement uncertainty. However, the comprehensiveness of the simulation method, e.g. considering all of the measurement uncertainties during the simulation process, is virtually impossible to achieve. The verification and validation of UES result is doubted by the final users of the UES.

2.3.2 The simulation methods for evaluating task-specific measurement uncertainty

The review paper [13] concerning task-specific measurement uncertainty has identified error components that may lead to the measurement uncertainties (Figure 14), and concluded six methods for evaluating task-specific measurement uncertainty, which are ‘sensitivity analysis’, ‘expert judgement’, ‘experimental method using calibrated objects’, ‘computer simulation’, ‘statistical estimations from measurement history’, and ‘ hybrid methods’. Various research efforts [12,109,110] have indicated that the main flexible method for determining the uncertainty is the computer simulation method.

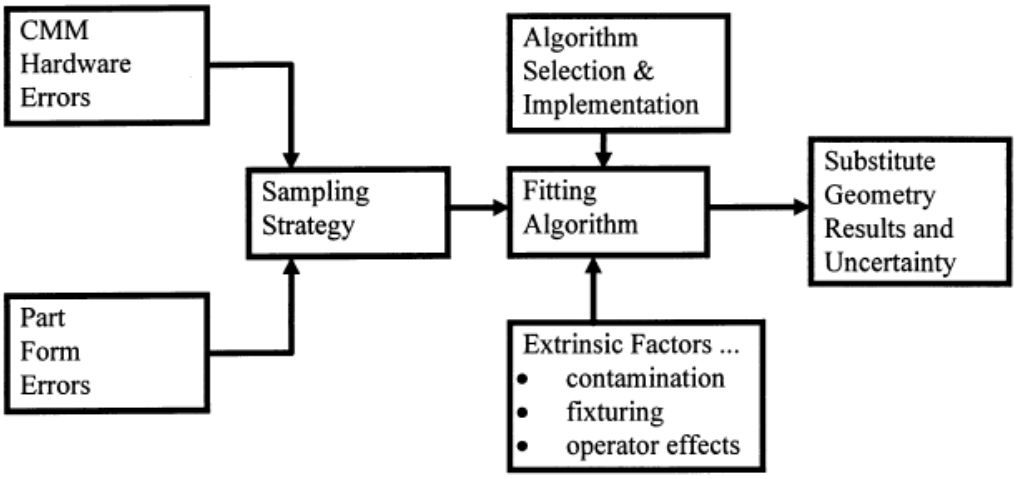

Figure 14. Error components that lead to uncertainties

The computer simulation method offers the potential to configure highly complicated CMM error models to the specific measurement task under consideration [15]. Various computer simulation packages have been developed, such as "Virtual CMM" [111], "PUNDIT/CMM" [112], and "Expert CMM" [113]. Most of the methods work on the basis of propagating uncertainty from the different sources to the measurement results, but may operate in a slightly different approach.

*A) **The virtual CMM (VCMM)***

The virtual coordinate measuring machine (VCMM) estimates task specific measurement uncertainty for a specific CMM machine. The process starts by assigning virtual probing points to an ideal geometry that represents the design specification. At each probing point on a particular feature, the VCMM generates a perturbed point [114]. The perturbed point is generated by modelling variations coming from the different contributors to the measurement task. Each contributor is simulated using a probability density function (PDF) and each perturbed point is simulated by combining the information from all input contributors (PDFs).

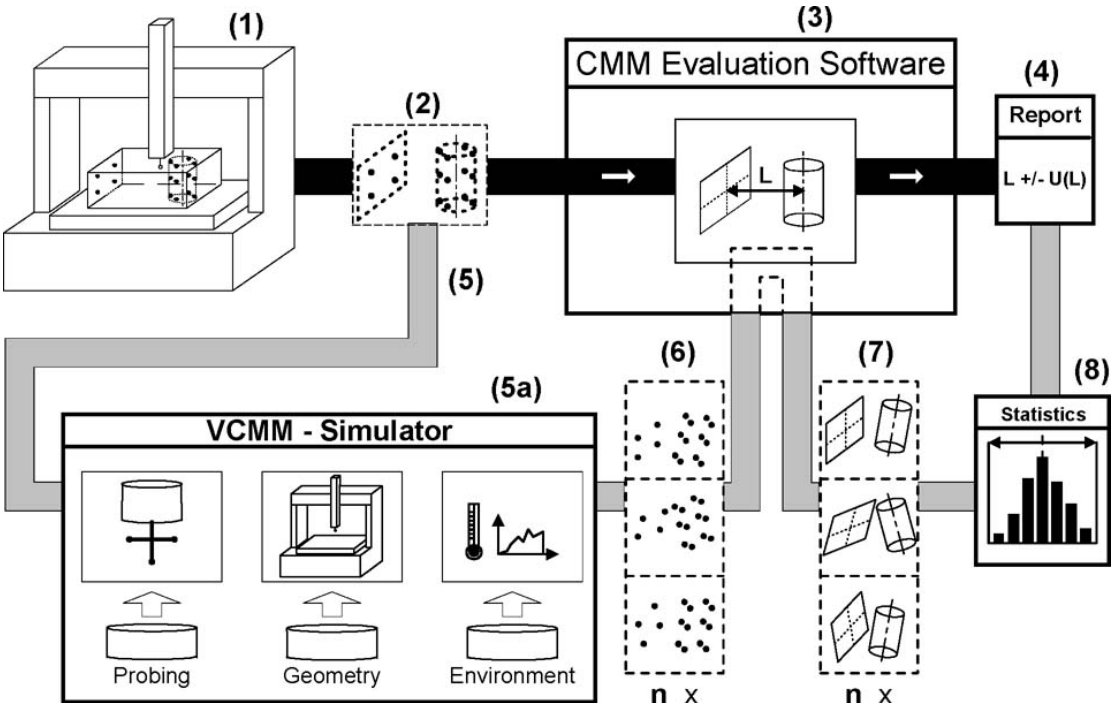

Figure 15. The VCMM concept [114]

Figure 15 shows the sequence of events related to both the physical CMM measurements and the VCMM simulator. Steps (1) to (3) represent the collection of data points, the application of substitute geometry to the collected data points and the computation of specified tolerances. The VCMM simulator considers three typical input factors:

- CMM geometric errors information;
- Probing uncertainty;
- Environment.

The input factors are used to perturb (5a in Figure 15) the original data points collected from the physical measurements via Monte Carlo simulation. This task allows several data sets to be created within the bounds set by the collective uncertainty due to the three input factors. A set of substitute geometries is then computed by the CMM software on the generated data. Statistical analysis (8) can then be used to report the uncertainty results.

The NEDO International Joint Research project [115] summarises a collection of projects from different working groups on VCMM, including the PTB (Physicalish-Technishe Bundesanstalt) Germany, NMIJ (National Metrology Institute of Japan) Japan, NML (National Measurement Laboratory) Australia, UT (The

University of Tokyo) Japan and TDU (Tokyo Denki University) Japan. A discussion [116] of how the VCMM concept could be generalised together with a general methodology to take into account prior calibration information in uncertainty estimation was also proposed by the NPL (National Physics Laboratory). Other VCMM have been developed [117,118] to include enhanced user interfaces and 3D simulation of the specific measurement task.

Several researchers have pointed out the disadvantages of VCMM. Firstly, VCMM relies heavily on the accuracy of the CMM geometric description [119,120]. Secondly, the VCMM inputs (uncertainty associated with each contributor) need to be assessed completely, but some of them cannot be economically measured or be easily estimated. Thirdly, some essential uncertainty contributors (e.g. form error, cleanliness, fixturing variability and operators) are not taken into account in the VCMM approach [121,122].

B) ***The expert CMM (ECMM)***

The Expert CMM project (ECMM) consisted of a collaboration between a national metrology institute and industry [114]. The ECMM is a GUM-consistent UES package dealing with task-specific measurement uncertainty. The ECMM developer claims that ECMM requires minimum involvement of the user, and is capable to work both online (for real-time inspection) and off-line (for alternative procedure comparison). The ECMM keeps uncertainty contributors (e.g. CMM machine, environment, workpiece) in separate groups, so it is easy to trace poor measurement accuracy.

The ECMM method considers individual points of the measurand instead of compound geometric features (e.g. diameters and angles), which is a breakthrough for evaluating measurement uncertainty. The overall scheme of ECMM is shown in Figure 16. The ECMM method assumes that the outputs, y, of the measuring system are related to the inputs, x, through a transfer function, h(x). Nominal measurement points, x_0, are perturbed with errors from an error simulator using a Gaussian pseudo-random number generator. The various simulated points are then fed through

the CMM software to produce a variety of outputs, y, which are statistically evaluated to compute the variance covariance matrix to produce a complete uncertainty statement as requested in GUM [21].

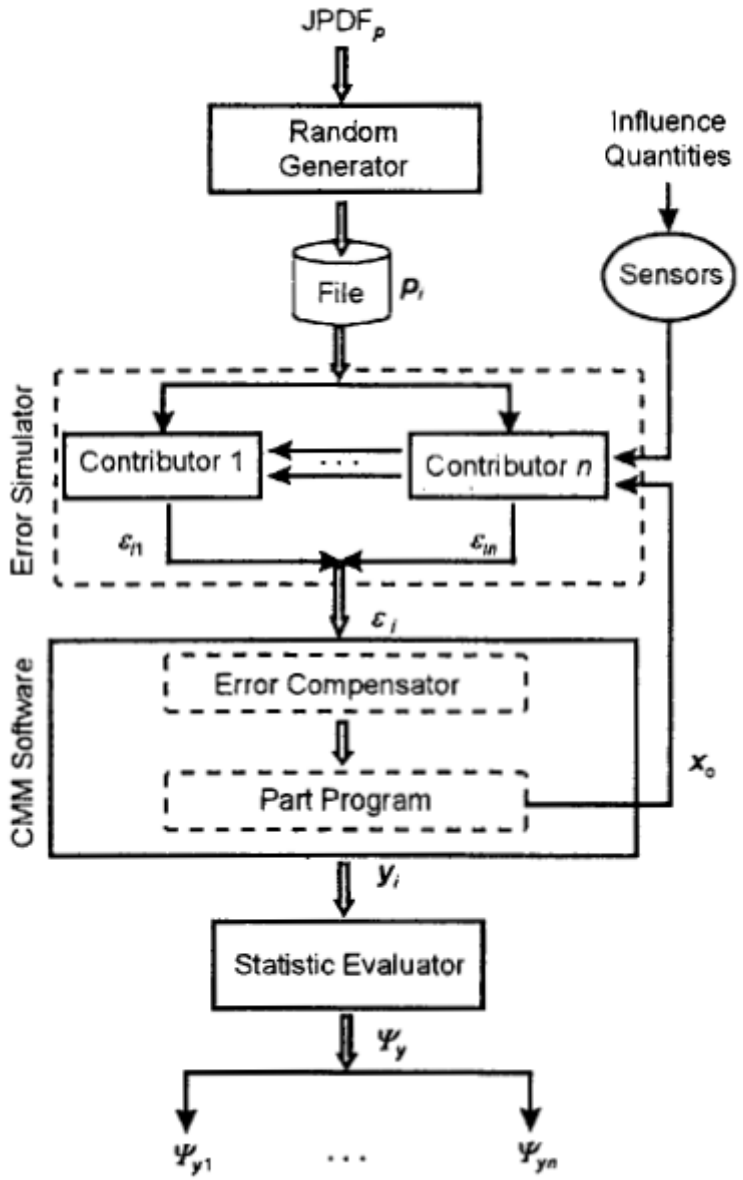

Figure 16. Overall scheme of the ECMM [12]

Testing of the ECMM has been done on a plate with two holes (60 mm and 20 mm in diameter, 60 mm apart). The plate was measured in 100 positions and the length and its uncertainty computed. In 89% of the cases the calibrated length was within the computed uncertainty with a coverage factor of 2. Only geometric errors were used as input factors during the ECMM simulation due to the fact that the machine was

located in a laboratory environment. The initial testing result is considered to be successful [12].

C) ***Simulation-by-constraints***

The simulation-by-constraints method [112,14] generalizes the VCMM simulation concept, and allows the calculation of task-specific measurement uncertainty based on standardized performance data, e.g. ANSI B89.4.1 CMM performance specifications [123]. The overall scheme is illustrated in Figure 17.

The simulation-by-constraints method treats performance tests specifications as mathematical constraints on the infinite number of possible virtual CMM states, each of which is defined by specific parametric errors. These constraints, together with reasonable assumptions (e.g. the CMM kinematic error model), greatly limit the number of permissible states that the CMM may occupy. For example, the ANSI B89.4.1 Standards provide volumetric performance test data for CMM. It includes the measurement of ball bar lengths near the extremes of the CMM work zone. This is, in effect, a boundary condition on the allowed parametric error functions. In order to be self-consistent, the constrained parametric errors (e.g. the permissible virtual CMM states) must faithfully reproduce the original performance specifications when a simulation of the performance test is computed. Standard specifications provide sufficient constraints to allow a reasonable calculation of task-specific uncertainty.

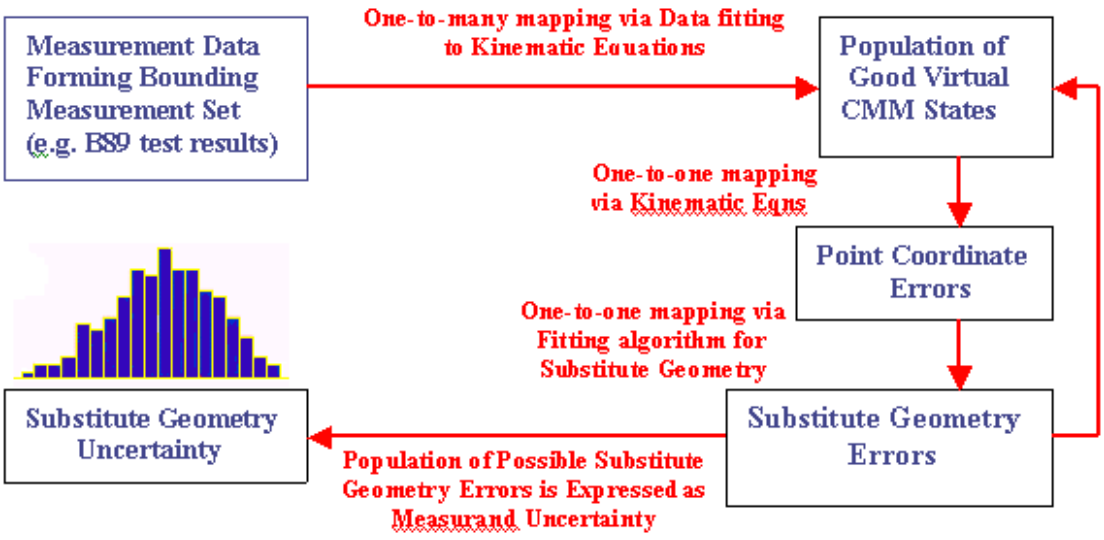

Figure 17. Overall scheme of simulation-by-constraints method

The simulation-by-constraints method does not require a full parametric error description of the CMM machine, which is a major difference between the previously described simulation methods*. The inspection engineers can use the simulation-by-constraints results as the guidance for setting up a practical CMM strategy as well as avoiding the need to physically error map all of the CMMs, which is an expensive and impractical activity for industry.

A comparison between the VCMM method and the simulation-by-constraints method [124] found that both methods approximated the experimental uncertainty values calculated from the physical measurements of two ring gauges. The main difference between the two methods is that the VCMM was likely to have a better description of the machine geometry when compared with the MPE values used to describe the machine geometry in the simulation-by-constraints method.

D) ***Hybrid approach***

There are several approaches in the literature where researchers mixed the simulation methods described above to address the task-specific measurement uncertainty [125,126]. Generally, the hybrid approach employs the Monte Carlo technique to generate the errors of each single measured point, and then uses the CMM

* Both of VCMM and ECMM require the assessment of the individual parametric errors of the CMM.

measurement program itself to propagate the measurement uncertainty. In the hybrid approach, the CMM is not modelled, but its role in the measurement uncertainty evaluation is emphasized as in the simulation-by-constraint method. The hybrid approach provides an approximate yet reasonable evaluation of CMM measurement uncertainty. Therefore it is supposed to fit an industrial production environment more than a calibration laboratory.

Conclusively speaking, the simulation techniques for evaluating task-specific measurement uncertainty have been developed for years. Nearly all of the simulation techniques have been claimed to be consistent with GUM, while different simulation methods require different accuracy levels of simulation parameter inputs. The more accurate the simulation parameter inputs (e.g. a full error model of CMM machine) fed to the simulation algorithm, the more accurate simulation result will potentially be provided. But it is costly to determine an extreme accuracy description of simulation parameters. Research is needed to scientifically explore the balance between the accuracy of simulation parameter description and the simulation result.

Furthermore, due to the large versatility of CMM measurement tasks and inspected features, it is virtually impossible to include all of the measurement uncertainty contributors into the simulation algorithm. For example, it is hard to mathematically define the interactions between the form error and the probing strategy, and hence it is difficult to develop a fitting algorithm taking into account of form error.

2.3.3 The verification of UES performance

The computer code of the UES is not often disclosed by the UES developer, making it difficult for the UES user to assess the reliability of the calculated uncertainty statements. For a UES user, it is very important to verify the UES performance before purchasing the software package. A set of UES verification procedures, which are able to quantify the UES capability, would be of interest to both the UES developer and the UES user.

The ISO 15530-4 [67] provides four verification methods for testing the UES performance, which are:

- Physical Testing on Individual CMM;

- Computer-Aided Verification and Evaluation;
- Comparison with Specific Reference Result;
- Statistical Long-Term Investigation.

Each of the verification methods has their own advantages and disadvantages, which are summarized in Table 5. Generally, the verification methods combine both physical measurements and software measurements. Each of the verification methods has its own advantages and disadvantages in terms of cost, application extension etc. A comprehensive verification method is virtually prohibitive. While passing one verification test may not necessarily guarantee a perfect UES, failing in one can possibly reflect significant problems in a UES. ISO 15530-4 [67] suggests carrying out multiple verification tests, and thus increases the UES result reliability.

Table 5 UES verification methods provided in ISO 15530-4

Verification Method	Procedure Highlight	Advantage	Disadvantage
Physical Testing on Individual CMM	➢ Perform measurement tasks in UES, determining measurement uncertainty *U*; ➢ Repeatedly perform physical measurement on a calibrated artefact, determining the measurement results *y*; ➢ Comparison criteria: $\lvert y - y_{cal} \rvert \Big/ \sqrt{U_{cal}{}^2 + U^2} \le 1$	➢ Close to the measurement scenario; ➢ Performed on real CMM; ➢ Able to detect physical measurement mistakes.	➢ Costly; ➢ Requiring many calibrated artefacts; ➢ Result is not promising on other CMMs.
Computer-Aided Verification and Evaluation	➢ Simulate a CMM measurement behaviour; ➢ Use the simulated CMM to generate MPE value; ➢ Supply the MPE value to obtain uncertainty U; ➢ Compute the measurement error, E, of the simulated CMM; ➢ Comparison criteria: $\lvert E \rvert < U$	➢ Cost saving; ➢ Able to simulate a large number of CMMs and artefacts; ➢ Verification procedure can be performed under specific focus; ➢ Easy for quantitative comparison.	➢ Difficult to simulate all of uncertainty contributor models; ➢ Difficult to cover all of the uncertainty contributors into UES algorithm; ➢ Requiring information exchange between UES developer and user.
Comparison with Specific Reference Result	➢ Specify a measurement scenario; ➢ Determine the uncertainty, u, from UES; ➢ Determine the reference uncertainty, u_{ref}, from physical measurements; ➢ Direct comparison criteria: $u \ge u_{ref}$	➢ Comparison is directly between two uncertainty values.	➢ Limited to very restricted measurement scenarios.

Statistical Long-Term Investigation	➢ Similar to 'Physical Testing on Individual CMM', also include historical measurement data as a consideration; ➢ A historical record is used to provide an understanding of CMM measurement behaviours under various situations.	➢ Allowing a large number of measurements over diverse measurement scenarios and long time.	➢ Difficult to trace the problem if there is inconsistency between UES and physical measurement results; ➢ Difficult to have historical measurement record.

Few formal UES verification studies have appeared in the past literature. But as the UES market emerges, the UES verification starts to be attached to metrology researchers, and rigorous verification efforts have been carried out. Beaman et Morse [124] carried out the simulation measurements in two commercially-available software products, PUDIT and VCMM, and repeated the same measurements in physical environments. By direct comparison between the three sets of the uncertainty evaluation results, it was concluded that the comparison strategy implemented in their experiments could reach general agreement with the software predictions. Abackerli et al. [127] carried out a direct comparison between VCMM results and physical measurement results by measuring the roundness and diameter of a ring. They noticed that in a simulation there will always be real measurement factors that are not fully represented, creating the need to account for uncertainty sources that are not included in the simulation.

UES verification work is starting to attract research attention as market demand emerges. ISO 15530 – 4 describes the general methods for UES verification. Some research has been carried out to verify several commercially-available UES packages. Although some research efforts showed general agreement between UES results and physical measurement results, such comparison results do not guarantee the full capability of UES. Nearly all of the verification work has been done in finely-controlled laboratories on relatively simple geometries and tolerance features. The robustness of UES packages needs to be verified under diverse measurement scenarios, and in realistic environment using a wide range of input and configuration parameters.

2.4 Chapter summary

In this chapter, the fundamentals of coordinate measurement, CMM measurement planning and uncertainty evaluation simulation have been reviewed. The concepts of coordinate measurement have been standardized in the international standard system. There are many systems for computer-aided CMM measurement planning having been developed to solve one or more CMM measurement challenges. These developments have created a good foundation for the development of Uncertainty Evaluation Software (UES), the software packages for evaluating task-specific measurement uncertainty for CMM inspection. However, the performance of UES is not universally agreed, hindering the industrial adoption of UES. One of the primary reasons is that evaluating the task-specific measurement uncertainty, the key aim of the UES, is a complex and sequential decision-making process, and there is a large diversity and complexity of CMM resources and tasks. Determining the measurement uncertainty as per ISO-VIM and ISO-GUM is complicated and abstract, and there is some inconsistency between the ISO GPS standards. It is virtually impossible to develop a CMM inspection planning algorithm which considers all of the problems and parameters in the measurement process. Verifying the UES performance in a physical environment has not been carried out comprehensively, and it is very difficult to verify the UES results under all of the measurement scenarios.

Therefore, it is necessary to extend the UES verification studies into more complicated and practical measurement scenarios. Moreover, it would be useful to explore alternative approaches of utilizing UES evaluation results, and hence to extend the applications of UES to a robust level. This is the major objective of the thesis.

Chapter 3 Research Aims, Objectives and Methodology

This chapter presents the aims and specific objectives of the research. The general research methodology in engineering has been discussed, and applied to this research project.

3.1 Aim of the Research

On the basis of the literature review of the previous chapter, the aims of the research are to verify the uncertainty simulation results of a particular UES software system and to investigate the alternative means of utilizing the UES results. The physical CMM measurement tasks will be carried out on a realistic-scale part under shopfloor conditions. The physical measurement results will be compared with simulation results in order to verify the UES performance and to identify alternative applications of UES results. A new approach will be developed to provide an alternative means to analysing UES results. The approach will analyse the UES results by embracing statistical data analysing techniques. The statistics methods and characterizations will be aligned into the CMM measurement. Hence, an approach suggesting a novel perspective on UES application for CMMs will be established and proved.
The other broad aim of the research is to evaluate the newly developed Quality Information Framework (QIF) from the perspective of using its constructs within CMM measurement and inspection modelling and planning.

3.2 Objectives of the Research

To meet the aim of the research the following specific objectives have been investigated:

1) To gain expert understanding on coordinate measurement, CMM measurement modelling and uncertainty evaluation by literature review and industrial visits;

2) To verify UES performance under meaningful complexity measurement scenarios. This objective will include:

a) Planning and carrying out the physical measurement on a real part under shopfloor working conditions;

b) Simulating the same measurements using a UES system, and generating simulation results;

c) Comparing physical and simulation measurement results;

3) To develop a novel measurement planning and implementation framework to analyse and integrate digital and physical measurement uncertainty. The tasks involved are:

   a) To explore alternative applications of the UES by analysing the simulation and physical measurement results;

   b) Selecting statistical analysis method(s) which can be used for the post-measurement data processing;

   c) Aligning the statistical data analysing methods to the CMM measurement reality;

4) To design and carry out test to validate the approach via the physical measurements, define the details of the validation program, and draw conclusions;

5) To summarize the outcomes of the research, write papers and indentify future research.

3.3 Methodology of the Research

3.3.1 Research methods in engineering

Generally, a research process follows either a deductive or inductive approach [128]. The inductive approach gathers data and then concludes a theory. The inductive approach is more applicable to social science research. The deductive approach firstly finds a theory (or a proposal) and is then tested with data. This is more appropriate to engineering and science research, and is also adopted by this research.

According to the University of Bath, Mechanical Engineering course in Research methods – ME50173 (2006), engineering research is described to have following steps:

- Encounter a problem;
- Propose a solution;
- Assess the consequences;
- Decide How to embody the solution;
- Embody it;
- Test it;
- Learn how dependable it was.

Blockley & Henderson [129] extended the above description, and further specified the actions taken for engineering research:

- Determine the basic area of the work;
- Find out what is already known (review of previous work);
- Identify the problem or gap exactly (problem definition and hypothesis generation);
- Develop a precise objective;
- Perhaps propose and build a trial artefact;
- Collect data on its performance;
- Analyse the data;
- Draw conclusions;
- Disseminate findings.

3.3.2 Methods for this research project

The research methodology described above deals with an applied manufacturing problem. It falls into our engineering research aim and objectives, and thus is adopted by this research. Figure 18 lists the general research methodology in engineering (highlighted in blue). The steps carried out in this research are underpinned by the framework of general research and highlighted in red in Figure 18.

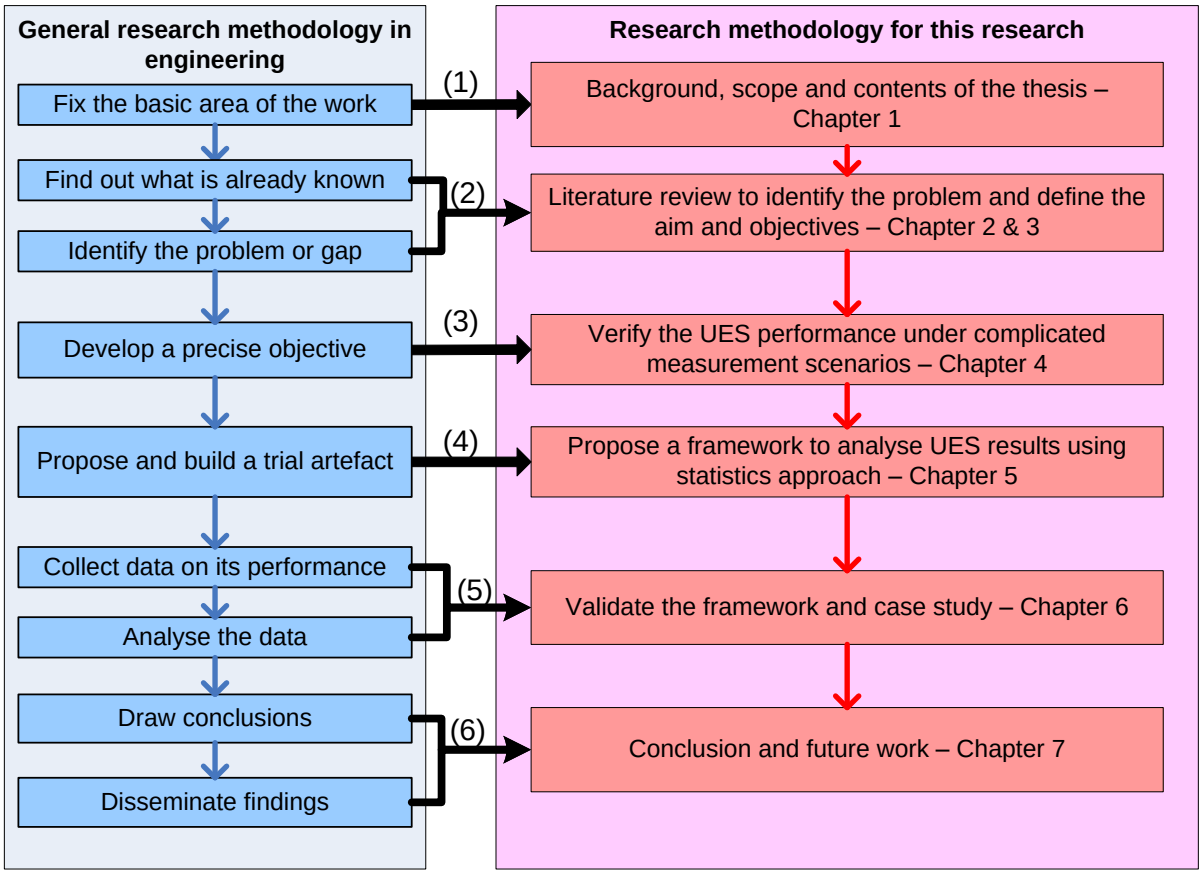

Figure 18. Research method of this project

(1) Determine the basic area of the work - *Background*

In Chapter 1 – Background, scope and justification, the basic research area of the work has been briefly introduced. The research area has been determined in the verification of CMM measurement simulation for the complex product inspection and assembly.

(2) Research problem definition and hypotheses - *Literature review*

As shown in Chapter 2, the literature review conducted in this research included a current review from the academic and industrial points of view. Literature on the fundamentals of coordinate measurements, computer-aided CMM measurement planning and the development of uncertainty simulation techniques were thoroughly surveyed and those relevant to the research reviewed. The literature review has been used extensively to aid the understanding of current research activities of the UES verification and application, to avoid repeating research, developing aims and objectives to aid the construction of the hypotheses.

Following Chapter 2, the gaps in CMM measurement planning and modelling were identified and hypotheses generated in this chapter (Chapter 3). The hypotheses can be summarised as:

- Metrology will play a vital role in the modern manufacturing, interlinking all of the phases within a product lifecycle, from design, manufacturing, in-service to maintenance;
- Task-specific measurement uncertainty will play a leading role in measurement uncertainty evaluation;
- The performance of task-specific measurement uncertainty evaluation software (UES) is not promising. There is a need to verify the UES performance particularly under complicated measurement scenarios;
- The UES results can be used to guide practical industrial production if being deployed with more dedicated data analysis approach, e.g. Design of Experiments (DOE);
- The Design of Experiments (DOE) framework in the research serves for the post-measurement data processing. It does not deal with the CMM inspection process improvement and conformance assessment.

(3) Developing precise objectives – *Pilot experiment*

The aims and objectives of the research have been described in Section 3.1 and 3.2. The more precise objectives have been developed in Chapter 4, where a pilot study of UES verification has been carried out in the shopfloor environment, and hence the limitation of UES capability has been realized.

(4) Proposing and building a prototype system – *Proposing a DOE framework*

To achieve the aims and objectives and realize the hypotheses, a novel framework which is deployed by the Design of Experiments (DOE) approach is firstly proposed and then implemented.

The proposed framework has three main modules: measurement scenario streamliner module, measurement uncertainty simulation module and post-measurement data

analysis module. The details of the proposed system and development of these modules are shown in Chapter 5.

(5) Data collection and analysis – *Case study*

One of the most significant research methods used to examine the industrial application of product development tools and methods is that of case studies [130]. In the context of this research, case studies are mainly used to test the validity of the DOE framework. The case study is carried out between university, national research agency and industry (Figure 19). The cooperation ensures the quality of the case study and confirms the scientific quality of the research.

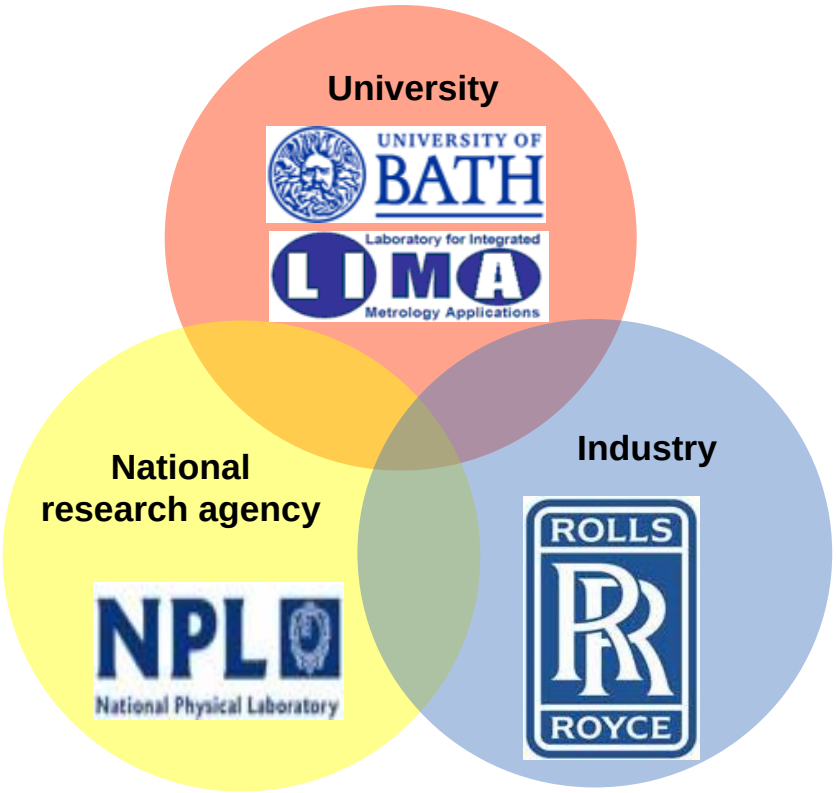

Figure 19. The case study is an honourable corporation between three prestige organizations.

The case study validates the process of DOE framework. In every step of the DOE framework, the data needs to be valid and feasible, otherwise the algorithm or/and knowledge database needs to be checked and modified to make sure output is correct.

Also by using the case studies, the performance of the DOE framework can be identified.

Data collection and analysis has been carried out through the case study. The DOE framework developed in the research is required to quantitatively evaluate the influences of the uncertainty contributors of the CMM measurement. The main concept of the case study is to validate the DOE results by the physical measurements. The simulation data sets are collected through the commercial UES package, PUNDIT/CMM, and analysed in the statistics software Minitab. In parallel, the physical measurement data sets are collected in a finely-controlled environment. At last, the two data sets are compared using NIST statistical comparison methods to find out the statistical significance. The details of the case study are presented in Chapter 6.

(6) Conclusion and dissemination of findings – *Conclusion and future work*

The findings are disseminated as a thesis, and as publications in conferences and journals. The conclusion and the future work of the research are presented in Chapter 7.

Chapter 4 Initial Study of Establishing Task Specific Uncertainty using a Digital CMM Model and Physical Measurements

4.1 Introduction to the Digital CMM Model

The digital CMM Model is usually a software package developed for evaluating the task-specific CMM measurement uncertainty. A commercial software system, PUNDIT, is employed in the research to demonstrate the performance of digital CMM model. Based on the uncertainty predicted by the CMM model, further research is developed. This section introduces the working principles and the operations flow of the simulation software, and provides a demonstration study of using the CMM modelling software.

The digital CMM system, PUNDIT, can be considered as a UES according to the description of the standards. However, as PUNDIT does much more than uncertainty estimation, it is only appropriate to describe it as digital CMM modelling system.

4.1.1 Working principle

The CMM measurement modelling software evaluates the task-specific measurement uncertainty by the Simulation-by-Constrain (SBC) method, an uncertainty simulation method reviewed in Chapter 2 – Literature Review. It performs the Monte Carlo simulations regarding principal sources of error in CMM measurements by taking into account machine geometry, probe, thermal conditions, feature surface characteristics, sampling patterns, etc, as shown in Figure 20. It has a modular architecture that facilitates enhancements of error models [22]. Deviation errors with random values are added to the actual figures on each parameter. The combined uncertainty is obtained by having the integration of the individual random errors into one uncertainty value [21].

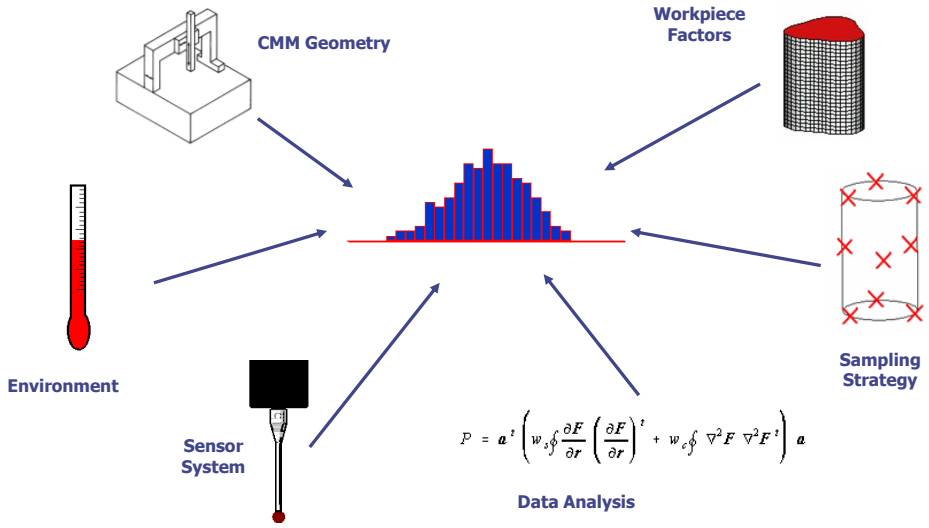

Figure 20 Error sources considered in CMM modelling software

As its first step in creating the uncertainty estimates, the CMM modelling software incorporates a 'Bounding Measurement Set', which is a hypothetical CMM error states found to be consistent with the ASME B89 test suite [123]. Since this set does not completely describe the CMM, the software then proceeds to simulate inspection of the part using each of the hypothetical CMMs in this set by randomly varying the errors of each error contributor within the 'Bounding Measurement Set'. Finally, for each GD&T parameter to be determined the population of substitute geometry errors is used to create an estimate of measurement uncertainty [131]. The inspection engineers can use this estimation of measurement uncertainty as the guidance for setting up the practical CMM probing strategy and companies can avoid the need to physically error map all of the CMMs, which is an expensive and impractical activity for industry.

4.1.2 Operations flow

The operations flow of the CMM modelling software is fairly straight forward and similar to the CMM measurement planning in a physical environment. Figure 21 shows the entire operations flows [131]. It starts from loading the workpiece CAD model to the system. Then the users can manually characterize the factors appearing during the CMM measurement process. These factors include the CMM, probe, environment (mainly thermal environment), measurement plan and manufacturing

information. At last, the software runs Monte-Carlo Simulation and calculates the measurement results.

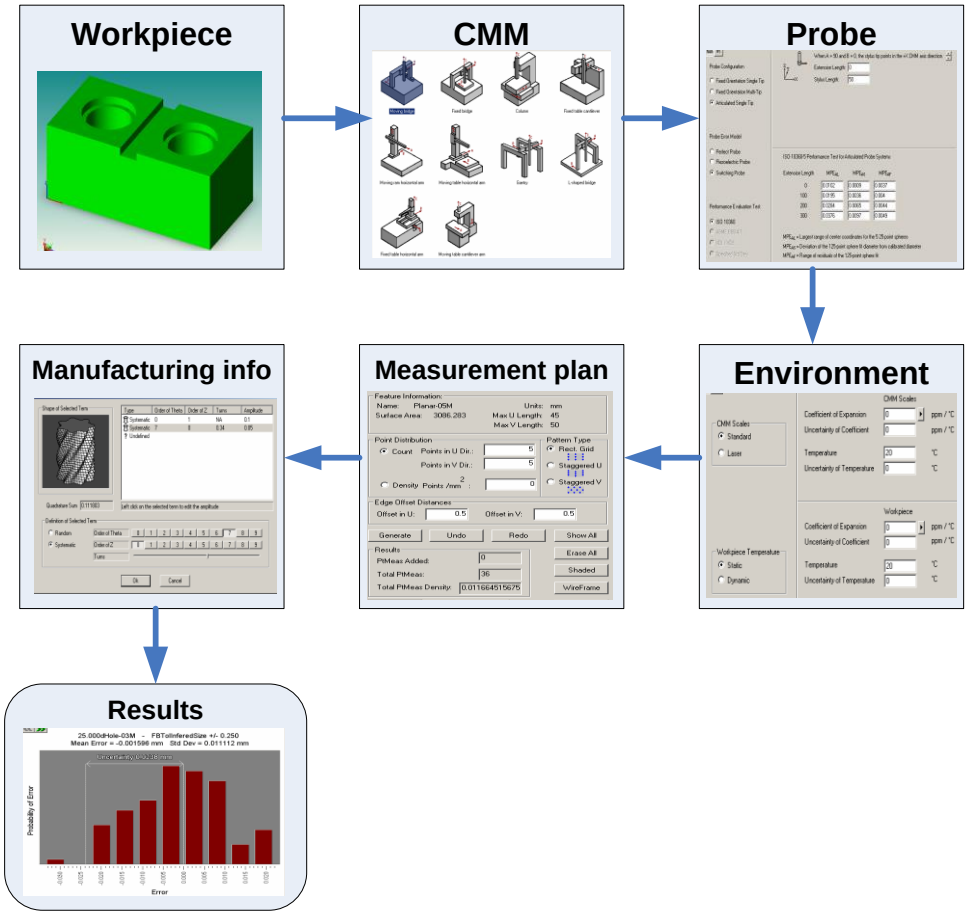

Figure 21 Operations flow (concluded from [131]).

Monte Carlo Simulation is a broad class of computational algorithms that rely on repeated random sampling to obtain numerical results [27]. As shown in Figure 22, $f(x)$ represents a measurement process. $g(x_1)$, $g(x_2)$ and $g(x_3)$ are the distribution functions of the input quantities, which represent the influence quantities of the measurement process. Through the function box $f(x)$, $g(y)$ is propagated to represent the distribution function of the measurement results.

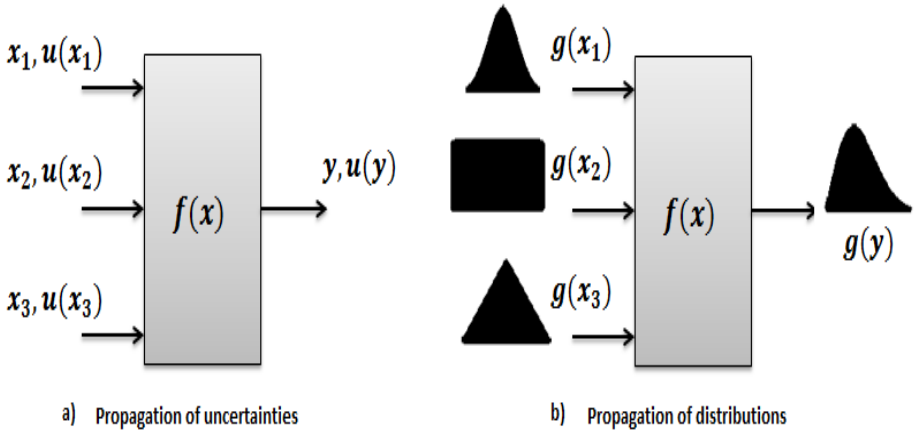

Figure 22 Monte Carlo simulation applied to metrology

To realize the operations flow of the digital CMM model, a brief study was organised for measuring a mechanical product with complex geometry.

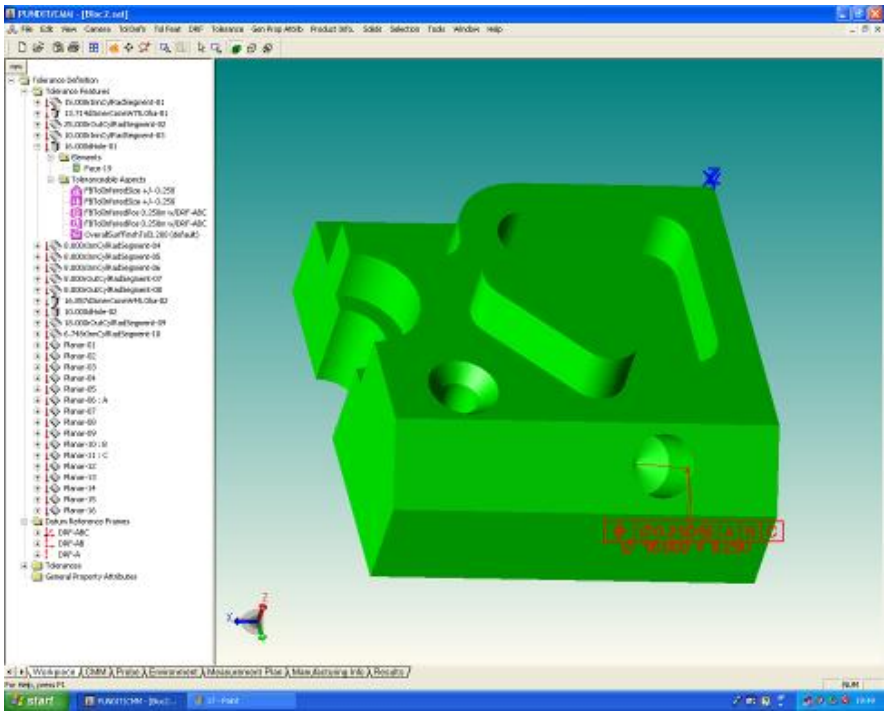

Figure 23 CAD model of the complex product for the case study.

The case study started by importing a CAD model representation (created in SolidWorks) of the workpiece to the digital environment along with the entire product's design specifications (as shown in Figure 23). 30 tolerance features were defined that had to be measured as well as defined the measurement datum reference frames and established specific tolerances for feature location, orientation, size and form. Similarly to the physical CMM verification process, the research chose the hardware and environment for the CMM measurement, such as a CMM gantry structure, probe and thermal conditions. The details are listed in Table 6.

Table 6 Hardware and Temperature Set-up in simulation

CMM	Geometry	Moving Bridge
	Error model	Perfect
Probe	Type	Fixed orientation single tip
	Error model	Perfect probe
Temperature		20°C, static

After setting up the inspection features, temperature and hardware specification, the uncertainty models of each inspection feature had to be considered individually and synchronously for the purpose of generating an appropriate inspection plan. In this research, one inspection feature is selected, the diameter of the oblique hole. As annotated in Figure 23, the diameter of the oblique whole 16mm, of which tolerance value is 0.25mm.

Figure 24 illustrates the points sampling when measuring the diameter of the oblique hole. The sampling strategy is deliberately designed for the task of measuring the oblique hole. Firstly, the sampling points are not evenly distributed along the hole circle. It is designated to sample more points on the lower side of the hole than on the upper side. This is because the hole is oblique. The uneven sampling point distribution would help to detect the oblique angle of the hole axis, and eliminate the impact of the oblique axis on diameter measurement. Secondly, the form error of the oblique hole is

considered. Form error describes the deviation of a machined feature from its nominal design. Form error is usually caused by the inaccuracy of machining process. Therefore, the mathematical model of form error needs to consider machining process and machining capability. In the case study, it is assumed the oblique hole is made by rough drilling, followed by machining to the finished size with a six-flute reamer. Based on this assumption, the form error is mathematically modelled by assigning into two categories, systematic form error and random for error. The systematic form error is the form error caused by the inaccuracy of machining instruments, of which value is derived from the principles of machining tool designs. In this case, the systematic error is modelled as a theta order of 0 (no angular variation) and a z order of 1. The random form error is the form error caused by the unpredictable disturbance during the machining process, of which value is judged on machining experts' experiences. Given the above information, In this case, the random error is defined at the amplitude 0.025.

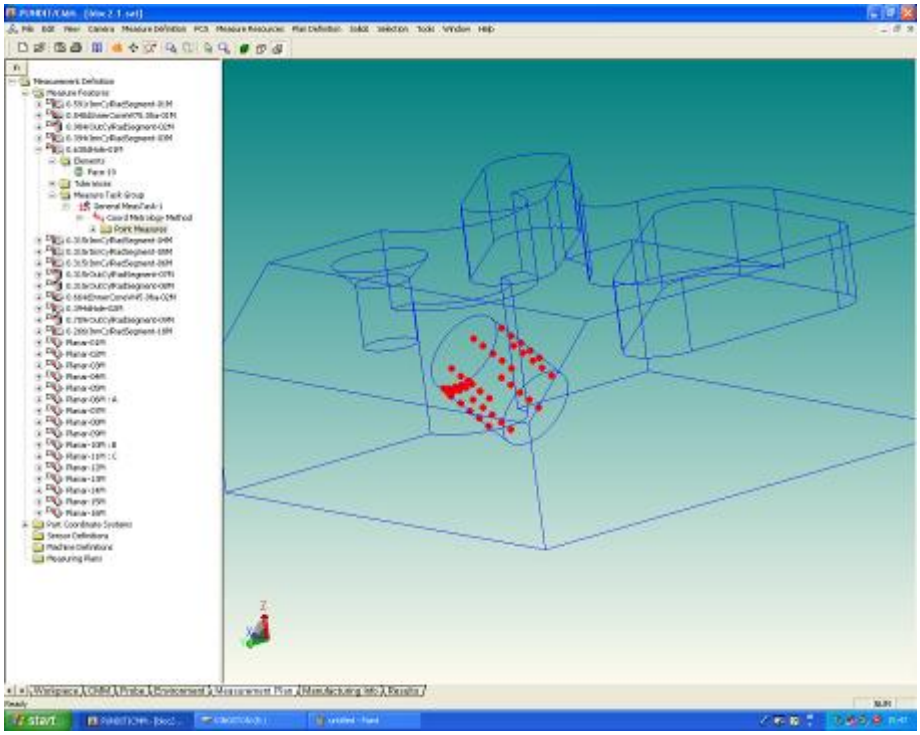

Figure 24 Points sampling of the oblique hole

When all the influencing parameters have been specified, the number of 1,000 simulation cycles was selected to run and launch the simulation process.

4.1.3 The outputs

The Monte-Carlo simulation runs in the CMM measurement modelling software, and outputs task-specific uncertainty estimates for the dimensions measured.

Figure 25 is the outputs of the simulation study in previous section. This simulation results state the bias, variability and uncertainty estimation of task-specific measurement. Ideally, the shape of the results is close to a normal distribution due to the Monte Carlo simulation used. For the inspected oblique hole, the task-specific measurement uncertainty statement can be expressed as “The uncertainty of the diameter of this nominally 16 mm diameter hole is 0.121 mm, at 95% confidence.”

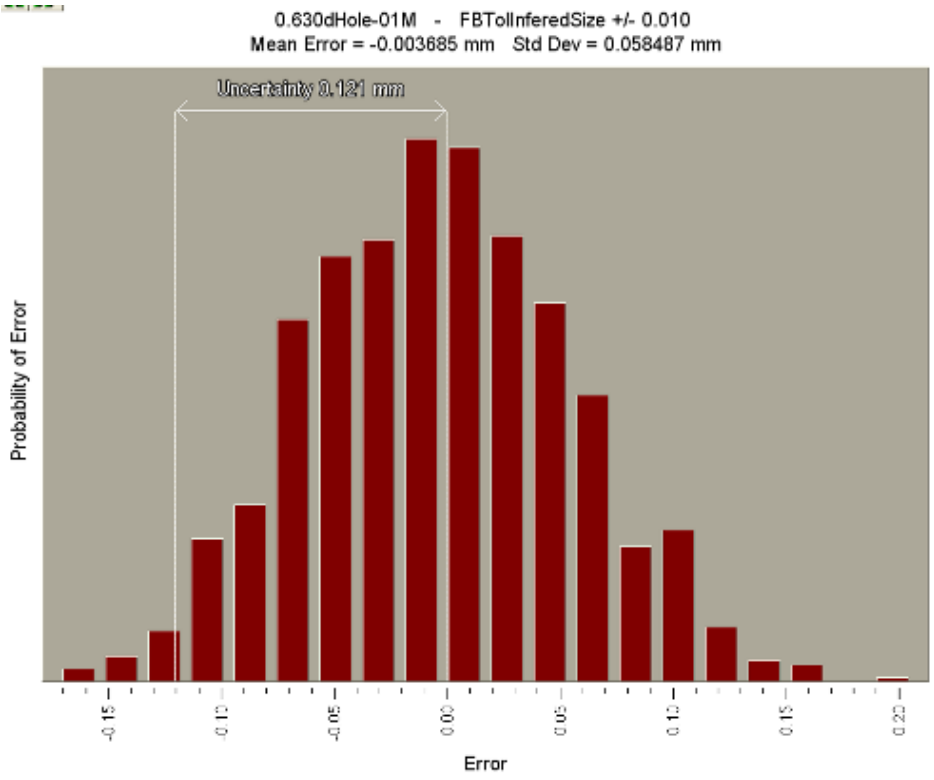

Figure 25 Simulation Result

4.2 Pilot case study on verifying Digital CMM Model simulation results by physical measurements on a large scale component

4.2.1 Background

As stated in previous sections, estimation of the CMM measurement uncertainty for real parts is a sophisticated undertaking. The ability of the uncertainty estimation software remains arguable in terms of their accuracy and precision. In order to test the performance of the uncertainty estimation software (UES) used, the physical and virtual measurements have been carried out on a large-scale part, on which the critical and relatively small-size features needed to inspected by CMM to meet their tight tolerance requirements. The part is an essential component on a high-quality aerospace product. The main challenge of the component is the fitting/assembly problem. The physical measurement was carried out in an industrial aerospace facility in the UK.

Prior to carrying out the physical measurements on the component, it is advised to firstly identify the likely sources that would affect the measurement uncertainty. The sources affecting the measurement uncertainty are identified as:

- Variation in ambient temperature;
- Variation in component temperature;
- Choice of probing stylus;
- Condition of the stylus (degree of wearing, damage or cleanliness);
- Location of the component on CMM measurement volume;
- Variation in the location of the part in any fixture used on the CMM table;
- Machine to machine variation if two or more CMM are used in parallel on the same part;
- Variation between part programmes if more than one programme version is used to control the inspection procedure on the same part;
- Operator influence through variation in set up, probe qualification, datuming practice or assessment of probe qualification results.

The above sources affecting measurement uncertainty are prioritized and grouped. According to the aims and objectives of this research and research facility availability, the following sources affecting measurement uncertainty are included in the study:

- CMM;
- Probe;
- Temperature;
- Measurement plan.

Although there are other uncertainty contributors, it is proposed that for the pilot study, these other uncertainties are assumed to be small, and, hence can be ignored.

Additionally the following assumptions have been made:

- Form errors are not a significant contributor to measurement uncertainty in this case, and consequently can be ignore;
- The error in machine location at any given point is not a function of how the CMM got to that point. In other words, the dynamic errors are not considered to be significant;
- The part is perfectly constrained and not deformed by its fixture.

These assumptions are established given the metrology experts' experiences and the aims and the objectives of the research. The assumptions have made the pilot study practicable in the shopfloor environment, and linked the study outcomes to the research aims. Not only have the assumptions been made on reasonable ground, but also they have provided an industrial focus to the case study.

4.2.2 Physical measurements on a large-scale part with relatively small-size feature

Due to the data protection agreement with the industrial partner, the specific information relating to the inspected part design and manufacturing are advised to be non-disclosure. Generally speaking, the inspected part is a key component of a gas turbine system which generates enormous and reliable power to drive high-tech engineering products. The inspected part is the stator of the gas turbine system. As circled in the red loop in Figure 26, it is located behind the rotary compressor to uniform the gas flow exiting the compressor.

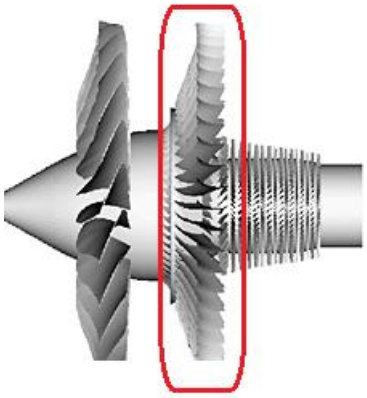

Figure 26 A representation of the gas turbine system

Figure 27 is a highly simplified representation of the inspected part. It is a large scale part, of which the diameter is approximately 3 meters. Various holes are drilled on the inspected part in order to rivet the inspected part with the housing hole. The positions of the holes and the geometries of the inspected part are constrained with tight tolerances. A very large coordinate measurement machine (CMM) is used to carry out measurement tasks. However, it is challenging to determine a confident measurement statement because of the unexceptionally large scales of the part and the CMM.

Figure 27 A representation of the inspected part

Prior to the CMM measurements, the critical features relating to the final assembly are identified. Given the feature natures and tolerance requirements, these critical features are grouped into 4 categories, of which details are listed in Table 7 lists. The IDs of the feature groups are named given the code of practice of the industrial partner. The meanings of the feature groups are explained as below:

- **CCF2a:** the feature group represents the basic geometries of the inspected part. By measuring the features, 'Outer Gauge Point Diameter/LE' and 'Inner Gauge Point Diameter/TE', the outer and inner radii of the inspected part is determined respectively. Despite the large dimensions of the diameters (nearly 3 meters), the tolerance requirements are very high, which have to be ±0.30mm. It is a major challenge of the inspection project;
- **CCF2b:** the features in this group represent the holes on the front side of the feature CCF2c. These holes allow the rivet abutment between the inspected

part and the housing shell. By measuring these holes, the positions of these holes are constrained to allow smooth joint between the inspected part and the housing shell;

- **CCF2d:** the features in this group represent the holes on the rear side of the feature CCF2c. These holes have the same function as the ones in the feature group CCF2b. By measuring these holes, the positions of these holes are constrained to allow smooth joint between the inspected part and the housing shell.

Table 7 The list of the inspected features

ID	Feature Description	Nominal (mm)	Tolerance (mm)
CCF2a	Outer Gauge Point Diameter/LE*	2981.8	±0.30
	Inner Gauge Point Diameter/TE§	2946.78	±0.30
CCF2b	Front Flange Bolt Hole Position/No1	791	±0.25
	Front Flange Bolt Hole Position/No15	791	±0.25
	Front Flange Bolt Hole Position/No45	791	±0.25
CCF2d	Rear Flange Bolt Hole Position/No1	805	±0.25
	Rear Flange Bolt Hole Position/No7	805	±0.25
	Rear Flange Bolt Hole Position/No14	805	±0.25
	Rear Flange Bolt Hole Position/No20	805	±0.25

Note: *LE: Leading Edge; §TE: Tailing Edge (*sic).*

The specifications of the CMM used in the test is listed in Table 8. The CMM is a bridge type CMM with exceptionally large working volume ($4m \times 4m \times 4m$). The CMM gantry is firmly embedded into the ground of shop floor. The maximum permitted error (MPE) of the CMM is $\pm 9\mu m \pm 10\mu m \times [L(mm)/1000mm]$ quoted by the manufacturer's manual. The probe is the Renishaw SP25M. According the temperature monitor in the shopfloor, the temperature control is $19.52°C \pm 0.05°C$. The inspected part is clamped on the ground by special fixtures within the CMM working volume. Considering the large scale of the inspected part, the form errors are assumed to be ignored.

Table 8 The physical test parameters of the CMM

Working Volume (approximate)	$4m \times 4m \times 4m$
MPE Quoted by Manufacturer	$\pm 9\mu m \pm 10\mu m \times [L(mm)/1000mm]$
Probe	Renishaw SP25M
Temperature	$19.52°C \pm 0.05°C$
Manufacturing	Assume no form error

The measurement plan is established as follows:

1) Calibration: Measure 4 points on a calibrated sample of holes to get the self-calibration;
2) Datum establishment: Probing 3 points on top face of the inspected part to create a plane. Then, probing 4 points on one of the Front Flange Bolt Holes to create a circle;
3) Feature Group CCF2a Measurement: Probing certain critical points by following the commands of the metrology experts in the shopfloor. The diameters of the inner circle and the outer circle of the inspected part are calculated and reported using the least-square fitting algorithm;
4) Feature Groups CCF2b and CCF2d Measurement: the holes are measured by probing 4 points at the 2mm depth of the hole. The position of the holes are calculated, and fitted using least square fitting algorithm.

All of the features listed in Table 7 have been measured by the CMM machine within 8 hours. The measurement results are listed in Table 9. The measurement results of Feature Groups CCF2b and CCF2d, which indicate the hole positions, were originally reported in polar coordinates. The results listed in Table 9 have been converted to Cartesian coordinates in order to calculate the positional deviation.

Table 9 Results of physical test

ID	Feature Description	Design Speciation		Physical Measurement Result
		Nominal Value (mm)	Tolerance (mm)	Standard Deviation (S_{phy})
CCF2a	Outer Gauge Point Diameter/LE*	2981.8	±0.30	0.00351
	Inner Gauge Point Diameter/TE§	2946.78	±0.30	0.00215
CCF2b	Front Flange Bolt Hole Position/No1	791	±0.25	0.00258
	Front Flange Bolt Hole Position/No15	791	±0.25	0.00204
	Front Flange Bolt Hole Position/No45	791	±0.25	0.00288
CCF2d	Rear Flange Bolt Hole Position/No1	805	±0.25	0.00097
	Rear Flange Bolt Hole Position/No7	805	±0.25	0.00151
	Rear Flange Bolt Hole Position/No14	805	±0.25	0.00233
	Rear Flange Bolt Hole Position/No20	805	±0.25	0.00166

The results indicate the repeatability of the measurement system (shown as Standard Deviation in Table 9), but cannot provide further information on bias. This is because the exact dimensions of the inspected part are unknown.

4.2.3 Simulation measurement results using Simulation-by-Constrain (SBC) method

The simulation experiments are performed in the digital environment. A solid body was created as shown in Figure 28. The outside conical surface was formed from a sweep through the outer gauge points. This is a simple approximation to allow the inspected features to be analysed using a circularity tolerance in the simulation software. The logic for this construction is based on the idea that the uncertainty of a circularity tolerance, applied to each set of gauge points, is equivalent to the uncertainty on the distance of any given gauge point to the datum origin.

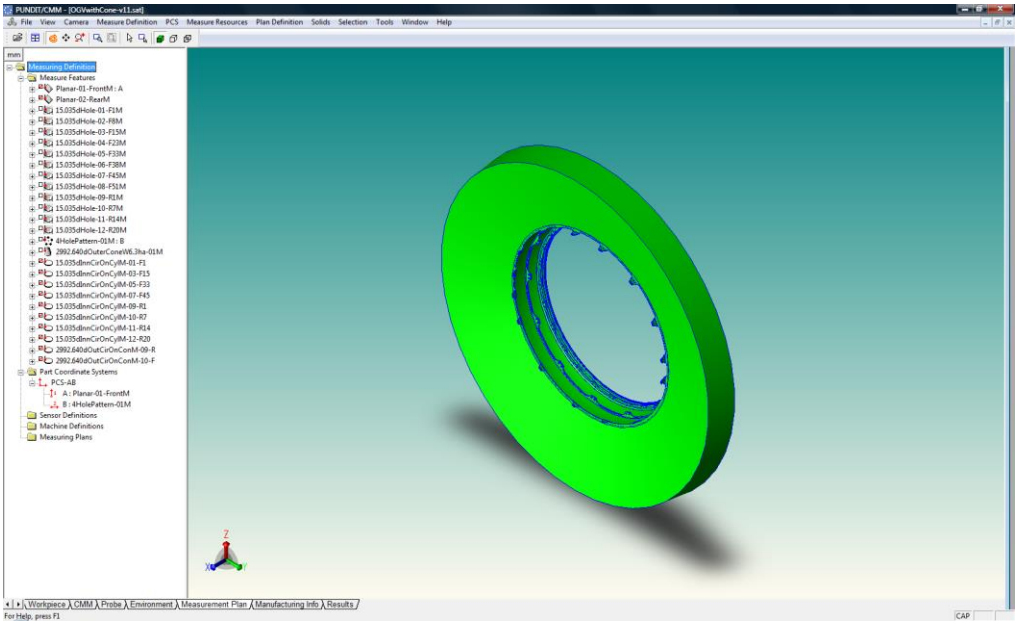

Figure 28 A generic compontent input model

The digital measurement process has been modelled using the 'Simulation-by-Constraints' method. In this method, the machine errors are not entered into to the model directly; rather the limits of permissible errors are entered consistent with the CMM machine specification in accordance with ISO 10360 calibration requirements.

The parameters used as the primary inputs are listed in Table 10. It is known that the CMM tends to behave better than the values a CMM manufacturer publishes for the Maximum Permissible Error (MPE). It has been suggested that it is not unusual for a CMM to perform to half its published MPE. Additionally, the temperature variation during the experiment was almost ideal (average of $19.52°C \pm 0.05°C$). Therefore, the temperature effects could be effectively ignored in the experiment. Finally, a small amount of random form error was introduced to the surface of the rear flange, the bolt holes, and outer conical surface.

Table 10 Simulation parameters

CMM	E = ±4.5μm + 5μm * [L (mm)/1000 mm] (*half the manufacturers' stated MPE*)
Probe	Standard Deviation 1.0μm for 100m stylus
Environment	$20°C \pm 0°C$ (*minor change – to remove temperature effects from the simulation*)
Manufacturing	5μm random error on rear flange, holes and conical surface

Each simulation trial was conducted with 3,000 runs. The simulation results are listed in Table 11.

Table 11 Simulation result

ID	**Feature**	**Simulation Result**	
		Standard Deviation (S_{pun})	**Uncertainty (U_{pun})**
CCF2a	**Gauge Points (LE)**	0.004377	0.0173
	Gauge Points (TE)	0.004300	0.0171
CCF2b	**Front Hole 1 (Pos)**	0.005707	0.0210
	Front Hole 15 (Pos)	0.006611	0.0262
	Front Hole 45 (Pos)	0.006639	0.0265
CCF2d	**Rear Hole 1 (Pos)**	0.005335	0.0197
	Rear Hole 7 (Pos)	0.006346	0.0249
	Rear Hole 14 (Pos)	0.005245	0.0196
	Rear Hole 20 (Pos)	0.006842	0.0275

4.2.4 Measurement results comparison

A) Comparison between physical and digital measurement results

The physical measurement results and the digital measurement results are listed together in Table 12. S_{pun} is the standard deviation predicted by the digital CMM model, and S_{phy} is the standard deviation of the physical tests. S_{pun}/S_{phy} is the ratio of standard deviation by simulation versus the standard deviation from the physical repeatability test.

Table 12 Comparison between digital and physical measurement results

ID	Feature	Tolerance (mm)	Physical Measurement	Digital Measurement		Ratio S_{pun}/S_{phy}
			Standard Deviation ($S_{phy,}$ mm)	Mean Error (mm)	Standard Deviation ($S_{phy,}$ mm)	
CCF2a	**Gauge Points (LE)**	0.30	0.00351	0.008575	0.004377	1.25
	Gauge Points (TE)	0.30	0.00215	0.008453	0.0043	2.00
CCF2b	**Front Hole 1 (Pos)**	0.25	0.00258	0.009567	0.005707	2.21
	Front Hole 15 (Pos)	0.25	0.00204	0.012934	0.006611	3.24
	Front Hole 45 (Pos)	0.25	0.00288	0.013244	0.006639	2.31
CCF2d	**Rear Hole 1 (Pos)**	0.25	0.00097	0.00901	0.005335	5.50
	Rear Hole 7 (Pos)	0.25	0.00151	0.012233	0.006346	4.20
	Rear Hole 14 (Pos)	0.25	0.00233	0.00907	0.005245	2.25
	Rear Hole 20 (Pos)	0.25	0.00166	0.013847	0.006842	4.12

Given the data in Table 12, Figure 29 is constructed.

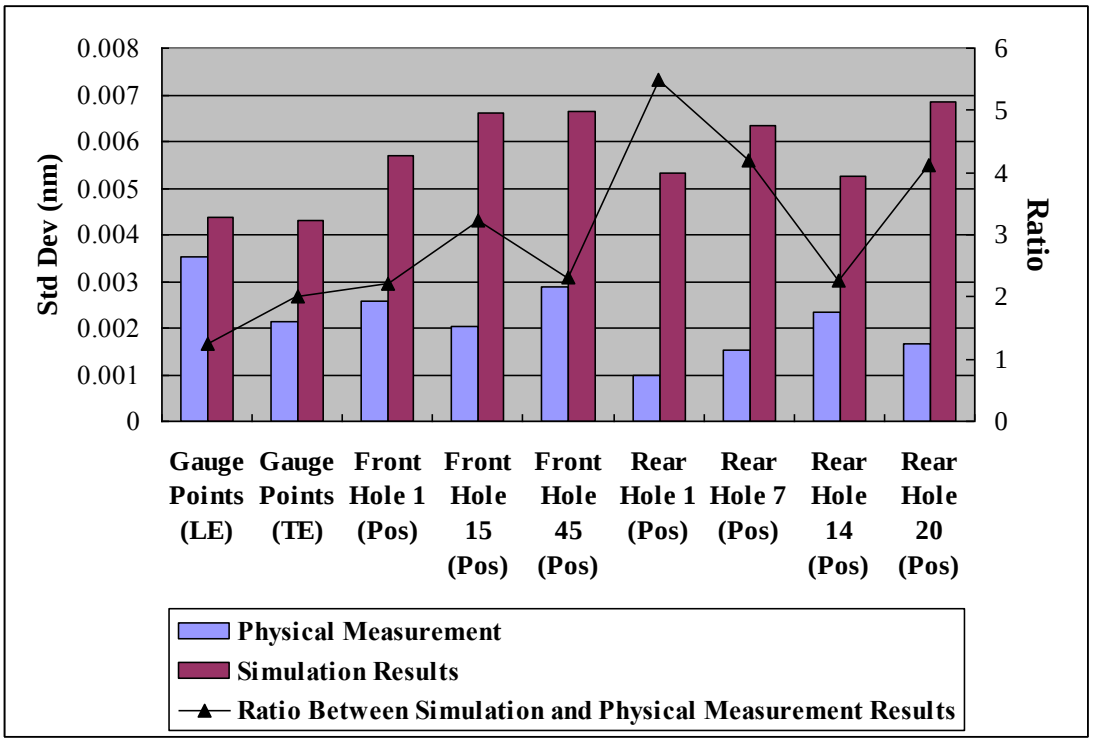

Figure 29 Comparison between physical measurement and simulation results

From Figure 29, several points can be concluded:

- The digital CMM model generally predicts higher measurement results than that obtained from the physical measurement environment. The standard deviations for positional measurements obtained from the digital measurement environment are generally higher than that obtained through physical experiments.

  This is caused by the nature of the SBC method. The SBC method does not require a full description of the physical measurement environment. The information loaded into the digital CMM model (which employs SBC method) does not completely cover all aspects of measurement process. Therefore, the measurement uncertainty predicted by the digital CMM model would be generally higher than that obtained from the physical measurement.

- The Ratio between Simulation and Physical Measurement Results varies significantly across the inspected features. The Ratio ranges from 1.25 to 5.50.

  For the Feature Group CCF2a, which includes 'Gauge Points (LE)' and 'Gauge Points (TE)', the Ratio is relatively lower, ranging between 1.25 to 2.00. In

particular, for the ‘Gauge Point (LE), the standard deviations predicted by simulation software become closer to physical measurement results. The Feature Group CCF2a represents the outer and inner diameters of the inspected part. The CCF2a measurements represent the measurements of size and dimension. The comparison result shows promising capability of the digital CMM model in predicting the dimension measurements.

For the Feature Group CCF2b, which includes three holes at the flange bolt fronts, the Ratio gets larger, and the variations are larger. It indicates that the performance of the digital CMM model is unstable in predicting the locations of these front holes.

For the Feature Group of CCF2d, which includes four holes at the flange bolt rears, the Ratio get significantly larger and variation increase. Despite disregarding the human errors during the physical measurement process, the Ratio values and its variation are not considered to be acceptable. In particular, there are significant differences in measurement results on Rear Hole 1.

The above examinations on the Ratio between Simulation and Physical Measurement Results indicate the unstable performance of the digital CMM model in predicting different feature. Generally, the digital CMM model is more capable of ‘measuring’ the dimension features (diameter in the pilot study) than the form features (hole positions in the pilot study). This conclusion is close to common understandings on uncertainty estimation software. Form features have high geometric complexity. Estimating measurement uncertainty for form measurement needs more comprehensive and sophisticated algorithms than that for dimension measurement. Consequently, in the pilot study, the digital CMM model performs better to predict the diameter measurement than the hole positions.

- The human-errors are considered. At the Rear Hole 1 (Pos), the ratio is significantly high. It is very difficult to give a definitive explanation. It is very possible that the significant high ratio value was caused by un-detected human errors over the physical measurement process.

Generally speaking, no obvious tendency can be derived by simply comparing physical measurements and simulation results. The performance of the digital CMM model is not convincing. The digital measurement results are not reasonably close to the physical measurement results. The large dimension and complex geometry of the inspected part is a major problem. Through the measurement modeling process of the pilot study, it is realized that the digital CMM model would be more suitable to measure conventionally machining products, of which dimensions are within traditional CMM working volume.

B) Calculating measurement uncertainty using GUM approach

Another approach to justifying the measurement results has been carried out by using the GUM approach, the standardized guidance for measurement uncertainty calculation. The GUM-approach measurement uncertainty is calculated given the mathematically idealized conditions of measurement instruments and measurement environments. The CMMs and measurement environments which vary in the ideal mathematical ways are nicknamed as 'being good' in the shopfloor. Therefore, the GUM-approach measurement uncertainty represents the measurement uncertainty of a 'good' CMM in a 'good' measurement environment. The comparisons between the GUM-approach measurement uncertainty and digital measurement uncertainty examine the consistence between the digital CMM model and the GUM method. Priory to the comparisons, the measurement uncertainties are calculated using the GUM approach.

The GUM advises that a value for uncertainty can be calculated by identifying the uncertainty component sources and adding these values in quadrature [21]. Generally, it is considered a CMM measurement system as having three major categories of uncertainty: the CMM machine itself, the temperature effects, and random error ('Type A'). In our case, the temperature, as monitored as $19.52°C \pm 0.05°C$, is likely to be a small contributor to the overall uncertainty, and therefore is ignored. Therefore, the uncertainty is approximated using the GUM method by considering just the MPE of CMM machine and the Type A contribution (as calculated from the standard deviation of the repeatability test).

In order to calculate the GUM-approach uncertainty (U_{Gum}), a combined standard uncertainty was calculated by adding constituent standard uncertainties in quadrature, and multiplying by a coverage factor of 2. This gives a value of expanded uncertainty of 95%. The CMM uncertainty used for calculation was taken by the value for the anticipated error from the MPE value at the nominal length and dividing by $\sqrt{3}$ (as the distribution is assumed to be rectangular). The Type A uncertainty is calculated by taking the standard deviation and dividing by $\sqrt{10}$, where 10 is the number of values used in the test.

The measurement uncertainties calculated given the GUM approach are listed in Table 13 together with the digital measurement uncertainty. The ratio between GUM-approach uncertainty and digital measurement uncertainty is also calculated and listed in Table 13.

Table 13 GUM-approach measurement uncertainty and digital measurement uncertainty

Feature	Digital Measurement		GUM-approach Uncertainty			Ratio U_{pun}/U_{GUM}
	Standard Deviation (S_{pun})	Uncertainty U_{pun}	CMM	Type A	U_{GUM}	
Gauge Points (LE)	0.004377	0.0173	0.0069	0.0011	0.0140	1.2
Gauge Points (TE)	0.0043	0.0171	0.0069	0.0007	0.0138	1.2
Front Hole 1 (Pos)	0.005707	0.0210	0.0049	0.0008	0.0099	2.1
Front Hole 15 (Pos)	0.006611	0.0262	0.0049	0.0006	0.0098	2.7
Front Hole 45 (Pos)	0.006639	0.0265	0.0049	0.0009	0.0099	2.7
Rear Hole 1 (Pos)	0.005335	0.0197	0.0049	0.0003	0.0099	2.0
Rear Hole 7 (Pos)	0.006346	0.0249	0.0049	0.0005	0.0099	2.5
Rear Hole 14 (Pos)	0.005245	0.0196	0.0049	0.0007	0.0100	2.0
Rear Hole 20 (Pos)	0.006842	0.0275	0.0049	0.0005	0.0099	2.8

Note: 1) In this table, uncertainty is calculated as the mean error plus two times of standard deviation, U=E+2σ;

2) The GUM-approach measurement uncertainty, U_{GUM}, is calculated in the following way:

a) Calculate type A uncertainties given the equation

$$U_A = \frac{\sqrt{\frac{1}{n-1}\sum_{i=1}^{n} x_i (x_i - \frac{1}{n}\sum_{i=1}^{n} x_i)}}{\sqrt{n}}$$

where the subscript A indicated the uncertainty type, and x_i represents the measurement results, and n represents the number of repeated measurements.

b) Calculate type B uncertainties: two 'systematic' uncertainty sources are included, which are CMM specification and temperature effects;

c) All type A and Type B uncertainties were combined in quadrature to derived the combined standard uncertainty;

d) Calculate effective degrees of freedom to derive the appropriate K value from a t-distribution table. In this calculation, K=2.

C) Comparison between digital measurement uncertainty and GUM-approach measurement uncertainty

To compare the digital measurement uncertainty with the GUM-approach measurement uncertainty, Figure 30 is drawn given the data in Table 13.

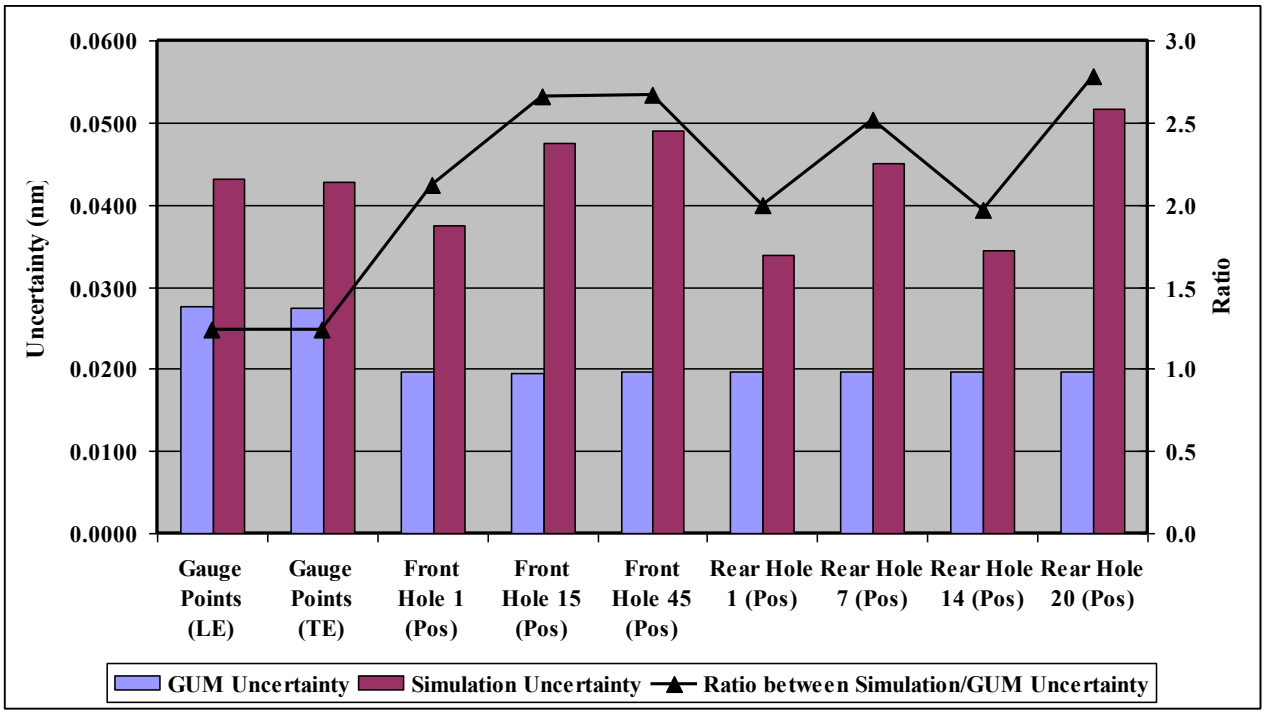

Figure 30 Uncertainty comparison between simulation result and GUM calculation

From Figure 30, it can be seen that the digital measurement uncertainty is significantly higher than the GUM-approach measurement uncertainty. It again reflects the nature of the SBC method, which the limited information input to the digital CMM model restrains the fidelity of the digital measurement result.

On the other hand, the values of the Ratio between the digital measurement uncertainty and the GUM-approach measurement uncertainty vary given the nature of the inspected features. At the features of 'Gauge Points (LE)' and 'Gauge Points (TE)' (Feature Group CCF2a), which represent the dimension measurement, the Ratio

values get close to 1 and become stable. However, for the rest of the feature measurements, which represent the geometry measurements, the Ratio values vary significantly, and few tendencies could be examined. It further proves that it is very complicated and difficult to simulate geometry measurement in the digital environment. The digital CMM model needs to improve the capability of predicting geometry measurement uncertainty.

For further analyzing the performance of the simulation results, the Simulation/GUM Ratio[*] and the Simulation/Physical Ratio[†] are compared, and their value variations are illustrated in Figure 31. The values of Simulation/GUM Ratio vary between 1.2 to 2.8, whereas the values of Simulation/Physical Ratio vary between 1.25 to 4.20. The Simulation/GUM ratio is generally lower than 'Simulation/Physical ratio', and the Simulation/GUM Ratio is more convergent than 'Simulation/Physical Ratio'. The digital measurement uncertainty tends to be closer to the GUM-approach measurement uncertainty to the physical measurement uncertainty. It indicates that the digital CMM model has relatively good consistence with the GUM approach. The uncertainty calculation algorithm utilized by the digital CMM model incorporates well with the GUM instructions which are fundamental to measurement uncertainty estimation. But the digital CMM model still needs to improve its performance in the physical measurement environment.

[*]Simulation/GUM Ratio: the Ratio between the digital measurement uncertainty and the GUM-approach measurement uncertainty;
[†] Simulation/Physical Ratio: the Ratio between the digital measurement uncertainty and the physical measurement uncertainty.

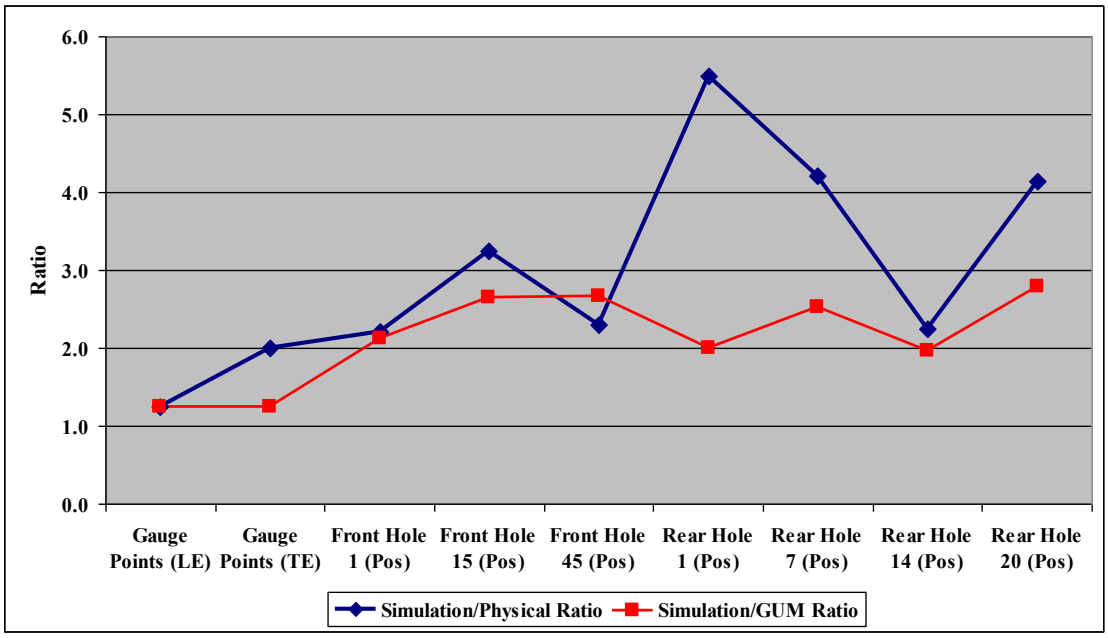

Figure 31 Comparison between simulation result, physical measurement result and GUM approach result.

Noticeably, in Figure 31, the difference between the Simulation/Physical Ratio and the Simulation/GUM Ratio at Rear Hole 1 (Pos) is significantly high. As explained in previous paragraphs, the unexpectedly high Simulation/Physical Ratio is possibly caused by human errors during the physical measurement process. Consequently, it causes the unexpected high difference between the two ratios. However, it suggests that the digital CMM model could be used to detect physical operation errors, which alert production managers to examine the physical measurement process to prevent the errors occurring again.

Conclusively, four major points can be made from the above comparisons:

1) The digital CMM model generally predicts higher measurement uncertainty than GUM-approach uncertainty and physical measurement uncertainty. This indicates the nature of the SBC methods;
2) The digital CMM model is more capable of predicting dimension measurement uncertainty than geometry measurement uncertainty. Estimating uncertainty for geometry measurement is sophisticated and difficult;
3) The digital CMM model has relatively good consistency with the GUM instructions, which are fundamental to measurement;

4) The digital CMM model can possibly be used to prevent operation errors. By comparing the results between digital measurement and physical measurement, the operation errors can be detected, and alert the production manager.

The overall project indicates enormous difficulty and complexity of verifying the performance of the digital CMM model in terms of controlling physical measurement environments and financial and labor cost. It is neither feasible to control all of the uncertainty contributors in the physical measurement environment, nor possible to establish the digital measurement environment to be exactly identical to the physical measurement environment. The nature of the SBC method also limits the fidelity of the digital measurement result. These conclusions explicitly suggest exploring an alternative approach to utilizing the digital CMM model and the SBC method. The approach needs to be innovative, robust and practical to industrial production.

4.2.5 Examining the impacts of measurement uncertainty contributors

Previous experimental evidence does not provide conclusive evidence for validating the use of the digital CMM model. Therefore, an extra set of experiments have been designed and carried out in order to explore the alternative means of utilizing the digital CMM model. In the extra set of experiments, the digital measurement uncertainty is implemented into the CMM measurement capability assessment. Special working conditions have been established in the digital environment, which allows the digital CMM model to carry out sensitivity analysis of the measurement uncertainty contributors.

The ratio between measurement and tolerance, noted as ‘Uncertainty/Tolerance Ratio’, is introduced in the extra set of experiments. In industry, Uncertainty/Tolerance Ratio is usually used for the measurement instrument selection. The rules of CMM instrument selection given the Uncertainty/Tolerance Ratio are listed in Table 14. If the CMM measurement uncertainty is lower than 15% of the designated tolerance, the CMM would be good enough to perform measurement tasks, and there is no need to act on further analysis. If the CMM measurement uncertainty is between 15% - 25% of the designated tolerance, the CMM is on borderline condition, where Gauge R&R

Study* will be carried out to statistically analyse the CMM performance. If the CMM measurement uncertainty is higher than 25% of the designated tolerance, the CMM measurement is not capable enough to perform the measurement tasks, and consequently, is rejected.

Table 14 Use of the Uncertainty/Tolerance metric for decision-making

Uncertainty / Tolerance	**Action**
< 15%	None. Measurement system is acceptable for the feature.
15% - 25%	Borderline Case. Conduct Type 1 Gauge R&R Study.
> 25%	Measurement system is unacceptable. Discuss with design.

Ideally, in this pilot study, the digital measurement uncertainty should have been utilized as the uncertainty input in the 'Uncertainty/Tolerance Ratio' judgement to assist the CMM machine selection. However, the validity of the digital measurement result is not definitively proved. As a consequence, the digital measurement results are deployed in the sensitivity analysis to evaluate the impacts of the measurement uncertainty contributors. And the 'Uncertainty/Tolerance Ratio' judgement rule is suggested to be used to assess the relative sensitivity of the environmental influence parameters.

Priory to the sensitivity analysis, special working conditions are established in the digital CMM model. Three major measurement uncertainty contributors, the CMM gantry, the probe specification and the temperature effect, are selected given the metrology experts' experiences. One or more measurement uncertainty contributors are set to be 'perfect' in due order, where the 'perfect' means the measurement uncertainty contributor has no effect on measurement result. The combinations of the uncertainty contributor states create 8 measurement scenarios as listed in Table 15. The code of the measurement scenarios represents the states of the measurement uncertainty contributors. The 'perfect' state is denoted as 0, whereas the 'effective' state is denoted as 1. For example, "1-0-0" means that only CMM gantry is

* Gauge R&R Study: Gage Repeatability and Reproducibility, a measurement systems analysis technique that uses an analysis of variance (ANOVA) random effects model to assess a measurement system. It measures the amount of variability induced in measurements by the measurement system itself, and compares it to the total variability observed to determine the viability of the measurement system (*ANOVA gauge R&R, Wikipedia*).

effective in affecting the measurement uncertainty, while the probe and temperature are perfect, having no effect on the measurement result.

Table 15 Codes for individual working conditions.

Code	Measurement Uncertainty Contributor		
	CMM Gantry	Probe	Temperature
0-0-0	Perfect	Perfect	Perfect
0-0-1	Perfect	Perfect	Effective
0-1-0	Perfect	Effective	Perfect
0-1-1	Perfect	Effective	Effective
1-0-0	Effective	Perfect	Perfect
1-0-1	Effective	Perfect	Effective
1-1-0	Effective	Effective	Perfect
1-1-1	Effective	Effective	Effective

The digital measurements are carried out respectively in the measurement scenarios. And the digital measurement results, the digital measurement uncertainties, are listed in Table 16*.

Table 16. Uncertainty/Tolerance Ratio under various measurement scenarios

Feature Group	Feature	Measurement Scenario							
		0-0-0	0-0-1	0-1-0	0-1-1	1-0-0	1-0-1	1-1-0	1-1-1
CCF2a	Gauge Points (LE)	0.0%	0.0%	2.4%	2.4%	8.8%	8.7%	8.8%	8.8%
	Gauge Points (TE)	0.0%	0.0%	2.4%	2.4%	8.6%	8.6%	8.7%	8.7%
	Average	0.00 %	0.00 %	2.40 %	2.40 %	8.70 %	8.65 %	8.75 %	8.75 %
CCF2b	Front Hole 1 (Pos)	0.0%	1.7%	7.0%	7.3%	3.2%	3.8%	5.9%	6.0%
	Front Hole 15 (Pos)	0.0%	1.7%	7.0%	7.1%	3.3%	3.7%	5.7%	5.9%
	Front Hole 45 (Post)	0.0%	1.7%	7.0%	7.2%	3.3%	3.7%	5.6%	5.8%
	Average	0.00	1.70	7.00	7.20	3.27	3.73	5.73	5.90

* Due to the data protection agreement with the industrial partner, the designed tolerance values are not allowed to publish. So only the values of the Uncertainty/Tolerance Ratios are listed.

		%	%	%	%	%	%	%	%
CCF2d	**Rear Hole 1 (Pos)**	0.0%	1.7%	6.9%	7.3%	3.3%	3.6%	5.6%	5.8%
	Rear Hole 7 (Pos)	0.0%	1.7%	6.9%	7.1%	3.3%	3.7%	5.7%	6.0%
	Rear Hole 14 (Pos)	0.0%	1.7%	6.9%	7.2%	3.3%	3.6%	5.7%	5.9%
	Rear Hole 20 (Pos)	0.0%	1.7%	6.9%	7.2%	3.3%	3.7%	5.7%	6.0%
	Average	0.00 %	1.70 %	6.90 %	7.18 %	3.30 %	3.68 %	5.70 %	5.98 %

Several points can be made by examining the data in Table 16:

1) For the Measurement Scenario 0-0-0 where all of the measurement uncertainty contributors are set to be 'perfect', the digital measurement uncertainties is 0 for all of the feature measurements;
2) In the same Feature Group, the values of Uncertainty/Tolerance Ratios are close to each other. This indicates the digital CMM model employs the task-specific, feature-based measurement simulation method. Therefore, the digital measurement results vary little against the feature nature;
3) The Uncertainty/Tolerance Ratio has marked changes across the measurement scenarios. This indicates the nature of the Simulation-by-Constraint (SBC) method deployed in the digital CMM model. The measurement uncertainty contributors are the 'constraint' inputs to the Simulation-by-Constraint method. The change of the constraints has obvious effect on the digital measurement results.

Given the above observations, the average values of the Uncertainty/Tolerance ratios are calculated in respect to Feature Groups and Measurement Scenario. The average values are also listed in Table 16.

Given the data in Table 16, Figure 32 is constructed. It shows how the impacts of the measurement uncertainty contributors on the digital measurement results for certain Feature Groups.

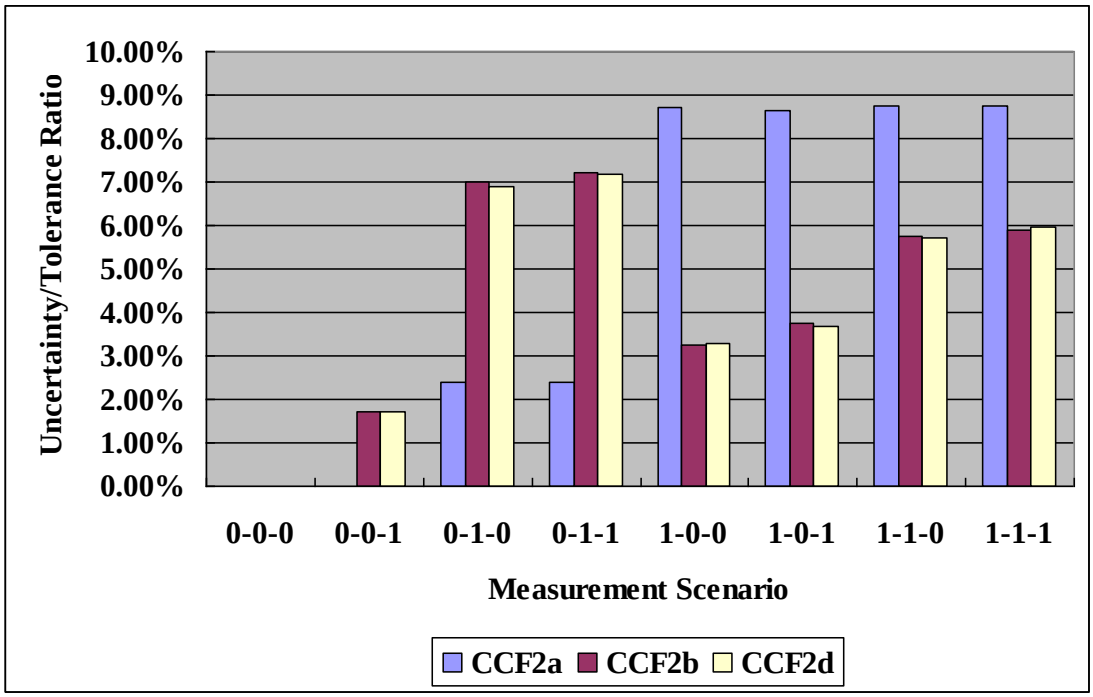

Figure 32 Uncertainty/Tolerance Ratios for Feature Groups CCF2a, CCF2b and CCF2d

Several points could be made by examining Figure 32:

1) Feature Groups CCF2b and CCF2d have similar patterns against the Measurement Scenarios, whereas Feature Group CCF2a has a separate pattern. This result is within the expectation. Feature Groups CCF2b and CCF2d are hole positional measurements which are geometry measurements. Feature Group CCF2a is the part diameter measurements which are dimension measurements. It is understood that the Uncertainty/Tolerance Ratio patterns would be different between dimension measurement and geometry measurement because of the different tolerance natures;

2) CMM gantry has significant impact on the diameter measurement.
   For Feature Group CCF2a (diameter measurement, the blue bar in Figure 32), the Uncertainty/Tolerance values differences significantly between the Measurement Scenarios '0-0-1', '0-1-0' and '0-1-1' and the Measurement Scenarios '1-0-0'. '1-0-1' and '1-1-1'. But, for the Feature Groups CCF2d and CCF2d (positional

measurement, the purple and yellow bars in Figure 32), there is no such pattern to be found.

The major differences between the Measurement Scenarios ‘0-0-1’, ‘0-1-0’ and ‘0-1-1’ and the Measurement Scenarios ‘1-0-0’. ‘1-0-1’ and ‘1-1-1’ are the effectiveness of the CMM Gantry uncertainty contributor. When the CMM gantry is effective, the uncertainty of diameter measurement (Feature Group CCF2a) is significantly. The CMM gantry has significant effects on diameter measurement, but not on positional measurement.

This judgement is reasonably consistent with the physical measurement environment. For the diameter measurements, the CMM gantry needs to move long distance due to the large scale of the part (about 3 meters in diameter). Enormous kinematic errors have been introduced during the CMM gantry movement. For the position measurements, the CMM gantry only needs to move within a relatively small area to inspect the hole. Therefore, the CMM gantry has an obvious impact on the diameter measurement uncertainty, but not on the positional measurement uncertainty.

This analysis result suggests metrology engineers should notice the nature of a feature when making the measurement plan, and to minimize the kinematic errors of the CMM gantry movements especially for large-scale dimension measurements.

3) Probe has lowest impact on the measurement uncertainty.

The Uncertainty/Tolerance Ratio is at the lowest on Measurement Scenario 0-0-1, where only ‘Probe’ contributor is effective. In particular, the Uncertainty/Tolerance Ratio value becomes nil on Measurement Scenario for the Feature Group CCF2a (diameter measurement). The low measurement uncertainty value and the relatively high tolerance value round up the Ratio value to nil. It indicates that the Probe is not a significant factor for the large-scale diameter measurement in this case.

This judgement is consistent with the common understanding on the physical measurement process. Given this judgement, metrology engineers could potentially save capital investment on purchasing better probes, and focus on improving the CMM gantry movements and temperature control.

4) Two non-normative patterns have been realized from Figure 32.

Firstly, it is expect that the Uncertainty/Tolerance Ratio reaches a peak value at the Measurement Scenario 1-1-1 where all of the three measurement uncertainty contributors are effective. However, for the Feature Groups CCF2b and CCF2d (positional measurement), the peak value of the Uncertainty/Tolerance Ratio appears at the Measurement Scenario 0-1-1. This non-normative pattern reflects the incapability of predicting the geometry measurement uncertainty in the digital environment. The complexity of the geometry measurement is a crucial challenge for measurement process modelling and measurement uncertainty estimation.

Secondly, the Temperature factor has little effect on the Feature Group CCF2a (diameter measurement). For example, the value of the Uncertainty/Tolerance Ratio of the Feature Group CCF2a (the blue bars in Figure 32) changes little between the Measurement Scenario 1-0-1 and the Measurement Scenario 1-1-1, the difference of which is the effectiveness of the Temperature factor. This digital measurement result counters common understandings on thermal expansion rules, and remains unexplainable. It indicates that the performance of the digital CMM model still needs to be improved, especially for the large-scale measurement and complex feature inspection.

Conclusively speaking, the reliability of the digital measurement results is critiqued again. Due to the availability of the physical measurement resources, it is difficult to design and perform an extra set of physical measurements to confirm the above judgments. However, it indicates an alternative way of utilizing the digital CMM measurement model, of which result can justify the impacts of measurement uncertainty contributors. The digital measurement uncertainty can have sensible applications to physical measurement, if the digital measurement uncertainty analysis could be analyzed and examined in more sophisticated approach.

4.2.6 In-depth analysis on the hole position measurement results

Given the research interest of the industrial partner, the digital measurement results for the hole position measurements (Feature Groups CCF2b and CCF2d) are further analysed. Since the Uncertainty/Tolerance Ratios shares similar pattern of Feature Groups CCF2b and CCF2d, the values of the Uncertainty/Tolerance Ratios of the hole position measurement are averaged and listed in Table 17.

Table 17 The Uncertainty/Tolerance Ratio of hole position measurements

Feature Group	Feature	0-0-0	0-0-1	0-1-0	0-1-1	1-0-0	1-0-1	1-1-0	1-1-1
CCF2b	Front Hole 1 (Pos)	0.00%	1.70%	7.00%	7.30%	3.20%	3.80%	5.90%	6.00%
	Front Hole 15 (Pos)	0.00%	1.70%	7.00%	7.10%	3.30%	3.70%	5.70%	5.90%
	Front Hole 45 (Post)	0.00%	1.70%	7.00%	7.20%	3.30%	3.70%	5.60%	5.80%
CCF2d	Rear Hole 1 (Pos)	0.00%	1.70%	6.90%	7.30%	3.30%	3.60%	5.60%	5.80%
	Rear Hole 7 (Pos)	0.00%	1.70%	6.90%	7.10%	3.30%	3.70%	5.70%	6.00%
	Rear Hole 14 (Pos)	0.00%	1.70%	6.90%	7.20%	3.30%	3.60%	5.70%	5.90%
	Rear Hole 20 (Pos)	0.00%	1.70%	6.90%	7.20%	3.30%	3.70%	5.70%	6.00%
Average		0.00%	1.70%	6.94%	7.20%	3.29%	3.69%	5.70%	5.91%

Given the data in Table 17, Figure 33 is constructed.

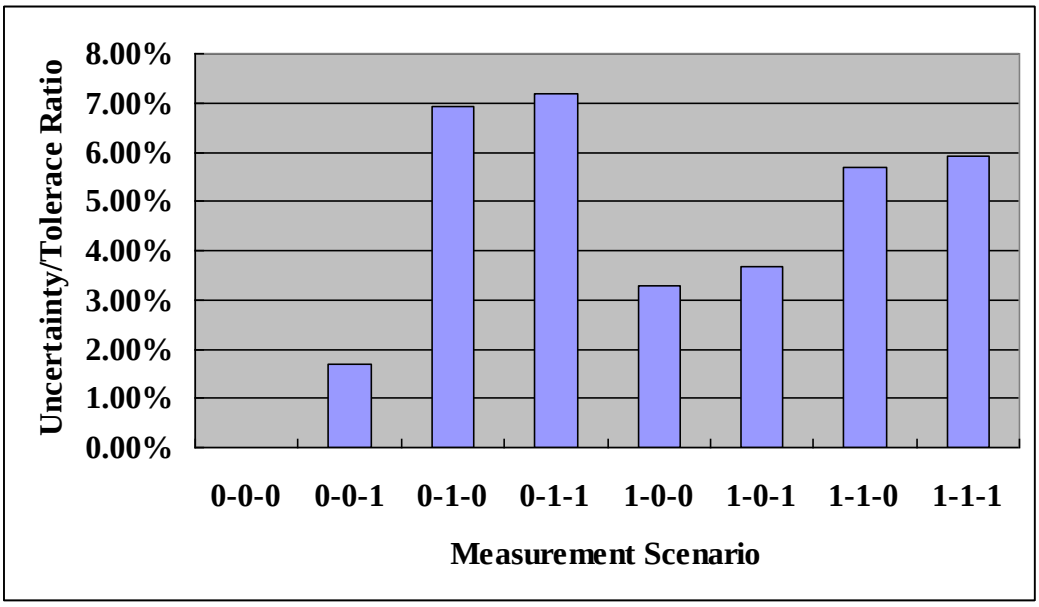

Figure 33 Uncertainty/Tolerance Ratio of hole position measurements

From Figure 33, it can be seen that the key uncertainty contributor impacting the hole position measurement is ‘Temperature’. For example, there is an obvious difference of the Uncertainty/Tolerance Ratio values between Measurement Scenarios 1-0-1 and 1-1-1. The key difference between the two Measurement Scenarios is the effectiveness of the ‘Temperature’ factor. Noticed from the previous section, the key uncertainty contributor for the diameter measurement is the CMM gantry. As stated in the previous analysis, this difference is understandable. For the diameter measurement, the CMM gantry needs to move long-distance. The kinematic error during the CMM gantry movements contributes the significant portion of measurement uncertainty. For the position measurement, the CMM gantry only needs to move within a relatively-small area, so the significant uncertainty contributor is temperature.

The temperature impact on hole position measurement is further explored. The digital measurements are repeatedly carried out under the Measurement Scenario 0-1-0, where only ‘Temperature’ factor is effective to measurement uncertainty. The Temperature inputs are modelled to different dynamic levels, that is to say the temperature setting is gradually changed from $19.52 \pm 0°C$ to $19.52 \pm 3°C$ in the digital CMM model. Then the digital measurements are carried out, and the digital measurement uncertainties are recorded for every 0.5°C temperature change. At last, the Uncertainty/Tolerance Ratios are calculated.

Figure 34 illustrates how the Uncertainty/Tolerance Ratio changes against the temperature uncertainty changes. The measurement uncertainty determined from the digital CMM model changes literally linear against the temperature uncertainty changes.

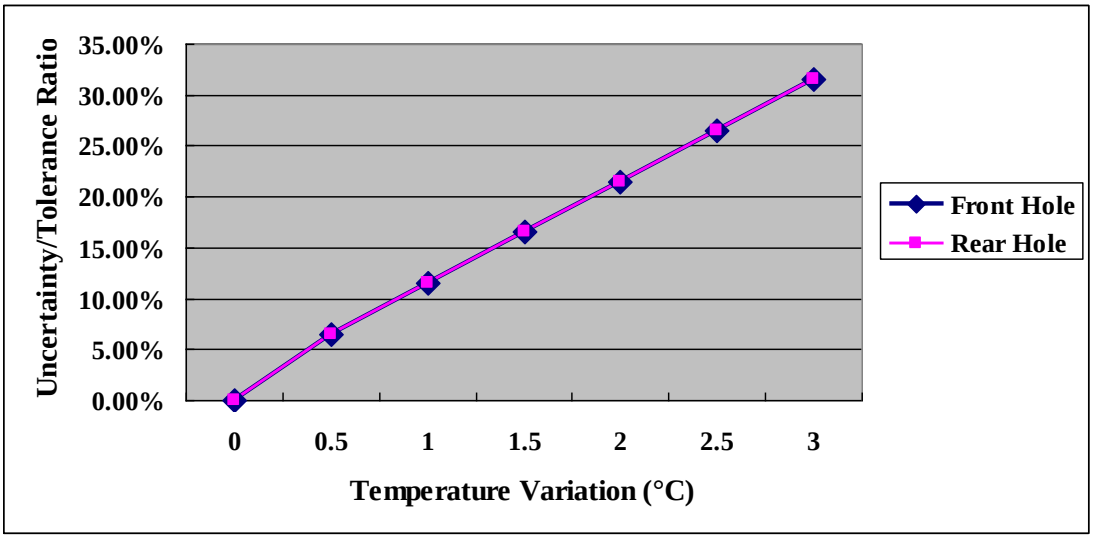

Figure 34 Effect of temperature variations on hole position measurements

Several points could be made by examining Figure 34:

1) The linear pattern in Figure 34 reveals how the digital CMM model calculates temperature effect on task-specific measurement uncertainty. Obviously, in the shopfloor environment, the uncertainty-temperature relationship would be much more sophisticated. This result indicates the digital CMM model needs to improve its capability in modelling the temperature effects on task-specific measurement uncertainty;
2) The pattern in Figure 34 suggests that it would be advisable to maintain the temperature variation within approximately 2°C in order to keep the Uncertainty/Tolerance ratio below the 25% threshold. If the magnitudes of the data in Figure 34 could be accepted, this result could guide the shopfloor temperature control before carrying out physical measurements. It provides anther possible means of utilizing the digital measurement result. The digital CMM model can provide certain guidance on measurement environment control with the existing information on measurement resources and measurement tasks. It will potentially save financial cost from physical measurement, and minimize production risk.

4.2.7 Summary

The pilot study carried above is a useful exercise for learning about the potential benefits and challenges of using the digital CMM model to predict task-specific measurement uncertainty and analyze the CMM measurement capability.

In order to verify the performance of the digital CMM model, the physical measurement environment has been established as identical as possible to the digital measurement environment. Then the physical measurements have been carried out on a large-scale component by measuring its dimension and geometry features. The physical measurement results are compared with the digital measurement results. Since the comparison results do not fully convince the performance of the digital CMM model, extra set of experiments are carried out to explore the alternative means of using the digital CMM model. Several conclusions have been drawn.

The uncertainty obtained from the digital measurement is generally higher than that obtained from the physical measurement. It reflects the nature of the Simulation-by-Constraint (SBC) method, which is employed by the digital CMM model. Since the SBC method does not require a complete description of the CMM process, the measurement uncertainty calculated by the SBC method tends to be higher. On the other hand, by comparing the digital measurement uncertainty with the GUM-approach uncertainty, it shows that the digital CMM model has relatively good consistent with the GUM instructions.

The digital measurement results vary against the feature natures. It indicates the digital CMM model carries out feature-based uncertainty calculation algorithm for task-specific measurement. In particularly, the digital CMM model is more capable of ‘measuring’ dimension features than geometry features;

The performance of the digital CMM model is not fully verified by the physical measurements. Due to the high complexity and diversity of the CMM measurement tasks, it is very difficult to provide a digital CMM model which includes all of measurement uncertainty contributors and measurement scenarios. Moreover, it is barely feasible to establish the physical measurement environment exactly the same as

the digital measurement environment. It is virtually impossible to verify the diverse measurement tasks by physical measurements for task-specific measurement uncertainty estimation.

The alternative applications of the digital CMM model are considered. The digital measurement results are further analyzed to examine the impacts of the measurement uncertainty contributors. The analysis results have shown promising perspective. By deploying delicate experiment design and data analysis techniques, the digital measurement uncertainty could be utilized to answer the questions such as which measurement uncertainty contributor(s) have the most significant impact on the overall measurement system, and consequently to guide the measurement system design in physical environment. It indicates the next step of the research is to establish a robust algorithm and procedures to achieve this objective.

4.3 Chapter summary

The chapter explores how to utilize the digital simulation techniques to model the CMM measurement process in the digital environment, and to determine the task-specific measurement result. The chapter firstly introduces a digital CMM model. It employs the Simulation-by-Constraint (SBC) method and performs Monte-Carlo simulation to predict CMM task-specific measurement uncertainty in the digital environment. Then a pilot study on ‘measuring’ a large-scale part in the digital CMM model has been carried out. The simulation measurement results have been compared with the physical measurement results to verify the performance the digital CMM model. Through the verification work, the strengths and the limitations of the digital CMM model have been explored. Further research on utilizing the digital measurement results has been suggested.

Chapter 5 A Measurement Planning and Implementation Framework to Compare Digital and Physical Measurement Uncertainty

5.1 Introduction

Task-specific measurement uncertainty plays an important role in the CMM measurement evaluation. Various digital CMM models have been developed to predict the task-specific measurement uncertainty before carrying out physical measurement. However, as concluded from the inspection study in Chapter 4, the performance of the digital CMM model is not fully verified. The digital measurement result depends highly on the inputs of measurement uncertainty contributors. The closeness between the digital and physical measurement results remains inconclusive. Moreover, it is virtually impossible to validate the simulation results under all of the measurement scenarios due to the variety of CMM measurement tasks. The effective integration between digital and physical measurement environments challenges both of the simulation software developer and the end-user.

A pilot study has been carried out using Design of Experiments (DOE) method to statistically analyze the simulation uncertainty and inform the integration between digital and physical environments. Based on the pilot study, this chapter proposes a novel measurement planning and implementation framework which employs the DOE method. The framework serves for the post-measurement data analysis and evaluation, aiming to provide closer integration between the digital and physical measurement environments.

The Chapter firstly identifies the limitations of the CMM digital model for evaluating task-specific measurement uncertainty. Then the design of a generic framework to analyze the simulation uncertainty is introduced. The details of the modules of the framework are explained in the following section. At last, the implementation of the framework is provided to prove the integration between the digital measurement environment and the physical measurement environment.

5.2 The limitations of task-specific uncertainty simulation model

The literature reviewed in Chapter 2 has pointed out the limitations of using simulation techniques to evaluate the task-specific measurement uncertainty. The pilot study has provided first-hand experience to realize the limitations of the CMM digital model. From the literature review and the pilot studies, we summarize the difficulties of verifying the performance of the CMM digital model, and align these difficulties under the stages of verifying the CMM digital model as shown in Figure 35. The stages of verification work include the 'CMM digital model' itself, 'running the CMM digital model' and 'verifying the performance of the CMM digital model'. The difficulties of each simulation stage are further explained in Figure 35.

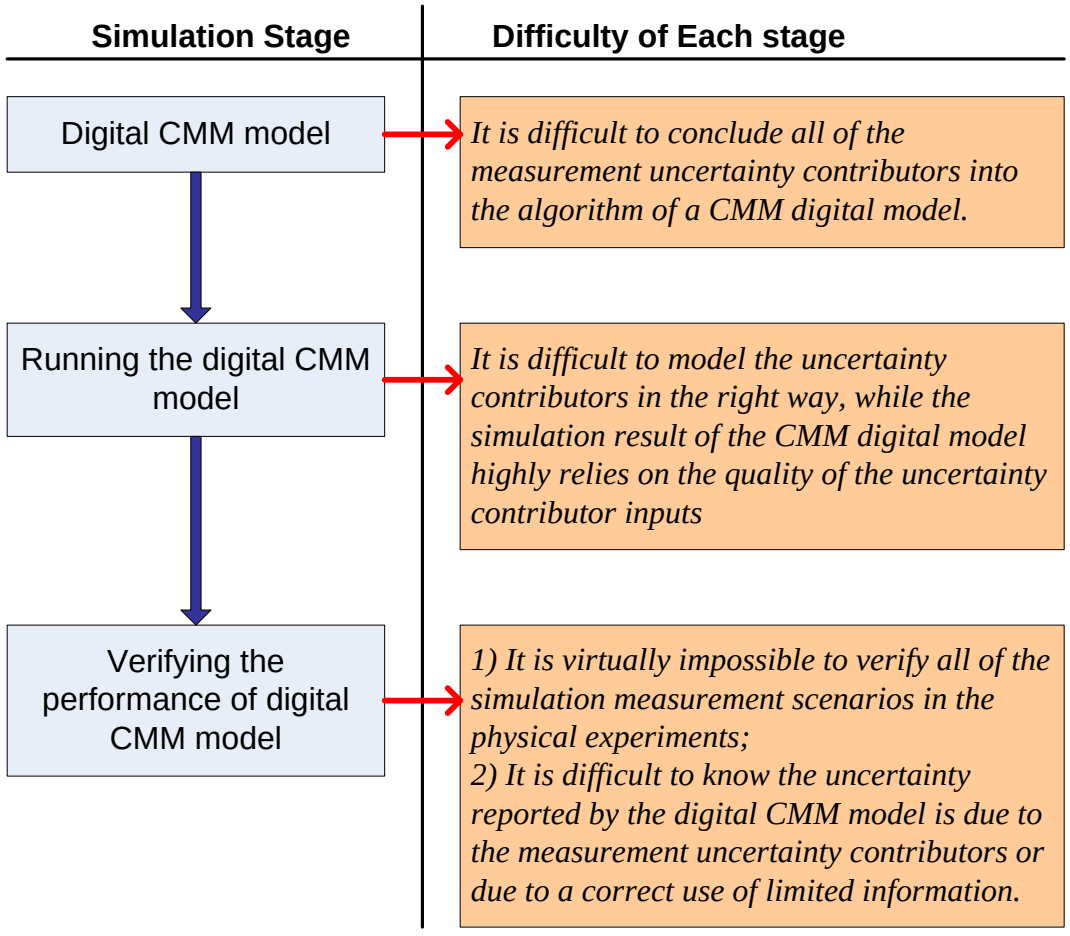

Figure 35 Limitations of the CMM digital model

To conclude, the difficulties of verifying the CMM digital model are due to the contradiction between the nature of task-specific measurement uncertainty and the

large diversity of the CMM measurement tasks. It is nearly impossible to simulate all of the scenarios of the task-specific measurements in the digital measurement environment The difficulties limit the development of evaluating task-specific measurement uncertainty in digital environment.

5.3 Examining uncertainty contributor effects by using Design of Experiments (DOE) approach

Given the limitations described in the previous section, the Design of Experiment (DOE) approach is considered to explore whether the simulation results can be used in statistical analysis for alternative purposes. A trial study has been carried out. The trial study statistically analyzes the simulation results aiming to make a technical contribution to decision-making through the quantification of uncertainties in the relevant variables. The classical statistical approach, Design of Experiments (DOE), is adopted in the trial study to process the post-measurement data given by the simulation software. It aims to quantitatively evaluate which uncertainty contributors have the biggest impact on the entire measurement system performance.

In order to determine the task-specific measurement uncertainty, a slotted block is loaded in the digital CMM model (Figure 36). The 30mm-diameter shallow hole on the slotted block is “measured”. The digital CMM model evaluates the measurement uncertainties of the diameter and position of the shallow hole (as denoted in Figure 36).

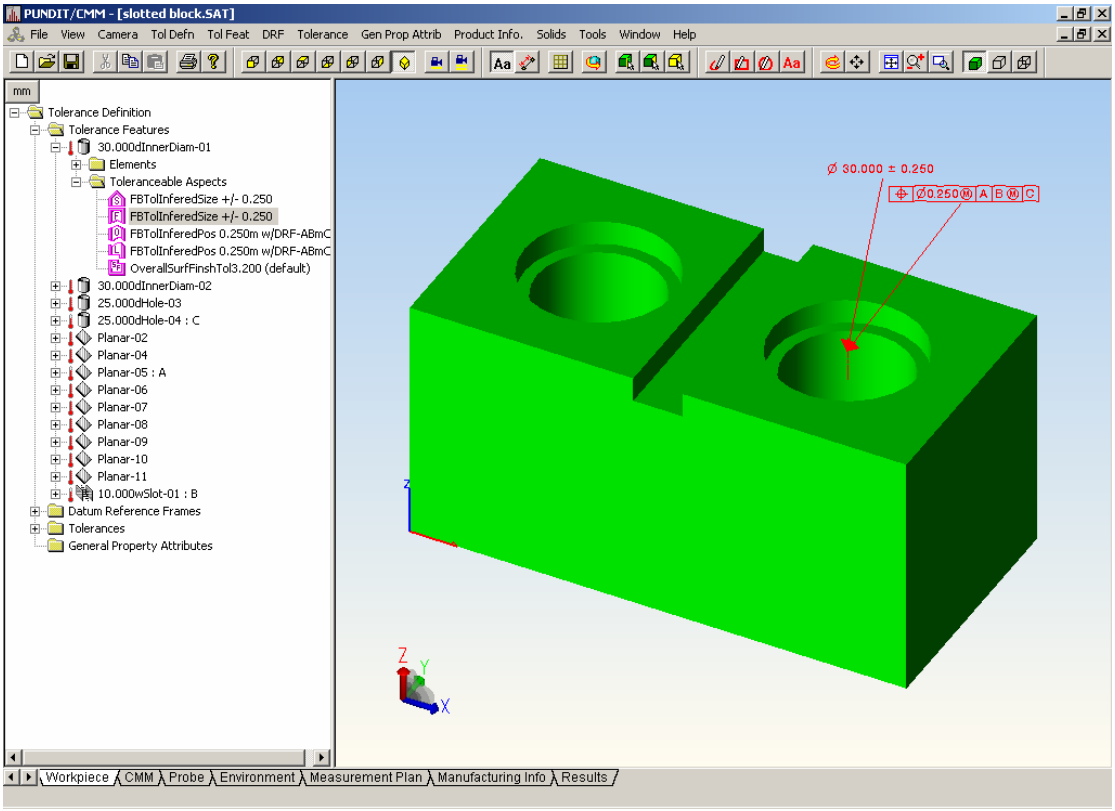

Figure 36 The artefact and measured features

A full factorial design* is carried out. Three factors influencing the CMM measurement uncertainty are selected; they are CMM Specification, Environment and Probing Strategy respectively. Each of the factors is designed to have three levels. The details of the factors and the factorial levels are listed in Table 18. One combination of the random factorial levels is called a 'measurement scenario'. For a full-factorial experiment, there are $3^3 = 27$ measurement scenarios.

* In statistics, a full factorial experiment is an experiment whose design consists of two or more factors, each with discrete possible values or "levels", and whose experimental units take on all possible combinations of these levels across all such factors.

Table 18 Factors and factorial levels for DOE analysis

Factor	Factorial Level
A. CMM Specification	A1: High Accuracy (HA): 1+3L/1000
	A2: Medium Accuracy (MA): 2+4L/1000
	A3: Low Accuracy (LA): 5+4L/1000
B. Environment	B1: Enclosed: 20±1°C
	B2: CMM Room, Class I: 22±2°C
	B3: Shop Floor: 25±5°C
C. Probing Strategy	C1: Low density: minimum, 3 points
	C2: Medium density: NPL guide, 7 points
	C3: High density: 3∗NPL guide, 21 points

The 27 measurement scenarios are reproduced in the digital CMM model. The orders of running measurement scenarios are randomized. Under each measurement scenario, the simulation runs three trials. There are $3\times(3^3)=81$ trials to run. For each trial, the digital CMM model executes a Monte-Carlo CMM . The 81simulation results for each tolerance features are collected respectively and listed in Appendix A. These results are the measurement uncertainties evaluated by the digital CMM model under the claimed measurement scenarios.

To analyse the simulation results, the factorial design is created using statistical and process management software, Minitab, and the simulation results are stored in Minitab as the worksheet format. Two types of factorial plots, main effect and interaction, are produced from the simulation results (Figure 37 to Figure 40). The plots show the factorial effects on the response (which is the measurement uncertainty in our case) and show how the response variable relates to one or more factors.

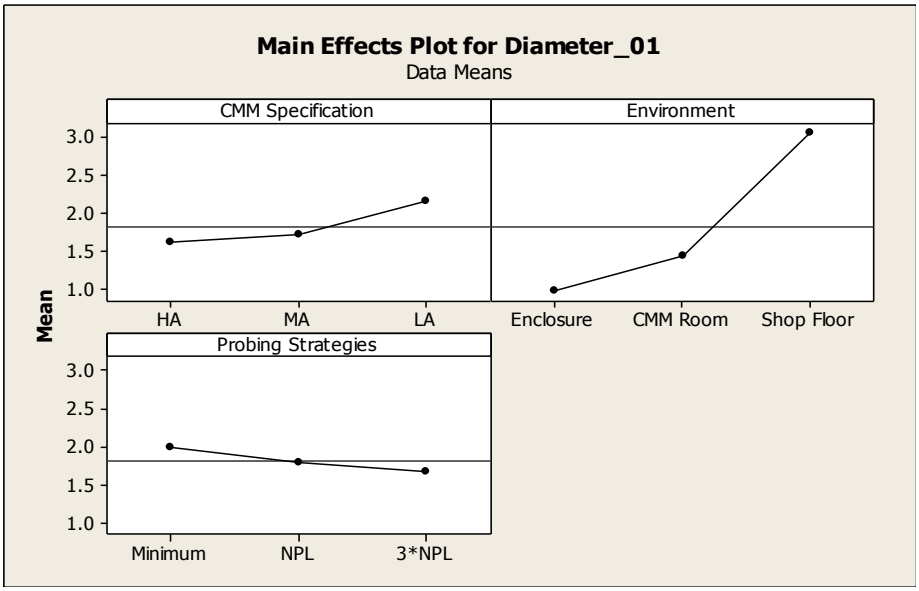

Figure 37 Main effects plot for position measurement

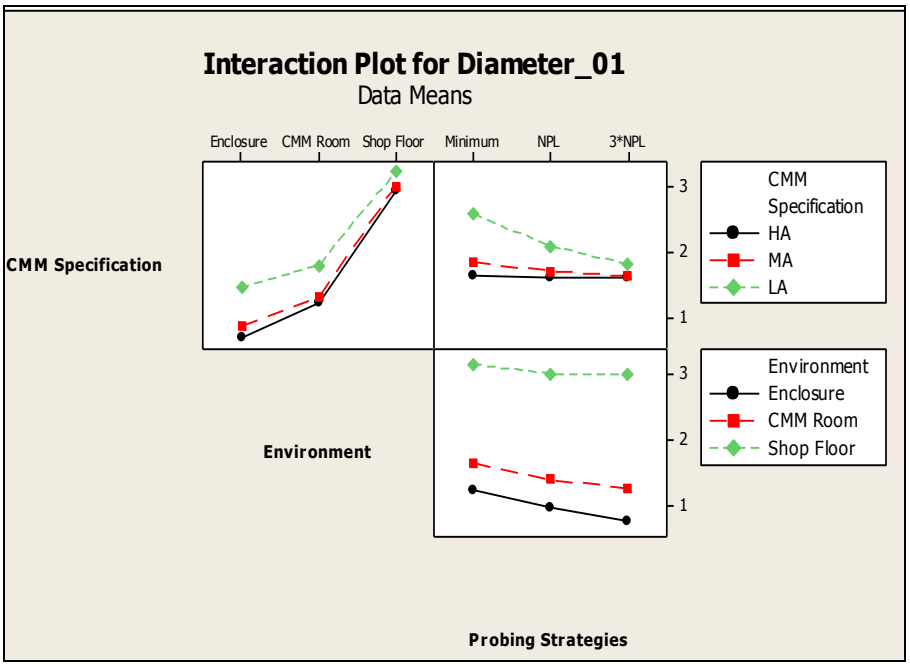

Figure 38 Interaction plot for diameter measurement

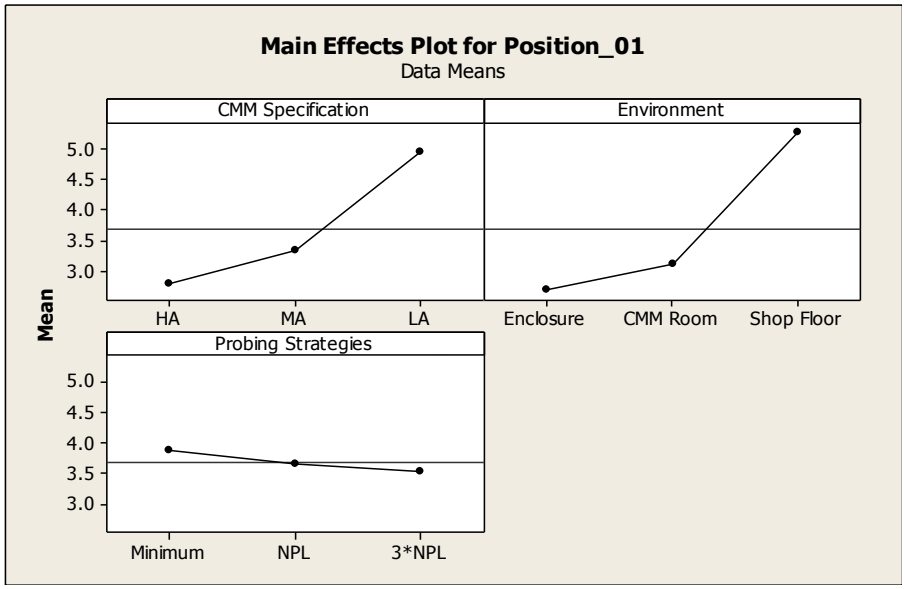

Figure 39 Main effects plot for position measurement

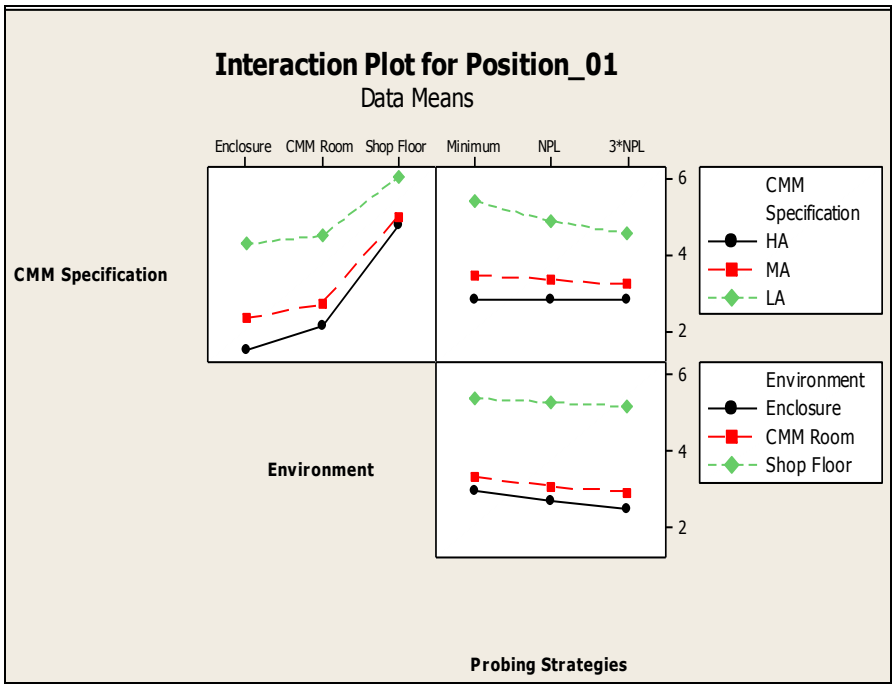

Figure 40 Main effects plot for position measurement

Figure 37 and Figure 39 show the main effects of the uncertainty factors on measuring diameter tolerance and position tolerance respectively. The plots reveal how a single factor will affect measurement uncertainty. For both diameter measurement and position measurement, the uncertainty increases as the CMM machine gets 'worse' and the thermal environment losses its control. On the other hand, the measurement

uncertainty decreases as the sampling points are intensified. The results are in accordance with the general rules of measurement practice.

Moreover, Figure 37 and Figure 39 show the influence power of the uncertainty factors in a quantitative way. For example, for the diameter measurement in Figure 37, the variability of main effect for the Environment factor is significantly bigger than the ones for the CMM Specification factor and the Probing Strategy factor. It suggests that the thermal environment has a greater influence on measurement uncertainty than the other uncertainty factors. By further comparison, we can rank the influence powers of the uncertainty factors as below:

$$"Environment" \succ "CMM\_Specification" \succ "Sampling\_Power"$$

This analytical result is consistent with the experiences of CMM measurement experts. It quantitatively shows how to control the uncertainty factors in order to minimize the measurement uncertainty. So when facing multiple yet limited choices of improving CMM measurement process, measurement engineers can reference the analytical result, and then decide how to control the measurement uncertainty contributors.

Figure 38 and Figure 40 respectively show the interactions of the uncertainty factors on measuring the diameter and the position. The interaction plots display the combined effects of the two factors on the measurement uncertainty. They provide the comparison between two uncertainty factors without accounting the third factor's effect, and hence give further guidance to measurement engineers to prioritize the choices of improving CMM inspection systems.

The Figure 38 and Figure 40 also show that thermal environment has the greatest influence on the measurement uncertainty. Additionally, more details of the factorial influences are shown up. For example, by examining the combined effect of CMM Specification and Sampling Strategy (in the top right box in), it can be concluded that the Sampling Strategy has very small effect on the measurement uncertainty when using a high-accuracy CMM machine, while still having a clear impact when using a low-accuracy CMM. It suggests that when using a high-accuracy CMM, the number of sampling points can be reduced, which consequently saves measurement time and improves production efficiency.

Although Figure 38 and Figure 40 indicate similar trends, there are still nuances exhibited in the two figures. The nature of the tolerance feature also has effect on the measurement uncertainty. For example, the three curves in the top right box in Figure 38 get very close at the end. These curves represent the combined effect of CMM Specification and Sampling Strategy when measuring the diameter. It suggests that for the diameter measurement, improving the number of sampling points can reduce the measurement uncertainty to a level close to which by improving the accuracy of CMM machine. The same effect does not reveal in the case of position measurement (the top right box in Figure 40). Measurement engineers need to take into account the types of features of the part, and then decide to purchase a new CMM machine or simply improve the sampling strategy.

The initial DOE analysis of the simulation results has shown promising results. The analysis results have certain logic coherence with the common understanding on CMM measurement process. Given the DOE analysis results, a framework to integrate the digital and physical environments is proposed in the next section.

5.4 Design of a generic framework to compare digital and physical measurement environments

The contradiction between the nature of task-specific measurement uncertainty and the diversity of CMM measurement tasks prevents the integration of digital and physical measurement environments. To solve the problem, a generic framework, is proposed, aiming to compare the two measurement environments (as shown in Figure 41). The framework employs Design of Experiments (DOE) techniques to process the post-measurement data sets, and evaluates the influence of measurement uncertainty contributors.

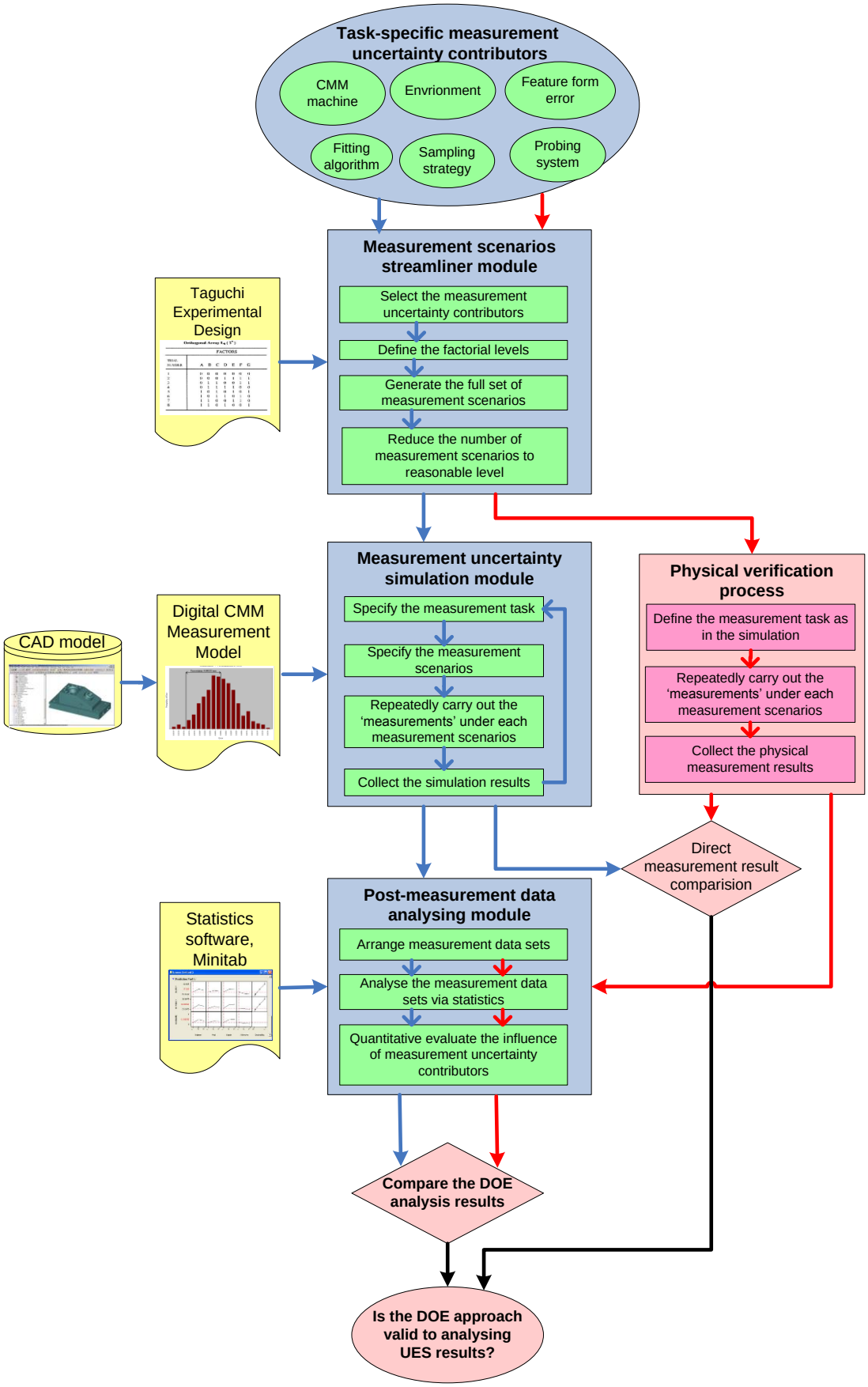

Figure 41 A Measurement Planning and Implementation Framework to Compare Digital and Physical Measurement Uncertainty

As shown in Figure 41, the entire framework is composed of three domains, which are the digital measurement environment (blue in Figure 41), the physical measurement environment (red in Figure 41) and the external resources (yellow in Figure 41) respectively. The blue arrows represent the operations flow in the digital environment, while the red arrows represent the operations flow in the physical environment. The details of the digital and physical measurement flows and the comparison methods are described separately in the following sub-sections.

5.4.1 The 'Task-specific Measurement Uncertainty Contributors'

The working flow starts from collecting the measurement uncertainty contributors. Six major uncertainty contributors are considered by the digital CMM model. These uncertainty contributors include CMM machine, thermal environment, feature form error, probing system, sampling strategy and fitting algorithm.

5.4.2 The 'Measurement Scenario Streamliner' module

The 'Measurement Scenario Streamliner' module collects the measurement uncertainty contributors. The end-user can select the uncertainty contributors (control factors) needed and define their factorial levels given the measurement aim. The combinations of the selected uncertainty contributors and their factorial levels create a full set of measurement scenarios.

The 'Taguchi Orthogonal Array' (shown in yellow in Figure 41) is deployed in the 'Measurement Scenario Streamliner' model to reduce the number of measurement scenarios to a reasonable level. The Taguchi DOE method and its implementation are described in sub-sections 5.5.2 and 5.6.1.

The 'Measurement Scenario Streamliner' module outputs the measurement scenarios, given which the digital and physical measurements are carried out. After the 'Measurement Scenario Streamliner' module, the measurements are carried out respectively in the digital measurement environment and the physical measurement environment, where the task-specific measurement uncertainties are obtained.

5.4.3 The ‘Measurement Uncertainty Simulation’ module

The ‘Measurement Uncertainty Simulation’ module represents the measurements carried out in digital environment.

The Module receives measurement scenarios information from the ‘Measurement Scenario Streamliner’ module. Meanwhile, it perceives the feature-based design information from the product CAD-model, and employs a standing-alone digital CMM model to calculate the task-specific measurement uncertainty (shown in yellow in Figure 41).

The Module integrates the above information, and allows the end-user to define the details of digital measurements. Measurement tasks are specified given product design information, and measurement scenarios are further clarified in the digital CMM model. Then digital measurements are repeatedly carried out under each measurement scenario. The digital measurement simulates CMM measurement process and runs Monte-Carlo simulation. The output of the Module is a set of the task-specific measurement uncertainty calculated by the digital CMM model under the selected measurement scenarios.

5.4.4 The ‘Physical Verification Process’

The ‘Physical Verification Process’ module represents the CMM measurements which are carried out in physical environment. The physical measurements are carried out as close as in the digital environment. Therefore, the Physical Verification Process includes similar operations as in the ‘Measurement Uncertainty Simulation’ module. The Physical Verification Process includes:

- Define measurement task as in the digital environment;
- Repeatedly carry out measurements under each measurement scenario;
- Collect the physical measurement results.

The output of the ‘Physical Verification Process’ is a set of measurement uncertainties of selected measurement scenarios in the physical measurement environment..

Both of the digital and physical measurement results are collected for comparison and verification.

5.4.5 The 'Post-Measurement Data Analyzing' module

The 'Post-Measurement Data Analyzing' module receives the measurement result data sets from both of digital measurements and physical measurements.

The Module collects the measurement results from the digital or physical environments. It employs professional statistics software, Minitab, to run the Design of Experiments (DOE) analysis, and obtains the DOE analysis results of the digital measurement and physical measurement respectively. The details of DOE method and implementation are described in subsections 5.5.2 and 5.6.3.

The outputs of the Module are a set of main effect plots, which represent influence levels of uncertainty contributors for the defined measurement task.

5.4.6 Comparison

In order to verify the simulation performance, the digital and physical measurement results are compared. Noticeably, there are two sets of measurement results obtained from the above measurement activities. One is the direct measurement results, and the other one is the DOE analysis results. The comparison of direct measurement results assesses the capability of the digital CMM model in predicting the task-specific measurement uncertainty. The comparison of DOE analysis results assesses the capability of the DOE approach on evaluating the influence of measurement uncertainty contributors. Consequently, it provides the verification of the digital CMM measurement model in the physical environment.

The digital and physical operation flows are described in details in the next two sections respectively.

5.5 Overview of framework methodologies

The measurement planning and implementation framework described in Section 5.4 is a robust framework deployed with several methodologies in metrology, statistics and software engineering. In this section, the principles of these methodologies are explained and further introduced.

5.5.1 Task-specific measurement uncertainty contributors

Task-specific measurement uncertainty is the measurement uncertainty of measuring a specific feature using a specific measurement strategy [13]. The definition of 'task-specific measurement uncertainty' addresses the traceability of measurement, and consequently facilitates the importance of the measurement uncertainty contributors. To determine the measurement uncertainty, it is vital to indentify the measurement uncertainty contributors prior to executing measurement.

In our research, we have considered six measurement uncertainty contributors, which are CMM machine, environment (temperature), feature form error, fitting algorithm, sampling strategy and probing system respectively. There are 4 reasons of selecting these measurement uncertainty contributors:

- Importance: these six factors have significant influence on CMM measurement uncertainty;
- Independence: the six factors are relatively independent from each other[*];
- Operation: the effects of the six factors can be validated in the laboratory environment;
- Manageable: the selection of the six factors is consistent with the research focus and expertise.

It is noticeable that the selection of measurement uncertainty contributors is expandable. The selection can be beyond the ones proposed. The CMM measurement planning and implementation framework proposed in this research is expected to be applicable in more sophisticated measurement scenarios which includes a broader diverse of measurement uncertainty factors.

[*] The independence of the factors will be quantitatively analyzed.

5.5.2 'Measurement Scenario Streamliner' module: Taguchi experimental design

'Taguchi experimental design' is deployed in the 'Measurement Scenario Streamliner' module. In classically designed experiments, the primary goal is to identify factors that affect the mean response and control them to desirable levels. Taguchi focuses on reducing variability, as well as setting the mean to target.

In Taguchi design of experiments, the control factors and their factorial levels are firstly defined. The combination of the control factor and the factorial levels settings produce a large number of experimental scenarios, which is possibly too high to be practiced in the laboratory environment. To reduce the number of experimental runs, the Taguchi Orthogonal Array is used.

The 'Taguchi orthogonal arrays' is a methodology of designing experiments that usually requires only a fraction of the full factorial combinations. Figure 42 shows a 'Taguchi Orthogonal Array Selector'. The column of 'Taguchi Orthogonal Array Selector' is the number of experimental factors, and the row is the number of factorial levels.

Number of Levels	Number of Parameters (P)																														
	2	3	4	5	6	7	8	9	10	11	12	13	14	15	16	17	18	19	20	21	22	23	24	25	26	27	28	29	30	31
2	L4	L4	L8	L8	L8	L8	L12	L12	L12	L12	L16	L16	L16	L16	L32	L32	L32	L32	L32	L32	L32	L32	L32	L32	L32	L32	L32	L32	L32	L32
3	L9	L9	L9	L18	L18	L18	L18	L27	L27	L27	L27	L27	L36	L36	L36	L36	L36	L36	L36	L36	L36	L36								
4	L'16	L'16	L'16	L'16	L'32	L'32	L'32	L'32	L'32																					
5	L25	L25	L25	L25	L25	L50	L50	L50	L50	L50	L50																			

Figure 42 Taguchi Orthogonal Array Selector [132]

Given to experimental factors selected, their factorial levels and 'Taguchi Orthogonal Array Selector', an appropriate orthogonal array is selected. Each column in the orthogonal array represents a specific factor with two or more levels. Each row represents a run; the cell values indicate the factor settings for the run. An orthogonal array allows the design to be balanced so that factor levels are weighted equally. Because of this, each factor can be evaluated independently of all the other factors, so the effect of one factor does not influence the estimation of another factor [132].

An example of Taguchi design of experiment is given in Appendix B.

5.5.3 Measurement Uncertainty Simulation module: the simulation-by-constraints method

The simulation-by -constraints method is deployed in the Digital CMM model, which allows the 'Measurement Uncertainty Simulation' module to generate measurement uncertainty. The simulation-by-constraints method has been reviewed in the Chapter 2 – Literature Review as one of four major simulation methods for evaluating task-specific measurement uncertainty.

The simulation-by-constraints method starts with populating a large amount of virtual CMMs, each of which has a random error state. Each virtual CMM is characterized by the 21 parametric errors. Theoretically the data sets which describe the virtual CMMs states could be infinite. But in practice, the random error state is "limited" by physical CMM calibrated results. For example, a CMM calibration result shows that the largest error of measuring a calibrated step gauge along the X-axis is 10μm, it is unlikely the X-axis scalar error of the CMM machine is significantly larger than 10μm.

Therefore, the large amount of virtual CMMs reasonably represents the complete state space of the CMM. This data set, which describes the virtual CMM states, is bounded by a bounding measurement set, which is a set of actual measurement results of certain reference length (e.g. a step gauge). The virtual CMMs carry out measurements on the bounding measurement set. If the virtual CMM state shows the same errors as the complete bounding measurement set, the virtual CMM is retained. Otherwise it is rejected. Majority of the virtual CMM states are rejected, and only a

few are retained. The retention rate is between 0.01% and 0.00001%. Consequently, the bounding measurement set defines a bounded area containing 'good CMM states'. Each of the 'good CMM states' could be the true state of the CMM during measurement process.

Figure 43 illustrates an idealized machine which has only two error sources denoted as α and β respectively. 'SBC' is short for 'simulation-by-constraints', and 'FPS' is short for 'full-parametric simulation'. Figure 43 shows the bounded region resulting from the simulation-by-constraints method is much larger than that from the full-parametric simulation method. If a very extensive bounding measurement set is used, the bounding region from the simulation-by-constraints method will be the same as the one with the full-parametric method.

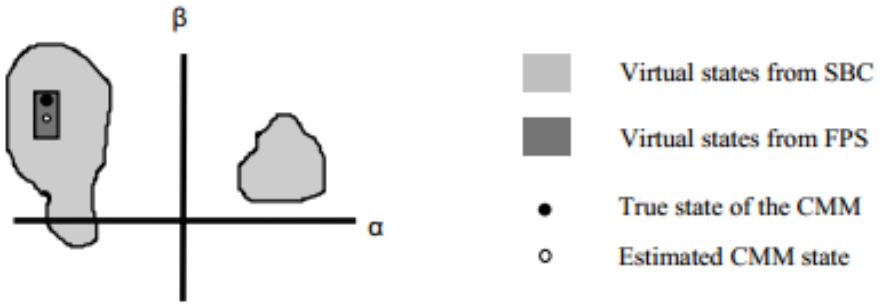

Figure 43 Schematic of the simulation-by-constraints method

The advantage of the simulation-by-constraints method can work with incomplete information of the CMM, whereas the full-parametric simulation requires a complete description of CMM state. The simulation-by-constraints method does not require a full error-mapping of CMM machine. The only requirement is that sufficient measurements are taken to obtain bounding measurement set.

There are three reasons why the simulation-by-constraints method is selected to be deployed in the Measurement Planning and Implementation Framework:

- The simulation-by-constraints method calculates the influences of the constraints on task-specific measurement uncertainty. This is consistent with the expected outcomes of Taguchi experimental design;

- Compared to the other simulation methods, the simulation-by-constraints method does not require full parametric error-mapping of the CMM machine, which is time-consuming and laborious to obtain. Using the simulation-by-constraints method in the Framework can potentially reduce the workload of the metrology engineers, if the Framework is validated;
- The simulation-by-constraints method is available in the laboratory resources.

5.6 Overview of framework implementation

The implementation of the Measurement Planning and Implementation Framework described here has been carried out in the digital and physical environments. In the digital environment, the Framework is implemented by using commercially-available software to determine task-specific measurement uncertainty and generate statistical analysis result. In the physical environment, physical measurements are carried out in the finely-controlled testing environment in collaboration with the National Physical Laboratory (NPL), UK. This section describes the key stages of the Framework implementation.

5.6.1 Measurement uncertainty generation using the simulation software

The primary objective of the Framework implementation is to generate task-specific measurement uncertainty in the digital environment. Therefore, the digital environment needs to have the following capabilities:

- Able to provide a CMM task-specific measurement simulation environment;
- Able to carry out the simulation-by-constraints approach;
- Able to calculate measurement uncertainty.

Given the above considerations, the SolidWorks and PUNDIT/CMM software package have been deployed to assist the Framework implementation.

The SolidWorks (coloured in green in Figure 44) is a commercial software package allowing feature-based design in the digital environment [133]. The workpiece CAD-model is created in SolidWorks, and converted into DMIS-coded file allowing the CAD-model to be accepted by the digital CMM model.

PUNDIT/CMM (coloured in blue in Figure 44) has a built-in database of common CMMs. It imports the CAD-model of a workpiece, and provides options allowing the user to establish the CMM measurement tasks, e.g. selecting a CMM, formulating feature form error, defining measurement plan [131]. The measurement uncertainty calculation is based on the simulation-by-constraints approach of NIST [131]. Monte Carlo simulation is also utilized to calculate the probability distribution of the simulated measurement results [22]*.

Given the research aim and the capability of PUNIT/CMM, the implementation plan of the Framework is designed and shown in Figure 44. It has three domains, which are, 'Task-specific Measurement Uncertainty Generation Flow', 'PUNDIT Operation Flow', and 'Supporting CAD/CAM Design Software', respectively.

The central domain of the implementation plan is the 'Task-specific Measurement Uncertainty Generation Flow'. It is in the centre of Figure 44 and is highlighted in red. The aim of the central domain is to generate task-specific measurement uncertainty in the digital environment. It has five elements repenting the key steps of CMM measurement. Over the operation of the 'Task-specific Measurement Uncertainty Generation Flow', the elements trigger the external applications, SolidWorks and PUNDIT/CMM, to realize the functionalities. The details of the five elements are presented in the following paragraphs.

* The working principle and operation flow of PUNDIT/CMM can be referenced from the previous Chapter.

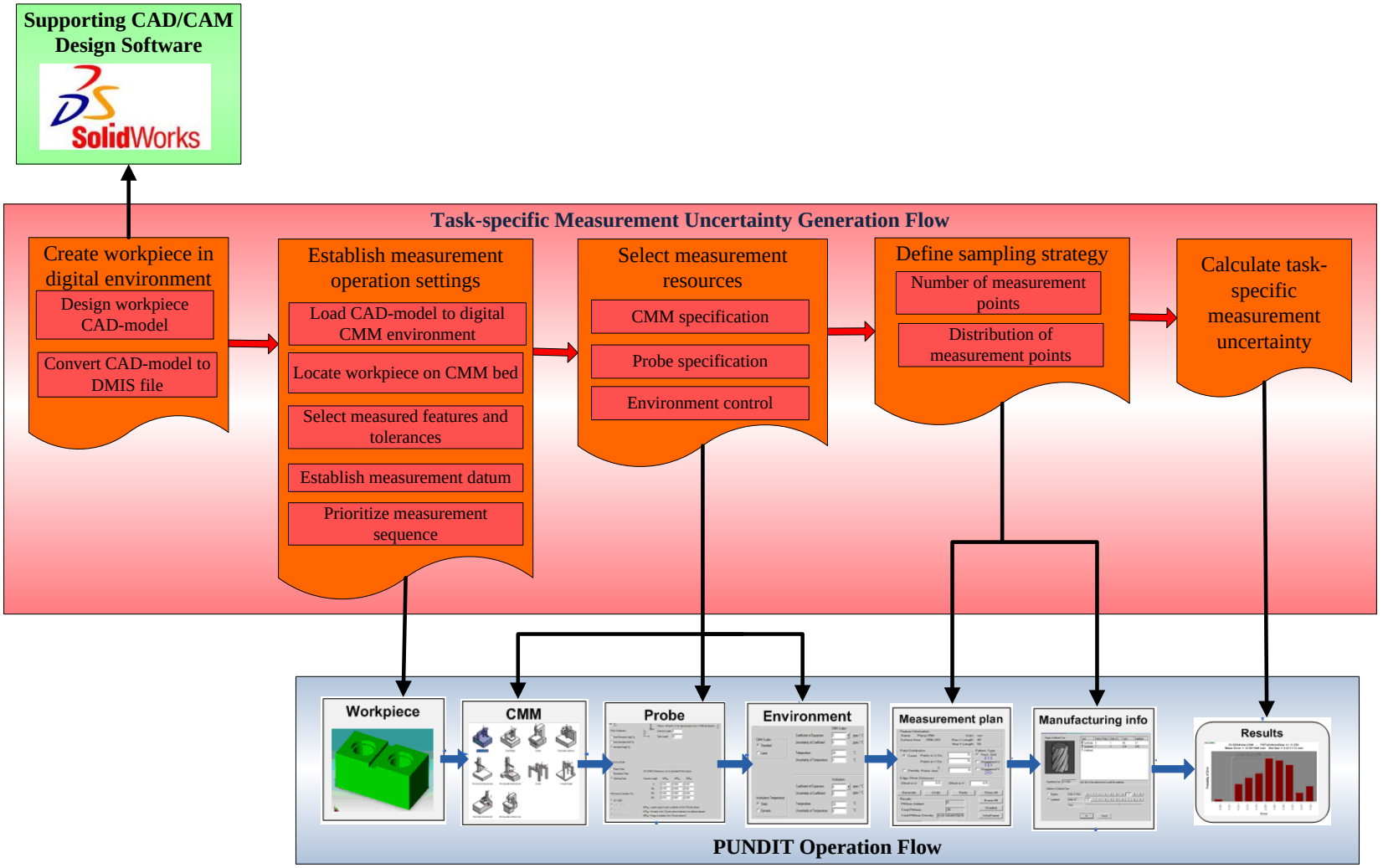

Figure 44 The Implementation plan to generate measurement uncertainty in digital environment

- *Create workpiece in digital environment:*

  This element has two functions, which are to create workpiece CAD-model and to convert the CAD-model into DMIS format. The element triggers the supporting CAD/CAM software, the SolidWork, to realize these two functions. The CAD-model of the measured part, including its dimension and geometry information, is created in the SolidWork, and converted into DMIS-coded file allowing the CAD-model to be accepted by the digital CMM model.

- *Establish measurement operation settings:*

  This element allows end-users to establish background information of measurement operations in the digital CMM model. It has five functions, including 'load CAD-model into the digital CMM environment', 'locate workpiece on CMM bed', 'select measured features and tolerance', 'establish measurement datum' and 'prioritize measurement sequence'. These functions are achieved by the 'Workpiece' tab in PUNDIT/CMM. The workpiece CAD-model is loaded into the PUNDIT/CMM environment, where the initial measurement operation settings are established.

- *Select measurement resources:*

  This element allows end-users to characterize measurement resources in the digital CMM model. It has three functions, including defining 'CMM specification', 'probe specification' and 'environment control' respectively. To achieve these functions, the element triggers the CMM tab, the Probe tab and the Environment tab in the PUNDIT/CMM. The information relating CMM measurement resources is implemented into the digital measurement environment.

- *Define sampling strategy:*

  This element allows end-users to establish the sampling strategy on features to be measured. It has two functions, including defining 'number of measurement points' and 'distribution of measurement points'. The element triggers the Measurement

Plan tab and the Manufacturing Info tab to realize the above functions. The sampling strategy of CMM measurement is implemented into the digital measurement environment.

- *Calculate the task-specific measurement uncertainty:*

  At last, the simulation-by-constraints is performed in the digital CMM model. The task-specific measurement uncertainty is generated in the digital environment.

5.6.2 Determining the uncertainty of physical measurements

Determining uncertainty in the physical environment is vital for verifying the digital part of the Measurement Planning and Implementation Framework. To ensure the scientific correctness of the physical measurement results, the physical measurement experiments are designed and executed in collaboration with the metrology scientists from National Physical Laboratory (NPL), where the measurement environments are finely controlled, and the measurement instruments are deliberately calibrated and maintained (Figure 45).

Figure 45 Finely-controlled measurement environment in NPL [134]

The fundamental of performing physical measurements is to ensure that the physical measurement tasks are as close as the ones in the digital environment. To achieve this objective, the physical measurement tasks have been deliberately designed by assessing the available resources and capability.

More details of performing the physical measurement are presented in the Chapter 6.

5.6.3 Evaluating the influence levels of uncertainty contributors

The influence levels of the uncertainty contributors are quantitatively evaluated through Taguchi experimental design. Statistical analysing software, Minitab, is utilized to carry out the Taguchi statistical calculation and to implement the evaluation algorithm into the Measurement Planning and Implementation Framework.

The implementation procedures have been carried out in seven steps as shown in Figure 46. The details of the implementation procedures are explained in the following paragraphs. The tests of the implementation will be discussed in the next chapter.

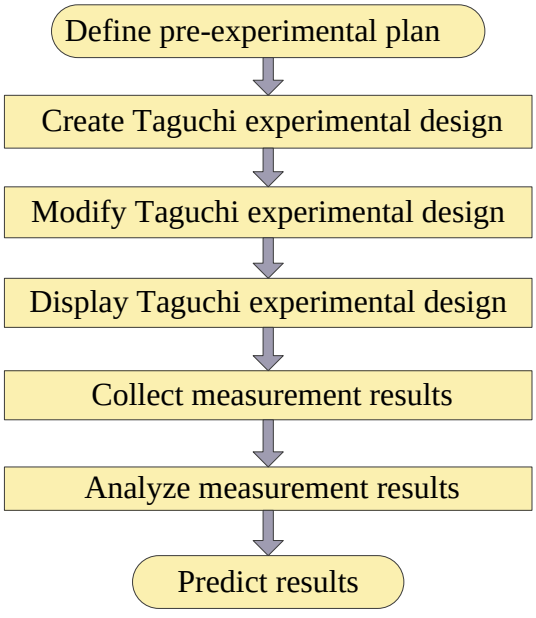

Figure 46 Steps of implementing Taguchi experimental design method

♦ *Define pre-experimental plan:*

Prior to carrying out the experiment, a plan is defined. The plan includes the control factors and their factorial levels. The uncertainty contributors are selected as the control factors in Taguchi experimental design, and their factorial levels are defined given to the measurement environments and the measurement tasks. The combinations of control factors and their factorial levels create a set of measurement scenarios.

♦ *Create Taguchi experimental design:*

In order to streamline the number of measurement scenarios, Taguchi experiment design is created as shown in Figure 47. The appropriate Taguchi orthogonal array is selected given to the number of control factors and the factorial levels defined in the previous step.

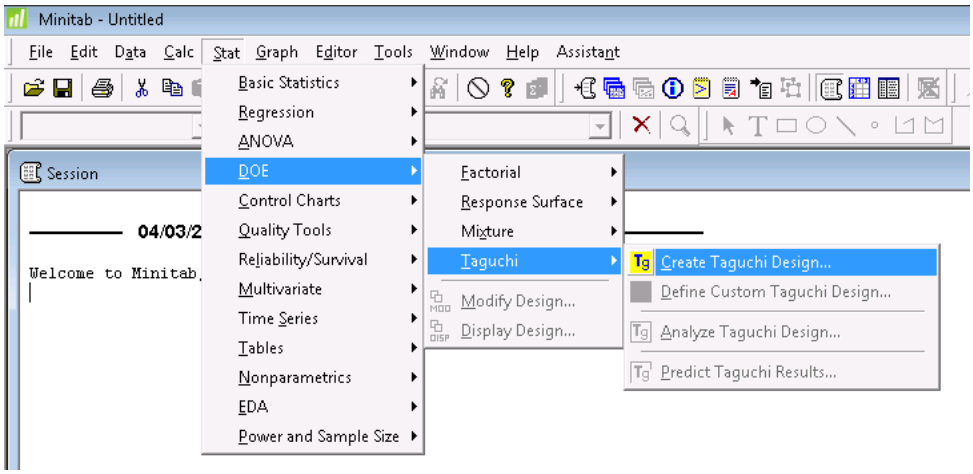

Figure 47 Create Taguchi experimental design

♦ *Modify Taguchi experimental design*:

The Taguchi experimental design is further modified as shown in Figure 48. The control factors are assigned to the names of the selected measurement uncertainty contributors of the CMM measurement tasks. The values of the factorial level are added to the existing control factors.

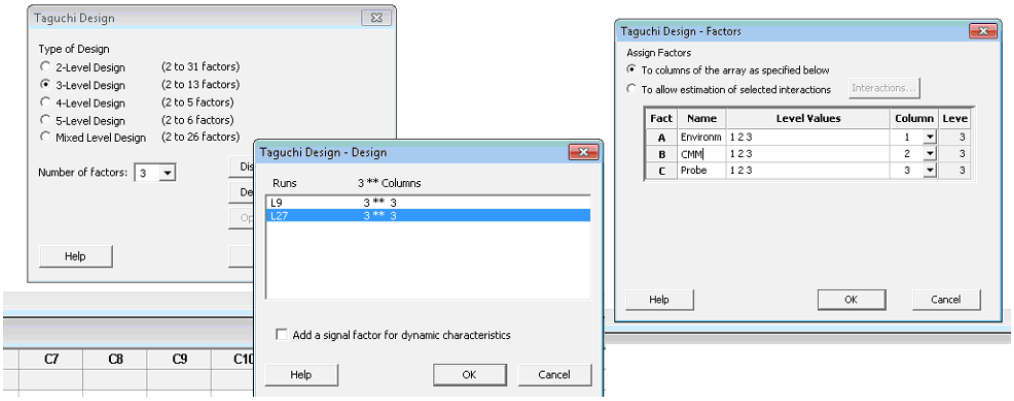

Figure 48 Modify Taguchi experimental design

♦ *Display Taguchi experimental design:*

Then the Taguchi experiment design is generated in the statistical software, as shown in Figure 49. The streamlined measurement scenarios are displayed as a Minitab worksheet. The rows of the worksheet show the uncertainty contributors, and the columns show the settings of the measurement scenarios after being applied Taguchi Orthogonal Arrays.

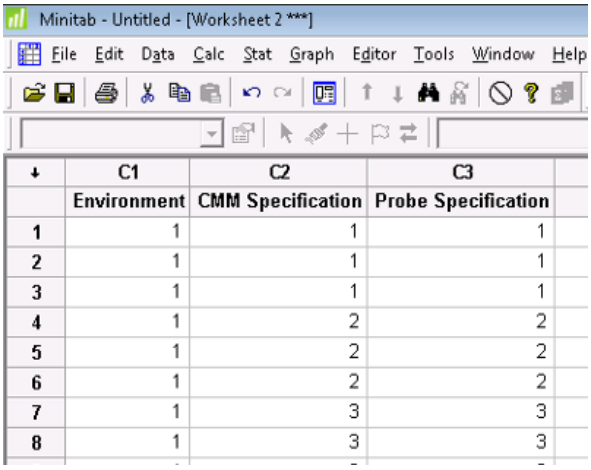

	C1	C2	C3
	Environment	CMM Specification	Probe Specification
1	1	1	1
2	1	1	1
3	1	1	1
4	1	2	2
5	1	2	2
6	1	2	2
7	1	3	3
8	1	3	3

Figure 49 Display Taguchi experimental design

♦ *Collect measurement results*:

The digital measurements are performed in the digital CMM mode. The measurement results are collected, and then entered into the Minitab worksheet as shown in Figure 50. These measurement results are the task-specific measurement

uncertainties attained from the digital or physical measurements. The worksheet is stored in data collection for the uncertainty analysis.

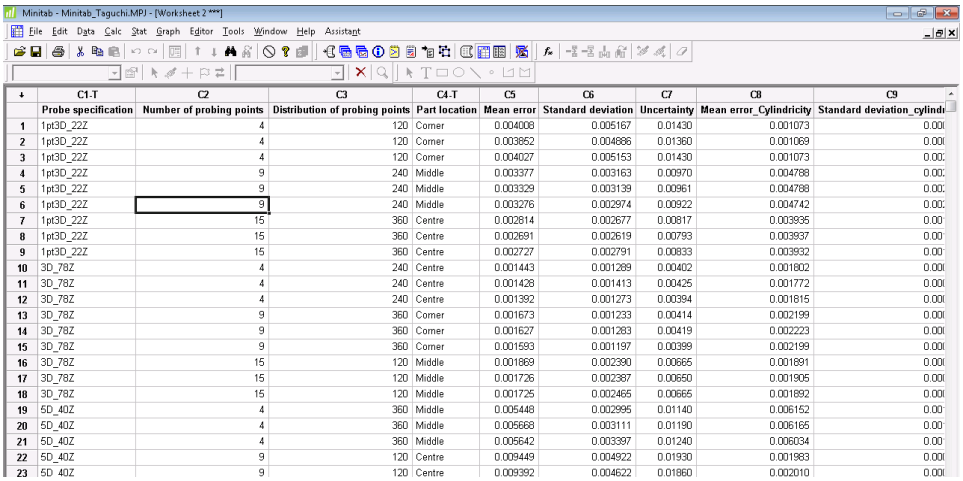

Minitab - Minitab_Taguchi.MPJ - [Worksheet 2 ***]

File Edit Data Calc Stat Graph Editor Tools Window Help Assistant

	C1-T	C2	C3	C4-T	C5	C6	C7	C8	C9
	Probe specification	Number of probing points	Distribution of probing points	Part location	Mean error	Standard deviation	Uncertainty	Mean error_Cylindricity	Standard deviation_cylindr
1	1pt3D_22Z	4	120	Corner	0.004008	0.005167	0.01430	0.001073	0.000
2	1pt3D_22Z	4	120	Corner	0.003852	0.004886	0.01360	0.001069	0.000
3	1pt3D_22Z	4	120	Corner	0.004027	0.005153	0.01430	0.001073	0.000
4	1pt3D_22Z	9	240	Middle	0.003377	0.003163	0.00970	0.004788	0.000
5	1pt3D_22Z	9	240	Middle	0.003329	0.003139	0.00961	0.004788	0.000
6	1pt3D_22Z	9	240	Middle	0.003276	0.002974	0.00922	0.004742	0.000
7	1pt3D_22Z	15	360	Centre	0.002814	0.002677	0.00817	0.003935	0.000
8	1pt3D_22Z	15	360	Centre	0.002691	0.002619	0.00793	0.003937	0.000
9	1pt3D_22Z	15	360	Centre	0.002727	0.002791	0.00833	0.003932	0.000
10	3D_78Z	4	240	Centre	0.001443	0.001289	0.00402	0.001802	0.000
11	3D_78Z	4	240	Centre	0.001428	0.001413	0.00426	0.001772	0.000
12	3D_78Z	4	240	Centre	0.001392	0.001273	0.00394	0.001815	0.000
13	3D_78Z	9	360	Corner	0.001673	0.001233	0.00414	0.002199	0.000
14	3D_78Z	9	360	Corner	0.001627	0.001283	0.00419	0.002223	0.000
15	3D_78Z	9	360	Corner	0.001593	0.001197	0.00399	0.002199	0.000
16	3D_78Z	15	120	Middle	0.001869	0.002390	0.00665	0.001891	0.000
17	3D_78Z	15	120	Middle	0.001726	0.002387	0.00650	0.001905	0.000
18	3D_78Z	15	120	Middle	0.001725	0.002465	0.00665	0.001892	0.000
19	5D_40Z	4	360	Middle	0.005448	0.002995	0.01140	0.006152	0.000
20	5D_40Z	4	360	Middle	0.005668	0.003111	0.01190	0.006165	0.000
21	5D_40Z	4	360	Middle	0.005642	0.003397	0.01240	0.006034	0.000
22	5D_40Z	9	120	Centre	0.009449	0.004922	0.01930	0.001983	0.000
23	5D_40Z	9	120	Centre	0.009392	0.004622	0.01860	0.002010	0.000

Figure 50 Collect the data

♦ *Analyze measurement results*:

After collecting experiment data, the measurement results are analysed as shown in Figure 51. The analysis generates main effects and interaction plots of the S/N ratios, means versus the control factors, and displays response tables and linear model results for S/N ratios and means.

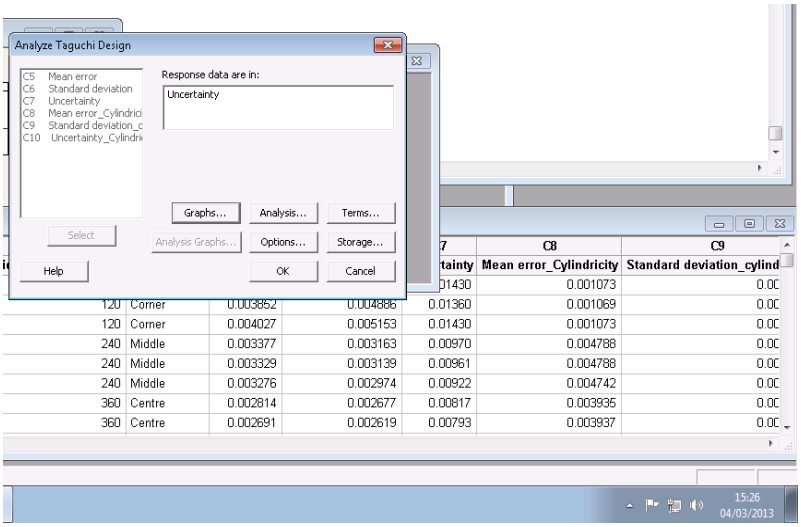

Figure 51 Analyze the data

- *Predict results*:

  Finally analysis results are generated. Analysis results indicate influence levels of uncertainty contributors, and how the factors affecting the measurement process are determined

By following the above steps, the algorithm which evaluates the influence levels of measurement uncertainty contributors is implemented into the Measurement Planning and Implementation Framework.

5.7 Chapter summary

The integration between digital and physical measurement environments is a critical challenge for the CMM measurement planning and modelling. The complexity of the CMM measurement tasks encounters against the fundamental concept of task-specific uncertainty simulation model.

In this chapter, the limitations of the task-specific uncertainty simulation model have been discussed. A full-factorial design has been performed to quantitatively compare the influences of the uncertainty factors. Though not being scientifically verified in the physical measurements, the DOE analysis results reveal certain agreement with the physical CMM measurement reality. Based on this, a Measurement Planning and Implementation Framework is proposed to analyze and integrate digital and physical measurement uncertainty. The mathematical modelling methodologies deployed in the Framework are deliberately investigated and extensively described. The details of implementation of individual modules of the Framework are presented.

Chapter 6 Experimental Work to Validate the Framework

The Measurement Planning and Implementation Framework has been proposed in the Chapter 5. It is a theoretical framework aiming to provide closer integration between digital and physical measurement environments. In this chapter, the step by step implementation of the proposed framework will be described. The experimental work is designed and performed to validate the theoretical framework.

6.1 Overall experiment plan

Given the aim and procedures of the Measurement Planning and Implementation Framework, this validation work has been designed. A set of experiments has been planned, and the overall experiment plan is presented in Figure 52.

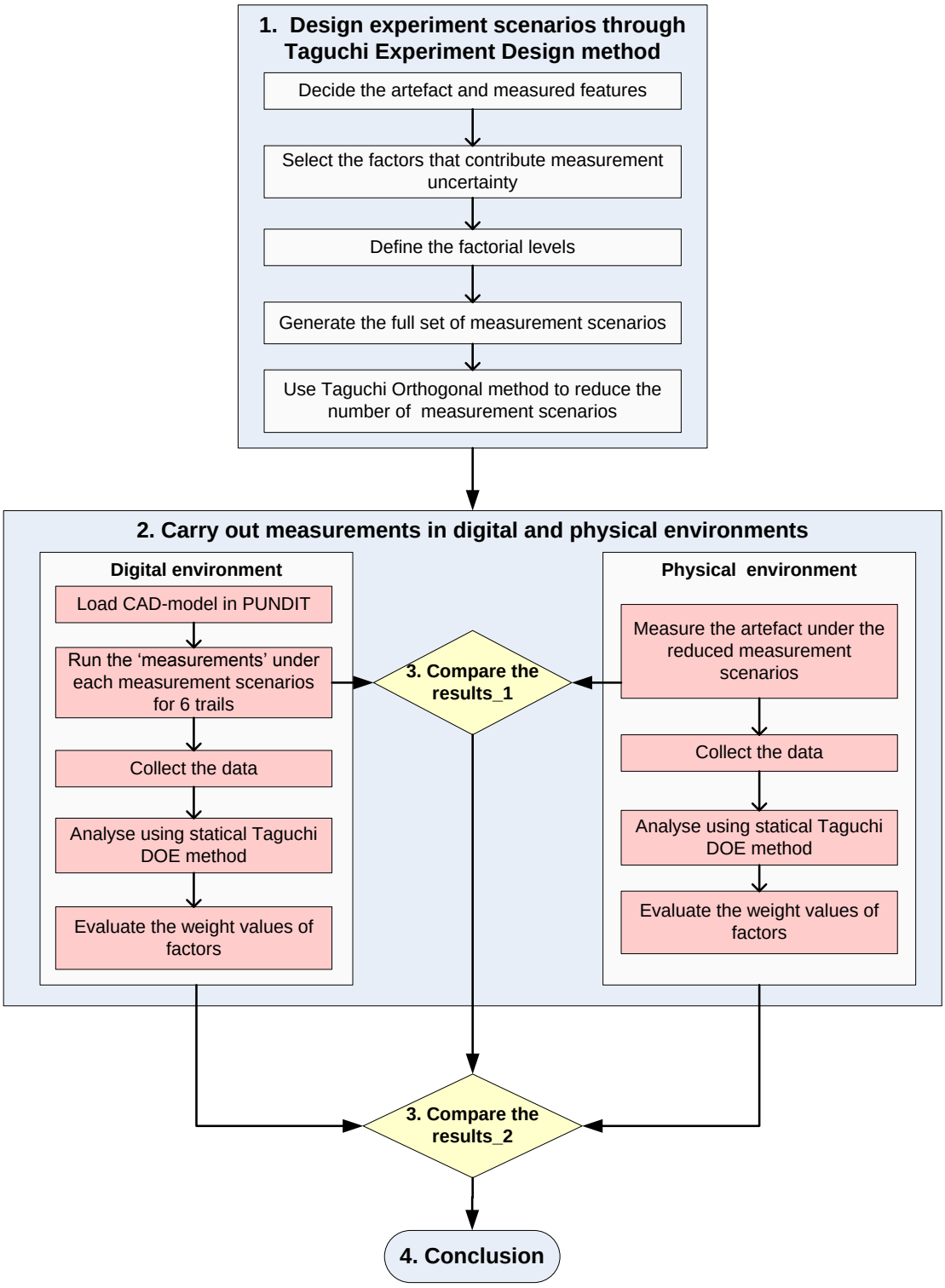

Figure 52 Overall experiment plan

As illustrated in Figure 52, the validation work is planned with four work packages. These four work packages are:

1) *Design experiment scenarios through Taguchi Experiment Design method:* The

part is created, and features to be measured are selected. The measurement uncertainty contributors are identified, which are ‘probe specification’, ‘number of probing points’, ‘distribution of probing points’ and ‘part location’. Each of the measurement uncertainty contributors are assigned with three factorial levels. The combination of measurement uncertainty contributors and the factorial levels produces a large number of measurement scenarios. The appropriate measurement scenarios are selected by applying the Taguchi Orthogonal Array method.

2) *Carry out measurements in the digital and physical environments:* The digital and physical measurements are carried out simultaneously. In the digital environment, the part CAD-model is loaded into a digital CMM model. The digital CMM model performs virtual measurements under the selected measurement scenarios, and predicts task-specific measurement uncertainties. The digital CMM model runs six trials for each measurement scenario. The simulation results are collected and analyzed statistically according to the Taguchi Experiment Design method. In the physical environment, physical measurements are carried out using the selected measurement scenarios. The physical measurements are planned to be conducted in the finely-controlled laboratory environment. So that the physical measurements can be performed in a manner that allows good simulation fidelity. The physical measurement results are collected and analyzed to determine the influences of measurement uncertainty contributors.
3) *Compare the results:* two comparisons are carried out. Firstly, the digital measurement results and the physical measurement results are compared directly under respective measurement scenarios. This is an obvious method of examining the validity of an uncertainty statement produced by computer simulation. Secondly, the DOE analysis results derived from the digital and physical experiments are compared. This comparison examines the validity of deploying the Taguchi Experiment Design approach into the post-measurement data processing as proposed in the Framework.
4) *Conclusion:* a conclusion is drawn from the experimental work. The validity of the Framework is discussed.

The experimental activities are performed according to the above experimental plan. The following sections respectively present the technical details of carrying out the experimental activities, including

- The experimental procedures in the digital measurement environment;
- The experimental procedures in the physical measurement environment;
- Data collection and experimental result analysis;
- Comparison between physical measurement results and digital measurement results.

6.2 Experiment procedures in the digital environment

The digital measurements are carried out simultaneously with the physical measurements. The experimental procedures in the digital environment are designed based on the needs of validating the digital CMM model and the Taguchi Experiment Design method, but also considering the availability of the physical measurement resources. The following sub-sections respectively present the key technical procedures of carrying out the digital measurement. These key technical procedures include:

- Define the part and features to be measured;
- Arrange the measurement process in the digital CMM model;
- Select the measurement uncertainty factors and their factorial levels;
- Reduce the number of measurement scenarios using the Taguchi Orthogonal Array method.

6.2.1 Define the part and features to be measured

One of the most direct methods of examining the validity of the digital measurement model is to measure calibrated artefacts [124]. Using calibrated artefacts can provide good simulation fidelity to the physical measurement environment. ISO 15530-4 suggests using calibrated artefacts in the physical measurement to test the performance of measurement uncertainty simulation software [67]. In previous research, ring gauges

have been frequently used to validate the performance of CMM task-specific measurement uncertainty software [22].

A ring gauge is selected to be the measurand in this research. To execute the measurement in the digital CMM model, the following steps are taken:

1) *Create a CAD model of the ring gauge:*

The CAD model of the ring gauge is created as shown in Figure 53. The CAD model is transformed into DMIS-formatted file in order to be comprehended by the CMM measurement model.

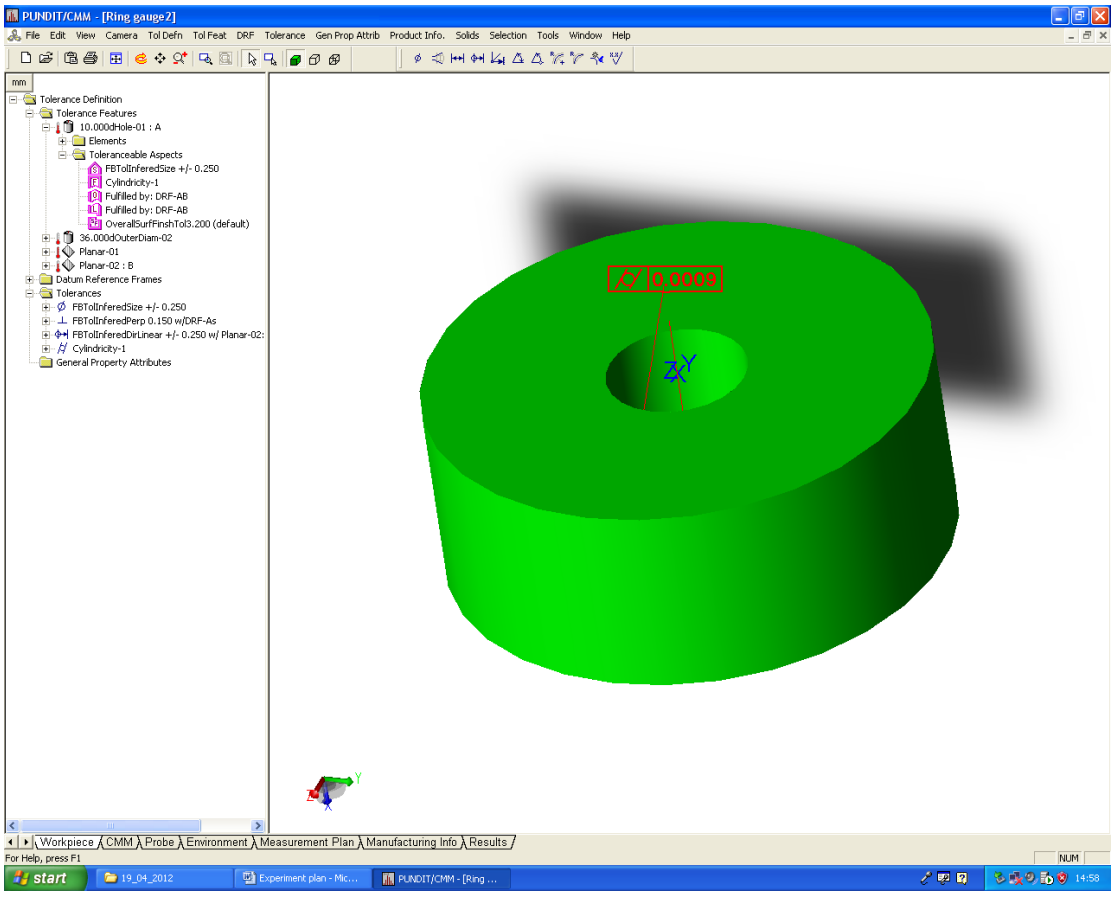

Figure 53 CAD-model of the ring gauge

2) *Define the specification of the ring gauge:*

The design specifications of the ring gauge are defined. Figure 54 illustrates the technical drawing of the ring gauge, and

lists the technical specifications of the ring gauge. The ring gauge is made of steel. The tolerance grade of the ring gauge is AA (+0.10μm to −0.05μm). This tolerance grade allows the form error of the ring gauge could be ignored. The inner and outer diameters of the ring gauge are 10mm and 26mm respectively. The thickness of the ring gauge is 14mm.

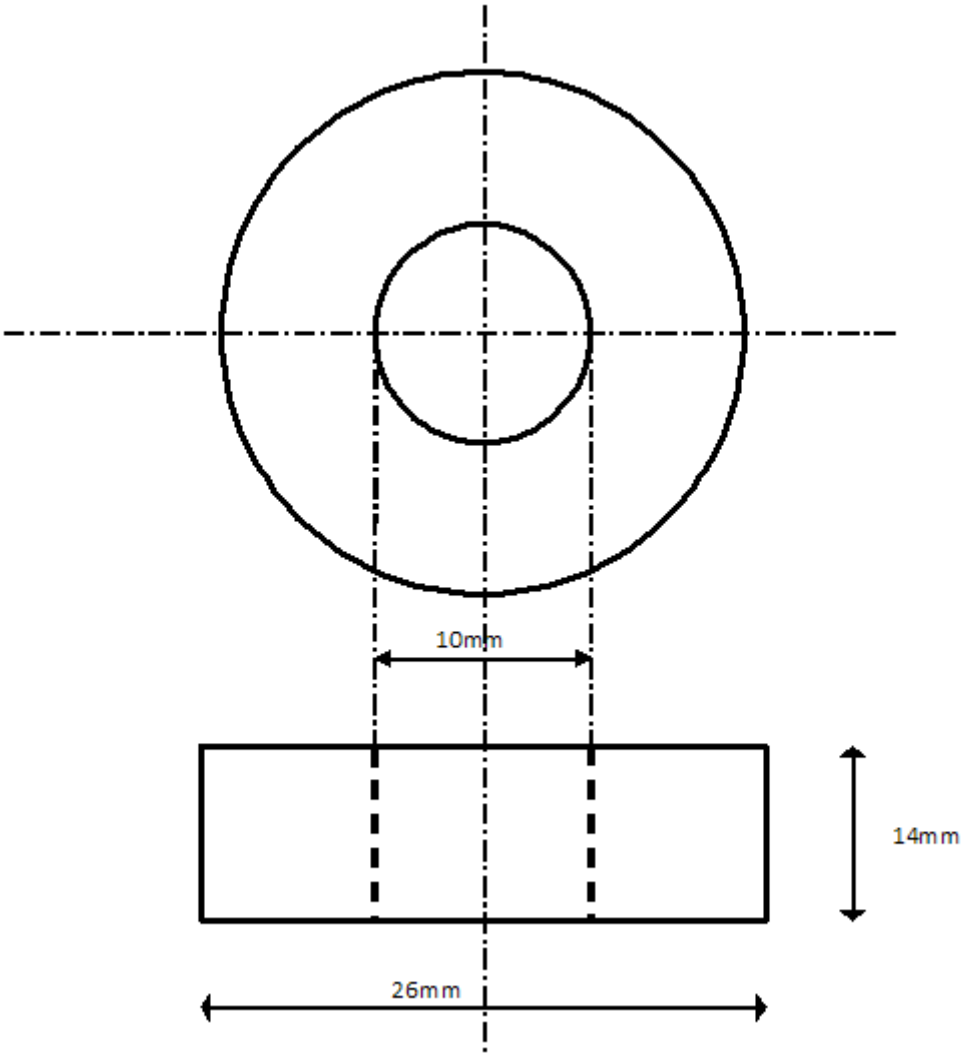

Figure 54 Technical drawing and specifications of the ring gauge

Table 19 Specifications of the ring gauge

Artefact Name	ϕ10 Nominal Ring Gauge	
Part No.	No. L5/004	
Tolerance Grade	AA	
Material	Steel	
Nominal Dimension (mm)	Inner diameter	ϕ10
	Outer diameter	ϕ26
	Thickness	14

3) *Select the feature to be measured:*

As shown in Table 20, the inner hole of the ring gauge is selected to the feature to be measured. The characteristics of the inner hole, diameter and cylindricity, are picked to be inspected. These characteristics represent major tolerance types of circular features. Diameter is the dimensional tolerance, and cylindricity is the form tolerance. The validation work, which is based on validating dimension and form tolerances, can provide a comprehensive evaluation on the digital CMM model performance.

Table 20 Details of the feature and the tolerances to be measured

Artefact Name	Ring gauge
Measured Feature	Inner hole
Measured Characteristics	Diameter ⌀
	Cylindricity ⌭

After defining the part and feature to be measured, the part CAD-model is ready to be imported into the digital measurement environment.

6.2.2 Select the measurement uncertainty contributors and their factorial levels

In the digital CMM model, the task-specific measurement uncertainty is calculated given the input values of measurement uncertainty contributors. As discussed in the pilot case study in Chapter 4, the uncertainty calculation result depends on the input quantities of the measurement uncertainty contributors. The selection and delimitation of the uncertainty contributors are important to the Framework validation.

As described in Chapter 5, the Measurement Planning and Implementation Framework compromises he following groups of measurement uncertainty contributors, 'CMM machine', 'environment', 'feature form error', 'fitting algorithm', 'sampling strategy' and 'probing system'. In terms of the diversity and complexity of CMM measurement tasks, each of the six groups is usually composed of sub-groups presenting specific measurement uncertainty contributors. In real CMM measure process, the measurement uncertainty contributors can go beyond these six groups.

Table 21 lists the specific measurement uncertainty contributors selected to be the factors in the Taguchi experiment design. There are four uncertainty contributors selected, which are 'probe specification', 'number of probing points', 'distribution of probing points' and 'part location'. They are numbered as 'Factor A', 'Factor B', 'Factor C' and 'Factor D' respectively. The four factors are from three uncertainty contributor groups, which are 'probing system', 'sampling strategy' and 'miscellaneous'.

Table 21 Uncertainty contributors selected as the factors in the Taguchi experiment design

Uncertainty Contributor Group	Factor Number	Factor Name
Probing system	Factor A	Probe specification
Sampling strategy	Factor B	Number of probing points
	Factor C	Distribution of Probing points
Miscellaneous	Factor D	Part location

To prepare for the Taguchi experiment design, the factorial levels of the four factors are defined as listed in Table 22. The selection of the factors and the delimitation of the factorial levels are based on the availability of the physical measurement resources, which is presented in the next section.

Table 22 Factorial levels

Level	Factor A Probe specification	Factor B Number of probing points	Factor C Distribution of Probing points	Factor D Part location
1	Probe 1	4	Evenly distributed within 120°	Corner of CMM bed
2	Probe 2	9	Evenly distributed within 240°	Middle point in-between
3	Probe 3	15	Evenly distributed along the circle (360°)	Centre of CMM bed

The explanations of these four factors and the factorial levels are described as below:

1) *Factor A - Probe specification*:

'Probe specification' represents hardware condition and performance of the probing system. It is the Factor A in the Taguchi experiment design. Three probes, Probe 1, Probe 2 and Probe 3, compose the three factorial levels. The details of the three

probes are listed in Table 23 together with their ‘name’, ‘stylus length in test’, ‘stylus tip point in the - z CMM axis direction’ and ‘range of residuals to 25-point sphere fit’.

Table 23 The details of probe specifications

Probe number	Name	Stylus length in test (mm)	Stylus tip point in the - z CMM axis direction (mm)	Range of residuals to 25-point sphere fit (mm)
Probe 1	1pt3D_22Z	22	67	0.0010
Probe 2	3D_78Z	78	128	0.0011
Probe 3	5D_40Z	40	98	0.0013

The meanings of the columns of Table 23 are explained as below:

- ‘Name’: the probe name is taken from NPL collection, where the physical measurements are performed;
- ‘Stylus length in test’ and ‘Stylus tip points in the - z CMM axis direction’: the meanings of these two columns are illustrated in Figure 55. The specific values of these two in the respective columns in Table 23.

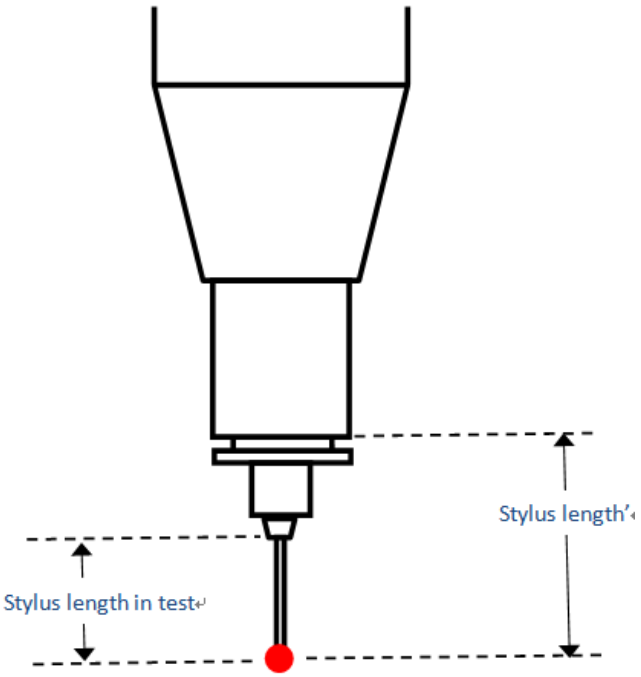

Figure 55 'Stylus Length' and 'Stylus length in test'

- 'Range of residuals to 25-point sphere fit': 'Range of residuals to 25-point sphere fit' literally represents probe measurement performance. The values of the ''Range of residuals to 25-point sphere fit' are determined from the physical probe tests, of which testing procedures are performed given to ISO 10360 requirements. The details of the physical probe tests are presented in the next section.

2) *Factor B - Number of probing points:*

'Number of probing points' represents the number of sampling points per level. It is the Factor B in the Taguchi experiment design.

It is expected that the larger the 'number of probing points', the lower the measurement uncertainty tends to be. However, there is a trade-off between the number of probing points and the working efficiency. Increasing probing points will increase the measurement time, and consequently will lower the working efficiency. It is sensible to select the 'number of probing points' as a factor in the Taguchi

experiment design. It estimates the influence of the ‘number of probing points’ on the measurement uncertainty, and hence helps to identify the worthiness of increasing the number of probing points during the CMM measurement process.

In this Taguchi experiment design, ‘number of probing points’ is designated to have three levels, which are 4, 9 and 15 respectively. NPL Best Practice Guide recommends to sampling 7 points of measuring a circle. The selection of the ‘number of probing points’ in this experiment have considered the NPL Best Practice as well as the feasibility of configuring the number of probing points in the digital CMM model.

3) *Factor C - Distribution of probing points:*

‘Distribution of probing points’ represents the pattern of probing point distribution as described in previous section. It is the Factor C in the Taguchi experiment design. As shown in Table 24, the ‘distribution of probing points’ is designated to have three levels, which are ‘evenly distributed within 120º’, ‘evenly distributed within 240º’ and ‘evenly distributed along the circle (360º)’ respectively. These distribution patterns are illustrated in Table 24.

Table 24 Description of the factorial levels of ‘Distribution of Probing Points’

Factorial Level	Factor C Probing Point Distribution Pattern	Description
1	Evenly distributed within 120º	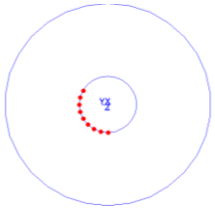
2	Evenly distributed within 240º	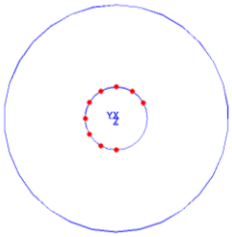
3	Evenly distributed along the circle (360º)	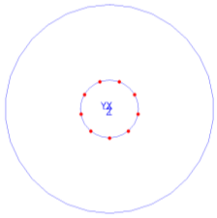

4) *Factor D - Part location:*

‘Part location’ represents the location of the ring gauge on the CMM bed. It is the Factor D in the Taguchi experiment design. In the digital CMM model, the adjustment of part location is done by the coordinate transition between the old and new part locations. In a practical CMM measurement process, the part is usually located as close as to the centre of CMM bed as possible, where the kinematic errors caused by CMM gantry movements have the lowest impacts on the measurement result.

As shown in Table 22, in the Taguchi experiment design, the ‘Part location’ is designated to have three levels, which are ‘corner of CMM bed’, ‘middle point in-between’ and ‘centre of CMM bed’ respectively. The definitions of the three levels are explained as below and illustrated in Table 25:

- Corner of CMM bed: the ‘corner of CMM bed’ is the origin (the (0,0,0) point) of the CMM bed as shown in the first row of Table 25;

- Centre of CMM bed: the ‘centre of CMM bed’ is the central point of the CMM bed. The working volume of the CMM is $550mm \times 500mm \times 400mm$. Therefore the coordinates of the ‘centre of CMM bed’ is (275, 250, 0). The location of the ‘centre of CMM bed’ is visualized in the digital CMM model as shown in the third row of Table 25;

- Middle point in-between: the ‘middle point in-between’ is the midpoint of the line between the ‘corner of CMM bed’ and the ‘centre of CMM bed’. Therefore the coordinates of the ‘middle point in-between’ is (137.5, 125, 0). The location of the ‘middle point in-between’ is shown in the second row of Table 25.

Table 25 Description of the factorial levels of 'Part Location

Factorial Level	Factor D Part Location	Description	Part location coordinates (x*y*z/mm)
1	Corner of CMM bed	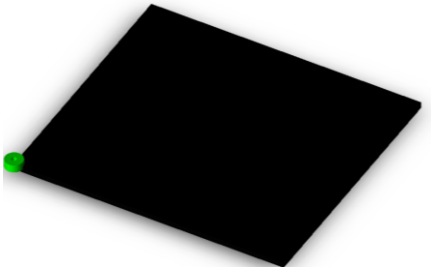	$0 \times 0 \times 0$
2	Middle point in-between	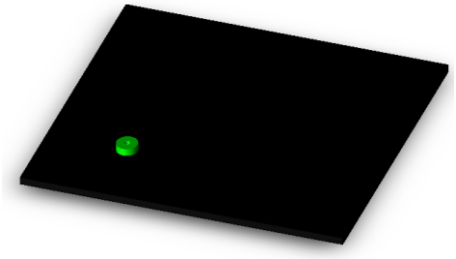	$137.5 \times 125 \times 0$
3	Centre of CMM bed	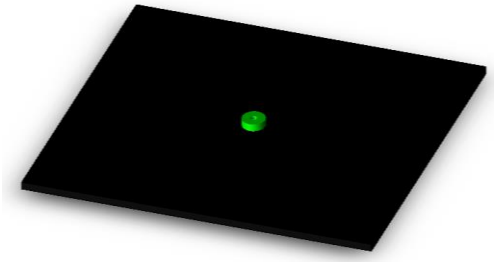	$275 \times 250 \times 0$

By this point, the factors for the Taguchi experiment design are established. Four factors are selected from the measurement uncertainty contributors. The four factors are ‘probe specification, ‘number of probing points’, ‘distribution of Probing points’ and ‘part location’. Each factor is aligned three factorial levels. Therefore, it produces 81 measurement scenarios which need to be performed in both the digital and physical measurement environment.

In the next section, the number of measurement scenarios is streamlined by using Taguchi Orthogonal Array. It reduces the number of digital and physical measurements, and makes the validation of the Measurement Planning and Implementation Framework feasible.

6.2.3 Reduce the number of measurement scenarios given to Taguchi Orthogonal Array

The Taguchi Orthogonal Array is deployed in the 'Measurement Scenario Streamliner' module of the Measurement Planning and Implementation Framework to reduce the number of measurement scenarios performed in the digital and physical measurement environments. The implementation of Taguchi Orthogonal Array is described in the previous Chapter. In this section, the Taguchi Orthogonal Array is used to streamline the measurement scenarios established by the combinations of the factors and factorial levels from the previous section. The procedures of streamlining the measurement scenarios are also presented in this section.

The measurement scenarios are streamlined in the digital environment with the assistance of professional statistical software, MiniTab.

1) *Create general Taguchi experiment design:*

A Taguchi experiment design is created by selecting appropriate menus and buttons in the statistical software (as shown in Figure 56). This design provides a basic structure for practicing Taguchi method, and is general to many statistics-based experimental circumstances.

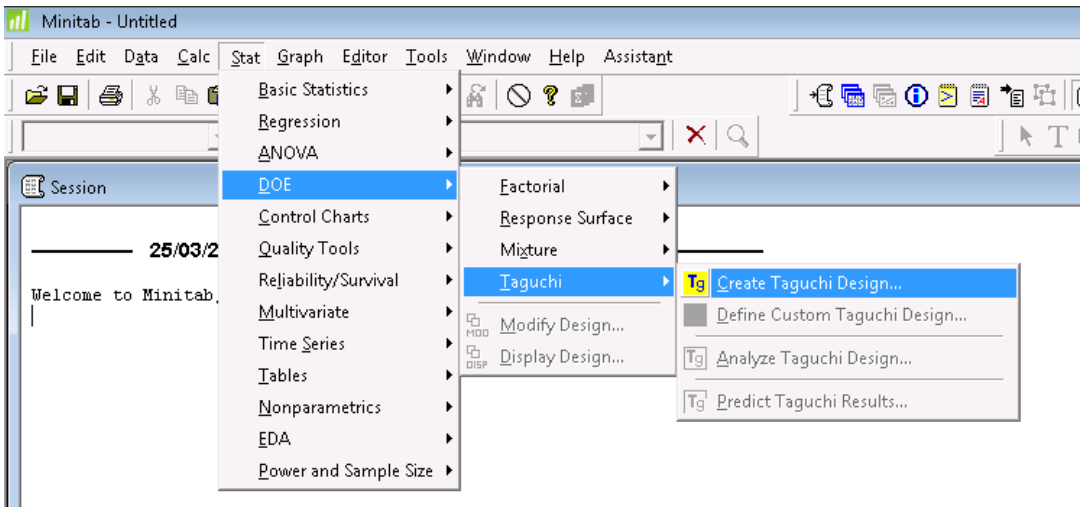

Figure 56 Create the Taguchi experiment design

2) *Customize Taguchi experiment design:*

The general Taguchi experiment design is customized according to the experiment design of this research. The sub-steps of customization are explained.

- Select the appropriate design:

  The layout appropriate Taguchi experiment design is selected by specifying the number of factors and the factorial levels (as shown in Figure 57). In this Taguchi experiment design, there are four factors, each of which has 3 factorial levels.

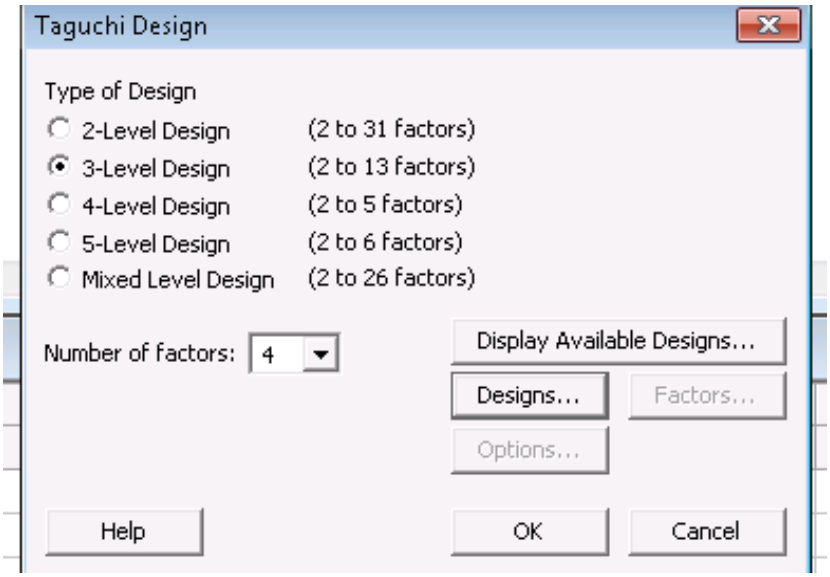

Figure 57 Select appropriate design

- Select proper Taguchi Orthogonal Array:

  By clicking 'Display Available Designs' button in Figure 57, another dialogue box comes out It shows the available Taguchi experiment designs which have four factors. The proper Taguchi Orthogonal Array is then selected given to the experiment plan.

  'Single-level' tab is selected, because in this experiment all of the factors are aligned to have the same number of factorial level.

A table is listed as in Figure 58, summarizing the single-level Taguchi designs available. The number following the "L" indicates the number of runs in the design. The numbers in the table indicate the minimum and maximum number of available factors for each design. Given to the requirements of this experiment design, L9 (2-4) is selected. It indicates that the ring gauge measurements need to run under nine measurement scenarios.

The experiment plan is a 4-factor and 3-factorial-level design, which originally requires 81 experimental runs. By applying the Taguchi Orthogonal Array, the number of experimental runs is reduced to 9.

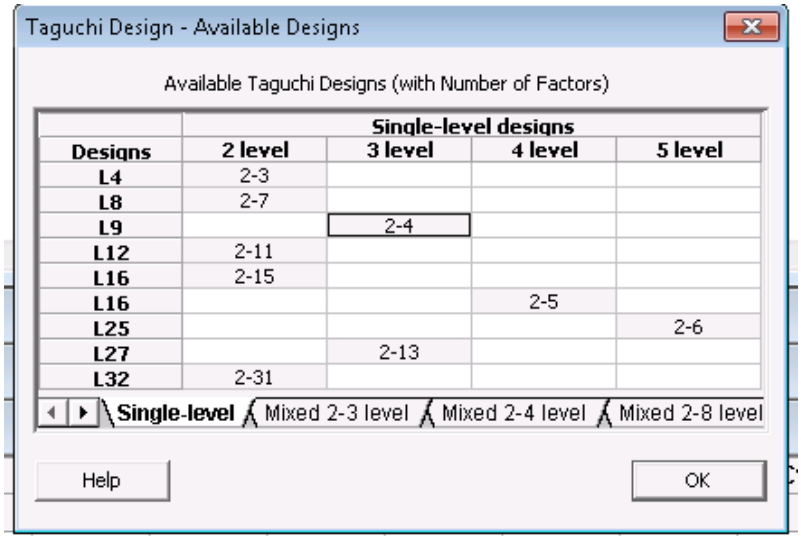

Figure 58 Select proper Taguchi Orthogonal Array

- Specify the number of trails for each run:

After specifying the number of runs, the number of trails for each run is selected. Figure 59 is the dialogue box where the number of trails is selected. According to the experiment plan, L27 (3-4) is selected. For each run, there are three trails to perform. It indicates that the ring gauge measurements are performed three times

under each selected measurement scenario. Therefore, there are totally 27 measurements to perform.

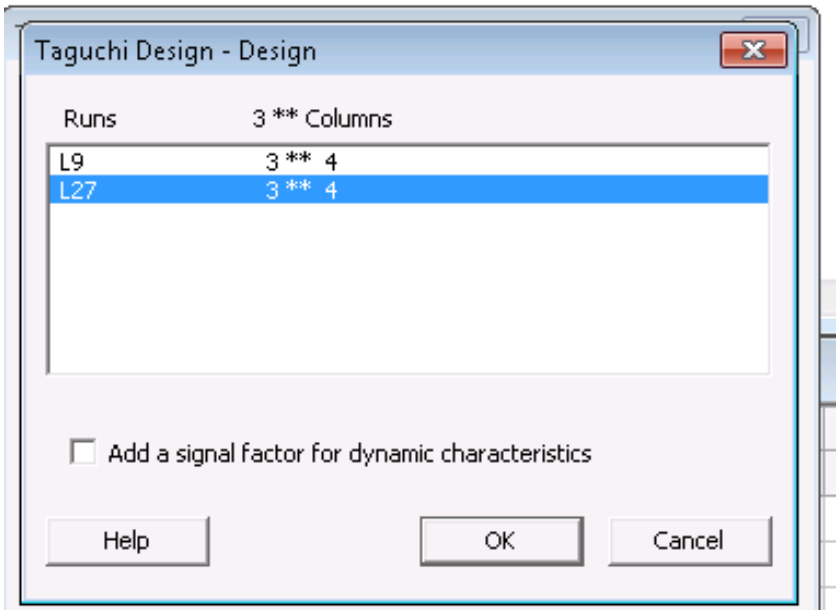

Figure 59 Specify the number of runs of each measurement scenario

- Align the factor names to the Taguchi experiment design:

  According to the experiment plan, the names of measurement uncertainty contributors are aligned to the Taguchi design factors through the dialogue box as shown in Figure 60. The four measurement uncertainty contributors are ‘probe specification’, ‘number of probing point’, ‘distribution of probing points’ and ‘part location’. Each of the factor has three factorial levels.

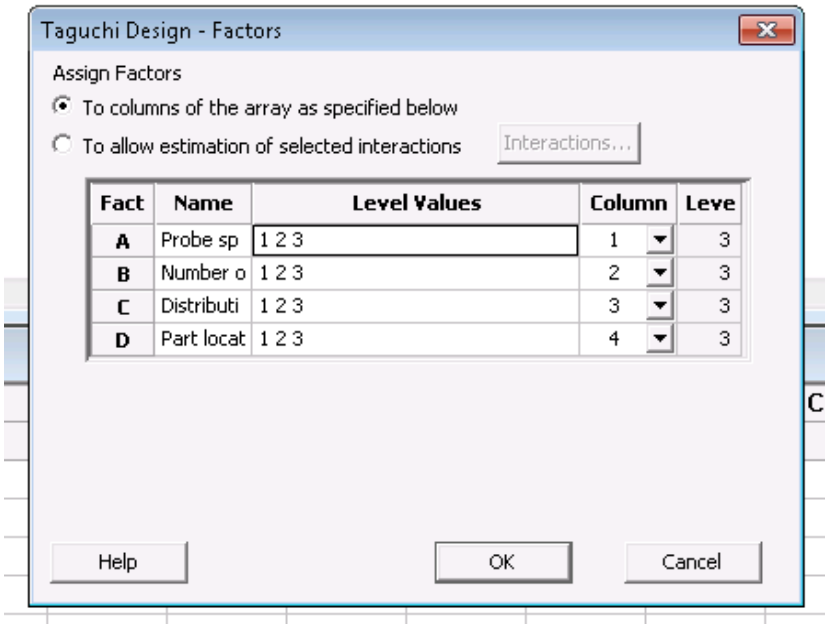

Figure 60 Align the factor names to the design

3) *Streamline measurement scenarios:*

By applying the Taguchi orthogonal array, the number of measurement scenarios is reduced from 27 to 9. Table 26 concludes the measurement scenarios after streamlining. The factors and the factorial levels appear equally in the selected measurement scenarios, so the analysis can give a comprehensive result on the overall experiment.

Table 26 The streamlining result of the measurement scenarios

Scenario No.	A Probe specification	B Number of probing points	C Distribution of probing points	D Part location
1	1 (1pt3D_22Z)	1 (4 points)	1 (Evenly distributed within 120°)	1 (Corner)
2	1 (1pt3D_22Z)	2 (9 points)	2 (Evenly distributed within 240°)	2 (Middle)
3	1 (1pt3D_22Z)	3 (15 points)	3 (Evenly distributed within 360°)	3 (Centre)
4	2 (3D_78Z)	1 (4 points)	2 (Evenly distributed within 240°)	3 (Centre)
5	2 (3D_78Z)	2 (9 points)	3 (Evenly distributed within 360°)	1 (Corner)
6	2 (3D_78Z)	3 (15 points)	1 (Evenly distributed within 120°)	2 (Middle)
7	3 (5D_40Z)	1 (4 points)	3 (Evenly distributed within 360°)	2 (Middle)
8	3 (5D_40Z)	2 (9 points)	1 (Evenly distributed within 120°)	3 (Centre)
9	3 (5D_40Z)	3 (15 points)	2 (Evenly distributed within 240°)	1 (Corner)

The streamlined measurement scenarios, including the repeated trails, are displayed in Figure 61.

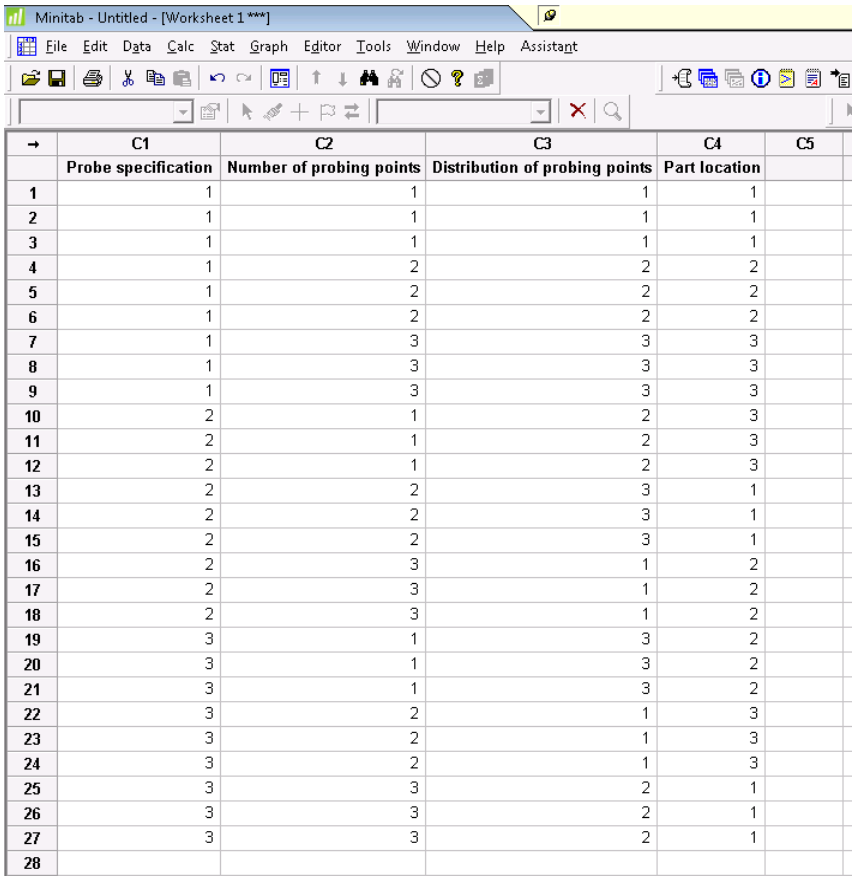

→	C1	C2	C3	C4	C5
	Probe specification	Number of probing points	Distribution of probing points	Part location	
1	1	1	1	1	
2	1	1	1	1	
3	1	1	1	1	
4	1	2	2	2	
5	1	2	2	2	
6	1	2	2	2	
7	1	3	3	3	
8	1	3	3	3	
9	1	3	3	3	
10	2	1	2	3	
11	2	1	2	3	
12	2	1	2	3	
13	2	2	3	1	
14	2	2	3	1	
15	2	2	3	1	
16	2	3	1	2	
17	2	3	1	2	
18	2	3	1	2	
19	3	1	3	2	
20	3	1	3	2	
21	3	1	3	2	
22	3	2	1	3	
23	3	2	1	3	
24	3	2	1	3	
25	3	3	2	1	
26	3	3	2	1	
27	3	3	2	1	
28					

Figure 61 The streamlined measurement scenarios

4) *Create data collection sheet:*

At last, the streamlined measurement scenarios are collectively organized in the Excel Table. The data collection sheet is created (as shown in Appendix C), which is used to record the digital and physical measurement results.

6.2.4 The measurement process in the digital CMM model

The fundamentals of the digital CMM model have been introduced in the previous chapters. The digital CMM model perceives the design and manufacturing information from the part CAD model, and simulates the CMM measurement process to predict task-specific measurement uncertainty. The digital CMM model provides options allowing the end-user to customize the digital measurement given to the conditions of the physical measurement. These options include diverse factors which

can potentially influence the CMM measurement process, e.g. temperature, CMM machine specification, probe specification and probing strategy etc. These options constrain the space of the CMM measurement uncertainty for the defined measurement tasks. Then the digital CMM model performs the simulation-by-constraints calculation to predict the task-specific measurement uncertainty.

The digital measurement process in this section basically follows the above workflow, but also is customized given to the special needs of the Framework validation. The digital measurement process in this case is shown in Figure 62.

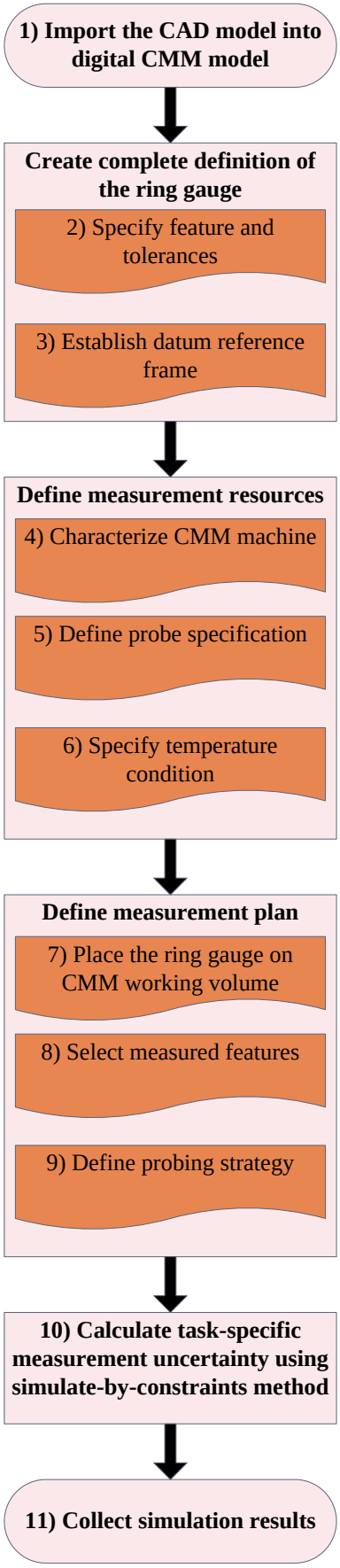

Figure 62 The measurement process in the digital CMM model

The individual steps of the digital measurement process are numbered in Figure 62. The details of these individual steps are described as below:

1) Import the CAD model into digital CMM model:

The CAD model of the ring gauge is transformed into DMIS format file, and loaded into the digital CMM model (as shown in Figure 63).

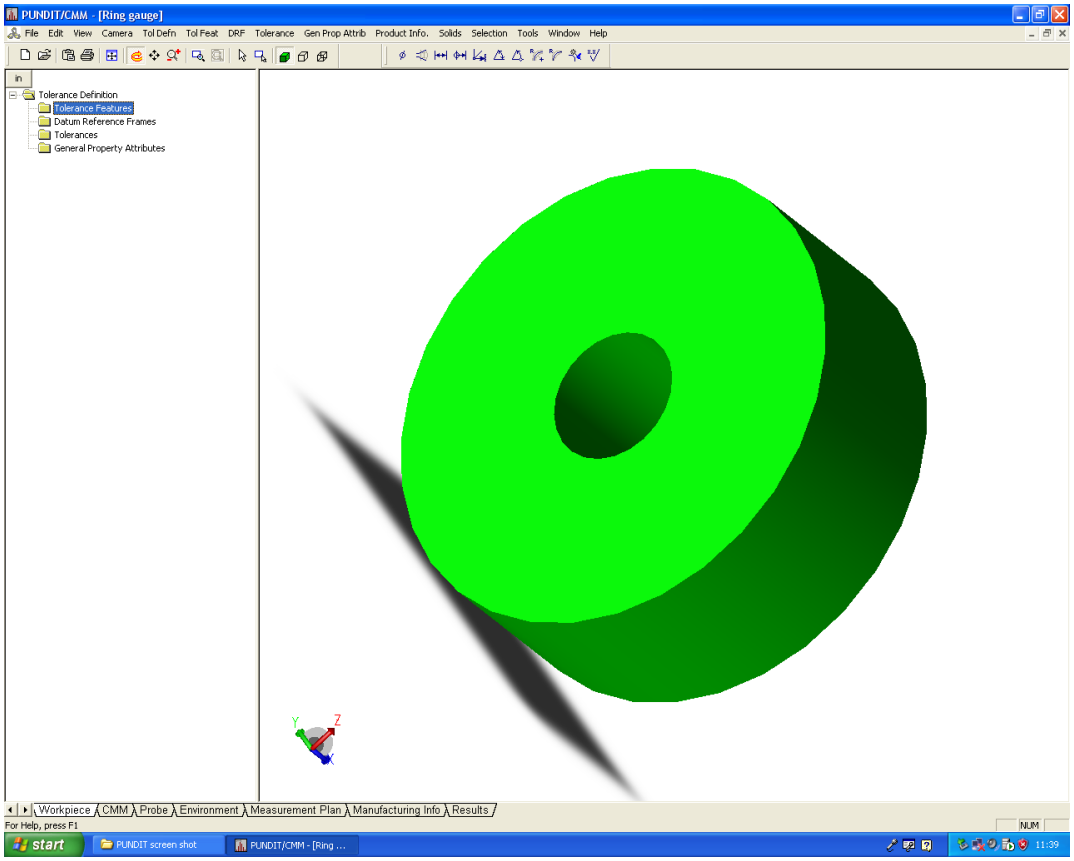

Figure 63 Import the CAD model of the ring gauge into the digital CMM model

2) Specify feature and tolerances:

The second step is to specify the tolerance characteristics of the measure feature. Although the CAD-model of the ring gauge is created in the feature-based design environment, this step is necessary. Because in the-state-of-the-art of computer-aided

inspection planning, the graphical entities that make up a solid model do not necessarily correspond on a one-to-one basis with the measurement features of the part. It is still necessary to create relationships between the graphical entities and the tolerance features.

In this experiment, the tolerance characteristics are manually assigned to the CAD-model of the ring gauge. As specified in the previous section, two tolerances are assigned, which are diameter and cylindricity (as shown in Figure 64). The values of the tolerances are also applied. The diameter of the inner hole is 10mm, of which tolerance is 0.0009mm. The cylindricity tolerance of the inner hole is 0.0009mm.

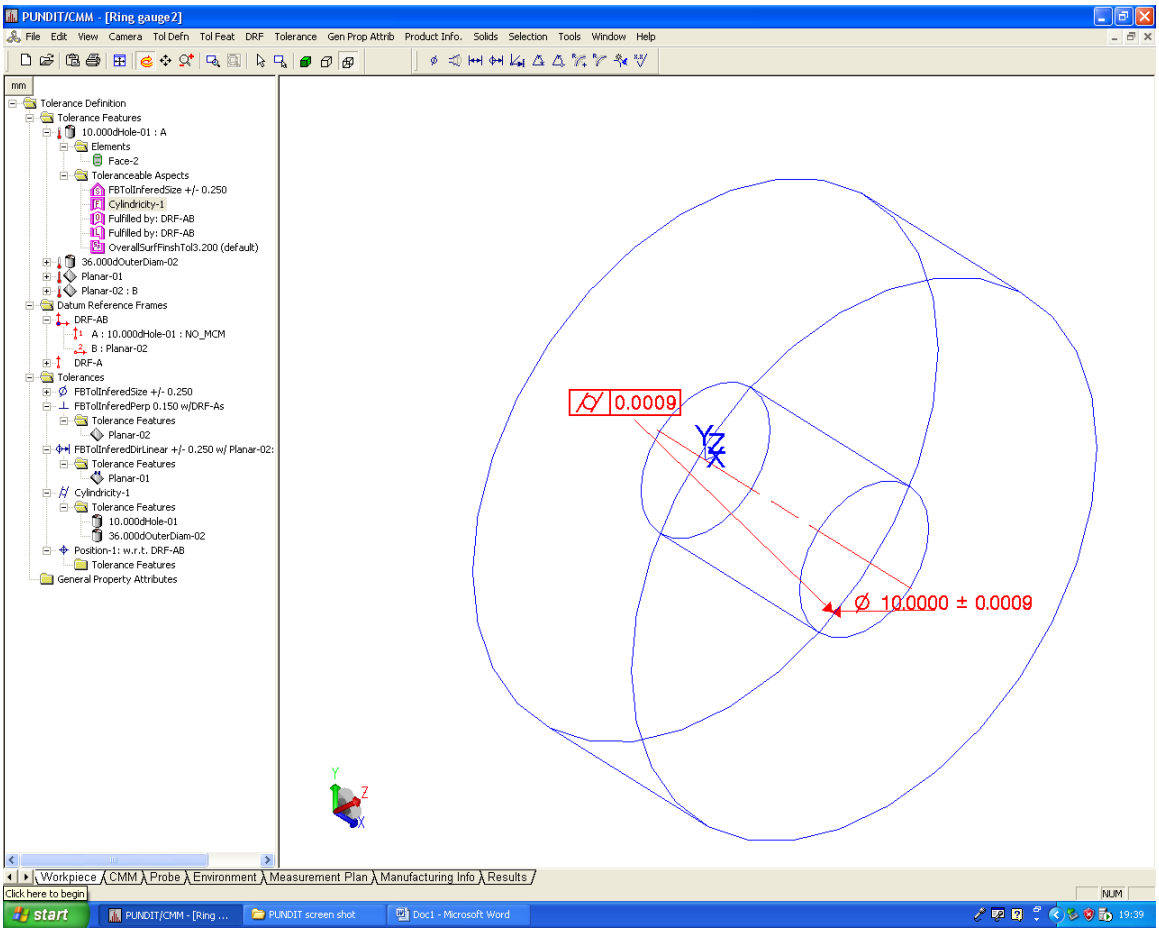

Figure 64 Assign the tolerances to the ring gauge CAD model

At this point, the measured characteristics are assigned to the part. The remaining tasks are to establish measurement datum, and to infer the measured characteristics with the measurement datum.

3) Establish datum reference frame:

The method and concerns of establishing measurement datum are the same in both of the digital CMM model and the physical measurement process. The datum reference frame is established given to the nature of the ring gauge and the measurement tasks. The top surface of the ring gauge serves as the primary datum feature, by measuring which a flat plane is created. The surface of inner hole serves as the secondary datum feature, by measuring which the central axis of the inner hole is created. The plane and the central axis intersect at one point, which creates the datum point. Based on this datum point, the datum reference frame is established.

In the digital CMM model, the top surface of the ring gauge is selected to be the primary datum and denoted as DRF-A. The surface of the inner hole is selected to be the secondary datum and denoted as DRF-B. On the computer screen, the DRF-B label is dragged under the DRF-A label, and a completed datum reference frame is created as shown in Figure 65.

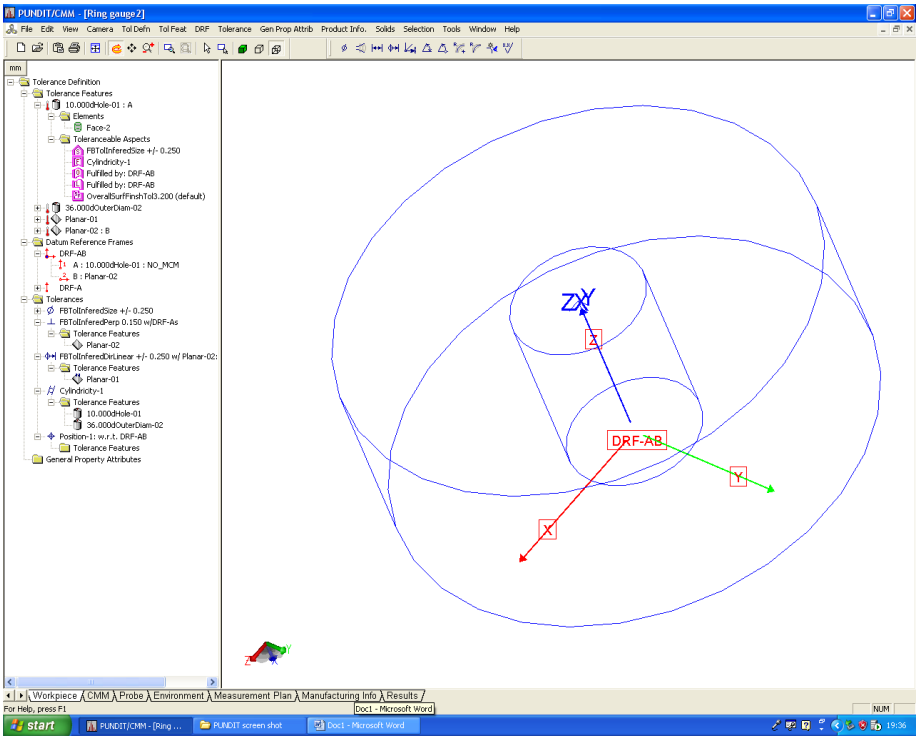

Figure 65 Datum establishment

By this point, the tolerances to be measured are assigned to the datum reference frame. The complete definition of the ring gauge in the digital CMM model has been created in the digital environment.

4) Characterize CMM machine

The resources needed through the measurement process are defined in this step. These resources include the CMM machine characteristics, the probe specification and the temperature condition.

The CMM characteristics are constrained given to the real CMM machine used in the physical measurement in NPL.

Firstly, the geometry of the CMM machine is selected as shown in Figure 66. The 'moving bridge' geometry is selected, because it is used in the physical measurement.

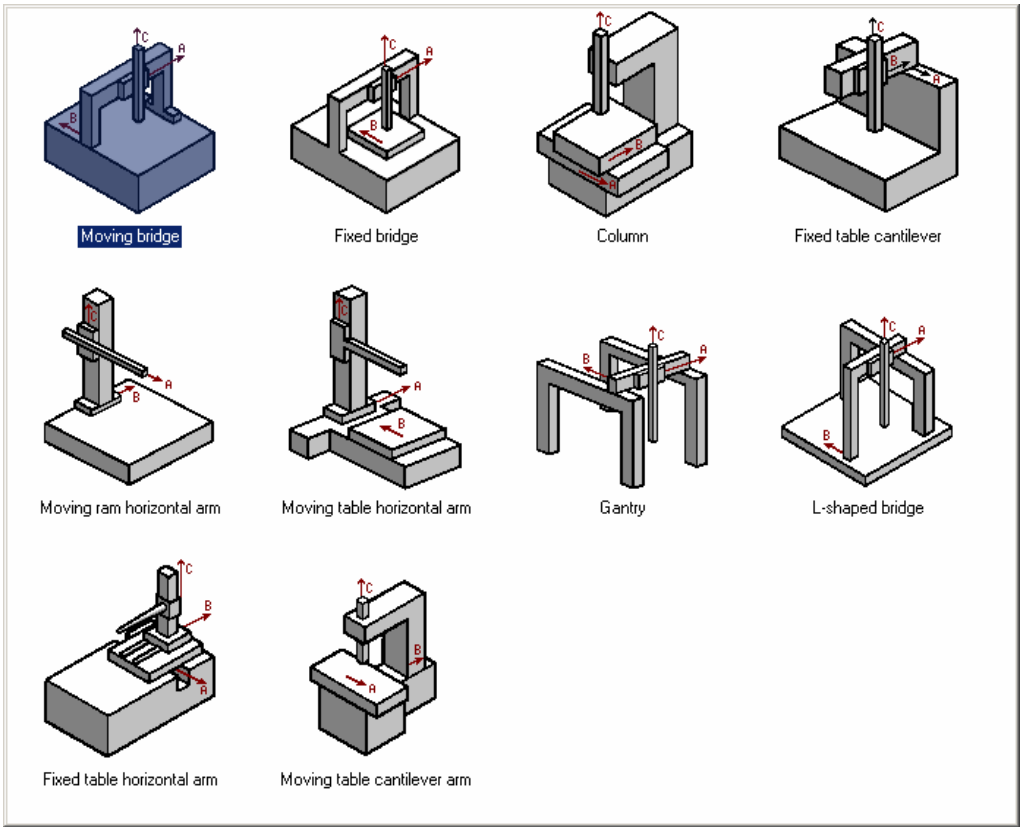

Figure 66 Select the geometry of the CMM machine

Secondly, the working volume of the CMM machine is defined in the digital CMM model (as shown in Figure 6768). Given to the CMM machine used in the physical measurement, the working volume of the digital CMM machine is defined as 550mm x 500mm x 400mm.

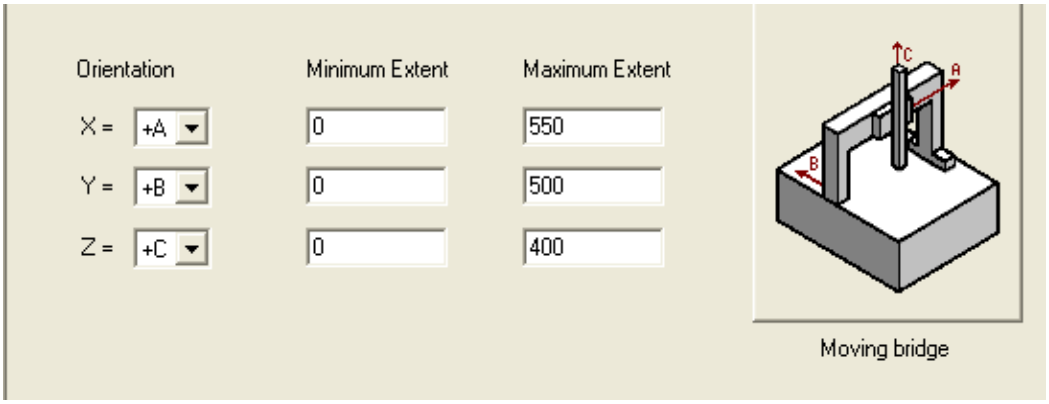

Figure 6768 Define working volume of the CMM machine

Thirdly, the verification information of the CMM machine is loaded in the digital CMM model (as shown Figure 69). The verification information requires the specification of four categories of information inputs, which are 'Error Model', 'Model Data Source', 'Artefact Type' and 'Error of Indication'. The details and specific input values to these modules are described below:

- 'Error Model': The 'Error Model' asks the end-user to specify the uncertainty calculation method. The digital CMM model provides three uncertainty calculation methods, which are 'Perfect Machine', 'Simulation by Constraints' and 'Full Parametric Specification'. Given the research aim, the Error Model is selected to be 'Simulation by Constraints'.

- 'Model Data Source': The 'Model Data Source' module asks the end-user to specify the verification standard based on which the CMM machine is tested. The verification methods and results create the CMM performance data set as mentioned in the previous sections. The CMM performance data set establishes the constraints of the CMM performance in the digital environment. Then the digital CMM model performs a simulation-by-constraints calculation to calculate task-specific measurement uncertainty.

  As shown in Figure 69, the digital CMM model provides three Model Data Sources, which are ASME B89, ISO 10360 and the USAF calibration test. ASME B89 requests full linear accuracy test, of which result is not supplied with the CMM machine in the physical measurement. USAF calibration is the verification standard used by US Air Force, which is not accessible. Therefore, ISO 10360 is selected to represent the CMM verification standard.

- 'Artefact Type' and 'Position': The 'Artefact Type' module and 'Position' module requests the end-user to specify the details during the full liner accuracy test, including which type of calibrated artefact is used and how the calibrated artefact is position on the CMM machine. ISO 10360, selected in the 'Model Data

Source', does not require the full liner accuracy test. Therefore, the two modules are left blank (as shown in Figure 69).

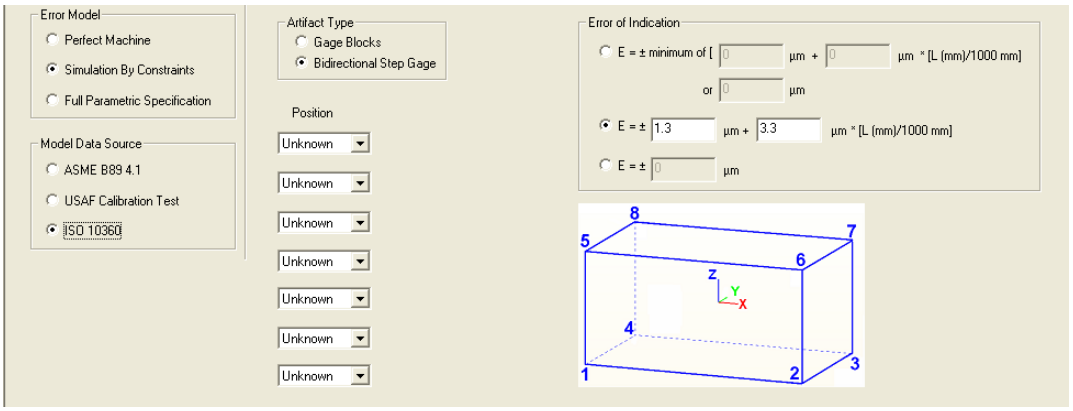

Figure 69 Load the verification information in the digital CMM model

- 'Error of Indication': The 'Error of Indication' module asks the end-user to specify the CMM verification result(s) given on the verification standard selected. In this case, the CMM verification result is 1.3 + L/300 µm, which is loaded in the digital CMM model as shown in Figure 69.

5) Define probe specification:

The probe used to measure the ring gauge is defined in this step. Figure 70 shows the dialogue box through which the probe specification is defined in the digital CMM model.

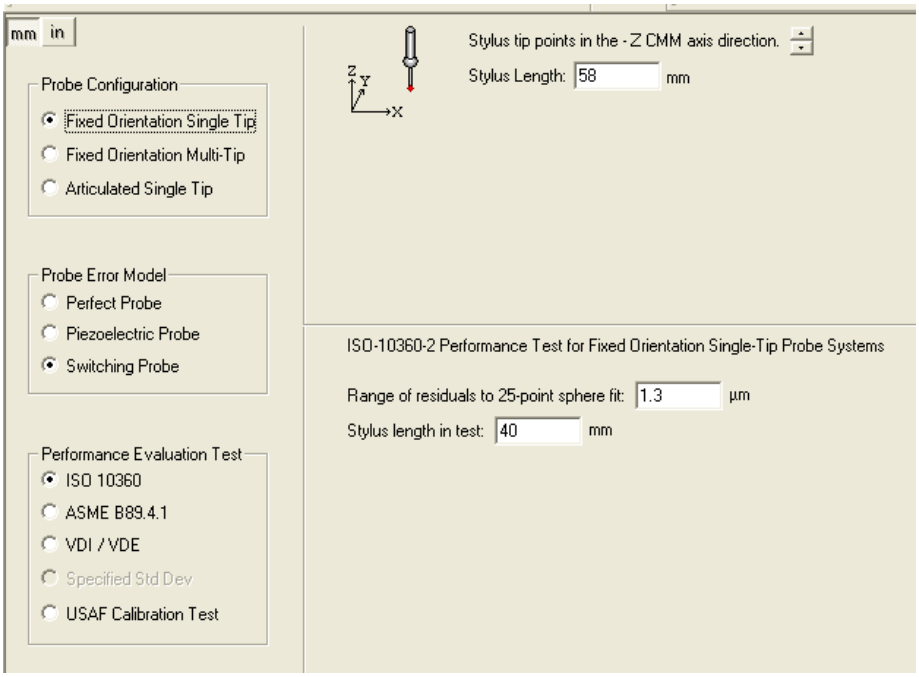

Figure 70 Define probe specification

There are two important input attributes in the dialogue box in Figure 70, which are 'Stylus Length' and 'Stylus length in test'. The definitive locations of 'Stylus Length' and 'Stylus length in test' are labelled in Figure 55 in the previous section.

The probe specification dialogue box requests to specify three categories of information inputs, which are 'Probe Configuration', 'Stylus Length' and 'Performance Evaluation Test'. The details and specific input values to these modules are described as below:

- 'Probe Configuration' and 'Probe Error Model': Given the probe used in the physical measurement*, 'Fixed Orientation Single Tip' and 'Switching Probe' are selected in respective modules (as shown in Figure 70).

* The specification of the probe used in the physical measurement is described in the previous section.

- ‘Stylus Length’ et al.: The ‘Stylus Length’ module in Figure 70 asks the end-user to specify how the probe head is mounted in the CMM machine by designating the axis direction that corresponds to the stylus tip pointing and stylus length.

  In the Taguchi experiment design, the ‘Stylus Length’ is selected to be an uncertainty contributor. Therefore, the input values of the ‘Stylus Length’ vary between the measurement scenarios, the details of which will be presented in the next section.

- ‘Performance Evaluation Test’ et al.: ‘Performance Evaluation Test’ and other modules ask the end-user to specify the probe testing procedure and testing results. The probes used in the physical measurements in NPL are tested accoording to the ISO 10360 requirements, and hence the option ‘ISO 10360’ in the ‘Performance Evaluation Test’ module is selected.

  The rest of two attribute inputs, ‘Range of residuals to 25-point sphere fit’ and ‘Stylus length in test’ represent the probe testing results, which is selected to be an uncertainty contributor in the Taguchi experiment design. The input values of these attributes vary between the measurement scenarios. The details of their input values are presented in the previous section.

6) Specify temperature condition:

The temperature condition during the measurement process is specified in this step. Figure 71 shows the dialogue box where end-user can define the temperature condition in the digital CMM model.

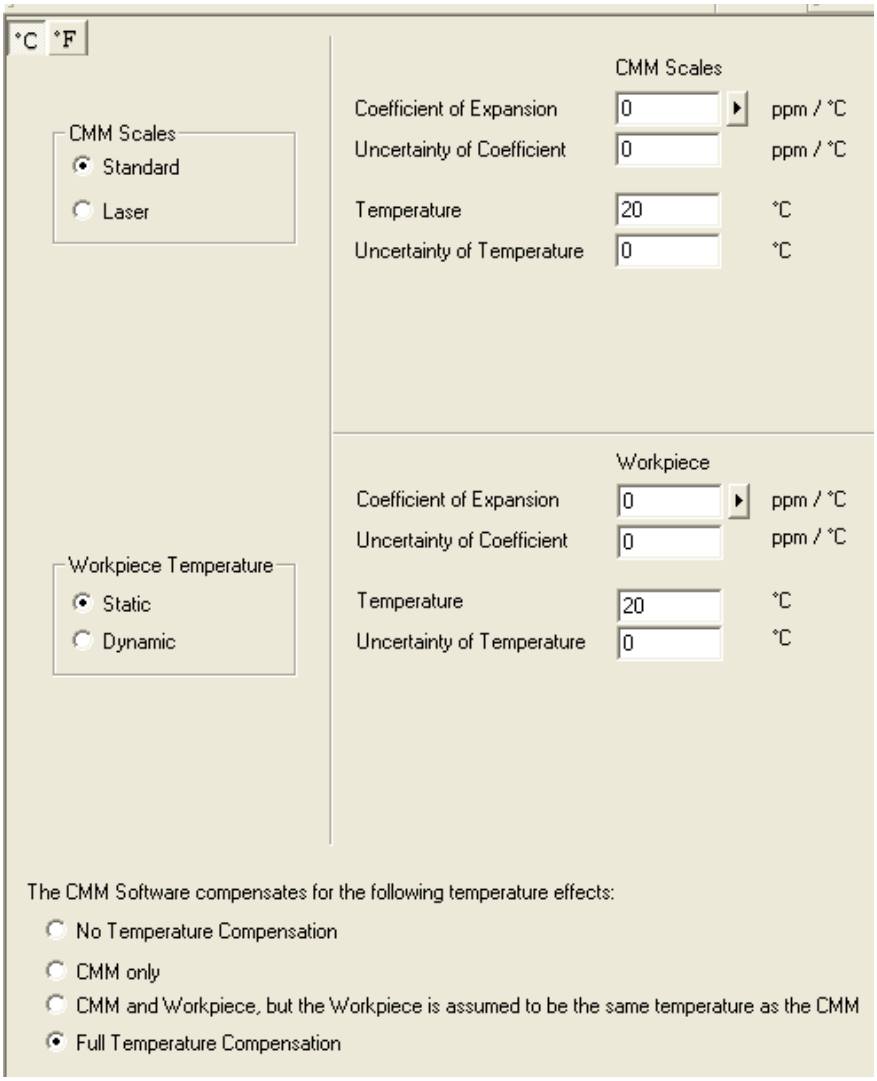

Figure 71 Specify temperature condition

Given to the particular physical measurement process, Celsius unit (°C) is used for data entry in the upper left corner of the dialogue box in Figure 71. Apart from the above information, the dialogue box also requests to specify five categories of information inputs, which are 'CMM Scales', 'Workpiece Temperature', CMM scales thermal condition, workpiece thermal condition and temperature compensation. The details and specific input values to these modules are described as below:

- 'CMM Scales': the 'CMM Scales' module represents the accuracy gradations of a CMM machine. As shown in Figure 71, the 'CMM Scales' module provides two

options, ‘Standard’ and ‘Laser’. The majority of CMMs are equipped with mechanical scales and optical reader heads that move along those scales to encode the axis positions. A few CMMs, primarily, those designed to produce measurements of extremely high accuracy are equipped with laser interferometer scales. For the CMM used in the physical measurement of this research, ‘Standard’ CMM scale is selected.

- ‘Workpiece Temperature’: the ‘Workpiece Temperature’ module represents the workpiece temperature changes over time. It provides two options, ‘Static’ and ‘Dynamic’. A ‘Static’ temperature model means that the temperature does not change over the time, while a ‘Dynamic’ temperature model means that the workpiece temperature may change with time. The physical measurements are carried out in the finely-controlled laboratory environment, where the temperature variation is very low. Therefore, in the digital CMM model, the ‘Static’ workpiece temperature model is selected (as shown in Figure 71).

- CMM Scales thermal condition: The attributes to define the CMM scales thermal condition is on the upper right side in the dialogue box in Figure 71. It concerns the thermal state of the CMM machine under the environment temperature change. The physical measurements are carried out in the finely-controlled laboratory where the temperature is maintained at 20°C. Therefore, in the digital CMM model, the CMM scales are established to work under the temperature of 20°C, and the dynamic thermal effects on the CMM machine are ignored (as shown in Figure 71).

- Workpiece thermal condition: the attributes to define the workpiece thermal condition is on the lower right side in the dialogue box in Figure 71. It concerns the thermal condition of the workpiece under the environment temperature change. The physical measurements are carried out in the finely-controlled laboratory where the temperature is maintained at 20°C. Therefore, in the digital CMM model, the workpiece is established to work under the temperature of 20°C, and the dynamic thermal effects on the workpiece are ignored (as shown in Figure 71).

- Temperature compensation: The temperature compensation module defines the extent to which the CMM software attempts to compensate for thermal effects. Four options are provided in the digital CMM model as shown in Figure 71. In the physical measurement process, the CMM control software employs the ‘full temperature compensation’ mode to manoeuvre the movements of CMM machine. Consequently, in the digital measurement environment, the digital CMM model is set to be ‘Full Temperature Compensation’ to follow the physical measurement environment.

By this point, the resources needed for the measurement have been defined in the digital CMM model. The next stage is to define the measurement plan as shown in Figure 62.

7) Place the ring gauge on CMM working volume:

In the digital CMM model, the measurement plan defines how the ring gauge is to be measured: where it will be placed in the CMM working volume, which features will be measured, how many data points are to be taken, where they are to be taken and with what probe(s).

The first step of defining the measurement plan is to specify where to place the ring gauge on the CMM working volume in the digital CMM model. The part location can be defined through the dialogue box shown in Figure 72. The part can be moved by entering the coordinates of the new location relative to the origin point which is at the corner of the CMM’s working volume. This transformation process can be visualized as shown in Figure 73.

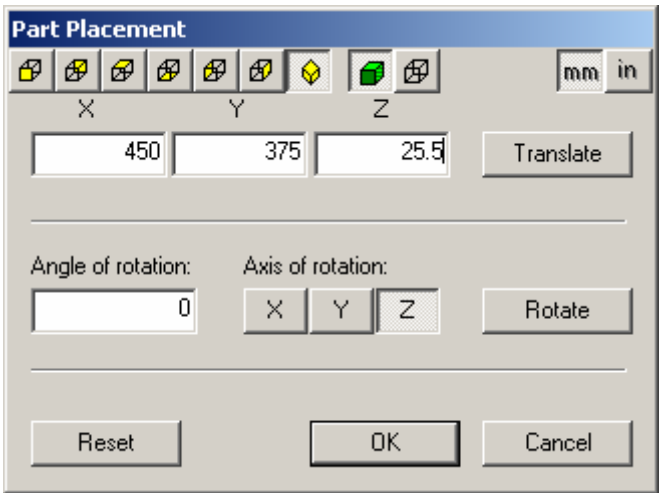

Figure 72 Place the part on CMM working volume

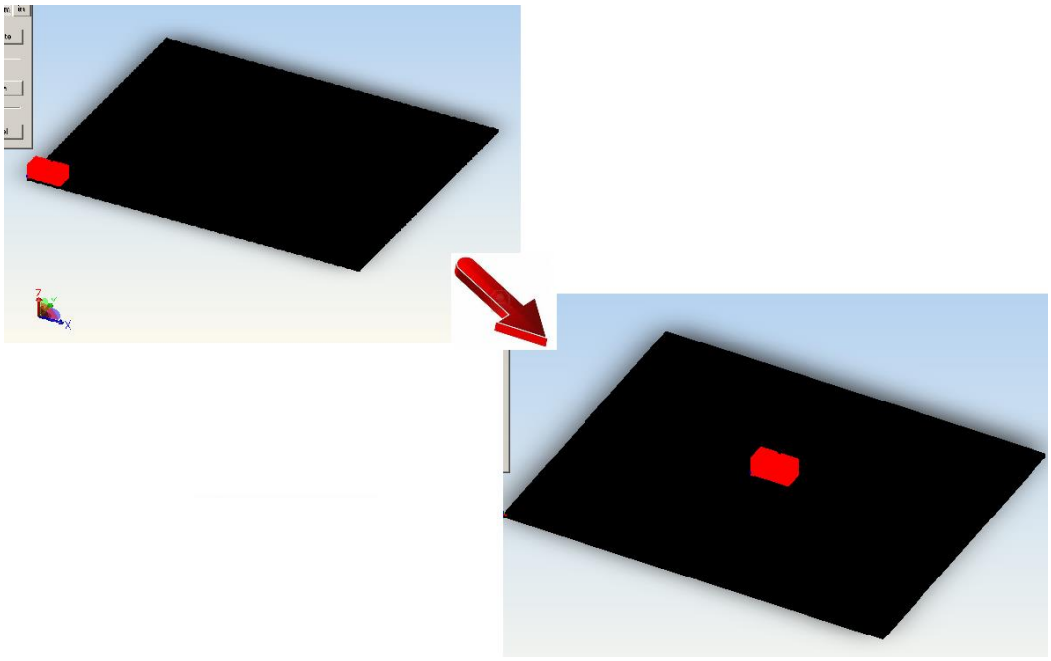

Figure 73 Transform the part location

The part placement is selected to be an uncertainty contributor in the Taguchi experiment design. The input values of these attributes vary between the measurement scenarios. The details of their input values are presented in the previous section.

8) Select measured features:

In this step, the features to be measured are edited, so that the digital definitions of the measurement tasks and operations can truly reflect the measurements needed in the digital CMM mode. A ‘Measurement Definition’ tree is generated as shown in Figure 74. The Measure Features folder is populated to list the key features of the ring gauge. For each Measure Feature there is an Elements sub-folder, a Datum Reference Frame sub-folder and a Tolerances sub-folder. Each Measure Feature also has a Measure Task Group folder.

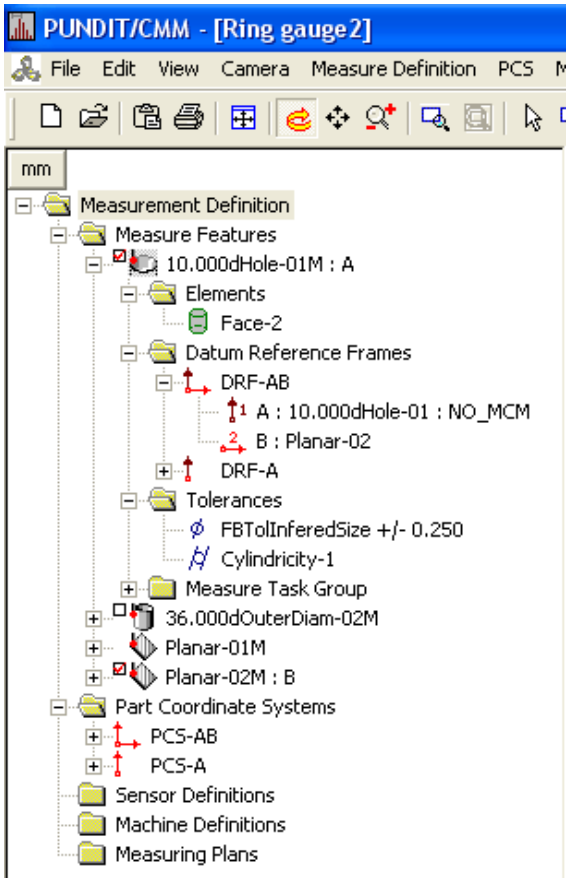

Figure 74 Select measured features

As shown in Figure 74, the ring gauge has four features, which are the inner circle (denoted as 10.000dHole-01M:A in Figure 74), the outer circle (denoted as 36.0000dOuter Diam-02M in Figure 74), the top surface (denoted as Planar-01M in

Figure 74) and the bottom surface (denoted as Plananr-02M:B in Figure 74). The inner circle is the feature to be measured, so the folder of '10.000dHole-01M:A' is expanded.

The '10.000dHole-01M:A' folder has four sub-folders, which contains the key information of measuring the inner circle of the ring gauge. The four sub-holders are 'Elements', 'Datum Reference Frames', 'Tolerance' and 'Measure Task Group'. The details of these four groups are described as below:

- Elements: The 'Elements' sub-folder shows the surfaces which compose the inner circle of the ring gauge. This sub-folder allows the end-user to define the measured features by directly clicking the surfaces of the part CAD model.
- Datum Reference Frames: The 'Datum Reference Frames' sub-folder shows the measurement datum to which the measure feature is referenced. As defined in the previous step, the datum for measuring the inner circle is composed by the intersection of the central axis of the inner circle and the top surface of the ring gauge, which are respectively denoted as 'A' and 'B' in the 'Measurement Definition' tree in Figure 74.
- Tolerance: The 'Tolerance' sub-folder shows the tolerances to be measured for the feature. As shown in Figure 74, there are two tolerances to be measured on the inner circle of the ring gauge, which are diameter and cylindricity.
- Measure Task Group: The 'Measure Task Group' sub-folder shows the probing strategy for measuring the feature. The details of defining the probing strategy, which supplies the content of the 'Measure Task Group' sub-folder, are presented in the next step.

9) Define probing strategy:

The details of the probing strategy are defined in this step. The number and placement of measurement points for each feature are designated in the digital CMM model.

Figure 75 shows the dialogue box through which the probing strategy is aligned to the inner circle of the ring gauge. For the geometric nature of the inner circle, the probing strategy is defined through three attributes, which are ‘Points per Level’, ‘Number of Levels’ and ‘Patter Type’. The values of the three attributes are manually inputted in the digital CMM model to generate a complete probing strategy.

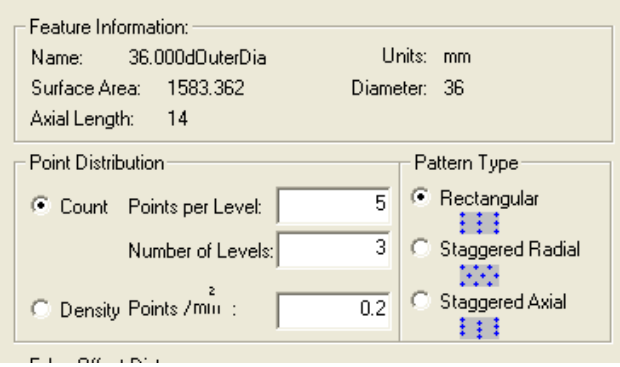

Figure 75 Probing strategy dialogue box

The result of arranging the probing strategy is visualized in the widow of the digital CMM model. Figure 76 shows one of the probing strategies defined for measuring the inner circle of the ring gauge. In this case, the ‘‘Points per Level’, ‘Number of Levels’ are set to be 20 and 5 respectively, meaning the sampling point distribution is 20 points per level, and 5 levels. And the point distribution pattern is ‘Rectangular’.

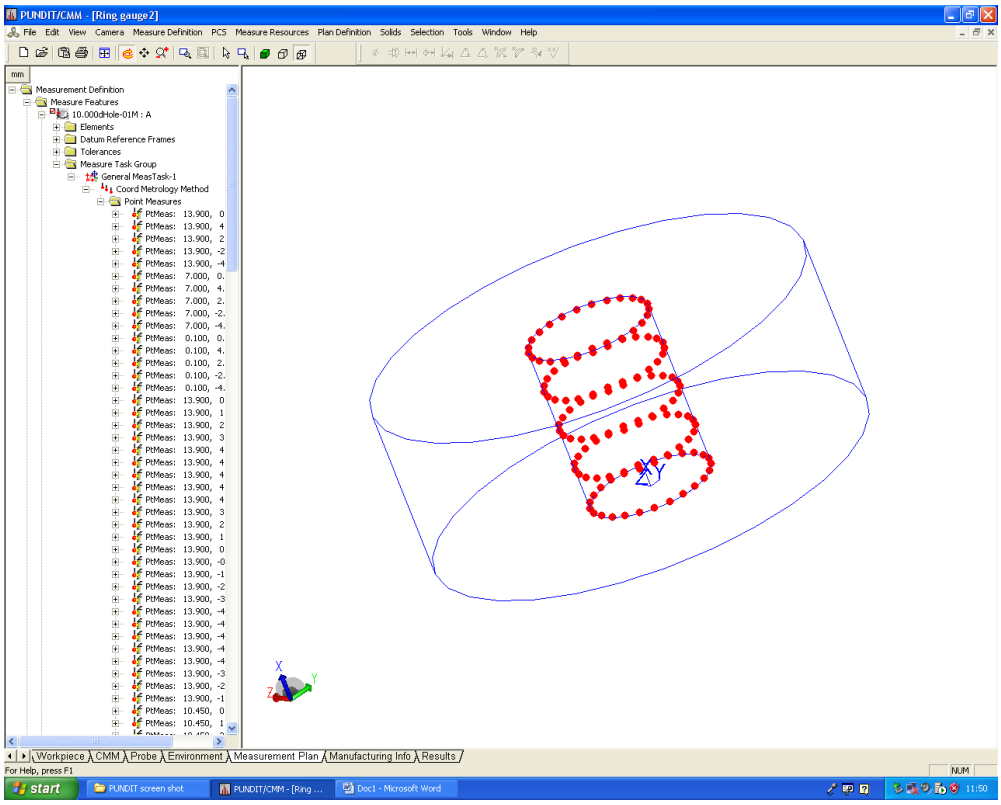

Figure 76 One of the probing strategies defined in the digital CMM environment

In the Taguchi experiment design, 'Probing Strategy' of the sampling points is selected to be an uncertainty contributor. Therefore, the input values of the 'Probing Strategy' vary between the measurement scenarios, the details of which has been presented in the previous section.

10) Calculate task-specific measurement uncertainty using the simulate-by-constraints method:

By this step, the simulation of measuring the inner circle of the ring gauge is ready to run. The digital CMM model employs a simulation-by-constraints method to calculate the task-specific measurement uncertainty for each tolerance under each measurement scenario.

Figure 77 shows the uncertainty calculation in the digital CMM model. Along the left side in Figure 77 there is a list of the tolerances that have been applied to the ring gauge CAD-model. Under each tolerance is a list of the measure features to which it applies. In the lower side in Figure 77, there is a control allowing selecting the number of times the simulation is to be run. To get stable values of uncertainty calculation results, 1000 times of simulation run is set to be in this research.

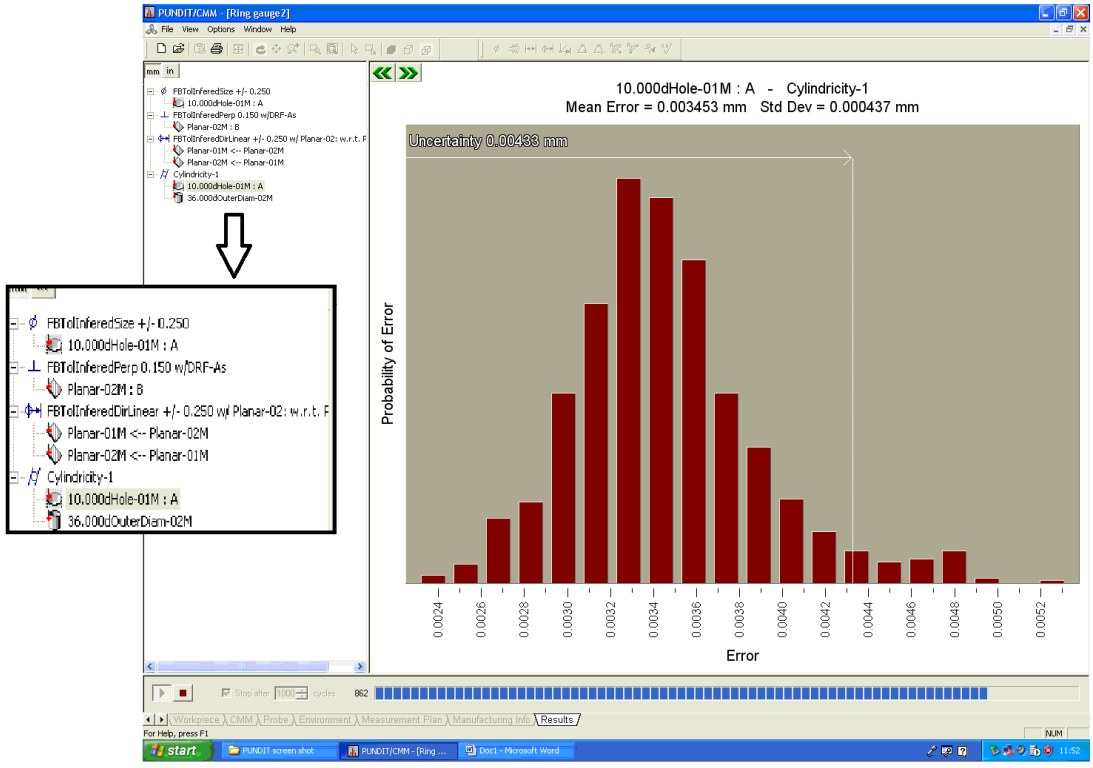

Figure 77 Uncertainty calculation in the digital CMM model

The main window of Figure 77 displays the uncertainty calculation result in histogram. It shows the results of measuring the cylindricity tolerance of the inner circle of the ring gauge under the specified measurement task. The mean error (E) is 0.003453mm, and the standard deviation (σ) is 0.000437mm. The uncertainty (U) is 0.00433mm, which is calculated as

$$U = E + 2|\sigma|.$$

6.2.5 Collect simulation results

The task-specific uncertainties calculated by the digital CMM model are recorded and kept in the Excel table(s) for further analysis.

By this point, the task-specific measurement uncertainties are generated in the digital CMM model based on the selected measurement scenarios. The input values of the digital CMM model are decided given to the resources availability of the physical measurements, and the measurement scenarios defined by the 'Measurement Scenario Streamliner' module in the Measurement Planning and Implementation Framework. The data collection from the digital measurement process is presented in the next section.

6.3 Digital measurement results and Taguchi experimental analysis

6.3.1 Digital measurement results

The digital measurements are carried out as defined by the experiment design. The measurement results are collected and presented in Table 27.

Table 27 Data collection of digital measurement results

Run No.	Measurement scenarios				Diameter result (μm)			Cylindricity result (μm)		
	Probe specification	Number of probing	Distribution of probing points	Part location	Mean error	Standard deviation	Uncertainty	Mean error	Standard deviation	Uncertainty
1	1pt3D_22Z	4	120	Corner	12.768	4.387	21.542	9.890	1.980	13.850
2	1pt3D_22Z	4	120	Corner	12.707	4.248	21.203	9.880	1.955	13.790
3	1pt3D_22Z	4	120	Corner	12.457	4.155	20.767	9.990	1.956	13.902
4	1pt3D_22Z	9	240	Middle	7.967	3.824	15.615	7.263	0.541	8.345
5	1pt3D_22Z	9	240	Middle	8.011	3.993	15.997	7.329	0.589	8.507
6	1pt3D_22Z	9	240	Middle	8.026	3.956	15.938	7.358	0.628	8.614
7	1pt3D_22Z	15	360	Centre	6.045	3.913	13.871	2.887	0.216	3.319
8	1pt3D_22Z	15	360	Centre	6.013	3.673	13.359	2.843	0.164	3.171
9	1pt3D_22Z	15	360	Centre	6.148	3.912	13.972	2.853	0.181	3.215
10	3D_78Z	4	240	Centre	4.157	1.655	7.467	2.812	0.439	3.690
11	3D_78Z	4	240	Centre	4.134	1.654	7.442	2.809	0.459	3.727
12	3D_78Z	4	240	Centre	4.134	1.654	7.442	2.788	0.447	3.682
13	3D_78Z	9	360	Corner	4.980	1.674	8.328	2.732	0.472	3.676
14	3D_78Z	9	360	Corner	4.966	1.647	8.260	2.726	0.466	3.658
15	3D_78Z	9	360	Corner	4.960	1.593	8.146	2.730	0.467	3.664
16	3D_78Z	15	120	Middle	6.487	1.868	10.223	2.487	1.440	5.367
17	3D_78Z	15	120	Middle	6.419	1.867	10.153	2.486	1.430	5.346
18	3D_78Z	15	120	Middle	6.431	1.856	10.143	2.488	1.470	5.428
19	5D_40Z	4	360	Middle	3.662	1.653	6.968	1.576	0.535	2.646
20	5D_40Z	4	360	Middle	3.576	1.560	6.696	1.564	0.536	2.636
21	5D_40Z	4	360	Middle	3.562	1.627	6.816	1.615	0.579	2.773

22	5D_40Z	9	120	Centre	5.518	1.678	8.874	3.570	0.840	5.250
23	5D_40Z	9	120	Centre	5.550	1.549	8.648	3.570	0.840	5.250
24	5D_40Z	9	120	Centre	5.556	1.633	8.822	3.570	0.940	5.450
25	5D_40Z	15	240	Corner	3.981	1.430	6.841	3.077	0.544	4.165
26	5D_40Z	15	240	Corner	3.899	1.480	6.859	3.087	0.554	4.195
27	5D_40Z	15	240	Corner	3.800	1.420	6.640	3.076	0.546	4.168

6.3.2 Taguchi experimental analysis of digital measurement results

The main effects plots of the means and S/N ratios are generated versus the control factors. The linear model results for S/N ratios and means are displayed with respects to diameter measurements and cylindricity measurements in the digital CMM model.

1) Diameter analysis result

The Taguchi analysis results of diameter measurements in digital environment are summarized in Table 28 and Table 30. Table 28 shows the response table and main effects plot for the means, and Figure 71 shows the response table and main effects plot for the S/N ratios. The interpretations of Table 28 and in Figure 71 are presented in the following paragraphs.

A. The effects of the control factors on the mean values

Table 28 reveals the effects of the selected control factors on the mean values of measurement uncertainty by measuring the diameter of the ring gauge in the digital CMM model. The numbers in Table 28 quantitatively represent the effects on the mean value of measurement uncertainty for each level of each control factor. Based on these numbers, the ‘Main Effects Plot for Mean’ is constructed. The Plot visually shows how the selected control factors influence the measurement results.

Table 28 Analysis of the means for diameter measurements in digital environment

Response Table for Means				
Factorial Level	**Control Factors**			
	Probe specification	**Number of probing points**	**Distribution of probing points**	**Part location**
1	16.918	11.816	13.375	9.989
2	8.623	10.959	10.027	12.065
3	7.463	10.229	9.602	10.950
Delta	9.456	1.587	3.773	2.077
Rank	1	4	2	3
Main Effects Plot for Means				

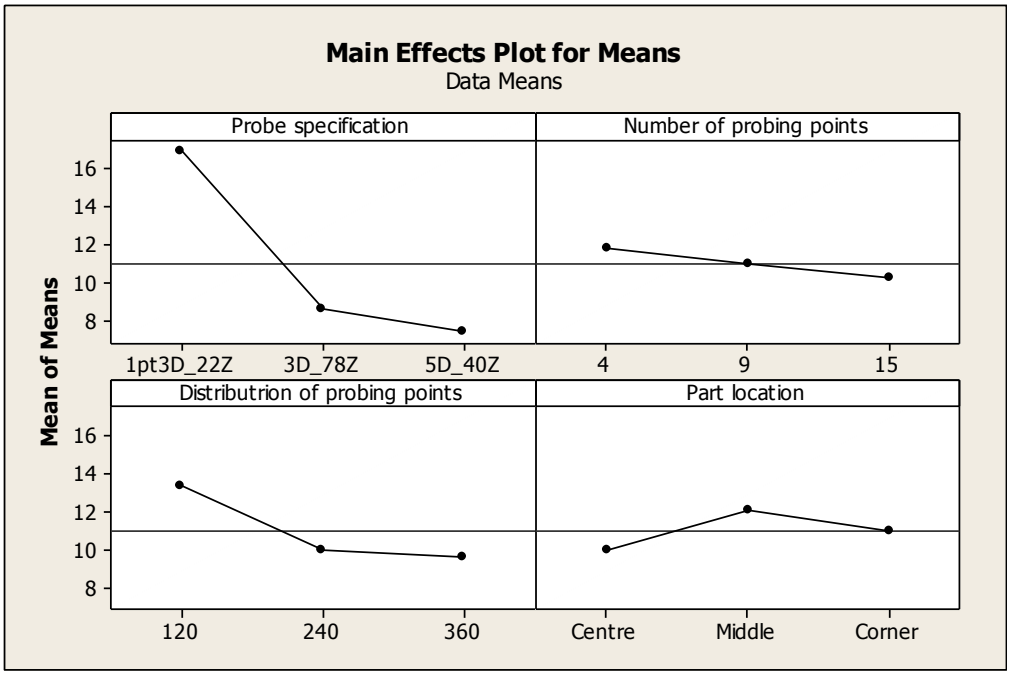

Key words:	*Digital measurement, diameter, mean.*

From the ‘Main Effects Plot for Mean’ in Table 28, two tendencies are observed directly: a) the diameter measurement is influenced by the selected measurement uncertainty contributors; b) Different measurement uncertainty contributors have different effects on the diameter measurement results. These two points are described and discussed in more detail in the following paragraphs.

a) The diameter measurement is influenced by the selected measurement uncertainty contributors. The mean value of the diameter measurement uncertainties,

determined from the digital measurements, changes over the changes of 'probe specification', 'number of probing points', 'distribution of probing points' and 'part location'. Several points are made by examining the 'Main Effects Plot for Mean' against the control factors:

- **Probe specification:** The mean value of measurement uncertainty decreases significantly when it is switched to better CMM probe. In particularly, the measurement uncertainty reduces significantly between Probe 1pt3D_22Z and 3D_78Z. The Taguchi analysis result of the factor effect conforms to common understandings on CMM measurement.
- **Number of probing points:** The mean value of measurement uncertainty decreases when the number of probing points increases. The measurement results are improved by probing more points on the feature. The Taguchi analysis result of the factor effect conforms to common understandings on CMM measurement.
- **Distribution of probing points:** The mean value of measurement uncertainty decreases significantly, when the probing points are distributed more evenly around the circle. In particularly, the measurement uncertainty reduces significantly between 120°-distribution and 240°-distribution. The Taguchi analysis result of the factor effect conforms to common understandings on CMM measurement.
- **Part location:** The mean value of measurement uncertainty changes over the change of part location. As the part is moved from the corner of the CMM bed to the centre, the Plot shows an overall decrease of the measurement uncertainty. However, on the middle point of the centre-corner line, the measurement uncertainty unexpectedly goes higher than the one on the corner point. The Taguchi analysis result of the factor effect conforms to common understandings on CMM measurement, except the one at the 'middle' point. It is possibly accounted by the nature of 'simulation-by-constraints' method, which popularizes a large amount of digital CMMs, and consequently is lack of the sensitivity to the part location adjustment on CMM bed.

b) Different measurement uncertainty contributors have different effects on the diameter measurement results. The range of the measurement uncertainty change varies between the selected control factors. The ranks of the factor effects are assigned based on the Delta statistics calculation[*], which compare the relative magnitude of effects. The Delta values of the control factors are presented in the 'Response Table for Means' in Table 28.

From Table 28, it can be seen that 'probe specification' has the greatest effect on the mean value of measurement uncertainty. 'Distribution of probing points' has the second greatest effect, followed by 'part location' and 'number of probing points'. This Taguchi analysis results suggest that, the most effective way to minimize the measurement uncertainty is to switch to a better CMM probe, and the second effective way is to evenly distribute probing points. Positioning the part in the centre of CMM bed is fairly effective, but not as effective as the former two options. Increasing the density of probing points has least effective impact on CMM measurement result.

The rank drawn from the digital measurement environment is fairly close to the rules-of-thumb in physical measurement. The rank of the control factor effects is discussed in Table 29.

[*] The Delta statistic is the highest minus the lowest average for each factor. Rank 1 assigns to the highest Delta value, rank 2 assigns to the second highest, and so on. Use the level averages in the response tables to determine which level of each factor provides the best result.

Table 29 Discussions of the control factor effects on diameter measurements in the digital environment

Rank	Factor	Discussion
1	Probe specification	Consistent to common understands on CMM measurement process. The quality of measurement hardware assets is primary to the measurement result
2	Distribution of probing points	Consistent to common understands on CMM measurement process. The even distribution of probing points is essential for circle measurement, and the probing points are impelled to be evenly distributed.
3	Part location	Raise concern. Part location has significant impact in physical measurement, where the part is positioned as close as to the centre of CMM bed. The Taguchi analysis on digital measurement results does not reveal the same situation. It is possibly accounted by the nature of 'simulation-by-constraints' method, which popularizes a large amount of digital CMMs, and consequently is lack of the sensitivity to the part location adjustment on CMM bed.
4	Number of probing points	The above Taguchi analysis result is consistent with the NPL recommendation. NPL suggests probing 7 points for circle measurement [135], beyond which the number of probing points has less effects on measurement result.

B. The effects of the control factors on the S/N ratios

S/N ratio is a measure used to identify control factors that reduce variability in a product or process by minimizing the effects of uncontrollable factors (noise factors). In a Taguchi experiment design, noise factors are manipulated to force variability to occur to identify optimal control factor settings that make the process or product resistant to variation from the noise factors. Higher values of the S/N ratio indicate control factor settings that minimize the effects of the noise factors. Generally, it is expected to maximize S/N ratio. In this Taguchi experiment design, S/N ratio is not a key measure to assess the effects of the selected control factors, but it provides further insights to examine the measurement process in digital CMM model.

Table 30 shows the control factor effects on the S/N ratios of the diameter measurements by the digital CMM model. The numbers in Table 30 quantitatively

represent the effects on the S/N ratios for each level of each control factor. Based on these numbers, the 'Main Effects Plot for S/N Ratios' is constructed. The Plot visually shows how the selected control factors are impacted by the noises during the digital measure process.

Table 30 Analysis of the S/N ratios for diameter measurements in digital environment

Response Table for S/N Ratios				
Factorial Level	**Control Factors**			
	Probe specification	**Number of probing points**	**Distribution of probing points**	**Part location**
1	24.42	20.21	21.85	19.69
2	18.64	20.40	19.36	20.49
3	17.39	19.84	19.26	20.28
Delta	7.03	0.55	2.59	0.80
Rank	1	4	2	3

Main Effects Plot for S/N Ratios

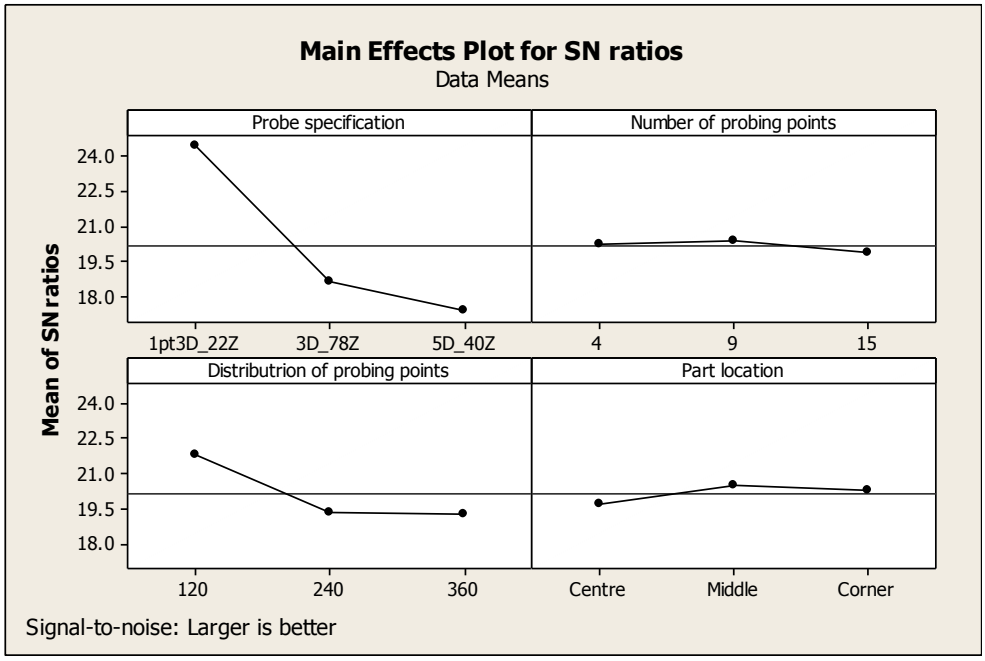

Key words: *digital measurement, diameter, S/N ratio*

Table 30 shows fairly good S/N ratios for diameter measurement. It indicates that the four control factors have significant impacts on the CMM measurement uncertainty, and are fairly independent from other measurement uncertainty contributors. Noticeably, the S/N ratio of 'probe specification' varies most greatly among the four control factors. This is because the independency of 'probe specification' is lower

than the other control factors. The ‘probe specification’ is composed by three components, ‘stylus length in test’, ‘stylus tip point in the - z CMM axis direction’ and ‘range of residuals to 25-point sphere fit’, which possibly contribute more noises over the measurement process. The digital analysis on S/N ratio conforms to the physical measurement reality.

To conclude, the above Taguchi analysis has produced reasonable results in predicting the effects of the control factors on measurement uncertainty of the diameter measurements in a digital environment. Although the effect of ‘part location’ does not completely conform to the rule-of-thumb in physical measurements, it can be explained by the natural blemish of the simulation-by-constraints method employed in the digital CMM model. The simulation-by-constraints method popularizes large amount of virtual CMMs, and ignores the characteristics of individual CMM machines. This limits the CMM digital model to sense the part location adjustments on individual CMM machine. Consequently, it leads to the defect in Taguchi analysis result of predicting the ‘part position’ effect on measurement uncertainty.

2) Cylindricity analysis result

The Taguchi analysis results of cylindricity measurements in the digital environment are summarized in Table 31 and Table 33. Table 31 shows the response table and main effects plot for the means, and Table 33 shows the response table and main effects plot for the S/N ratios. The explanations of Table 31 and Table 33 are presented in the following paragraphs.

A. *The effects of the control factors on the mean values*

Table 31 reveals the effects of the selected control factors on the mean values of measurement uncertainty by measuring the cylindricity of the ring gauge in the digital CMM model. The effects of the control factors observed from cylindricity measurement are similar to the ones from diameter measurement.

Two tendencies are noted: a) The cylindricity measurement is influenced by the selected measurement uncertainty contributors; b) Different measurement uncertainty contributors have different effects on the cylindricity measurement results. These two points are described and discussed in more detail in the following paragraphs.

Table 31 Analysis of the means for the cylindricity measurements in the digital environment

Response Table for Means				
Factorial Level	**Control Factors**			
	Probe specification	**Number of probing points**	**Distribution of probing points**	**Part location**
1	6.699	4.769	5.326	3.078
2	2.673	4.539	4.400	5.243
3	2.745	2.809	2.392	3.796
Delta	4.026	1.960	2.934	2.165
Rank	1	4	2	3

Main Effects Plot for Means

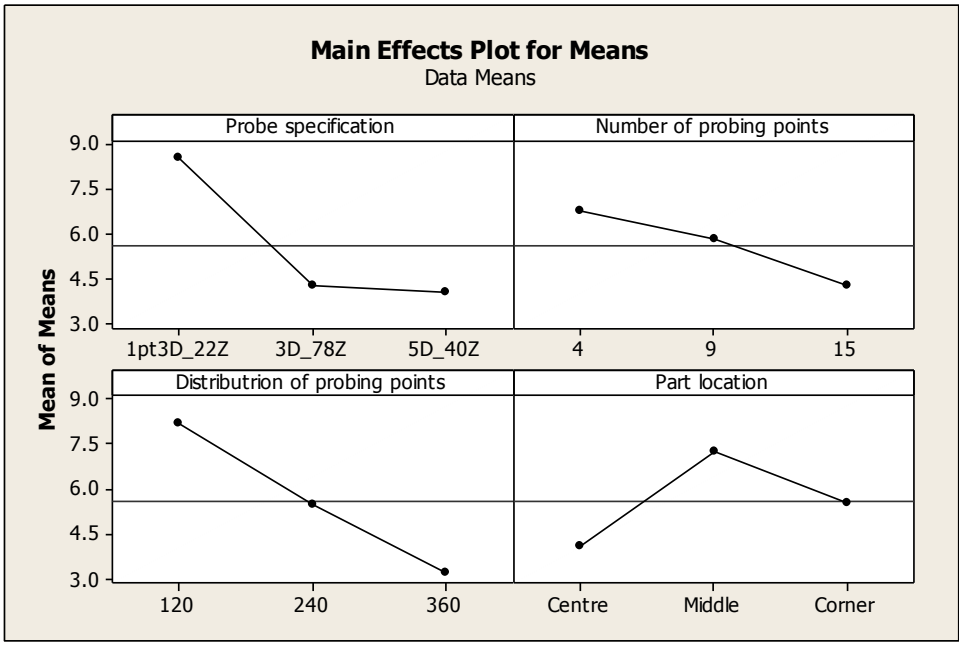

Key words: *digital measurement, cylindricity, mean*

a) The cylindricity measurement is influenced by the selected measurement uncertainty contributors. The mean value of the cylindricity measurement uncertainties, determined from the digital measurements, changes over the

changes of ‘probe specification’, ‘number of probing points’, ‘distribution of probing points’ and ‘part location’. Several points are made by examining the ‘Main Effects Plot for Mean’ against the control factors.

- **Probe specification:** The mean value of measurement uncertainty decreases significantly when it is switched to better CMM probe. In particularly, the measurement uncertainty reduces significantly between Probe 1pt3D_22Z and 3D_78Z. This digital analysis result conforms to common understandings on CMM measurement.
- **Number of probing points:** The mean value of measurement uncertainty decreases when the number of probing points increases. The measurement results are improved by probing more points on the feature. This digital analysis result conforms to common understandings on CMM measurement.
- **Distribution of probing points:** The mean value of measurement uncertainty decreases fairly significantly, when the probing points are distributed more evenly around the circle. This digital analysis result conforms to common understandings on CMM measurement.
- **Part location:** The mean value of measurement uncertainty changes over the change of part location. As the part is moved from the corner of the CMM bed to the centre, the Plot shows an overall decrease of the measurement uncertainty. However, on the middle point of the centre-corner line, the measurement uncertainty unexpectedly goes higher than the one on the corner point. This digital analysis result generally conforms to common understandings on CMM measurement, except the one at the ‘middle’ point. It is possibly accounted by the nature of ‘simulation-by-constraints’ method, which popularizes a large amount of digital CMMs, and consequently is lack of the sensitivity to the part location adjustment on CMM bed.

b) Different measurement uncertainty contributors have different effects on the cylindricity measurement results. The range of the measurement uncertainty change varies between the selected control factors.

From Table 31, it can be seen that ‘probe specification’ has the greatest effect on the mean value of measurement uncertainty. ‘Distribution of probing points’ has the second greatest effect, followed by ‘part location’ and ‘number of probing points’. This Taguchi analysis results suggest that, the most effective way to minimize the measurement uncertainty is to switch to a better CMM probe, and the second effective way is to evenly distribute probing points. Positioning the part in the centre of CMM bed is fairly effective, but not as effective as the former two options. Increasing the density of probing points has the least effective impact on the CMM measurement result.

The rank drawn from the digital measurement environment is fairly close to the rules-of-thumb in physical measurement. The discussions of the control factor effects are summarized in Table 32.

Table 32 Discussions of the control factor effects on cylindricity measurements

Rank	Factor	Discussion
1	Probe specification	Consistent with the rule-of-thumb in physical measurement. The quality of measurement hardware assets is primary to the measurement result
2	Distribution of probing points	Consistent with the rule-of-thumb in physical measurement. The even distribution of probing points is essential for circle measurement, and the probing points are impelled to be evenly distributed.
3	Part location	Raise concern. Part location has significant impact in physical measurement, where the part is positioned as close as to the centre of CMM bed. The Taguchi analysis on digital measurement results does not reveal the same situation. It is possibly accounted by the nature of 'simulation-by-constraints' method, which popularizes a large amount of digital CMMs, and consequently is lack of the sensitivity to the part location adjustment on CMM bed.
4	Number of probing points	The Taguchi analysis result is consistent with the NPL recommendation. NPL suggests probing 7 points for circle measurement [135], beyond which the number of probing points has less effects on measurement result. The above Taguchi analysis result is consistent with the NPL recommendation.

B. *The effects of the control factors on the S/N ratios*

Table 33 shows the control factor effects on the S/N ratios of the cylindricity measurements by the digital CMM model.

Table 33 Analysis of the S/N ratios for cylindricity measurements in digital environment

Response Table for S/N Ratios				
Factorial Level	**Control Factors**			
	Probe specification	**Number of probing points**	**Distribution of probing points**	**Part location**
1	15.449	10.961	12.966	9.712
2	8.529	12.354	12.003	12.808
3	8.275	8.938	7.284	9.734
Delta	7.174	3.415	5.681	3.095
Rank	1	3	2	4

Main Effects Plot for S/N Ratios

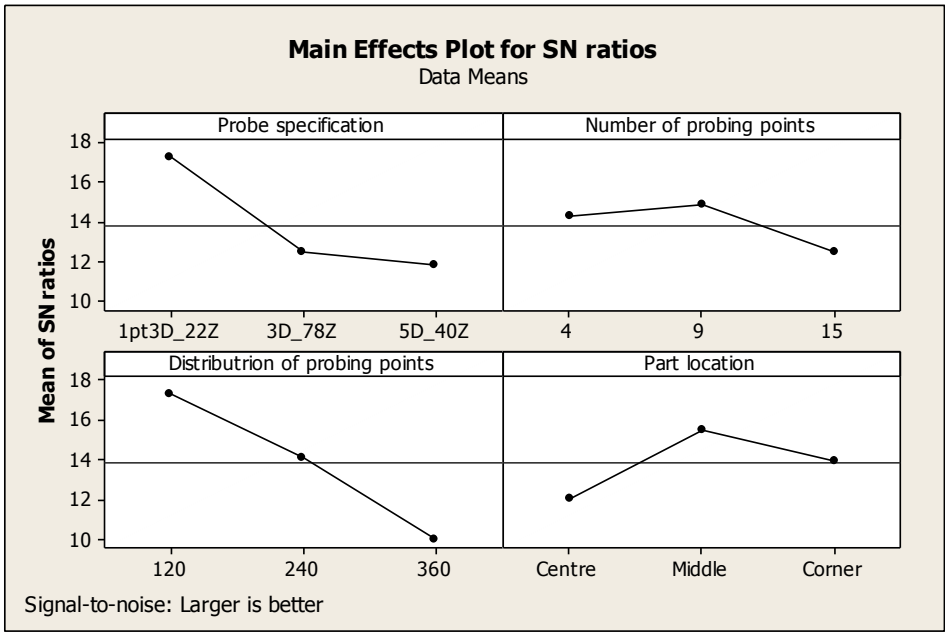

Key words: *digital measurement, cylindricity, S/N ratio*

Similar to diameter measurement, Table 33 shows fairly good S/N ratios for cylindricity measurement. The four control factors have significant impacts on the CMM measurement uncertainty, and they are fairly independent from other measurement uncertainty contributors.

Noticeable, there are sheer differences between the cylindricity S/N ratios and diameter S/N ratios. In term of the factor effect, the diameter S/N ratio tends to be more consistent with physical measurement. This again confirms the capability

variance of the digital CMM model, which performs superior in length measurement than in form measurement in uncertainty calculations.

Table 34 lists The ‘Main Effects Plot(s) for SN ratios’ for both of diameter and cylindricity measurements, by comparing which several differences are realized:

a) The S/N ratio of diameter measurement is generally higher than the one of cylindricity measurement. In the digital measurement environment, signal from diameter measurement is generally stronger than from cylindricity measurement. This confirms that it is easier to estimate task-specific measurement uncertainty for length measurement than for form measurements by digital measurement models;

b) For a single control factor, the S/N ratios in cylindricity measurements generally have greater variations than the ones in diameter measurements. Cylindricity uncertainty estimation is affected by more noises than diameter uncertainty estimation. Again, this indicates that uncertainty estimation for form tolerance is more complicated than for length tolerance. The algorithm for calculating cylindricity measurement uncertainty requires more efforts to determine the complete mathematical description of the CMM task-specific measurement process. On the other hand, this Taguchi analysis result reflects that the digital CMM is not as capable in predicting form measurement uncertainty compared with length measurement uncertainty;

c) The factor effects on S/N ratios in cylindricity measurement and diameter measurements are different. Fox example, in cylindricity measurements the ‘distribution of the probing points’ has the greatest, while in diameter measurements, the ‘probe specification’ has the greatest effect. In term of the factor effect, the diameter S/N ratio tends to be more consistent with physical measurement. This again confirms the capability variance of the digital CMM

model, which performs superior in length measurement than in form measurement in uncertainty calculations.

Table 34 Taguchi analysis result comparison between digital diameter measurement and digital cylindricity measurement

	Diameter	Cylindricity
S/N Ratio	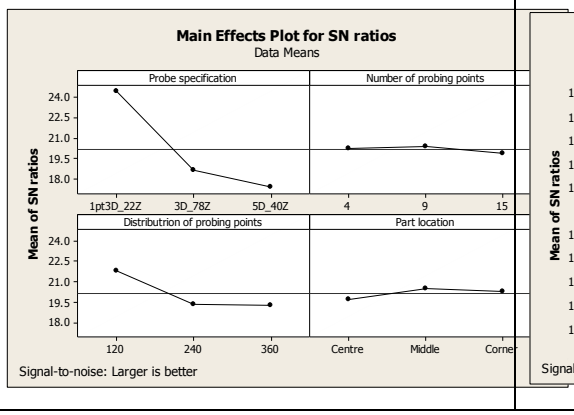	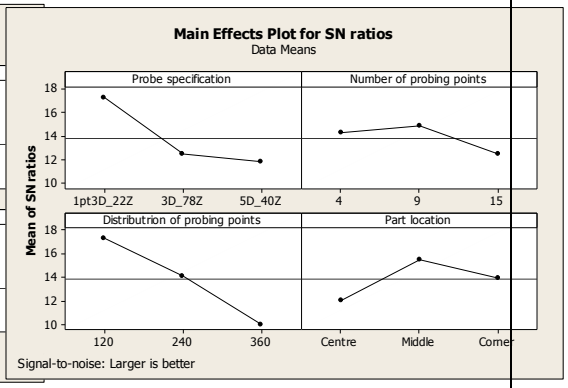

The above Taguchi analysis has produced reasonable results in predicting the effects of the control factors on measurement uncertainty for the cylindricity measurements in a digital environment. Although the effect of 'part location' does not completely conform to the rule-of-thumb in physical measurements, it can be explained by the natural defect of the simulation-by-constraints method employed in the digital CMM model. By comparing the S/N ratios between cylindricity measurement and diameter measurement, it is found that the measurement result produced by a digital CMM model is more reliable for length measurement than for form measurement.

6.3.3 Conclusion of the Taguchi experiment in digital environment

The digital measurement results are collected and analysed using Taguchi experiment design method. The control factor effects on the mean values and S/N ratios are deliberately examined. The Taguchi analysis results have produced reasonable results in predicting the effects of the control factors on measurement uncertainty for both the diameter and cylindricity measurements in a digital environment.

The defects in the Taguchi analysis results can be explained. Two major defects are:

a) The simulation-by-constraints method, deployed in the digital CMM model, is not capable of sensing the individual characteristics of a CMM machine. It limits the CMM digital model to sense the part adjustments on individual CMM machine. Consequently, it leads to the defect in the Taguchi analysis result of predicting the 'part position' effect on measurement uncertainty;

b) Calculating uncertainty for form measurement needs more complex mathematical descriptions than for length measurements. Therefore, the digital CMM model performs better in predicting length measurement uncertainty than form measurement uncertainty. Consequently, it leads to the defect of generating convincing S/N ratios for cylindricity measurements in the Taguchi analysis result.

The above findings have been approved by other scientific researches, and lead further understandings on the digital CMM model. The defects in the Taguchi analysis results are caused by the imperfections of the digital CMM model, and therefore do not disapprove the Taguchi analysis approach proposed in this research.

6.4 Experiment procedures in the physical environment

The physical measurements are designed and performed simultaneously with the digital measurements. To ensure the scientific correctness of the research, the physical measurements are carried out in collaboration with the National Physics Laboratory (NPL). The following procedures are taken to assure the physical measurements accomplish the research objectives:

1) Assessing and selecting measurement resources;
2) Defining measurement environment and artifact;

3) Performing physical measurements.

In the following sub-sections, these procedures are further introduced individually.

6.4.1 Assessing and selecting measurement resources

The measurements in the physical environment are limited by the availability of the measurement resources. The availability and capability of the measurement resources are assessed, given the result of which, the appropriate ones are selected to perform physical measurements.

1) Selecting appropriate CMM machine:

Table 35 lists the available CMM machines in NPL and their technical specifications, given to which the appropriate CMM machine is selected. Zeiss UPMC is selected, because it is equipped with appropriate control software and Virtual CMM (VCMM) package allowing further investigation of the digital CMM performance.

Table 35 Available CMM machines in NPL

CMM Machine	Control Software	VCMM Availability	MPE (μm)	Working Volume	Temperature Control
Leitz PMM	Unknown	Get soon	0.3	1.2m x 1m x 0.6m	20±0.1°C
Leitz PMM	Unknown	Get soon	0.3	1.2m x 1m x 0.6m	20±0.1°C
Zeiss UPMC	Calypso	Yes	1	1.2m x 1m x 0.5m	20±0.1°C
Zeiss F25	Calypso	No	0.25	0.1m x 0.1m x 0.1m	20±0.1°C
Mitutoyo	MCOSMOS	No	2~3	N/A	20±0.1°C
Underlined	Selected for physical measurements				

2) Probe calibration tests and selecting appropriate probe:

Before performing the physical measurement, '25-point sphere fit' tests are carried out on five probes. The testing procedures follow the requirements in ISO

10360. The specifications of the probes-in-test and their testing results are listed in Table 36.

The probe testing result, reflected in the column of ‘range of residuals of 25-point sphere fit’ in Table 36, is the main indicator of the probe performances. The probe performance is jointly influenced by the probe specifications which are listed in the rest of the columns in Table 36. For example, the longer the ‘stylus length in test’ is, the lower the value of ‘range of residuals of 25-point sphere fit’ is expected to be, and the better performance of the probe tends to be. The physical testing results could possibly be contrary to the theoretical expectation due to the unpredictable factors affecting the test procedure.

Table 36 Probe testing results

Probe No.	**Name**	**Ball diameter (mm)**	**Stylus length in test (mm)**	**Shank diameter (mm)**	**Material**	**Stylus tip point in the - z CMM axis direction (mm)**	**Range of residuals to 25-point sphere fit (mm)**
1	1pt3D_22Z	1.35	22	1	Tung. Carbide	67	0.0010
2	2D_40ZC	2	40		Tung. Carbide	99	0.0018
3	3D_78Z	3.5	78	3	Tung. Carbide	128	0.0011
4	3D_20Z	3	21		Tung. Carbide	66	0.0009
5	3D_45Z	3	46		Tung. Carbide	96	0.0012
6	5D_40Z	5	40	4	Tung. Carbide	98	0.0013
Underlined	Selected for physical measurements						

Three probes are selected to be used in the physical measurements (as highlighted in Table 36). Because the testing results of these three probes conform most reasonably with the probe specifications. And the CMM controller has most confidence in dealing with these three probes.

6.4.2 Defining measurement environment and artefact

The measurement resources are selected, and the ring gauge is chosen as the measured artifact (as specified in the previous section). Table 37 summarizes the physical measurement environments, including the CMM machine specifications and the measurement temperature. Figure 78 is the photo of the ring gauge used in the physical measurements. The CAD-model and specifications of the ring gauge are identical that used in the digital measurements. The details could be referenced to Figure 53, Figure 54, Table 1 and Table 2 in the previous section.

Table 37 Physical measurement environment

CMM machine	Zeiss UPMC
Control Software	Calypso
VCMM availability	Yes
MPE (μm)	1.3 + L/300 μm
Working Volume	1.2m x 1m x 0.5m
Temperature Control	20±0.5°C

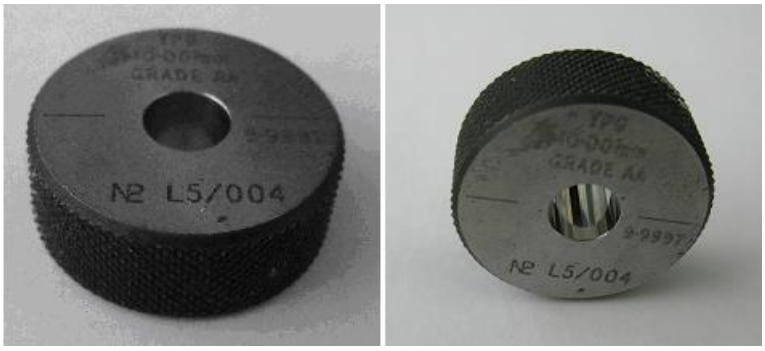

Figure 78 The ring gauge

After defining the measurement environment and the measured artefact, it is ready to perform the physical measurements.

6.4.3 Performing physical measurements

1) Implement the measurement scenarios as in the digital measurement:

The physical measurements are performed in the measurement scenarios as specified in the Taguchi experimental design in the previous section. Figure 79 shows the physical measurements in progress.

Figure 79 Measurements in progress

The measurement results are collected and stored in an Excel table. The data collection and discussion are presented in the next section.

2) Complementary study:

A complementary study is carried out to further study the performance of the digital CMM model. The uncertainty calculation result of the digital CMM model is evaluated against the one of the VCMM which is partnered with the selected CMM machine. The goal is to compare the uncertainty evaluation performances between the simulation-by-constraints method and the full-parametric method.

Probe No 6 is selected to use in the complementary study. The specifications of Probe No 6 are listed in Table 38. Five measurement scenarios (as shown in Figure 64) are selected where the ring gauge measurements are performed. For each measurement scenario, the CMM machine and the VCMM perform three repeated measurements, by averaging which the measurement uncertainty is calculated. The measured features are the cylindricity and the diameter of the inner circle of the ring gauge (as listed in Figure 65).

Table 38 Probe used in the complementary study

Probe No.	**Name**	**Ball diameter (mm)**	**Stylus length in test (mm)**	**Shank diameter (mm)**	**Material**	**Stylus tip point in the -z CMM axis direction (mm)**	**Range of residuals to 25-point sphere fit (mm)**
6	5D_40Z	5	40	4	Tung. Carbide	98	0.0013

Table 39 Measurement scenarios in the complementary study

Scenario No.	**Number of probing points**	**Distribution of probing points**	**Part location**
1	1 (4 points)	1 (Evenly distributed within 120°)	1 (Corner)
4	1 (4 points)	2 (Evenly distributed within 240°)	3 (Centre)
5	2 (9 points)	3 (Evenly distributed within 360°)	1 (Corner)
8	2 (9 points)	1 (Evenly distributed within	3 (Centre)

		120°)	
9	3 (15 points)	2 (Evenly distributed within 240°)	1 (Corner)

Table 40 The measured features in the complementary study

Artefact Name	Ring gauge
Measured Feature	Inner hole
Measured Characteristics	Diameter ⌀
	Cylindricity 

The data is collected in an Excel table, and then numerically analysed. The results and data analysis of the complementary study is presented in the next section. The result from the complementary study further examines the validity of the digital measurement result against the physical measurement, and explains the data analysis result from the Taguchi experiment.

6.5 Physical measurement results and Taguchi experimental analysis

6.5.1 Physical measurement results

The physical measurements are carried out given to the experiment design. The measurement results are collected and presented in Table 41.

Table 41 Data collection for physical measurement results

Run No.	Measurement scenarios				Diameter	Cylindricity		
	Probe specification	Number of probing points	Distribution of probing points	Part location	Uncertainty	X_value	Y_value	Uncertainty
1	1pt3D_22Z	4	120	Corner	0.8	0.1	0.9	0.906
2	1pt3D_22Z	4	120	Corner	0.6	0.2	0.7	0.728
3	1pt3D_22Z	4	120	Corner	1.1	0.5	0.9	1.030
4	1pt3D_22Z	9	240	Middle	0.9	0.1	0.6	0.608
5	1pt3D_22Z	9	240	Middle	0.4	0	0.4	0.400
6	1pt3D_22Z	9	240	Middle	0.7	0.1	0.6	0.608
7	1pt3D_22Z	15	360	Centre	0.1	0.1	0.1	0.141
8	1pt3D_22Z	15	360	Centre	0	0	0	0.000
9	1pt3D_22Z	15	360	Centre	0.1	0	0.1	0.100
10	3D_78Z	4	240	Centre	0.1	0.1	0.2	0.224
11	3D_78Z	4	240	Centre	0.1	0	0	0.000
12	3D_78Z	4	240	Centre	0.2	0	0.1	0.100
13	3D_78Z	9	360	Corner	0.2	0	0.1	0.100
14	3D_78Z	9	360	Corner	0.2	0	0	0.000
15	3D_78Z	9	360	Corner	0.1	0	0	0.000
16	3D_78Z	15	120	Middle	0.3	1	0	1.000
17	3D_78Z	15	120	Middle	0.3	0.1	0.1	0.141
18	3D_78Z	15	120	Middle	3	1	0	1.000
19	5D_40Z	4	360	Middle	0.3	0.1	0.1	0.141

20	5D_40Z	4	360	Middle	0.2	0.1	0.1	0.141
21	5D_40Z	4	360	Middle	0.4	0.2	0.1	0.224
22	5D_40Z	9	120	Centre	0.1	0.1	0.2	0.224
23	5D_40Z	9	120	Centre	0.1	0.1	0.2	0.224
24	5D_40Z	9	120	Centre	0	0.1	0.2	0.224
25	5D_40Z	15	240	Corner	0.1	0.1	0.1	0.141
26	5D_40Z	15	240	Corner	0.2	0.1	0.1	0.141
27	5D_40Z	15	240	Corner	0.1	0.1	0	0.100

6.5.2 Taguchi experimental analysis of physical measurement results

The main effects plots of the means and S/N ratios are generated versus the control factors. The linear model results for S/N ratios and means are displayed with respects to diameter measurements and cylindricity measurements in the physical measurement environment.

1) Diameter analysis result

The Taguchi analysis results of diameter measurements in the physical measurement environment are summarized in Table 42 and Table 44. Table 42 shows the response table and main effects plot for the means, and Table 44 shows the response table and main effects plot for the S/N ratios. The interpretations of Table 42 and Table 44 are presented in the following paragraphs.

A. The effects of the control factors on the mean values

Table 42 reveals the effects of the selected control factors on the mean values of measurement uncertainty by measuring the diameter of the ring gauge in the physical measurement environment.

Table 42 Analysis of the means for cylindricity measurements in physical environment

Response Table for Means				
Factorial Level	**Control Factors**			
	Probe specification	**Number of probing points**	**Distribution of probing points**	**Part location**
1	0.52222	0.42222	0.40000	0.08889
2	0.20000	0.30000	0.31111	0.37778
3	0.16667	0.16667	0.17778	0.42222
Delta	0.35556	0.25556	0.22222	0.33333
Rank	1	3	2	4
Main Effects Plot for Means				

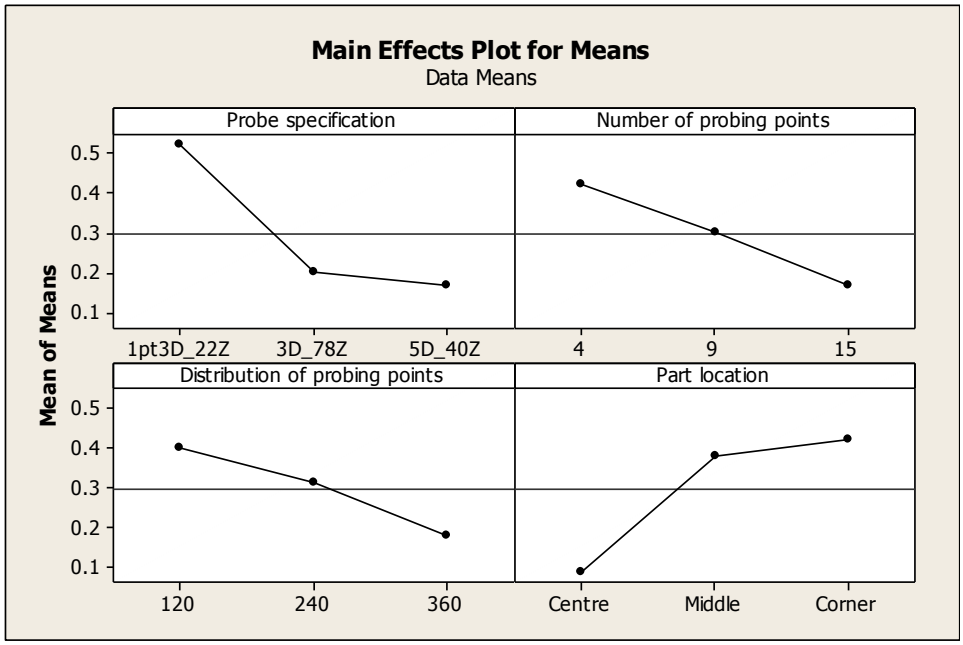

Key words: *physical measurement, diameter, mean*

From the 'Main Effects Plot for Mean' in Table 42, two tendencies are observed: a) the diameter measurement is influenced by the selected measurement uncertainty contributors; b) Different measurement uncertainty contributors have different effects on the diameter measurement results. These two points are described and discussed into more details in the following paragraphs.

a) The diameter measurement is influenced by the selected measurement uncertainty contributors. The mean value of the diameter measurement uncertainties, determined from the physical measurements, changes over the changes of 'probe specification', 'number of probing points', 'distribution of probing points' and 'part location'. Several points are made by examining the 'Main Effects Plot for Mean' against the control factors:

   - **Probe specification:** The mean value of measurement uncertainty decreases significantly when it is switched to better CMM probe. In particularly, the measurement uncertainty reduces significantly between Probe 1pt3D_22Z and 3D_78Z. The Taguchi analysis result of the factor effect conforms to common understandings on CMM measurement.
   - **Number of probing points:** The mean value of measurement uncertainty

decreases when the number of probing points increases. The measurement results are improved by probing more points on the feature. The Taguchi analysis result of the factor effect fairly conforms to common understandings on CMM measurement. NPL suggests probing 7 points for circle measurement [135], beyond which the number of probing points has less effects on measurement result.

- **Distribution of probing points:** The mean value of measurement uncertainty decreases as the probing points are distributed more evenly around the circle. The Taguchi analysis result of the factor effect conforms to common understandings on CMM measurement.
- **Part location:** The mean value of measurement uncertainty decreases, as the part is moved toward to the centre of the CMM bed. The Taguchi analysis result of the factor effect conforms to common understandings on CMM measurement.

b) Different measurement uncertainty contributors have different effects on the diameter measurement results. The range of the measurement uncertainty change varies between the selected control factors. The ranks of the factor effects are assigned based on Delta statistics calculation, and are presented in the 'Response Table for Means' in Table 42.

From Table 42, it can be seen that 'probe specification' has the greatest effect on the mean value of measurement uncertainty. 'Distribution of probing points' has the second greatest effect, followed by 'number of probing points' and 'part location'. The rank is fairly consistent with the common understandings on CMM measurement. The rank of the control factor effects is discussed in Table 43.

Table 43 Discussions of the control factor effects on diameter measurements in the physical environment

Rank	Factor	Discussion

1	Probe specification	Consistent with common understanding on CMM measurement. The quality of measurement hardware assets is primary to the measurement result
2	Distribution of probing points	Consistent with common understanding on CMM measurement. The even distribution of probing points is essential for circle measurement, and the probing points are impelled to be evenly distributed.
3	Number of probing points	Raising concern. The 'number of probing points' should have less effect on measurement result in this physical experiment.
4	Part location	Raising concern because of the concern from 'number of probing points' effect. The ranks of 'part location' and 'number of probing points' are not consistent with common understandings on CMM measurement.

B. The effects of the control factors on the S/N ratios

Table 44 reveals the effects of the selected control factors on the S/N ratios of measurement uncertainty by measuring the diameter of the ring gauge in the physical measurement environment.

Table 44 Analysis of the S/N ratios for diameter measurements in physical environment

Response Table for S/N Ratios				
Factorial Level	**Control Factors**			
	Probe specification	**Number of probing points**	**Distribution of probing points**	**Part location**
1	16.25	18.92	18.38	24.77
2	24.77	20.51	20.51	20.51
3	23.18	24.77	23.18	15.99
Delta	8.53	5.85	4.80	8.78
Rank	2	3	4	1

Main Effects Plot for S/N Ratios

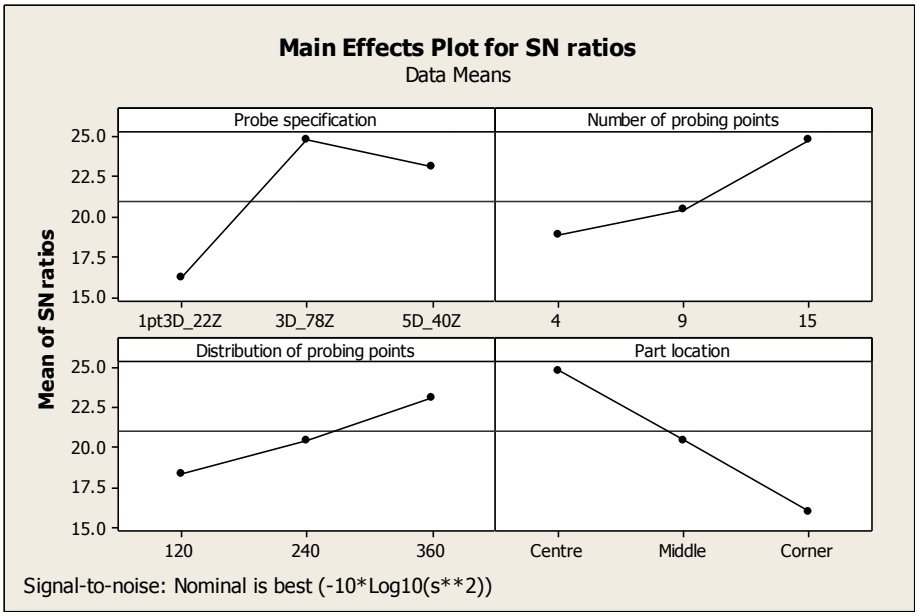

Key words: *physical measurement, diameter, S/N ratio*

Table 44 shows fairly good S/N ratios for diameter measurement. It indicates that the four control factors have significant impacts on the CMM measurement uncertainty, and are fairly independent from other measurement uncertainty contributors. Noticeably, the S/N ratio in physical measurements varies greatly against the factorial level changes. It indicates that the physical measurement environment is influenced by more measurement uncertainty contributors. Similar to the digital measurement environment, the 'probe specification' has greater impact on the S/N ratio, because the 'probe specification' is composed by three components, 'stylus length in test', 'stylus tip point in the - z CMM axis direction'

and ‘range of residuals to 25-point sphere fit’, which possibly contribute more noises over the measurement process.

To conclude, the above Taguchi analysis have produced fairly reasonable results in predicting the effects of the control factors on measurement uncertainty of the diameter measurements in physical environment. But the effect of ‘number of probing points’ does not approve the NPL experimental result [135], and the disapproval can not be explained.

2) Cylindricity analysis result

The Taguchi analysis results of cylindricity measurements in physical measurement environment are summarized in Table 45 and Table 46. Table 45 shows the response table and main effects plot for the means, and Table 46 shows the response table and main effects plot for the S/N ratios. The interpretations of Table 45 and Table 46 are presented in the following paragraphs.

A. The effects of the control factors on the mean values

Table 45 reveals the effects of the selected control factors on the mean values of measurement uncertainty by measuring the cylindricity of the ring gauge in the physical measurement environment.

Table 45 Analysis of the means for cylindricity measurements in physical environment

Response Table for Means				
Factorial Level	**Control Factors**			
	Probe specification	**Number of probing points**	**Distribution of probing points**	**Part location**
1	0.50234	0.38813	0.50837	0.13732
2	0.18500	0.26526	0.25811	0.34955
3	0.17335	0.20730	0.09421	0.37382
Delta	0.32900	0.18083	0.41416	0.23651
Rank	2	4	1	3

Main Effects Plot for Means

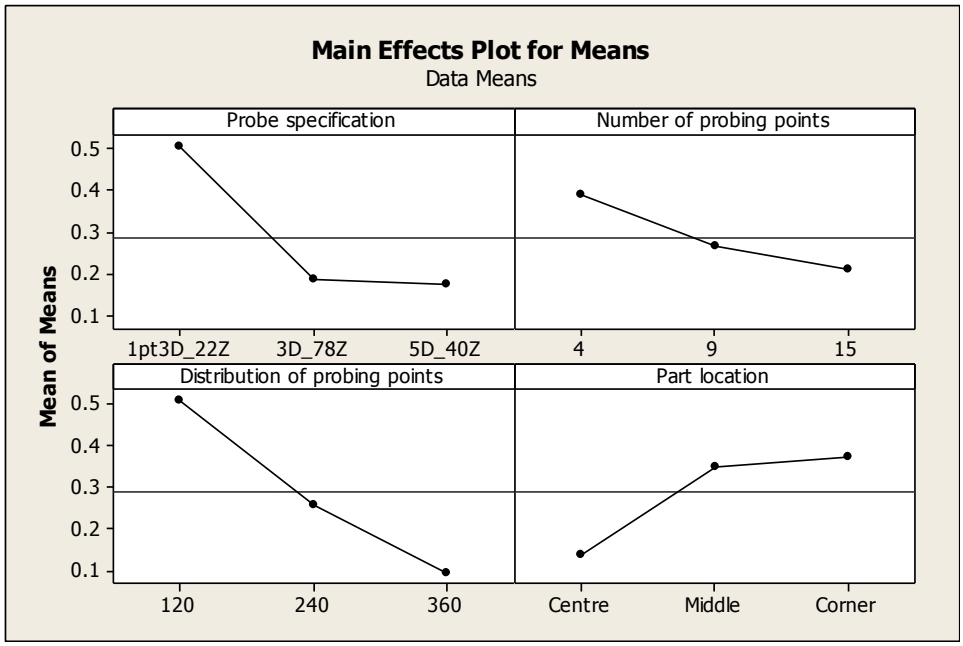

Key words: *physical measurement, cylindricity, mean*

Two tendencies are noted from Table 45: a) The cylindricity measurement is influenced by the selected measurement uncertainty contributors; b) Different measurement uncertainty contributors have different effects on the cylindricity measurement results. The two points are discussed in the following paragraphs:

a) The cylindricity measurement is influenced by the selected control factors. The mean value of the cylindricity measurement uncertainties, determined from the physical measurements, changes over the changes of ‘probe specification’, ‘number of probing points’, ‘distribution of probing points’ and ‘part location’.

Several points are made by examining the 'Main Effects Plot for Mean' against the control factors:

- **Probe specification:** The mean value of measurement uncertainty decreases significantly when it is switched to better CMM probe. In particularly, the measurement uncertainty reduces significantly between Probe 1pt3D_22Z and 3D_78Z. The Taguchi analysis result of the factor effect conforms to common understandings on CMM measurement.
- **Number of probing points:** The mean value of measurement uncertainty decreases when the number of probing points increases. The measurement results are improved by probing more points on the feature. The Taguchi analysis result of the factor effect conforms to common understandings on CMM measurement.
- **Distribution of probing points:** The mean value of measurement uncertainty decreases fairly significantly, when the probing points are distributed more evenly around the circle. The Taguchi analysis result of the factor effect conforms to common understandings on CMM measurement.
- **Part location:** The mean value of measurement uncertainty decreases, as the part is moved toward to the centre of the CMM bed. In particularly, the measurement uncertainty reduces more significantly when the part is moved from the 'middle' point to the centre of the CMM bed. The Taguchi analysis result of the factor effect conforms to common understandings on CMM measurement.

b) Different measurement uncertainty contributors have different effects on the cylindricity measurement results. The range of the measurement uncertainty change varies between the selected control factors.

From Table 45, it can be seen that 'Distribution of probing points' has the greatest effect on the mean value of measurement uncertainty. 'Probe specification' has the second greatest effect, followed by 'number of probing points' and 'part

location'. This Taguchi analysis result suggests that, the most effective way to minimize the measurement uncertainty is to encourage an even distribution of probing points, and the second effective way is to switch to a better CMM probe. Increasing the density of probing points is also effective, but not as effective as the former two options. Positioning the part in the centre of CMM bed has least effective impact.

B. The effects of the control factors on the S/N ratios

Table 46 reveals the effects of the selected control factors on the S/N ratios of measurement uncertainty of cylindricity measurements in the physical environment.

Table 46 Analysis of the S/N ratios for cylindricity measurements in physical environment

Response Table for S/N Ratios				
Factorial Level	**Control Factors**			
	Probe specification	**Number of probing points**	**Distribution of probing points**	**Part location**
1	9.754	8.683	109.977	105.639
2	-2.294	108.206	9.082	8.376
3	113.977	4.548	2.378	7.423
Delta	116.270	103.658	107.599	98.216
Rank	1	3	2	4

Main Effects Plot for S/N Ratios

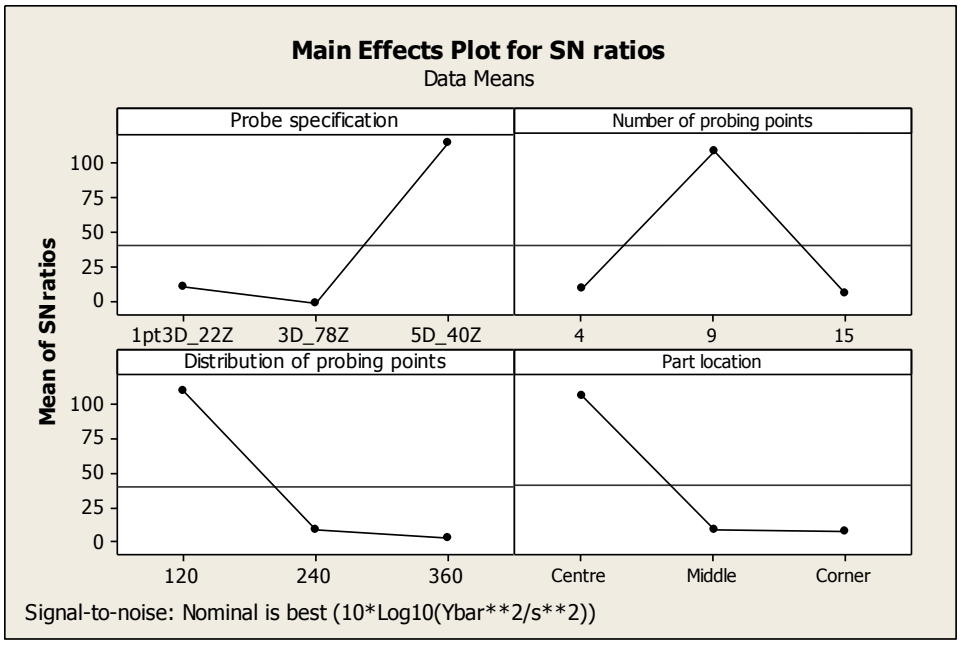

Key words: *physical measurement, cylindricity, S/N ratio*

Table 46 shows fairly good S/N ratios for cylindricity measurement. The four control factors have significant impacts on the CMM measurement uncertainty, and they are fairly independent. The variance of S/N ratios in the physical measurements is generally higher than in the digital measurements.

The above Taguchi analysis has produced reasonable results in predicting the effects of the control factors on measurement uncertainty for the cylindricity measurements in the physical environment.

6.5.3 Conclusion of Taguchi experiment method in physical environment

The physical measurement results are collected and analysed using Taguchi data analysis method. The control factor effects on the mean values and S/N ratios are deliberately examined. The Taguchi analysis results have produced reasonable results in predicting the effects of the control factors on measurement uncertainty for both of diameter and cylindricity measurements in physical environment.

There are defects in the Taguchi analysis results. These defects build on the high complexity of CMM measurement tasks. The complete traceability of uncertainty chain is virtually impossible to model and manage. Despite the defects, the physical measurement results are still of very high quality. The Taguchi analysis results from the physical measurements are used to benchmark that from the digital measurements, and therefore to verify the digital CMM measurement model.

The comparisons between digital and physical measurements are provided in the next section.

6.6 Comparison between physical measurement results and digital measurement results

The digital measurement results and the physical measurement results are compared in this section in order to assess the validity of the Measurement Planning and Implementation Framework. Firstly, the two sets of measurement results are compared directly under each measurement scenario. The direct comparison concerns the verification of the digital CMM model. Secondly, the two sets of Taguchi analysis results are compared. This comparison assesses the validity of the Taguchi analysis method proposed in the Framework.

6.6.1 Direct comparison

In this section, the digital measurement results and physical measurement results are compared for the two feature measurements, diameter and cylindricity.

1) Diameter measurements

Table 47 ties the digital measurement results and the physical measurement results. The measurement results in Table 47 are the average value of the three measurement runs for each measurement scenario. The ratios the digital measurement results and the physical measurement results are calculated and listed in the last row of Table 47. Figure 80 is constructed based on Table 47.

Table 47 Data collection for comparing diameter measurement results

Measurement Scenario No.	Measurement Uncertainty Contributors				Diameter		
	Probe specification	Number of probing points	Distribution of probing points	Part location	Average of digital measurement results	Average of physical measurement results	Ratio
1	1pt3D_22Z	4	120	Corner	21.171	0.833	25.405
2	1pt3D_22Z	9	240	Middle	15.850	0.667	23.775
3	1pt3D_22Z	15	360	Centre	13.734	0.067	206.010
4	3D_78Z	4	240	Centre	7.450	0.133	55.878
5	3D_78Z	9	360	Corner	8.245	0.167	49.468
6	3D_78Z	15	120	Middle	10.173	0.300	33.910
7	5D_40Z	4	360	Middle	6.827	0.300	22.756
8	5D_40Z	9	120	Centre	8.781	0.067	131.720
9	5D_40Z	15	240	Corner	6.780	0.133	50.850

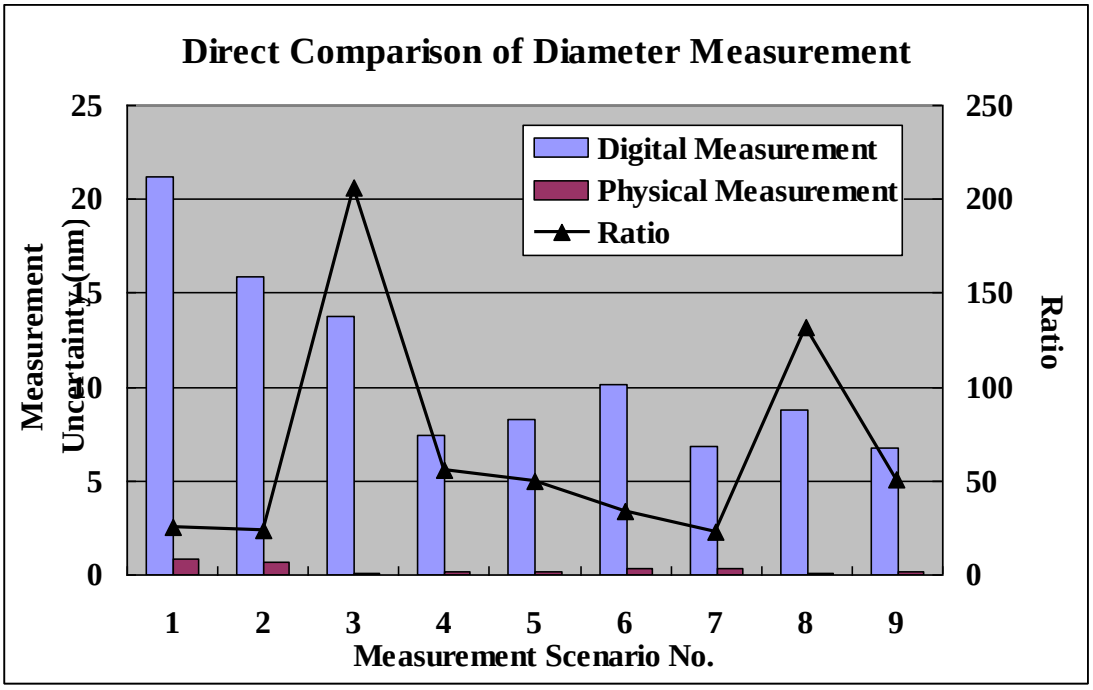

Figure 80 Direct comparison of diameter measurement results

Figure 80 underline the difference between the digital and physical measurement results of the select measurement scenarios for the diameter measurement of the ring gauge. By observing Figure 80, several points are made as below:

- The digital measurement results are significantly higher than the physical measurement results. This observation agrees with the theoretical analysis on the limitation of the simulation-by-constraints method. The simulation-by-constraints method predicts the measurement uncertainty based on the concise information of the measurement tasks. It lowers the fidelity of the digital measurement process, and consequently raises the uncertainty of the measurement result.
- The ratios between digital measurement results and physical measurement results vary greatly and irregularly among the measurement scenarios. It indicates that the performance of the CMM digital model is unstable. The digital measurement process highly relies on the input quantities of the measurement uncertainty contributors. The accountability of the digital CMM model needs to be improved before deployed into shop floor production;
- The ratios of Scenario 3 and Scenario 8 are exceptionally higher. It is found

difficult to interpret this interpret. However, it proves that uncertainty estimation in digital environment is a challenging task because of the complexity of CMM measurement tasks. The verification and validation are of primary importance as they ultimately influence and define the functionality of the digital measurement process [17].

2) Cylindricity measurements

Table 48 ties the digital measurement results and the physical measurement results for the cylindricity measurement. The measurement results in Table 48 are the average value of the three measurement runs for each measurement scenario. The ratios of the digital measurement results to the physical measurement results are calculated and listed in the last row of Table 48. Figure 81 is constructed based on Table 48.

Table 48 Data collection for comparing cylindricity measurement results

Measurement Scenario No.	Measurement Uncertainty Contributors				Diameter		
	Probe specification	Number of probing points	Distribution of probing points	Part location	Average of digital measurement results	Average of physical measurement results	Ratio
1	1pt3D_22Z	4	120	Corner	13.847	0.888	15.599
2	1pt3D_22Z	9	240	Middle	8.489	0.539	15.753
3	1pt3D_22Z	15	360	Centre	3.235	0.080	40.199
4	3D_78Z	4	240	Centre	3.700	0.108	34.300
5	3D_78Z	9	360	Corner	3.666	0.033	109.980
6	3D_78Z	15	120	Middle	5.380	0.414	13.002
7	5D_40Z	4	360	Middle	2.685	0.169	15.905
8	5D_40Z	9	120	Centre	5.317	0.224	23.777
9	5D_40Z	15	240	Corner	4.176	0.128	32.724

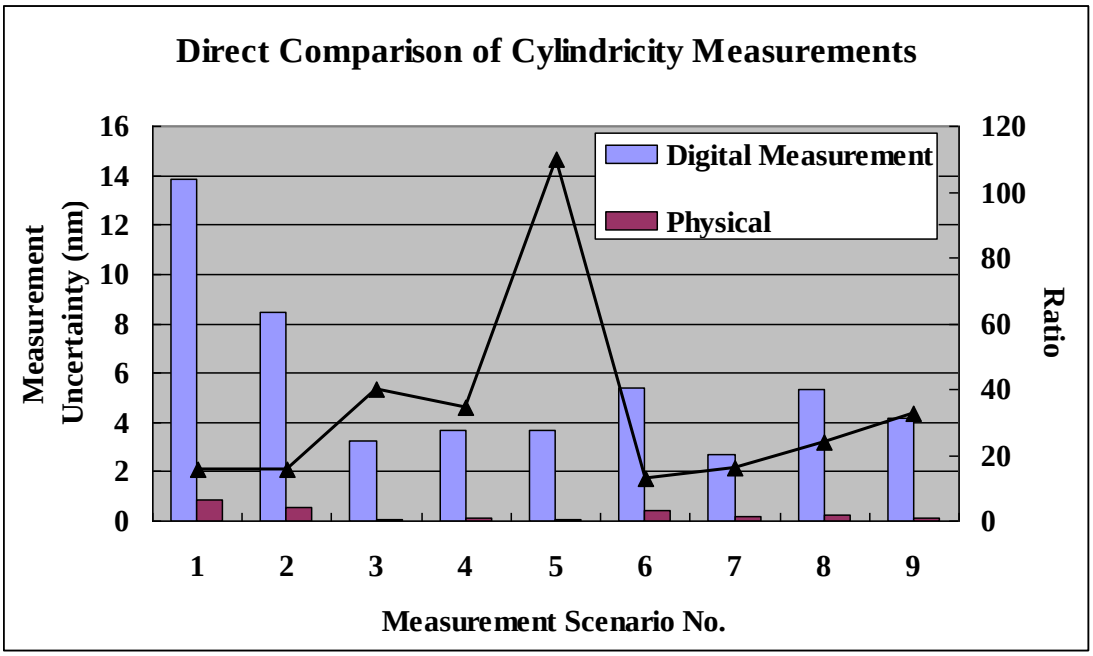

Figure 81 Direct comparison of cylindricitiy measurement results

Similar conclusions could be made from the cylindricity measurement results by observing Figure 81. Although the comparison results of the cylindricity measurement results and diameter measurements are numerically different, both of them have proven that the accountability of the digital measurements needs to be enhanced. The fidelity of the digital measurement results highly depend on the accuracy of the mathematical description of the measurement uncertainty contributors. The digital CMM model needs to improve this aspect before it is used in practical production environment.

6.6.2 Taguchi experimental result comparison

In this sector, the Taguchi experimental results of the digital measurements are compared with that of physical measurements. The Taguchi analysis results of two measured features, diameter and cylindricity, are compared respectively. The computing results of Taguchi experimental analysis, mean value and S/N ratio, are examined in the comparison.

1) Diameter measurement

Table 49 ties the Taguchi analysis results of the diameter measurements in the digital environment and the physical environment. The rows of ‘Mean’ and ‘S/N Ratio’ respectively contain the Taguchi analysis results of the mean values and of the S/N ratios from the two measurement environments.

Table 49 Comparison of Taguchi analysis results of diameter measurements

	Digital Measurement	Physical Measurement
Mean	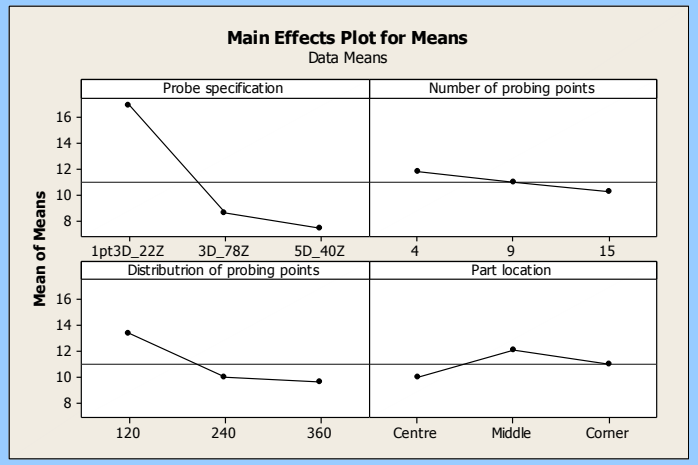	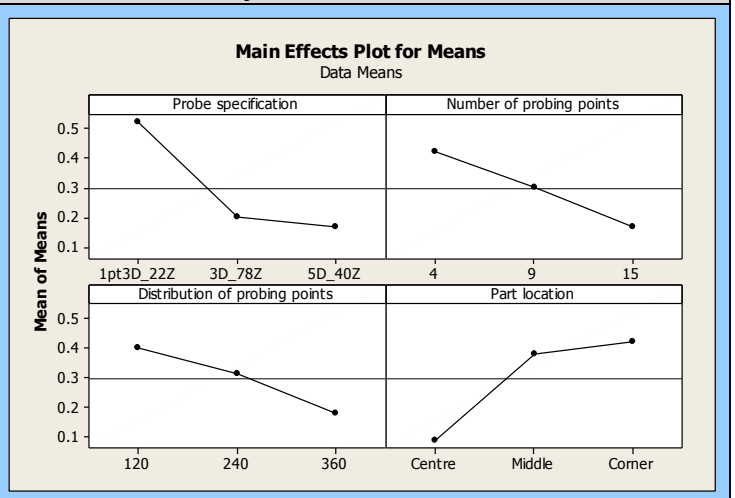
S/N Ratio	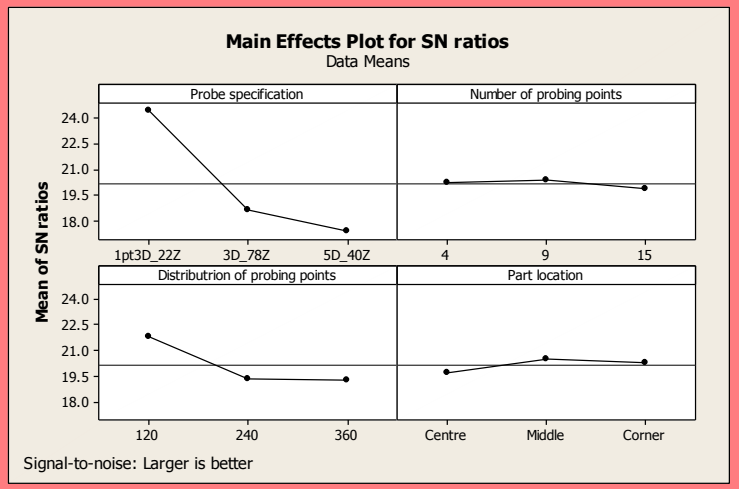	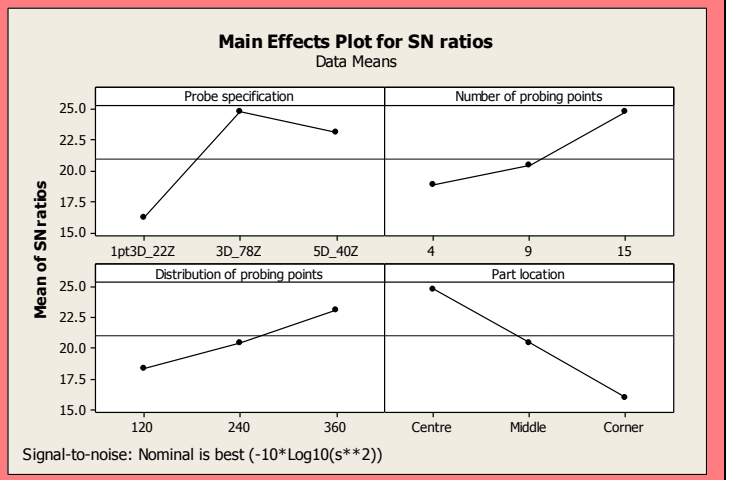

- Comparison of mean values

  As shown in Table 49, the mean values from the digital measurements are generally higher than that from the physical measurements. It indicates that the simulation-by-constraints method tends to overstate the measurement uncertainty. This problem is caused by the nature of the simulation-by-constraints method, which requires the partial information feed of the measurement task. It suggests the end-users to provide as fully complete description of CMM measurement scenarios as possible to the digital CMM model. On the other hand, it implicates that the simulation-by-constraints method is possibly more appropriate for instructing CMM measurement process than merely evaluating the measurement uncertainty of specific CMM measurement task.

  For the diameter measurements, the trends of the mean value changing against the control factors show noticeable consistency between the digital measurement results and the physical measurement results. Several points are made by comparing the mean value trends against the selected control factors:

  - **Probe Specification:** The mean values of measurement uncertainty decrease as switching to better probe. The measurement uncertainty decreases more significantly between Probe 1pt3D_22Z and Probe 3D_78Z. The trend in digital measurements is consistent with that in physical measurements.
  - **Number of probing points:** The mean values of measurement uncertainty decrease as the number of probing points increase. The mean value of measurement uncertainty in physical environment has bigger variation against the factorial level changes than that in digital environment. The trend in digital measurements is generally consistent with that in physical measurement. But intensifying the probing points is more effective in the physical measurement environment than in the digital measurement environment. It implicates that the simulation-by-constraints method is less sensitive on individual uncertainty contributors because of its nature.
  - **Distribution of probing points:** The mean value of measurement uncertainty

decreases as the probing points is distributed more evenly along the circle. The trend in digital measurements is fairly consistent with that in physical measurements.

- **Part location:** In the digital measurement environment, the measurement uncertainty is at the peak when the part is located at the quarter of the diagonal line of the CMM bed. However, in the physical measurement results, the measurement uncertainty increases greatly as the part moves from the centre to the corner of the CMM bed. The trend in digital measurements is inconsistent with that in physical measurement. The digital measurement results deviate from common understanding of CMM measurement process, and therefore are identified as bad data. The trend comparison of 'part location' indicates the limited nature of the simulation-by-constraints method, but does not refute the feasibility of Taguchi analysis approach proposed in this research.

From the Taguchi analysis on the physical measurement results, it could be seen that the 'probe specification' factor has the biggest impact on the measurement result. The 'part location' factor has second biggest impact. The rest of the two factors have similar impact, while the 'number of probing points' has slightly bigger impact than 'distribution of probing points'. The Taguchi analysis on the digital measurement results shows fairly logical coherence with the physical ones, but also shows certain degree of misalignment. The 'probe specification' has the biggest impact, which is the same with the analysis on the physical measurements. Although the analysis on digital measurements shows that the 'distribution of probing points' has the second biggest impact on measurement uncertainty, the impacts of 'number of probing points' is not significantly lower than that of 'distribution of probing points'. This is similar to the analysis on the digital measurements. The digital analysis result of 'part location' is inconsistent with common sense of CMM measurement, and consequently it is not proper to refer the 'part location' analysis result for the comparison. However, it suggests that

the digital CMM model needs to improve its sensibility on the part location change.

- Comparison of S/N ratios

  In general Taguchi experimental design, S/N ratio reflects the robustness of the experiment process and analysis result. In this Taguchi experimental design, S/N ratio is neither the key index for assessing the capability of the digital CMM model and nor for validating the Measurement Planning and Implementation Framework. Given the aims and objectives of this experimental research, it is not necessary to compare the S/N ratio values between the digital measurement environment and the physical measurement environment.

  The S/N ratios are discussed here in order to examine the robustness of the Taguchi experimental approach proposed in this research, in particular, to indentify the effects of the selected control factors on the measurement uncertainty against the un-selected control factors (other measurement uncertainty contributors).

  As shown in Table 49, the S/N ratios in both of digital and physical environments show good values, varying between 15 to 25. It confirms the robustness of the Taguchi experimental design in both of the digital measurement environment and the physical environment. Moreover, it indicates the prospect of incorporating the design of experiments (DOE) methods into the measurement uncertainty analysis to enable the knowledge management in task-specific measurements and to create the adoption of measurement experiences to the overall manufacturing process control.

2) Cylindricity measurement

Table 50 ties the Taguchi analysis results of the cylindricity measurements in the digital environment and the physical environment.

Table 50 Comparison of Taguchi analysis results of cylindricity measurements

	Digital Measurement	Physical Measurement
Mean	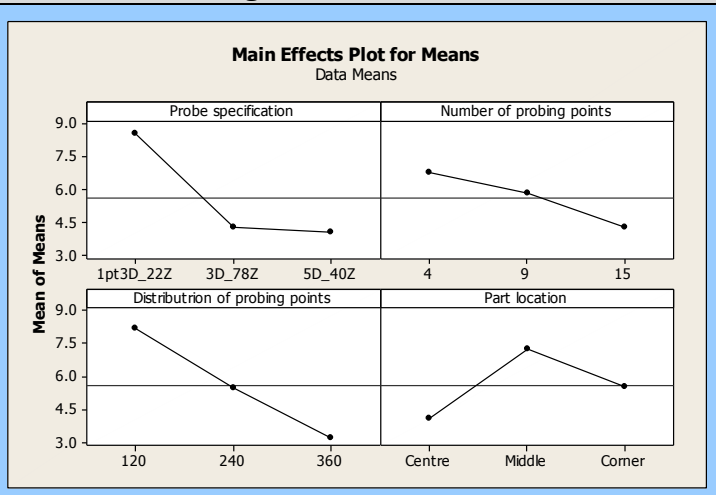	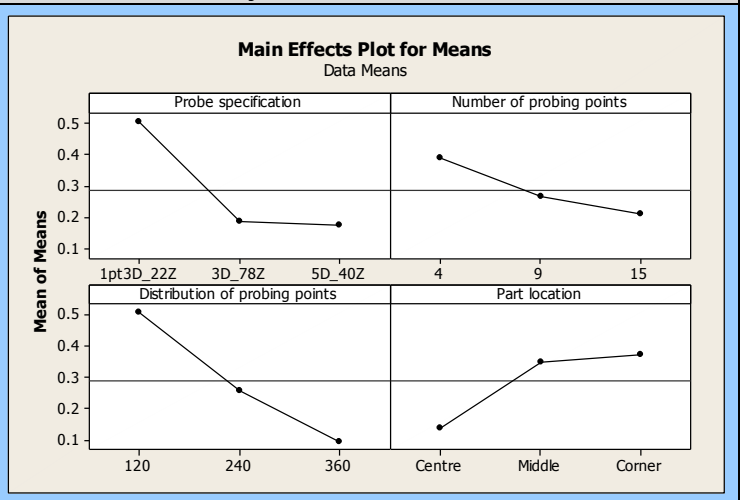
S/N Ratio	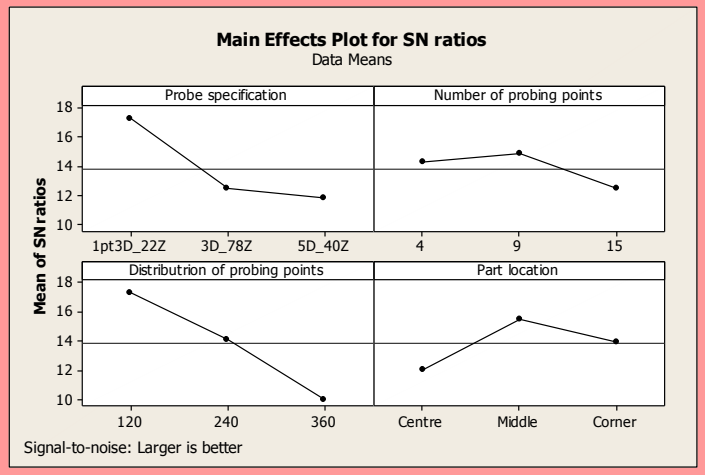	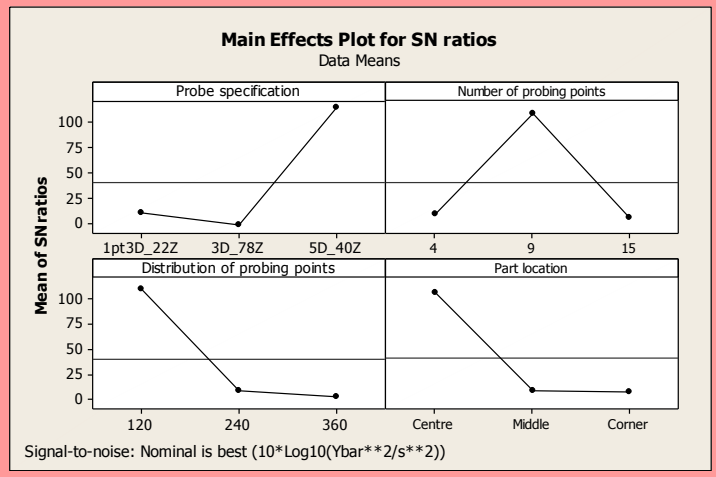

- Comparison of mean values

  Table 50 shows that the mean values of the cylindricity measurements in the digital environment are generally higher than that in the physical environment. This is similar to the diameter measurements, and once again indicates that the simulation-by-constraints method tends to overstate the measurement uncertainty.

  For the cylindricity measurements, the trends of the mean value changing against the control factors also show good consistency between the digital measurement results and the physical measurement results. Several points are made by comparing the mean value trends against the selected control factors:

  - **Probe Specification:** The mean values of measurement uncertainty decrease as switching to better probe. The measurement uncertainty decreases more significantly between Probe 1pt3D_22Z and Probe 3D_78Z. The trend in digital measurements is consistent with that in physical measurements.
  - **Number of probing points:** The mean values of measurement uncertainty decrease as the number of probing points increase. The trend in digital measurements is consistent with that in physical measurements.
  - **Distribution of probing points:** The mean value of measurement uncertainty decreases as the probing points is distributed more evenly along the circle. The trend in digital measurements is consistent with that in physical measurements.
  - **Part location:** In the digital measurement environment, the measurement uncertainty is at the peak when the part is located at the quarter of the diagonal line of the CMM bed. However, in the physical measurement results, the measurement uncertainty increases greatly as the part moves from the centre to the corner of the CMM bed. The trend in digital measurements is inconsistent with that in physical measurement. The digital measurement results deviate from common understanding of CMM measurement process, and therefore are identified as bad data. The trend comparison of 'part location' indicates the limited nature of the simulation-by-constraints method,

but does not refute the feasibility of Taguchi analysis approach proposed in this research.

Similar comparison results are observed from the cylindricity measurements as from the diameter measurements. In the physical measurement environment, the 'distribution of probing points' factor has the biggest impact on the measurement result for cylindricity measurement. The 'probe specification' factor has second biggest impact, followed by 'part location' and 'number of probing points'. The Taguchi analysis on the digital measurement results shows logical coherence with the physical ones, although has slight misalignment on the 'part location' factor. The analysis results from the digital measurements have the same patterns with the ones from physical measurements in terms of 'probe specification', 'distribution of probing points' and 'number of probing points'. In the digital analysis results, the 'distribution of probing points' factor has the biggest impact on the measurement uncertainty, followed by 'probe specification' and 'number of probing points'. The digital measurement results of 'part location' are inconsistent with common sense of CMM measurement, and consequently it is not proper to refer the 'part location' analysis result for the comparison.

Therefore, generally speaking, the control factor rank obtained from the digital measurements is aligned with that from the physical measurements. The approach proposed in the Measurement Planning and Implementation Framework has been validated and verified in the physical environment by measuring the cylindricity of the ring gauge using the procedures in this experiment design. To a certain degree, it is proved that the Framework, which statistically analyses the task-specific measurement uncertainty calculated by the digital CMM model, is capable to provide closer integration between digital and physical measurement environments.

In addition, the Framework strengthens the ability of the digital CMM model in measuring form tolerances. Although the digital measurement result and the physical measurement result are significantly different for the cylindricity measurements in this research, the Taguchi analysis results on both of the digital measurements and the physical measurements reveal similar patterns indicating the impact levels of the control factors.

- Comparison of S/N ratios

  As claimed in the previous paragraph, S/N ratio is not the key index for validating the Measurement Planning and Implementation Framework in this Taguchi experimental design. It is not necessary to compare the S/N ratio values between the digital measurement environment and the physical measurement environment. The S/N ratios are discussed here in order to examine the robustness of the Taguchi experimental approach proposed in this research, in particular, for the cylindricity measurements.

  As shown in Table 50, the S/N ratios in both the digital and physical environments reasonably high values. It confirms the robustness of the Taguchi experimental design in both of the digital measurement environment and the physical environment. Moreover, it indicates the prospect of incorporating the design of experiments (DOE) methods into the measurement uncertainty analysis to enable the knowledge management in task-specific measurement and to create the adoption of measurement experiences to the overall manufacturing process control.

6.6.3 Conclusion

In this section, the Taguchi analysis results from the digital and physical measurements have been compared in terms of the diameter and cylindricity measurements. The comparison shows generally positive results, proving promising

prospects of the Measurement Planning and Implementation Framework for integrating digital and physical measurement results.

The comparison results indicate the interesting points regarding the digital measurements and verification. The accountability of the digital CMM model needs to improve, especially in the regard of sensing the part location change on the CMM bed. Although the direct comparison shows that the digital CMM model is not capable of predicting form measurement results, the Taguchi analysis results on both of the digital measurements and the physical measurements reveal similar patterns indicating the impact levels of the control factors. The Framework strengthens the ability of the digital CMM model in measuring form tolerances.

The relatively high S/N ratios from the Taguchi experiment design prove the robustness of the Framework. It indicates the prospect of incorporating the design of experiments (DOE) methods into the measurement uncertainty analysis, which will enable the knowledge management in task-specific measurements and to create the adoption of measurement experiences to the overall manufacturing process control.

6.7 Chapter Summary

In this Chapter, the experimental works to validate the Measurement Planning and Implementation Framework have been carried out. The experimental plan has been carefully designed, including selecting proper measured artifact, assessing available measurement resources and defining the measurement uncertainty contributors. Following the procedures in the experimental design, the digital measurements and the physical measurements are carried out respectively. The results from the digital measurements and the physical measurements have been collected and analyzed using the approach proposed in the Framework. Finally, the measurement results and the analyzed results have been compared respectively. The direct comparisons between the digital and physical measurement results have shown that the digital measurement

generally produces higher measurement uncertainty than the physical measurement. On the other hand, the Taguchi analyzing comparisons have shown good consistency between the digital and physical measured results.

The Framework indicates a promising prospect of deploying the digital CMM model in a shopfloor environment to direct measurement resource allocation. In this environment, the measurement uncertainty contributors could be established on more significant levels (e.g. temperature control and CMM machine). By analysing the digital measurement results using the method in the Framework, the measurement manager could estimate the significance levels of the measurement uncertainty contributors, and decide the capital investments on the measurement capability improvement and the production control.

Additionally, the scientific validation of the Framework shows an encouraging future in the introduction of statistical methods to post-measurement data processing, especially for digital measurement result analysis. By deploying proper statistical methods, the digital measurement results could be used to direct the physical measurement environment in a robust manner. It extends the application fields of the digital CMM model. Moreover, it promotes the knowledge management in task-specific measurements and creates the adoption of measurement experiences to the overall manufacturing process control.

Chapter 7 Conclusions and Further Work

7.1 Conclusions

The developed Measurement Planning and Implementation Framework and the stand-alone Quality Information Framework for CMM measurement processes are considered to have met the research objectives given in Section 3.2. The primary aim of developing a metrology-based process modelling framework for integrating digital and physical measurement environments has been achieved. The workflow and the general structure of the Framework have been given in Chapter 5. The four major modules that form the Measurement Planning and Implementation Framework, namely *Measurement Scenario Streamliner Module, Measurement Uncertainty Simulation Module, Physical Verification Process* and *Post-Measurement Data Analysing Module*, have been designed and implemented. A case study shown in Chapter 6 has proved that the representation model of metrology-based process modelling framework works correctly. Through the case study, the results form the digital measurements and the physical measurements have been analyzed and compared using the approach proposed in the Measurement Planning and Implementation Framework. The comparisons have shown good consisteny between the digital and physical measure results. It indicates the promising prospect of introducing the statistical analysis approach into post-measurement uncertainty processing, which will promote the knowledge management in task-specific measurements and create the adoption of measurement experiences to the overall manufacturing process control.

7.2 Contribution to knowledge

Evaluating measurement uncertainty in digital environments has been an established topic in the metrology community. As shown in the literature review in Chapter 2,

many systems have been developed for measurement process modelling, and various uncertainty estimation techniques have been deployed to calculate measurement uncertainty in digital environments [4,12,13,14]. However, the integration between digital and physical measurement environments is not fully verified, primarily because of the large diversity and complexity of measurement tasks. It is virtually impossible to develop an algorithm which considers all of the problems in the measurement process. On the other hand, it tends to be impossible to verify the performance of digital measurement models under all of the measurement scenarios.

From the literature review, these functions are not complete in the current research:

(1) Verification of digital measurement model performances in physical measurement environments;
(2) Integration between digital and physical measurement environments in realistic measurement scenarios;
(3) Robust framework which standardizes measurement process, and therefore, leads measurement into manufacturing system integration.

Given the above points, the following contributions are considered to have been made.

(1) The performance of a digital CMM model has been verified under meaningful complexity measurement scenarios.

- The physical measurements have been planned and carried out on a realistic part in a shop floor environment;
- The physical measurements have been simulated in the digital CMM model, and generated simulation results;
- The physical and digital measurement results have been compared directly;

- The performance of the digital CMM model has been assessed, and the limitations of the digital CMM model have been realized.

(2) A metrology-based process modeling framework for digital and physical measurement environments integration has been developed.

- The limitations of task-specific uncertainty simulation model have been analyzed on technical level;
- A Measurement Planning and Implementation Framework has been proposed. The Framework analyzes measurement uncertainty to integrate digital and physical measurement environments. And the statistical analyzing methods and sophisticated algorithm models have been deployed in the Framework;
- The experimental works to validate the Measurement Planning and Implementation Framework have been carried out. Supplementary capabilities of the digital CMM model have been discovered by the experimental works. More importantly, the validation works have shown good consistence between the digital and physical measure results by deploying the Framework;
- The validation work has indicated the promising prospect of introducing the statistical analysis approach into post-measurement uncertainty processing, which will extends the application fields of the measurement uncertainty simulation model. Moreover, it promotes the knowledge management in task-specific measurements and creates the adoption of measurement experiences to the overall manufacturing process control.

7.3 Future work

The laboratory verification works have proved the validity of the proposed framework, but future work is still required to increase the Framework capabilities as well as to enhance the standardization and integration of measurement process modelling. The recommendations for future work are included.

(1) Extension of the verification work to complex features

Limited by the availability of the physical measurement resources, the developed Framework was verified by measuring a simple part. It is recommended to expand the physical verification work to complex feature measurements, which are highly demanded in high-value manufacturing.

(2) Extension of the verification work in shop floor environment

The scientific correctness of the proposed Framework has been verified in the finely-controlled laboratory environment by delicate experiment design and highly skilled metrology scientists. To enrich the industrial applicability of the Framework, it is necessary to perform the physical measurements in the shop floor environment to prove its validity in real production environment.

(3) Improvement of statistic methods for uncertainty analysis

The successful validation of the Framework has indicated the importance of deploying statistic methods for post-measurement uncertainty analysis. Proper deployment of statistics can release the practicality of measurement uncertainty in real production environment, and improve the integration of measurement process with overall product lifecycle. Future efforts should be paid to improve the statistical methods for uncertainty analysis.

(4) Establishment of the relationship between the CMM measurement planning and modelling to the Quality Information Framework (QIF)

The Quality Information Framework (QIF) is a robust conceptual framework aiming to provide seamless data transition between the key stages of quality measurement systems. [136].The QIF is expected to be the next generation platform for integrating manufacturing quality systems based on the metrology concepts

Relating the CMM measurement process planning with the QIF is vital for the measurement process standardization, and the quality system integration. The CMM measurement will get closer integration with the entire quality systems.

The CMM measurement modelling proposed in this research needs to be related with the QIF module. And the validation of the QIF-derived CMM measurement process modelling is needed to prove its functionality.

Appendix A. Data collection of the simulation results

Standard Order	Run Order	CMM Specification	Environment	Probing Strategy	Diameter (µm)	Position (µm)
80	1	LA	Shop Floor	NPL	3.21	6.08
20	2	LA	Enclosure	NPL	1.35	4.32
5	3	HA	CMM Room	NPL	1.22	2.14
78	4	LA	CMM Room	3*NPL	1.32	4.04
2	5	HA	Enclosure	NPL	0.665	1.48
37	6	MA	Enclosure	Minimum	1.01	2.52
28	7	HA	Enclosure	Minimum	0.753	1.56
57	8	HA	Enclosure	3*NPL	0.604	1.39
41	9	MA	CMM Room	NPL	1.3	2.71
11	10	MA	Enclosure	NPL	0.816	2.27
24	11	LA	CMM Room	3*NPL	1.38	4.18
72	12	MA	Shop Floor	3*NPL	3.02	5.06
64	13	MA	Enclosure	Minimum	1.02	2.47
74	14	LA	Enclosure	NPL	1.41	4.16
56	15	HA	Enclosure	NPL	0.665	1.44
33	16	HA	CMM Room	3*NPL	1.18	2.11
53	17	LA	Shop Floor	NPL	3.12	6.01
66	18	MA	Enclosure	3*NPL	0.697	2.17
71	19	MA	Shop Floor	NPL	2.99	5.03
81	20	LA	Shop Floor	3*NPL	3.12	5.8
21	21	LA	Enclosure	3*NPL	0.98	4
1	22	HA	Enclosure	Minimum	0.748	1.54
54	23	LA	Shop Floor	3*NPL	3.04	5.78
22	24	LA	CMM Room	Minimum	2.23	5.08
65	25	MA	Enclosure	NPL	0.831	2.29
75	26	LA	Enclosure	3*NPL	0.988	3.52
59	27	HA	CMM Room	NPL	1.18	2.09
77	28	LA	CMM Room	NPL	1.69	4.36
23	29	LA	CMM Room	NPL	1.7	4.36
15	30	MA	CMM Room	3*NPL	1.22	2.61
63	31	HA	Shop Floor	3*NPL	2.89	4.66
17	32	MA	Shop Floor	NPL	3.07	5.04
67	33	MA	CMM Room	Minimum	1.44	2.93
35	34	HA	Shop Floor	NPL	2.97	4.8
70	35	MA	Shop Floor	Minimum	3.05	5.02
49	36	LA	CMM Room	Minimum	2.36	4.92
68	37	MA	CMM Room	NPL	1.26	2.71
19	38	LA	Enclosure	Minimum	1.97	4.82
45	39	MA	Shop Floor	3*NPL	2.98	4.92

48	40	LA	Enclosure	3*NPL	0.977	3.96
10	41	MA	Enclosure	Minimum	0.998	2.5
73	42	LA	Enclosure	Minimum	1.87	4.86
62	43	HA	Shop Floor	NPL	2.93	4.82
29	44	HA	Enclosure	NPL	0.665	1.48
13	45	MA	CMM Room	Minimum	1.41	2.78
50	46	LA	CMM Room	NPL	1.75	4.5
26	47	LA	Shop Floor	NPL	3.02	5.9
6	48	HA	CMM Room	3*NPL	1.21	2.1
47	49	LA	Enclosure	NPL	1.42	4.21
42	50	MA	CMM Room	3*NPL	1.21	2.48
52	51	LA	Shop Floor	Minimum	3.56	6.56
30	52	HA	Enclosure	3*NPL	0.618	1.44
69	53	MA	CMM Room	3*NPL	1.2	2.55
3	54	HA	Enclosure	3*NPL	0.614	1.44
36	55	HA	Shop Floor	3*NPL	2.92	4.79
7	56	HA	Shop Floor	Minimum	2.86	4.7
32	57	HA	CMM Room	NPL	1.21	2.09
76	58	LA	CMM Room	Minimum	2.21	4.99
51	59	LA	CMM Room	3*NPL	1.38	4.12
61	60	HA	Shop Floor	Minimum	2.86	4.71
46	61	LA	Enclosure	Minimum	1.91	4.7
58	62	HA	CMM Room	Minimum	1.19	2.1
16	63	MA	Shop Floor	Minimum	3.08	4.99
79	64	LA	Shop Floor	Minimum	3.41	6.27
38	65	MA	Enclosure	NPL	0.824	2.32
9	66	HA	Shop Floor	3*NPL	3.13	5
4	67	HA	CMM Room	Minimum	1.22	2.15
43	68	MA	Shop Floor	Minimum	3.03	5.1
39	69	MA	Enclosure	3*NPL	0.667	2.14
60	70	HA	CMM Room	3*NPL	1.2	2.1
31	71	HA	CMM Room	Minimum	1.26	2.14
8	72	HA	Shop Floor	NPL	2.9	4.76
25	73	LA	Shop Floor	Minimum	3.53	6.39
55	74	HA	Enclosure	Minimum	0.728	1.55
34	75	HA	Shop Floor	Minimum	2.93	4.68
44	76	MA	Shop Floor	NPL	2.89	4.97
40	77	MA	CMM Room	Minimum	1.41	2.78
27	78	LA	Shop Floor	3*NPL	3.03	5.68
18	79	MA	Shop Floor	3*NPL	2.92	4.82
14	80	MA	CMM Room	NPL	1.24	2.65
12	81	MA	Enclosure	3*NPL	0.668	2.17

Appendix B. Example of Taguchi design of experiments

Table 51 shows the L8 (2^7) Taguchi orthogonal array. The table columns represent the control factors, the table rows represent the runs (combination of factor levels), and each table cell represents the factor level for that run. L8 means 8 runs. 2^7 means 7 factors with 2 levels each. If the full factorial design were used, it would have 2^7 = 128 runs. The L8 (2^7) array requires only 8 runs a fraction of the full factorial design. This array is orthogonal; factor levels are weighted equally across the entire design. For example, levels 1 and 2 occur 4 times in each factor in the array. If you compare the levels in factor A with the levels in factor B, you will see that B1 and B2 each occur 2 times in conjunction with A1 and 2 times in conjunction with A2. Each pair of factors is balanced in this manner, allowing factors to be evaluated independently.

Table 51 L8 (2^7) Taguchi Orthogonal Array (reproduced from[132])

Experiment Scenario Number	**Factor**						
	A	**B**	**C**	**D**	**E**	**F**	**G**
1	1	1	1	1	1	1	1
2	1	1	1	2	2	2	2
3	1	2	2	1	1	2	2
4	1	2	2	2	2	1	1
5	2	1	2	1	2	1	2
6	2	1	2	2	1	2	1
7	2	2	1	1	2	2	1
8	2	2	1	2	1	1	2

After the experimental plan has been defined and the experiments have been carried out according to the selected experimental scenarios, the measured performance characteristic from each experimental scenario can be used to analyze the relative

effect of the different factors. To explain the data analysis procedure, the L8 (2^7) array in Table 52 is used, but the principles can be used in any type of array.

Following the L8 (2^7) array in , the certain repeated observations are carried out under the selected experiment scenarios. These repeated observations are named as trails and form a matrix as shown in Table 52. $T_{i,j}$ represents the different trials, where i is the experiment scenario number, and j is the trial number under a certain experiment scenario.

Table 52 Example of Data Collection of Taguchi Experimental Design

Experiment Scenario Number (i)	**Trail ($T_{i,j}$)**			
	T_1	**T_2**	…	**T_N**
1	$t_{1,1}$	$t_{1,2}$	…	$t_{1,N}$
2	$t_{2,1}$	$t_{2,2}$	…	$t_{2,N}$
3	$t_{3,1}$	$t_{3,2}$	…	$t_{3,N}$
4	$t_{4,1}$	$t_{4,2}$	…	$t_{4,N}$
5	$t_{5,1}$	$t_{5,2}$	…	$t_{5,N}$
6	$t_{6,1}$	$t_{6,2}$	…	$t_{6,N}$
7	$t_{7,1}$	$t_{7,2}$	…	$t_{7,N}$
8	$t_{8,1}$	$t_{8,2}$	…	$t_{8,N}$

To obtain the factors' effects on the output, the signal-to-noise ratio (SN) is calculated for each experiment scenario. The calculation of the SN for the first experiment scenario in Table 52 is

$$SN_i = 10\log\frac{\overline{y_i}^2}{s_i^2}$$

where $\overline{y_i}$ and s_i are the mean value and the standard deviation of the trails under the first experiment scenario respectively. $\overline{y_i}$ also represents the value of the

performance characteristic for a given experiment. The calculations of $\overline{y_i}$ and s_i are:

$$\overline{y_i} = \frac{1}{N_i}\sum_{u=1}^{N_i} y_{i,u}$$

$$s_i^{\,2} = \frac{1}{N_i - 1}\sum_{u=1}^{N_i}(y_{i,u} - \overline{y_i})$$

where i is the experiment scenario number, u is the trial number, and N_i is the number of the trails for the Experiment i.

For the case of minimizing the performance characteristic, SN ratio should be calculated as:

$$SN_i = -10\log\left[\frac{1}{N_i}\sum_{u=1}^{N_i} y_u^{\,2}\right].$$

For the case of maximizing the performance characteristic, SN ratio should be calculated as:

$$SN_i = -10\log\left[\frac{1}{N_i}\sum_{u=1}^{N_i}\frac{1}{y_u^{\,2}}\right].$$

After calculating the SN ratio of each experiment scenario, the average SN value is calculated for each factor and level. Following the example of Table 51 and Table 52, Table 53 lists the SN ratios of each experiment scenario for Factor C. Factor C is designed to have 2 level, which are highlighted in yellow and red respectively in Table 53. The SN ratios relating to the same factorial level are highlighted in the same color. The SN ratio values for Factor C on 2 factorial levels are calculated as:

$$SN_{FC,1} = \frac{SN_1 + SN_2 + SN_7 + SN_8}{4}$$

$$SN_{FC,2} = \frac{SN_3 + SN_4 + SN_5 + SN_6}{4}$$

Table 53 Example of Data Analysis of Taguchi Experimental Design

Experiment Scenario Number	Factor							SN Ratio
	A	B	C	D	E	F	G	C
1	1	1	1	1	1	1	1	SN_1
2	1	1	1	2	2	2	2	SN_2
3	1	2	2	1	1	2	2	SN_3
4	1	2	2	2	2	1	1	SN_4
5	2	1	2	1	2	1	2	SN_5
6	2	1	2	2	1	2	1	SN_6
7	2	2	1	1	2	2	1	SN_7
8	2	2	1	2	1	1	2	SN_8

After calculating the SN ratio values for each factor and level, they are assembled into a matrix as shown in Table 54. The range (R) between SN values for each factor is calculated. The higher the R value is, the more significant effect the factor has on the process. This is because the same change in signal causes a larger effect on the output variable being measured [132]. Consequently, the influences of the factors are ranked and identified through the quantitative analytical approach.

Table 54 Example of Analysis Result of Taguchi Experimental Design

Level	Factor						
	A	B	C	D	E	F	G
1	$SN_{A,1}$	$SN_{B,1}$	$SN_{C,1}$	$SN_{D,1}$	$SN_{E,1}$	$SN_{F,1}$	$SN_{G,1}$
2	$SN_{A,2}$	$SN_{B,2}$	$SN_{C,2}$	$SN_{D,2}$	$SN_{E,2}$	$SN_{F,2}$	$SN_{G,2}$
Range (R)	R_A	R_B	R_C	R_D	R_E	R_F	R_G
Rank	…	…	…	…	…	…	…

Appendix C. Data Collection Sheet to record the digital and physical measurement results

Measurement scenarios				Diameter result (μm)			Cylindricity result (μm)		
Probe specification	**Number of probing points**	**Distribution of probing points**	**Part location**	**Mean error**	**Standard deviation**	**Uncertainty**	**Mean error**	**Standard deviation**	**Uncertainty**
1pt3D_22Z	4	120	Corner						
1pt3D_22Z	4	120	Corner						
1pt3D_22Z	4	120	Corner						
1pt3D_22Z	9	240	Middle						
1pt3D_22Z	9	240	Middle						
1pt3D_22Z	9	240	Middle						
1pt3D_22Z	15	360	Centre						
1pt3D_22Z	15	360	Centre						
1pt3D_22Z	15	360	Centre						
3D_78Z	4	240	Centre						
3D_78Z	4	240	Centre						
3D_78Z	4	240	Centre						
3D_78Z	9	360	Corner						
3D_78Z	9	360	Corner						
3D_78Z	9	360	Corner						
3D_78Z	15	120	Middle						
3D_78Z	15	120	Middle						
3D_78Z	15	120	Middle						
5D_40Z	4	360	Middle						
5D_40Z	4	360	Middle						
5D_40Z	4	360	Middle						

5D_40Z	9	120	Centre						
5D_40Z	9	120	Centre						
5D_40Z	9	120	Centre						
5D_40Z	15	240	Corner						
5D_40Z	15	240	Corner						
5D_40Z	15	240	Corner						

Reference

1 Wikipedia, 2008, *Dimensional metrology* [online]. Wikipedia. Available at: https://en.wikipedia.org/wiki/Dimensional_metrology [Accessed 28 May 2013].

2 Tang, X. Q. and Yun H., 2008. Data model for quality in product lifecycle. *Computers in industry*, 59 (2-3), pp.167-179.

3 Maropoulos, P., Guo, Y., Jamshidi, J. and Cai, B., 2008. Large Volume Metrology Process Models: A framework for integrating measurement with assembly planning. *CIRP Annals - Manufacturing Technology*, 57(1), pp.477–480.

4 Van Gestel, N., 2011. *Determining measurement uncertainties of feature measurements on CMMs*. Thesis (PhD). Katholieke Universiteit Leuven, Belgium.

5 Llewellyn, J., 2013. Introduction: *Measurement good practice in the supply chain* [Online]. BMTA: British Measurement and Testing Association. Available at: https://connect.innovateuk.org/c/document_library/get_file?p_l_id=10355645&folderId=11590307&name=DLFE-137688.pdf [Accessed 28 May2013].

6 Bamforth, P., 2013. *Product verification and its value for the aerospace industry* [Industrial presentation]. Rolls-Royce Plc [presented on Tue 19/03/2013].

7 Kruth, J. P., Bartscher, M., Carmignato, S., Schmitt, R., De Chiffre, L. and Weckenmann, A., 2011. Computed tomography for dimensional metrology. *CIRP Annals - Manufacturing Technology*, 60 (2), pp. 821–842.

8 Shen, W., Wang and L., Hao, Q., 2006. Agent-based distributed manufacturing process planning and scheduling: a state-of-the-art survey. *IEEE Transactions on Systems, Man and Cybernetics—Part C: Applications and Reviews*, 36 (4), pp. 563–577

9 Kimura, F., 1993. Product and process modelling as a kernel for virtual manufacturing environment. *CIRP Annals - Manufacturing Technology*, 42(1), pp. 147–151.

10 Baxter, D., Gao, J., Case, K, Harding, J., Young, B., Cochrane, S. and Dani, S., 2007. An engineering design knowledge reuse methodology using process modelling. *Research in Engineering Design*, 18(1), pp. 37–48.

11 Zhao, Y., Kramer, T., Stone, R., Hoffman, M., Hoffman, S. and Rippey, W., 2012. *Design and usage guide for version 0.92 of the Quality Information Framework data model and XML (Extensible Markup Language) Schemas*. Washington: National Institute of Standards and Technology (NIST).

12 Balsamo, A., Di Ciommo, M., Mugno, R., Rebaglia, B.I., Ricci, E. and Grella, R., 1999. Evaluation of CMM uncertainty through Monte Carlo simulations. *CIRP Annals - Manufacturing Technology*, 48(1), pp. 425–8.

13 Wilhelm, R.G., Hocken, R. and Schwenke, H., 2001. Task specific uncertainty in coordinate measurement, *CIRP Annals - Manufacturing Technology*, 50 (2), pp. 553–563.

14 Summerhaysa, K., Henkea, M., Brownb, C., Henke, R. and Baldwin, J., 2002. *A tool for determining task-specific measurement uncertainties in GD&T parameters obtained from coordinate measuring machines* [online]. USA: MetroSage LLC and Honeywell Inc. Available from: http://www.aspe.net/publications/Annual_2002/PDF/PAPERS/4stdmet/911.PDF [accessed 12 March 2013].

15 Baldwin, J., Summerhays, K., Campbell, D. and Henke, R., 2007. Application of simulation software to coordinate measurement uncertainty evaluations. *Measure*, 2 (4), pp. 40–52.

16 Arenhart, F., Donatelli, G. and Porath, M., 2012. An experimental method for assessing the contribution of the production process variations to the task-specific uncertainty of coordinate measurements. *Measurement*, 45(3), pp. 507–516.

17 Maropoulos, P.G. and Ceglarek, D., 2010. Design verification and validation in product lifecycle. *CIRP Annals - Manufacturing Technology*, 59(2), pp. 740-759.

18 Zhao, Y. F., Kramer, T., Rippey, W., Horst, J. and Proctor, F., 2012. An integrated data model for quality information exchange in manufacturing systems.

Proceedings of the 37th MATADOR Conference, 25-27 July 2012 Manchester, Manchester: University of Manchester, pp. 5-9.

19 Bell, S., 1999. *Measurement good practice guide No. 118: a beginner's guide to uncertainty of measurement*, 2nd ed. Teddington, UK: National Physical Laboratory.

20 JCGM 200:2008. *International vocabulary of basic and general terms in metrology (VIM), 3rd edition.* International Organisation for standardisation (ISO).

21 JCGM 100:2008. *Evaluation of measurement data — Guide to the expression of uncertainty in measurement (GUM).* International Organisation for standardisation (ISO).

22 Phillips, S., Borchardt, B. and Abackerli, A., 2003. The Validation of CMM Task Specific Measurement Uncertainty Software. *Proceedings of the ASPE 2003 summer topical meeting "Coordinate Measuring Machines"*, June 25 –26 2003 North Carolina, USA. USA: American Society for Precision Engineering (ASPE), pp. 1-6.

23 Forbes, A.B., 2006. Measurement uncertainty and optimised conformance assessment. *Measuremen*t, 39 (9), pp. 808–814.

24 Pendrill, L.R., 2008. Operating 'cost' characteristics in sampling by variable and attribute. *Accreditation and Quality Assurance*, 13(11), pp 619-631.

25 Baldwin, J.M., Summerhays, K.D. and Campbell, D.A., 2010. Evaluating the Economic Impact of CMM Measurement Uncertainty. *Proceedings of Measurement Science Conference*, Pasadena, USA.

26 JCGM 104:2009. *Evaluation of measurement data – An introduction to the "Guide to the expression of uncertainty in measurement" and related documents*. International Organisation for standardisation (ISO).

27 JCGM 101:2008. *Evaluation of measurement data – Supplement 1 to the "Guide to the expression of uncertainty in measurement" – Propagation of distributions using a Monte Carlo method.* International Organisation for standardisation (ISO).

28 John, H., Lehman, C., Wang, M., Dowell, L.M. and Hadler, J.A., 2009. Uncertainty calculation for spectral-responsivity measurements. *Journal of Research of the National Institute of Standards and Technology*, 114(5), pp. 287-291..

29 Oliveira, S.P., Rocha, A.C., Filho, T.J. and Couto P.R.G., 2008. Uncertainty of measurement by Monte-Carlo simulation and metrological reliability in the evaluation of electric variables of PEMFC and SOFC fuel cells. *Measurement*, 42(10), pp.1497-1501.

30 Müller, M. andRink, C., 2009. On the convergence of the Monte Carlo block design. *Metrologia*, 46(5), pp. 404-408.

31 Ellison, S.L.R., 1998. Using validation data for ISO measurement uncertainty estimation - Part 1. Principles of an approach using cause and effect analysis. *The Analyst*, 123(6), pp. 1387-1392.

32 Bich, W., Cox, M. G. and Harris, P. M., 2006. Evolution of the Guide to the Expression of Uncertainty in measurement. *Metrologia*, 43(4), pp. S161–S166.

33 Cox, M. and Harris, P., 2003. The GUM and its planned supplemental guides. *Accreditation and Quality Assurance*, 8(7-8), pp. 375-379.

34 Ridler, N., Lee, B., Martens, J. and Wong, K., 2007. Measurement uncertainty, traceability, and the GUM. *IEEE Microwave Magazine*, 8(4), pp. 44-53.

35 Krulikowski, A., 1997. *Fundamentals of geometric dimensioning and tolerancing*. 2nd ed. New York: Delmar Cengage Learning.

36 ASME Y14.5M: 1994. *Dimensioning and Tolerancing*. American Society of Mechanical Engineers (ASME).

37 Shah, J. J., Ameta, G., Shen, Z. and Davidson, J., 2007. Navigating the tolerance analysis maze. *Computer-Aided Design & Applications*, 4(5), pp.705-718.

38 Tsai, J.C. and Cutkosky, M.R., 1997. Representation and reasoning of geometric tolerances in design. *Artificial Intelligence for Engineering Design Analysis and Manufacturing*, 11(4), pp.325-341.

39 Chiabert, P., Lombardi, F. and Orlando, M., 1998. Benefits of geometric dimensioning and tolerancing. *Journal of Materials Processing Technology*, 78(1-3), pp.29-35.

40 Shah, J.J., Yan, Y. and Zhang, B.C., 1998. Dimension and tolerance modeling and transformations in feature based design and manufacturing. *Journal of Intelligent Manufacturing*, 9(5), pp.475-488.

41 Zhang, Y., Hu, W. and Rong, Y., 2001. Graph-based set-up planning and tolerance decomposition for computer-aided fixture design. *International Journal of Production Research*, 39(14), pp.3109-3126.

42 Shen, Z.S., Shah, J.J. and Davidson, J.K., 2008. Analysis neutral data structure for GD&T. *Journal of Intelligent Manufacturing*, 19(4), pp.455–472.

43 Kong, Z., Huang, W. and Oztekin, A., 2009. Variation propagation analysis for multistation assembly process with consideration of GD&T factors. *Journal of Manufacturing Science and Engineering*, 131(5), pp. 051010-1-10.

44 Hunter, R., Perez, J., Marquez, J. and Hernandez, J.C., 2007. Modelling the integration between technological product specifications and inspection process. *Journal of Materials Processing Technology*, 91(1-3), pp.34-38.

45 Mohib, A., Azab, A. and ElMaraghy, H., 2009. Feature-based hybrid inspection planning: A mathematical programming approach. *International journal of computer integrated manufacturing*, 22(1), pp.13-29.

46 Prieto, F., Boulanger, P., Lepage, R. and Redarce, T., 2002. Automated inspection system using range data. *Proceedings of IEEE International Conference on Robotics and Automation*, 3, pp.2557-2562.

47 Prieto, F., Redarce, T., Lepage, R. and Boulanger P., 2002. An automated inspection system. *International Journal of Advanced Manufacturing Technology*, Issue 19, pp. 917–925.

48 Son, S., Park, H. and Lee, K. H., 2002. Automated laser scanning system for reverse engineering and inspection. *International Journal of Machine Tools Manufacturing*, Issue 2, pp.889–897.

49 Gao, J., Gindy N., and Chen, X., 2006. An automated GD&T inspection system based on non-contact 3D digitization. *International Journal of Production Research*, 44(1), pp.117.

50 Rennels, K.E., 2003. Current methodologies for geometric dimensioning and tolerancing. *Proceedings of the Electrical Insulation Conference and Electrical Manufacturing & Coil Winding Technology Conference*, 23-25 September 2003, pp.565–569.

51 Watts, D., 2007. The ‘‘GD&T Knowledge Gap’’ in Industry. *Proceedings of the ASME International Design Engineering Technical Confere*nces, 4th-7th September 2007 Las Vegas, NV, USA. New York: ASME, pp. 597–604.

52 Zhang, Y. and Yang, M., 2009. A coordinate SPC model for assuring designated fit quality via quality-oriented statistical tolerancing. *Computers and Industrial Engineering*, 57(1), pp.73–79.

53 BS 8888:2008. *Technical Product Specification – Specification*. British Standard Institution (BSI)..

54 Henzold, G., 2006. Geometrical Dimensioning and Tolerancing for Design, Manufacturing and Inspection. *In A Handbook for Geometrical Product Specification using ISO and ASME standards*. 2nd ed. London: Butterworth-Heinemann, Page(s): 372 – 373.

55 ISO/TS 17450-1:2011. *Geometrical product specifications (GPS) – General concepts -- Part 1: Model for geometrical specification and verification*. International Organisation for standardisation (ISO).

56 ISO/TS 17450-2:2002. *Geometrical product specifications (GPS) – General concepts -- Part 2: Basic tenets, specifications, operators and uncertainties*. International Organisation for standardisation (ISO).

57 Nielsen, H.S., 2003. Specifications, operators and uncertainties. *Proceedings of the 8th CIRP International Seminar on Computer Aided Tolerancing*, April 2003 Charlotte, NC, USA.

58 Lu, W., Jiang, X., Scott, P.J. and Lan, X., 2009. A host system for form tolerance specification in the next-generation GPS based on AutoCAD. *Proceedings of he 11th CIRP Conference on Computer Aided Tolerancing - "Geometric Variations within Product Life-Cycle Management"*, 26th-27th March 2009 Annecy, France.

59 Dantan, J., Bruyere, J., Baudouin, C. and Mathieu, L., 2007. Geometrical Specification Model for Gear-Expression, Metrology and Analysis. *CIRP Annals-Manufacturing Technology*, 56(1), pp.517-520.

60 N Nielsen, H.S., 2006. New concepts in specifications, operators and uncertainties and their impact on measurement and instrumentation. *Measurement Science Technology*, 17(3), pp.541–544.

61 ISO 10360-2:2002. *Geometrical Product Specifications (GPS) - Acceptance and Reverification Tests for Coordinate Measuring Machines (CMM) - Part 2: CMMs used for measuring size*. British Standard Institution (BSI).

62 ISO 10360-5:2010. *Geometrical Product Specifications (GPS) - Acceptance and Reverification Tests for Coordinate Measuring Machines (CMM) - Part 5: CMMs using single and multiple stylus contacting probing systems*. British Standard Institution (BSI).

63 Schwenke, H., Wäldele, F. and Wendt, K., 1998. *Abnahme, Überwachung und Kalibrierung von flexiblen Industriemeßsystemen mit CCD-Kameras*. Braunschweig, Germany: Physikalisch-Technische Bundesanstalt (PTB).

64 Luhmann, T. and Wendt, K., 2000. Recommendations for an acceptance and verification test of optical 3-D measurement systems. *International Archives for Photogrammetry and Remote Sensing*, 33(5) pp.493-499.

65 Keferstein, C. P. and Züst, R., 2004. Minimizing technical and financial risk when integrating and applying optical sensors for in-process measurement. *International Intelligent Manufacturing Systems Forum*, Italia, Vol. 17, pp. 475-482.

66 Pumm, C. and Präzision, W., 2005. New ISO standards. *ia.cmm International Conference*, Germany, April 28th, 2005.

67 ISO/TS 15530-4: 2000. *GPS – CMM: Techniques for evaluation of uncertainty of measurement - Part 4: Evaluating task-specific measurement uncertainty using simulation*. International Organisation for standardisation (ISO).

68 Zhao, F., Xu, X. and Xie, S.Q., 2009. Computer-aided Inspection Planning – The State of the Art. *Computers in Industry*, 60(7), pp.453–466.

69 Cho, M.W., Lee, H., Yoon, G.S. and Choi, J., 2005. A feature-based inspection planning system for coordinate measuring machines. *The International Journal of Advanced Manufacturing Technology*, 26(9-10), pp.1078–1087.

70 Lin, Y.J., Mahabaleshwarkar, R. and Massina, E., 2001. CAD-based CMM Dimensional Inspection Path Planning: A Generic Algorithm. *Robotica*, 19(2), pp.137–148.

71 Lee, G., Mou, J. and Shen, Y., 1997. Sampling strategy design for dimensional measurement of geometric features using coordinate measuring machine. *International Journal of Machine Tools and Manufacture*, 37(7), pp.917–934.

72 Zhang, S.G., Ajmal, A., Wootton, J. and Chisholm, A., 2000. A feature-based inspection process planning system for coordinate measuring machine. *Journal of Materials Processing Technology*, 107(1-3), pp.111–118.

73 Limaiem, A. and ElMaraghy, H.A., 1999. CATIP: a computer-aided tactile inspection planning system. *International Journal of Production Research*, 37(2), pp.447–465.

74 Hwang, Y., Tsai, C.Y., and Chang, C.A., 2004. Efficient inspection planning for coordinate measuring machines. *International Journal of Manufacturing Technology*, 23(9-10), pp.732–742.

75 Wong, F.S.Y., Chuah, K.B. andVenuvinod, P.K., 2006. Automated inspection process planning: algorithmic inspection feature recognition, and case representation for CBR. *Robotics and Computer-Integrated Manufacturing*, 22(1), pp.56–68.

76 Lee, H., Cho, M.W., Yoon, G.S. and Choi, J.H., 2004. A computer-aided inspection planning system for online measurement-Part I: Global inspection planning. *KSME International Journal*, 18 (8), pp.1349–1357.

77 Chung, S.C., 1999. CAD/CAM integration of on-the-machine measuring and inspection system for free-formed surfaces. *Proceedings of American Society for Precision Engineering*, 20, pp. 267–270.

78 Cho, M.-W. and Seo, T.-L., 2002. Inspection planning strategy for the online measurement process based on CAD/CAM/CAI integration. *International Journal of Manufacturing Technology*, 19 (8), pp. 607–617.

79 Vafaeesefat, A. and EIMaraghy, G.A., 2000. Automated accessibility analysis and measurement clustering for CMMs. *International Journal of Production Research*, 38(10), pp.2215–2231.

80 Lu, C.G., Morton, D., Wu, M.H. andMyler, P., 1999. Genetic algorithm modelling and solution of inspection path planning on a coordinate measuring machine. *The International Journal of Advanced Manufacturing Technology*, 15(6), pp.409–416.

81 Huang, H.L. and Ha, S., 2002. Hybrid Neuro-fuzzy approach to the generation of measuring points for knowledge-based inspection planning. *International Journal of Production Research*, 40(11), pp.2507-2520.

82 Cho, M.-W., Lee, H., Yoon, G.-S. and Choi, J.-H., 2004. A computer-aided inspection planning system for online measurement-Part II: Local inspection planning. *KSME International Journal*, 18, pp.1358–1367.

83 Woo, T. and Liang, R., 1993. Optimal sampling for coordinate measurement: its definition and algorithm. *Quality through Engineering Design*, 16, pp. 333–346.

84 Dowling, M.M., Griffin, P.M., Tsui, K.-L. and Zhou, C., 1997. Statistical issues in geometric feature inspection using coordinate measuring machines. *Technometrics*, 39(1), pp.3–17.

85 Jiang, B.C. and Chiu, S.D., 2002. Form tolerance-based measurement points determination with CMM. *Journal of Intelligent Manufacturing*, 13(2), pp.101–108.

86 Elkott, F., ElMaraghy, H.A. and Elmaraghy, W.H., (2002). Automatic sampling for CMM inspection planning of free-form surfaces. *International Journal of Production Research*, 40(11), pp.2653–2676.

87 Moroni, G., Polini, and W., Rasella, M., 2003. *Manufacturing Signatures and CMM Sampling Strategies* [online]. Available from: http://www.aspe.net/publications/Summer_2003/03SU%20Extended%20Abstracts/Moroni.PDF [accessed 13 July 2012].

88 Cui, C., Fu, S. and Huang, F, 2009. Research on the uncertainties from different form error evaluation methods by CMM sampling. *The International Journal of Advanced Manufacturing Technology*, 43(1-2), pp.136-145.

89 Liu, Q., Zhang, C.C. and Wang, H.P.B., 2001. On the effects of CMM measurement error on form tolerance estimation. *Measurement*, 30(1), pp.33–47.

90 Odayappan, O., Raja, J., Hocken, R.J. and Chen, K., 1993. Sampling strategies for circles in coordinate measuring machines. *Proceedings of the American Society of Precision Engineering*, 8, pp. 70–72.

91 Dhanish, P.B. and Mathew, J., 2006. Effect of CMM point coordinate uncertainty on uncertainties in determination of circular features. *Measurement*, 39(6), pp.522–531.

92 Chan, F.M.M., King, T.G. andStout, K.J., 1996. The influence of sampling strategy on a circular feature in coordinate measurements. *Measurement*, 19(2), pp.73–81.

93 Elkott, D.F., Elmaraghy, H.A. and Elmaraghy, W.H., 2002. Automatic sampling for CMM inspection planning of free-form surfaces. *International Journal of Production Research*, 40(11) , pp.2653-2676.

94 Barini, E. M., Tosello, G. and De Chiffre, L., 2007. Uncertainty analysis of point-by-point sampling complex surfaces using touch probe CMMs: DOE for complex surfaces verification with CMM. *Precision Engineering*, 34(1), pp.16-21.

95 Lu, E., Ni, J. and Wu, S. M., 1994. An algorithm for the generation of an optimum CMM inspection path. *ASME Journal of Dynamic Systems, Measurements, and Control*, 116, pp.396-404.

96 Albuquerque, V.A., Liou, F.W. and Mitchell, O.R., 2000. Inspection point placement and path planning algorithms for automatic CMM inspection. *International Journal of Computer Integrated Manufacturing*, 13(2), pp.107–120.

97 Ainsworth, I., Ristic, M. and Brujic, D., 2000. CAD-based measurement path planning for free-form shapes using contact probes. *International Journal of Advanced Manufacturing Technology*,16 (1), pp.23–31.

98 Lin, Y.J. and Murugappan, P., 1998. A new algorithm for CAD-directed CMM dimensional inspection. *International Journal of Advanced Manufacturing Technology*, 16 (2), pp. 107–112.

99 Yu, D., Li, X.J., Xiong, Y. and Gao Z.H., 2010. Reconstructing of Prototype Surface with Reverse Engineering and Data Process Technology. *Key Engineering Materials*, 458, pp. 368-373.

100 Javidrad, F. and Rahmati, R., 2009. An integrated re-engineering plan for the manufacturing of aerospace components. *Materials & Design*, 30(5), pp.1524–1532.

101 Chang, D.Y. and Chang, Y.M., 2002. A freeform surface modelling system based on laser scan data for Reverse Engineering. *The International Journal of Advanced Manufacturing Technology*, 20(1), pp9-19.

102 Zhang, Y., 2003. Research into the engineering application of reverse engineering technology. *Journal of Materials Processing Technology*, 139(1–3), pp.472–4755.

103 Zhang, Y., Fan, Y. and Chu, X., 1999. Principle and key technologies of reverse engineering. *Journal of Kunming University Science and Technology*, 24(4), pp. 42–46.

104 Rajamohan, G., Shunmugam, M.S., Samuel, G.L., 2011. Effect of probe size and measurement strategies on freeform profile deviations using coordinate measuring machine. *Measurement*, 44(5), 832-841.

105 Tosello, G., Hansen, H.N. and Gasparin, S., 2009. Applications of Dimensional Micro Metrology to the Product and Process Quality Control in Manufacturing of Precision Polymer Micro Components. *CIRP Annals – Manufacturing Technology*, 58(1), pp. 467–472.

106 Fleischer, J., Lanza, G. and Schlipf, M., 2008. Statistical Quality Control in Micro-manufacturing Through Multivariate μ-EWMA Chart. *CIRP Annals – Manufacturing Technology*, 57(1), pp.521–524.

107 Kunzmann, H., Pfeifer, T., Schmitt, R., Schwenke, H. and Weckenmann, A., 2005. Productive Metrology—Adding Value to Manufacture, *CIRP Annals – Manufacturing Technology*, 54 (2), pp.691–713.

108 Pendrill, L.R., 2010. Optimised uncertainty and cost operating characteristics: new tools for conformity assessment - Application to geometrical product control in automobile industry. *International Journal of Metrology and Quality Engineering*, 1(02), pp.105-110.

109 Henke, R.P., Summerhays, K.D., Baldwin, J.M., Cassou, R.M. and Brown, C.W., 1999. Methods for evaluation of systematic geometric deviations in machined parts and their relation to process variables. *Precision Engineering*, 23(4), pp.273–292.

110 Takamasu, K., 2011. Present problems in coordinate metrology for nano and micro scale measurements, *Mapan*, 26(1) pp.3-14.

111 Trapet, E. and Waldele, F., 1996. The virtual CMM concept. *In: Advanced Mathematical Tools in Metrology II*. Singapore: World Scientific Publishing Company, pp.238–247.

112 Phillips, S.D., Borchardt, B.R., Sawyer, D., Estler, W.T., Ward, D., Eberhardt, K., and Levenson, M. S., 1997. The Calculation of CMM Measurement Uncertainty via the Method of Simulation by Constraints. *American Society for Precision Engineering*, 16, pp.443-446.

113 Haitjema, H., Van Dorp, B., Morel, M. and Schellekens, P.H.J., 2001. Uncertainty estimation by the concept of virtual instruments. *Proceedings of SPIE - Recent Developments in Traceable Dimensional Measurements*, 18th June 2001 Munich, Germany.

114 Trenk M., Franke, M. and Schwenke, H., 2004. The "Virtual CMM" a software tool for uncertainty evaluation – practical application in an accredited calibration lab. *ASPE Proceedings on Uncertainty Analysis in Measurement and Design*, pp. 1-6.

115 Takamasu, K., 2002. *Final Research Report - International Standard Development of Virtual CMM (Coordinate Measuring Machine)*. Tokyo: New Energy and Industrial Technology Development Organization (NEDO).

116 Forbes, A.B. and Harris, P.M., 2000. Simulated Instruments and Uncertainty Estimation. London: National Physical Laboratory (CMSC 01/00).

117 Pahk, H.J., Burdekin, M. and G N Peggs, 1998. Development of virtual coordinate measuring machines incorporating probe errors. *Proceedings of the Institution of Mechanical Engineers, Part B: Journal of Engineering Manufacture*, 212(7), pp.533-548.

118 Hu, Y., Yang, Q. and Wei P., 2009. Development of A Novel Virtual Coordinate Measuring Machine. *Proceedings of MTC 2009 - International Instrumentation and Measurement Technology Conference*, 5th-7th May 2009 Singapore. New York: IEEE, pp.230-233.

119 Zhang, G., Veale, R., Charlton, T., Borchardt, B. and Hocken, R., 1985. Error compensation of coordinate measuring machines. *CIRP Annals - Manufacturing Technology*, 34(1), pp.445–448.

120 Barakat, N.A., Elbestawi, M.A. and Spence, A.D., 2000. Kinematic and geometric error compensation of a coordinate measuring machine. *International Journal of Machine Tools & Manufacture,* 40(6), pp.833–850.

121 Van Dorp, B., Haitjema, H., Delbressine, F., Bergmans, R., and Schellekens, P., 2001. A virtual CMM using Monte Carlo methods based on frequency content of the error signal. *Proceedings of SPIE,* vol. 4401, pp. 58-167.

122 van Dorp, B., Delbressine, F., Haitjema, H., and Schellekens, P., 2001, Calculation of measurement uncertainty for multi-dimensional machines using the method of surrogate data. *In: Advanced Methematical and Computational Tools in Metrology.* Singapore: World Scientific Publishing Company, pp. 344-351.

123 ANSI/ASME B89.4.1:1997. *Methods for Performance Evaluation of Coordinate Measuring Machines*. ASME.

124 Beaman, J. and Morse, E., 2010. Experimental evaluation of software estimates of task specific measurement uncertainty for CMMs. *Precision Engineering,* 34(1), pp.28–3.

125 Salsbury, J.G., 1995. *A Simplified Methodology for the Uncertainty Analysis of CMM Measurements*. Indianapolis, USA: Society of Manufacturing Engineers, (IQ95-155:1 – 22).

126 Phillips, S.D., Borchardt, B., Estler, W.T. and Buttress J., 1998. The estimation of measurement uncertainty of small circular features measured by coordinate measuring machines. *Precision Engineering*, 22(2), pp.87-97.

127 Abackerli, A.J., Pereira, P.H. and Calônego, N., 2010. A case study on testing CMM uncertainty simulation software (VCMM). *Journal of the Brazilian Society of Mechanical Sciences and Engineering*, 32(1), pp.8-14.

128 Guo, Y., 2006. *Integrated process planning and scheduling for common prismatic parts in a 5-axis CNC environment*. Thesis (PhD), University of Bath, Bath, UK.

129 Blockley, D.I. and Henderson, J. R., 1980. Structural failures and the growth of engineering knowledge. *ICE Proceedings*, 70(3), pp.567 –579

130 Mebrahtu H., Walker R. and Mileham T., 2005. Manufacturing simulation optimization: an expert mechanism approach. *Proceedings of the Institution of Mechanical Engineers, Part B: Journal of Engineering Manufacture*, 223(12), pp.1625-1634.

131 Metrosage, 2003. *PUNDIT/CMM User Manual*. California, USA: MetroSage LLC.

132 Taguchi, G., Konishi, S. and Konishi S., 1987. *Methods, Orthogonal Arrays and Linear Graphs Tools for Quality Engineering*. USA: American Supplier Institute.

133 Wikipedia, 2012. *SolidWorks* [online]. Wikipedia. Available from: http://en.wikipedia.org/wiki/SolidWorks [accessed on 03/03/2013].

134 Flack, D., 2001. *Measurement Good Practice Guide No. 41: CMM measurement strategies*. London: National Physical Laboratory (NPL).

135 Flack, D., 2001. *Measurement Good Practice Guide No. 41: CMM measurement strategies*. London: National Physical Laboratory (NPL).

136 Lindqvist, R., 2011. *Geometrical and dimensional Measurement Planning: - a systematic and holistic approach*. Thesis (PhD). The Royal Institute of Technology, Stockholm, Denmark.